2018

Rapid bridge deck joint repair investigation - Phase III

David Andres Morandeira-Alonso
Iowa State University

Rapid bridge deck joint repair investigation - Phase III

by

David Morandeira

A thesis submitted to the graduate faculty

in partial fulfillment of the requirements for the degree of

MASTER OF SCIENCE

Major: Civil Engineering (Structural Engineering)

Program of Study Committee:
An Chen, Major Professor
Jennifer Shane
Brent Phares

The student author, whose presentation of the scholarship herein was approved by the program of study committee, is solely responsible for the content of this thesis. The Graduate College will ensure this thesis is globally accessible and will not permit alterations after a degree is conferred.

Iowa State University

Ames, Iowa

2018

DEDICATION

To my parents, Dania and Angel Luis, for their unconditional love and support.

To my brother, Angel Daniel, for providing me guidance.

TABLE OF CONTENTS

Page

LIST OF FIGURES

Page

LIST OF TABLES

Page

NOMENCLATURE

AADT	Annual Average Daily Traffic
AASHTO	American Association of State Highway and Transportation Officials
ABC	Accelerated Bridge Construction
ACI	American Concrete Institute
ASCE	American Society of Civil Engineers
ASTM	American Society for Testing and Materials
BEP	Break-Even Point
DBT	Deck Bulb Tee
DOT	Department of Transportation
CIP	Cast-In-Place
CTA	Chicago Transit Authority
EC	Elastomeric Concrete
FE	Finite Element
FEA	Finite Element Analysis
FHWA	Federal Highway Administration
FWS	Future Wearing Surface
HRWR	High-range Water Reducers
IDOT	Illinois Department of Transportation
LDF	Load Distribution Factor
LRFD	Load and Resistance Factor Design

MDOT	Michigan Department of Transportation
MPC	Magnesium Phosphate Cement
MPC	Multi-Point Constraints
NCDOT	North Carolina department of Transportation
NJDOT	New Jersey Department of Transportation
NYSDOT	New York State Department of Transportation
PBES	Prefabricated Bridge Elements and Systems
UHPC	Ultra-High Performance Concrete
WMU	Western Michigan University

ACKNOWLEDGMENTS

First and foremost, I would like to thank Dr. An Chen for his support along my graduate studies. I would like to express my appreciation for his advice, support and motivation throughout the course of this research and other aspects of life.

I would also like to thank Dr. Jennifer Shane for her guidance and continuous support throughout the course of this research. I would also like to thank Dr. Brent Phares for serving on my POS committee.

Special thanks to Dr. Charles Jahren for being a big proponent of mine since I started my graduate studies in Iowa State University. His input has been invaluable in the development of this research.

I would like to thank the Iowa DOT personnel for their input throughout the course of this research. Thanks to Michael Nop, Dean Bierwagen, James S. Nelson, Curtis Carter, and Eliezer Ramirez.

I would like to extend my gratitude to Douglas Wood and Owen Steffens for their help in developing the experimental investigation plan.

In addition, I would also like to thank Dr. Mostafa Yossef and Hao Wu for their help in developing the FE models and other aspects of this research.

Furthermore, I would like to thank all my friends and colleagues: Connor Schaeffer, Ahmed Alateeq, Mohammed Bazroun, Yinglong Zhang, Jin Yan, Elizabeth Miller, Yuderka Trinidad, Philip Iekel, Niles Quick, and many more.

Finally, I want to thank my family. Special thanks to my parents, Dania and Angel Luis, and my brother, Angel Daniel.

ABSTRACT

Accelerated Bridge Construction (ABC) technologies are changing the ways State Departments of Transportation (DOTs) do business. Subsequently, a three-phase project on the Rapid Bridge Deck Joint Repair Investigation is originated with the Iowa DOT. Phase I of this project focused on documenting the current means and methods of bridge expansion joint maintenance and replacement, and then identifying improvements. Based on the findings from Phase I, Phase II focused on the concept development. It was decided that a desirable approach would be to develop a design to move the joint away from the bridge deck at the face of the abutment to the approach slab that acts as a transition between roadway pavement and the previously mentioned bridge deck. By using this concept, a more effective joint can be created, where possible deicing chemical laden water leakage on the substructure components is no longer a concern for deterioration and its construction time can be comparable to that required for traditional joint replacements.

Phase III is tasked with the further development of this concept, the deck over backwall concept. The research team proposed various joint detailing options taking numerous factors into account. With this information, the Iowa DOT developed a more detailed joint considering their construction practices, experiences, and preferences. Full-scale finite element (FE) models of two different bridges were realized. These models were analyzed with various loading conditions from dead loads, temperature loading, and live loads which corresponds to various truck loading conditions. Both models were validated using the original drawing plans and the American Association of State Highway and Transportation Officials (AASHTO) Specifications providing deflection

limits for vehicular bridges in the absence of other criteria. The impact of the deck over backwall concept on the existing bridge elements was studied with the FE models alongside a parametric study of various bridge skew angles. The concept along with the approach slab were modeled in the FE models. Results show an increment in bearing loads due to the dead loads and live loads alongside relevant deflection values and stress levels at certain points of interest across the new joint and approach slab.

A cost estimate of different types of joints including the deck over backwall concept was developed. An initial estimate of the construction cost of the concept was realized to be used in the overall cost estimate. Results show that the deck over backwall concept over a bridge service life of 25 years constantly ranked 3th or 4th out of the nine types of joints that were considered. Over a bridge service life of 50 years, the concept produced the lowest cost in all possible combinations of inflation rates and fluctuations in installation cost and joint service life. In average, a break-even point (BEP) of 44 years was determined with a 2% interest rate and lowers as the interest rate is increased.

An experimental investigation plan was realized with the Iowa DOT joint. Test results will be compared and correlated with the FE models. A plan for construction observation and post-construction testing was developed with an instrumentation plan and various real-life truck loading cases to be correlated with the FE models. Implementation of the deck over backwall concept and the post-construction plan is expected to be conducted in a future Iowa DOT construction season.

With the results obtained from the FE models and, in the future, with the experimental investigation and the post-construction testing, the Iowa DOT can confidently design and further develop the deck over backwall concept.

CHAPTER 1. INTRODUCTION

1.1 Background

Phase I of this research project focused on documenting the current means and methods of bridge expansion joint maintenance and replacement, and then identifying improvements as part of workshop objectives. In Phase II, a literature review of topics including types of joints used or tested in other states, common and reported modes of failures in other states, integral abutments and the differences in their use between states, other methods of eliminating deck joints from existing bridges, and surveys of the average life span of particular types of expansion joints. Workshop were held with the emphasis on replacement of expansion joints. Discussions during the two workshops that were previously completed indicated that a desirable approach would be to develop a design to (1) minimize the amount of required concrete removal and to (2) move the joint away from the bridge deck at the abutment interface and instead place it on the approach slab. A schematic cross section of both concepts can be seen in in Figure 1.1 and Figure 1.2.

By minimizing concrete removal amounts, the impact on schedule time can also be minimized. Concrete removal has been recognized as one of the factors that affects construction time the most during expansion joint replacement projects. The other schematic cross section, Figure 1.2, shows a precast or cast-in-place (CIP) panel that is used to span the existing abutment backwall and push the joint out onto the approach slab. By using this concept, a more effective joint can be created, where possible deicing chemical laden water leakage on the substructure components is no longer a concern for deterioration and its construction time can be comparable to that required for traditional joint replacements.

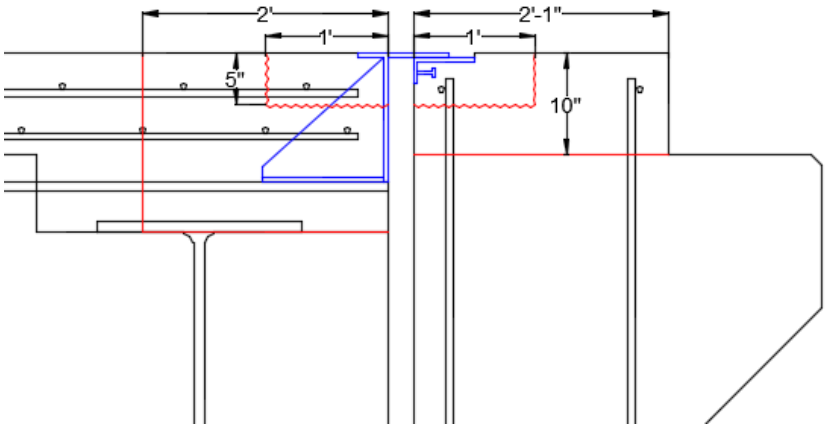

Source: Miller and Jahren (2015)

Figure 1.1: Minimum Concrete Removal Concept

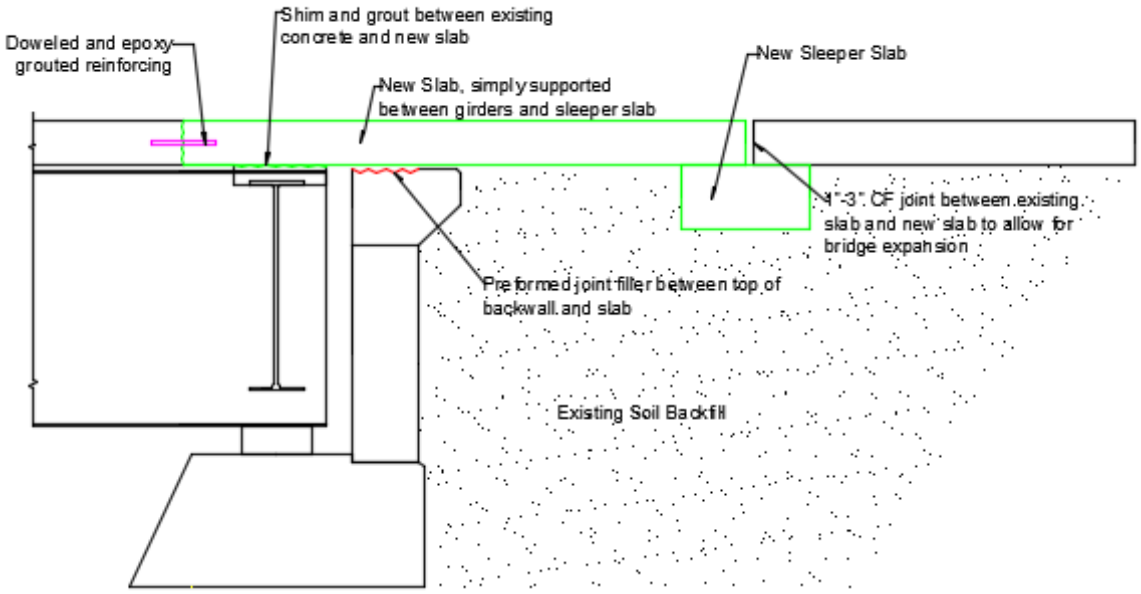

Source: Miller and Jahren (2015)

Figure 1.2: Example of Deck Over Backwall Concept

1.2 Problem Statement

Accelerated Bridge Construction (ABC) initiative is changing the way that bridges are built across the country. Accounting for an ever-increasing number of vehicle traveling over the nation's road infrastructure, reducing lane closure times has been identified as an integral part of ABC techniques and practices. In recent years, extensive research has been conducted on ABC. However, less attention has been devoted to accelerated repair and replacement of bridge deck expansion joints. For bridges requiring expansion joints, there is a need for accelerated replacement techniques that would lengthen the life cycle of the bridge in areas with high Annual Average Daily Traffic (AADT) and limited time for lane closures.

Many of the aging multiple span bridges utilize some form of expansion joints to properly counteract thermal movement alongside other factors. These joints also try to prevent the passage of winter de-icing chemicals and other corrosives applied to bridge decks from penetrating and damaging substructure components of the bridge. Majority of these expansion joints require frequent repair and multiple replacements during the normal service life of a bridge. Over the years, extensive research has been done to improve the longevity of these joints but with limited success. Eliminating deck joints instead of repair or replacement has been identified as a suitable and preferred option for bridges with moderate length and can be done in an accelerated fashion and minimize traffic interruption. When deck joints are eliminated, possible deicing chemical laden water leakage on the substructure components would no longer be a concern.

This three-phase project, Rapid Bridge Deck Joint Repair Investigation, is originated to address the dire need of further research into accelerated options for repair, replacement, and elimination of deteriorating conditions of bridge deck expansion joints in the state of Iowa and across the US.

1.3 Objectives

The objectives of this research are to:

(1) Conduct a literature review on repair, replacement, and elimination of bridge deck expansion joints.

(2) Further develop the deck over backwall concept with plans that conform to the design concepts.

(3) Create FE models of the selected bridges and study the impact of the concept on existing bridge structures.

(4) Compare the cost of application of the concept over other types of joints.

(5) Develop a plan for construction observation and post-construction testing where the concept can be further studied after implementation.

By achieving these objectives, the concept will be furthered developed and the Iowa Department of Transportation (DOT) can confidently design and implement the deck over backwall concept.

1.4 Limitations And Constraints

Multiple limitations and constraints were identified across all aspects of the research. For the FE modeling, it can be said that limitations and constraints exist in every FE model. The FE models can always be more detailed. Simplifications were made when necessary to accelerate processing time. In the cost analysis, assumptions and omissions were made to realize the analysis within time constraints. Many additional factors could be introduced in the cost analysis to present a more in-depth study into the different types of joints. For the experimental investigation plan, laboratory space constraints limited the test specimen size. Also, the plan was made without the presence of soil supporting the approach slab.

1.5 Thesis Organization

The thesis was organized in eight chapters each corresponding to various tasks that were needed to realize the research. The eight chapters are shown below with a brief summary into its tasks.

Chapter 1 Introduction: provide background into the problem that the research is attending and present the objectives of the research

Chapter 2 Literature Review: review of published literature of relevant topics

Chapter 3 Joint Detailing: further develop the joint detailing of the deck over backwall concept

Chapter 4 Finite Element Modeling and Analysis: create FE models and evaluate the impact of the deck over backwall concept at various points of interest in bridge elements

Chapter 5 Cost Analysis: realize a cost comparison of various types of joints including the deck over backwall concept

Chapter 6 Experimental Investigation Plan: develop a plan to conduct laboratory testing for the concept

Chapter 7 Construction Observation and Post-Construction Testing Plan: develop a plan for post-construction evaluation of the deck over backwall concept when implemented

Chapter 8 Conclusions and Future Work: provide the conclusions obtained throughout the various tasks of the research and future work recommendations

CHAPTER 2. LITERATURE REVIEW

A review of the published literature was conducted by the research team on three relevant topics. The first topic is the current practices and accelerated options of repairing and replacing expansion joints. Related to the first topic, the use of Ultra-High Performance Concrete (UHPC) in bridge joints and connections was reviewed. Finally, the different practices of modeling and analyzing bridge structures and soil properties with commercial software was studied.

2.1 Repair, Replacement, And Elimination Of Expansion Joints

A thorough review of the literature of accelerated methods of repair, replacement, and elimination of expansion joints has been realized in the past phases of this research, Phase I and Phase II. In conjunction with the Iowa DOT, Miller and Jahren (2014) conducted an investigation focused on determining the best ways to rapidly repair and replace expansion joints in Iowa and in other states. Their findings were synthesized by Phares and Cronin (2015). Their findings will be discussed and summarized in the following pages.

2.1.1 Joint Repair And Replacement

The study revealed that demolition and concrete cure times account for the longest segments of construction time in expansion joints replacement projects (Miller and Jahren 2015). From these conclusions, hydrodemolition was identified as an effective and quick way to remove concrete from the surrounding areas of the expansion joint; however, it is costly and runoff containing small concrete particles is an issue that must be dealt with (Phares and Cronin 2015).

To repair or replace sliding plate expansion joints, the Iowa DOT personnel stated that it would be best to remove the joint entirely. The open space would be filled with new concrete while leaving a flat gap between the abutment and deck for expansion and contraction of the bridge (Miller and Jahren 2014). This method of replacement avoids any unnecessary traffic delay (Phares and Cronin 2015).

There are various methods of repair and replacement of strip seal and compression seal expansion joints. These methods depend on the condition of the expansion joint mechanism in question. The use of compressed air or pressurized water to remove debris from the joint is acceptable as long as the seal or the extrusion is not damaged. If the strip seal or compression seal is damaged, it may need to be removed and cleaned or a new seal could also be installed. The new section may be spliced in or the entire length of the seal may be replaced (Miller and Jahren 2014). Miller and Jahren (2014) pointed out that a new section should not be spliced between two existing sections due to buckling concerns.

Various methods were recognized to replace the compression seal armoring. The armoring can be replaced by removing and replacing the existing concrete with new concrete for a flat riding surface. However, the process takes several hours to realize. Miller and Jahren (2014) found and alternative method that can be installed in as little as 30 minutes per lane if no repair of the vertical face of the concrete is required is also discussed. The method is the Silicoflex joint sealing system from R.J. Watson, Inc. This system is an inverted strip seal installed using adhesives instead of extrusions. The system has to be installed to a clean, flat vertical face below the damaged extrusion (Miller and Jahren 2014).

Other types of joints were also considered in the investigation. Finger and modular expansion joints were found to be easily repaired by simply replacing the damaged joint component. If a torn neoprene gland is discovered, the entire joint does not have to be replaced. A new neoprene gland can be installed after removing the damaged one (Miller and Jahren 2014).

Integral abutment joints were also looked at. Miller and Jahren (2014) found that possible locations of damage can unusually be found on the tire buffing and silicon sealant. To repair these deteriorated items, missing pieces from the tire buffing are replaced and new silicon is poured into the joint (Miller and Jahren 2014).

2.1.2 Joint Elimination

In Phase II of this research, Miller and Jahren (2015) stated that most bridge engineers would consider the best type of joint to be no joint. Tying into the statement, Palle et al. (2012) developed and distributed surveys to all the state highway agencies. Most state highway agencies sough to eliminate joints where ever possible. Several noted that joint elimination was a goal for new bridge designs (Palle et al. 2012). In their investigation, Miller and Jahren (2015) thoroughly conducted a review of the literature for possible joint elimination options. Elimination options were seen in the applications of integral abutments, semi-integral abutments, link slabs, and the concept originated in Phase II of this research and being further developed, the deck over backwall concept. Their findings will be summarized and discussed in the following pages.

2.1.2.1 Integral abutments

The trend of accelerated methods of repair and replacement of expansion joints seems to be toward eliminating deck joints altogether by utilizing the integral abutment design. A few agencies are using them as their sole selection for new construction (Baker Engineering & Energy 2006). It is for this reason that integral abutment bridges are becoming increasingly popular in the US.

Integral abutments differ from the most commonly known stud abutments in that they encompass the ends of the bridge girders in its own backwall. The integral abutment moves with respect to the movement of the girders due to thermal loading, dynamic loading, and other factors. The pile supports in the abutment move alongside as well. A typical cross section of integral abutments can be seen in Figure 2.1.

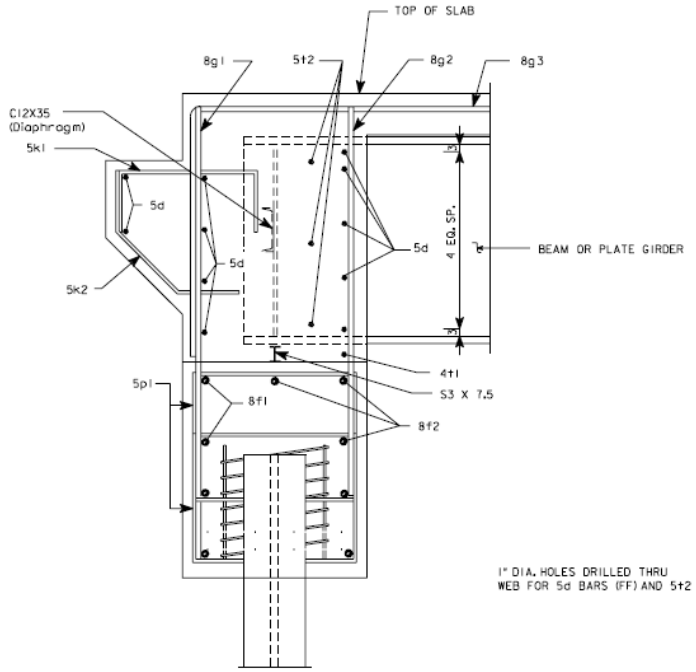

Source: Miller and Jahren (2015)

Figure 2.1: Integral Abutment Cross Section

Most states that employ the use of these abutments have reported that they are satisfied with the performance of integral abutment bridges. Maruri and Petro (2005) surveyed all the transportation agencies in the US regarding their use of integral abutment bridges. A large number of agencies responded to the survey. The survey had a 79% response rate because of this. From the survey results, an estimated number of in-service integral abutment bridges increased by almost 200% from an estimated 4,000 integral abutment bridges in 1995 to an estimated 13,000+ integral abutment bridges in 2004 (Miller and Jahren 2015).

Since deicing chemicals and snowplows are widely used in the Northern states of the US versus the Southern, integral abutments are much more common in the former states than in the latter states. Survey results showed that the usage of integral abutments is surely going to continue in the future as 77% of the respondents answered that they will continue with the use of integral abutments in bridges where they could be considered. While most states reported that they were satisfied with the performance of integral abutment bridges, three states in particular deviated from those feelings. Arizona encountered problems with their approach slabs while Vermont encountered scour issues. These two states abandoned the application of integral abutments in future bridges. The third state, Washington, encountered seismic issues and decided to move forward with semi-integral abutments in bridges where integral abutments could have been considered.

2.1.2.2 Semi-integral abutments

As an alternative to integral abutments, semi-integral abutments were originated. This option functions in many of the same ways as an integral abutment. These abutments still encompass the ends of the bridge girders in its own backwall. The semi-integral abutment also moves with respect to the movement of the girders due to thermal loading, dynamic loading, and other factors. The main difference between the two is that the entire backwall and girder system is situated on bearings and allowed to slide over a fixed foundation (Miller and Jahren 2015). A typical cross section of semi-integral abutments can be seen in Figure 2.2.

In the state of Iowa, semi-integral abutments are not used often on new construction of bridge structures. Instead semi-integral abutments are used as a joint retrofit where an integral abutment previously discussed is not compatible with the existing bridge design. Expansion joints across the states have been replaced with semi-integral abutments making possible deicing chemical laden water leakage on the substructure components no longer a concern. While their use has been rising, semi-integral abutments have received much less attention than integral abutments bridges. States also stated that semi-integral abutments were largely used in unique situations where integral abutments do not work well such as bridges with large skew angles, high backwalls, or those built on difficult soil conditions (Miller and Jahren 2015). One soil condition in particular that was mentioned was the situation where bedrock is close to the surface and piles cannot develop sufficient horizontal resistance to provide fixity for the footing (Yanotti et al, 2005).

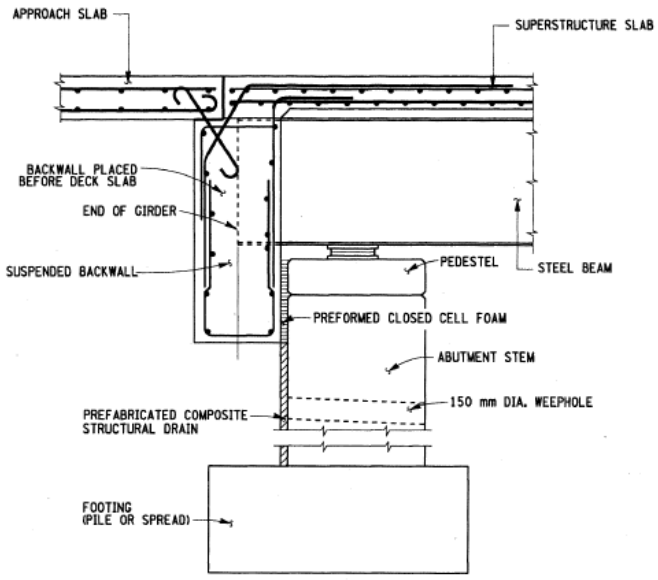

Source: Miller and Jahren (2015)

Figure 2.2: New York Semi-Integral Abutment

2.1.2.3 Link slabs

While the options previously discussed are all alternatives of eliminating expansion joints at the abutment interface, options for eliminating expansion joints above the piers are also available. Link slabs have been used in numerous projects across the US to replace expansion joints located over bridge piers. Link slabs do exactly what the name says, link the existing bridge deck between two girders over the pier supports.

Miller and Jahren (2015) explained that the stiffness of the continued deck is so small in comparison to the girders that continuity is assumed to not be provided. This means that the bridge will continue to act as a series of simply supported members thus not affecting the original bridge design. The link slab acts as a beam with a moment caused by the rotation at the end of the girders. To provide the necessary flexibility of the link slab a portion of the

deck is debonded at the end of the girders (Aktan et al, 2008). A typical cross section of link slabs can be seen in Figure 2.3 with the moment and rotation detailing.

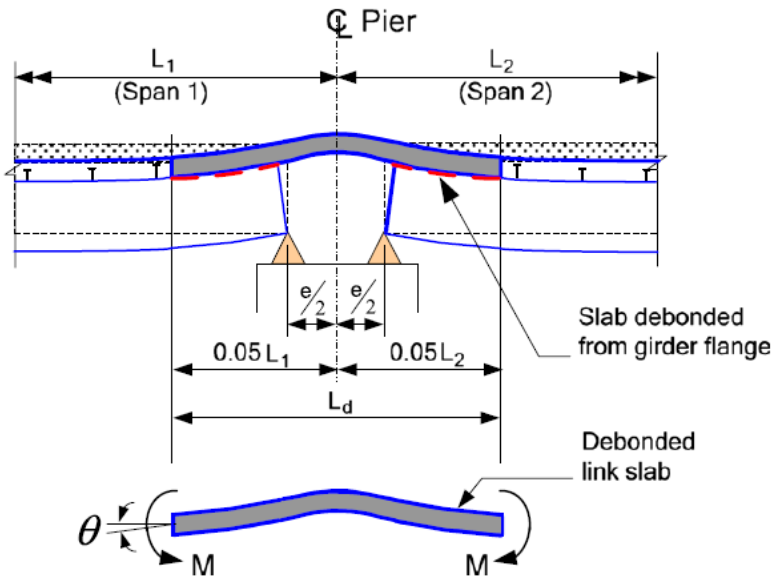

Source: Miller and Jahren (2015)

Figure 2.3: Debonded Link Slab System

Since link slabs have not been implemented as much as other methods of bridge deck joint repair, replacement, and elimination, there is a limited amount of knowledge in terms of its performance when implemented. Miller and Jahren (2015) detailed a pilot link slab that was built in 1998 by the North Carolina DOT (NCDOT). The pilot link slab was instrumented, monitored, and tested after implementation. Beam end rotations of 0.02 radians were taken into account in the design of the link slab. The link slab is also meant to have fine cracks under service loads. The maximum width of these fine cracks was designed to be 0.013 inches.

At no point over the next year of monitoring did the link slab exceed the 0.02 radians of bend end rotations. A crack higher than 0.013 inches was noticed in the middle of the link slab. This crack had a width of 0.063 inches. The crack was present before live load testing and did not increase during the tests. It was ultimately believed that this crack was larger than designed due to localized debonding of the reinforcement (Wing and Kowalsky, 2005).

Michigan installed numerous link slabs in the early 2000's as part of several deck rehabilitation projects across the state. Inspections of these bridges were held in 2006 showing observations similar to those by Wing and Kowalsky (2005) previously discussed. In every link slab inspected, a full depth crack was found approximately at the centerline of the pier, regardless of whether a sawcut had been provided at these locations. However, other than the transverse cracking at the pier centerlines little other cracking or damage was reported at the link slab locations (Aktan et al, 2008).

Aktan et al. (2008) completed a detailed FE analysis used to predict how certain parameters affect the performance of link slabs for use in the state of Michigan. The investigated design parameters of the link slab were as follows: the link slab debonded length with respect to adjacent span lengths, girder height, adjacent span ratio, and support conditions. Several conclusions were arrived at from the FE results:

- Top and bottom layer of steel should be continuous throughout the link slab.
- Additional moment and axial loads should be considered in the design of link slabs to account for thermal gradients.
- Sawcuts should be provided at the centerline of the pier and at each end of the link slab. These sawcuts concentrate cracking to areas where the performance of the link slab would not be diminished.

2.1.2.4 Deck over backwall concept

Miller and Jahren (2015) held various workshops with the objective of identifying improvements of bridge deck joint maintenance and replacement. Workshop participants came up with a concept that eventually evolved into the deck over backwall concept shown in Chapter 1, Figure 1.2. Further review of the literature was conducted to study possible implementation of this concept in other states.

According to a 2004 survey, there are approximately 3900 bridges with deck extensions currently in use in the United States (Miller and Jahren 2015). This type of bridge is stated to be particularly prominent in the Northeast region of the US as opposed to the Midwestern and Northern regions where full integral abutment designs are more common (Maruri and Petro 2005). The New York State DOT (NYSDOT) in particular has been building bridges with deck extensions since the 1980's or earlier (Alampalli and Yannotti 1998).

Alampalli and Yannotti (1998) detailed 105 deck extensions that were inspected by the NYSDOT, 72 with concrete superstructures and 33 with steel superstructures. These bridges were found to be performing as anticipated with minor deck cracking as the only significant problem. Miller and Jahren (2015) identified several conclusions with regards to deck extensions.

- Steel structures were usually less prone to deck cracking than prestressed-concrete superstructures.
- Performance typically worsened with increased skew or span length.

Miller and Jahren (2015) compared jojntless bridges and other types of joints, mainly compression seals, utilizing NYSDOT bridge inspection and inventory data. Results of the data show that components of jointless bridges performed better than components of compression seal bridges.

Construction details were provided for a typical deck extension of the NYSDOT. This is shown in Figure 2.4. Discussing the detail, Alampalli and Yannotti (1998) mentioned that the deck and approach slab were previously included in a single placement, and the formed joint is merely a sawcut to promote full depth cracking at the correct location. This has been changed since. The approach slab and deck are placed separately now, eliminating the need for a sawcut. This joint is provided to allow superstructure rotation with the bottom layer of longitudinal deck steel continuous through the joint to keep the deck and approach slab from separating (Alampalli and Yannotti 1998).

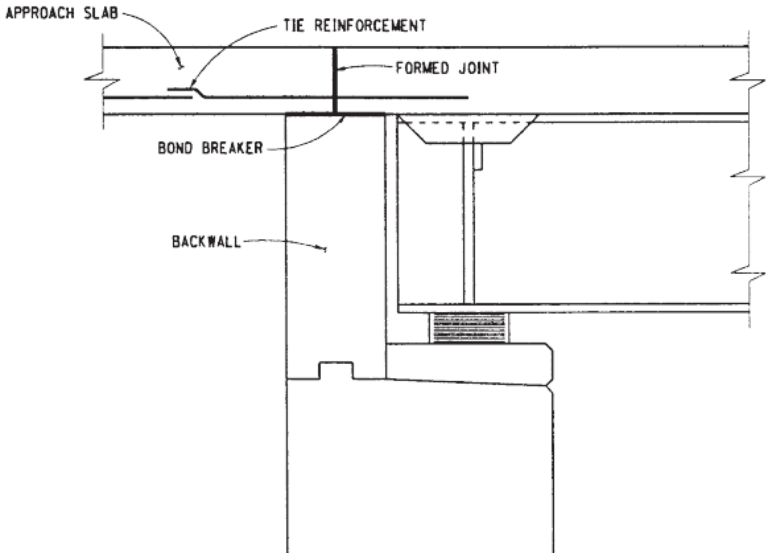

Source: Miller and Jahren (2015)

Figure 2.4: NYDOT Deck Extension Detail

Other DOT's have also developed jointless bridge decks with similar deck extension details as the NYSDOT joint and the concept brought up in the workshop that eventually evolved into the deck over backwall concept.

Michigan DOT (MDOT) has worked on developing jointless bridge decks to combat deterioration to the leaking expansion joints. Their detailing is shown in Figure 2.5.

Various differences can be seen between the NYSDOT joint and the MDOT joint. These differences are outlined below.

- location of the construction joint (in line with the center of the backwall for NYDOT, in line with inside edge of the backwall for MDOT)
- location of the continuous longitudinal reinforcing (bottom reinforcement for NYSDOT and top reinforcement for MDOT)
- sleeper slab incorporation in MDOT

Miller and Jahren (2015) pointed out that continuing the top layer of reinforcing through the joint should allow negative moment transfer across the construction joint as opposed to allowing the joint to act as a hinge.

Approach slab standards differ from the Iowa DOT and MDOT. Iowa DOT uses 20 feet approach slabs while MDOT only uses a 20 feet approach slab for bridges with integral and semi-integral abutments. However, for deck extension details, MDOT extends the approach slab 5 feet from the near edge of the backwall to rest on a sleeper slab. This sleeper slab would help mitigate possible settlement issues between the existing pavement and the new approach slab. MDOT's sleeper slab detailing can be seen in Figure 2.6.

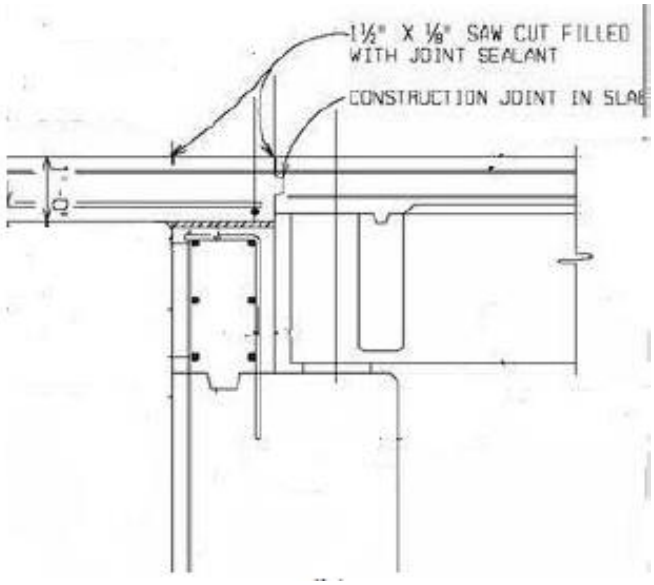

Source: Miller and Jahren (2015)

Figure 2.5: MDOT Deck Extension Detail

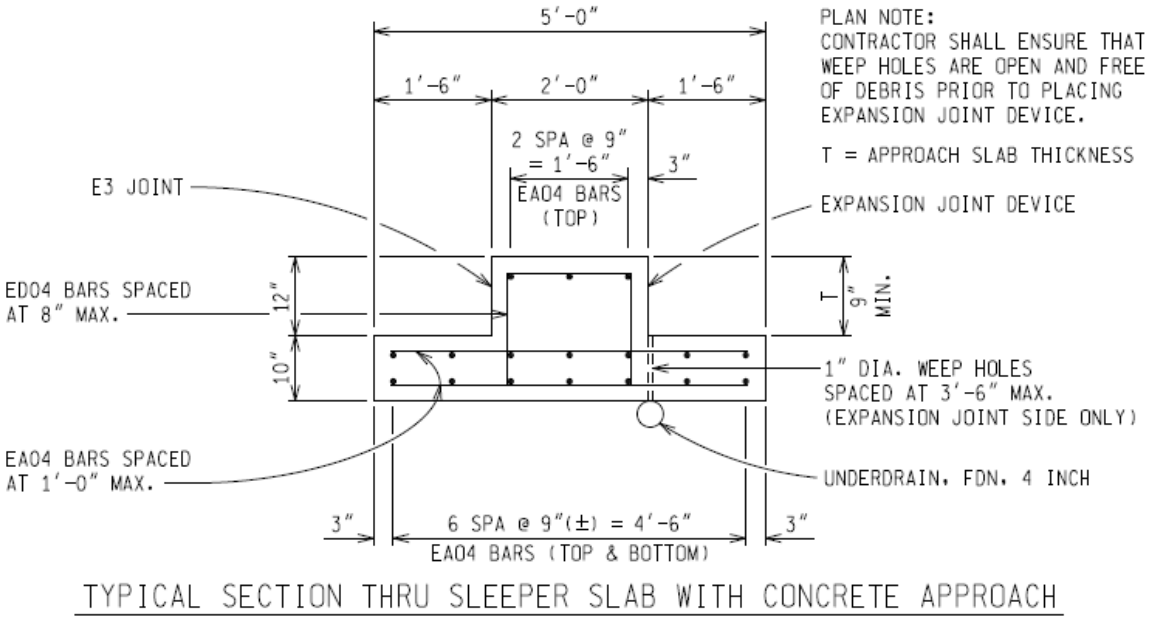

Source: Miller and Jahren (2015)

Figure 2.6: MDOT Sleeper Slab

Western Michigan University (WMU) developed FE models for MDOT to analyze deck extension details to further improve their designs. The difference between continuing the top layer of steel reinforcement versus bottom reinforcement was of particular interest. FE results show that continuing the top layer of reinforcing caused the construction joint to transfer negative moment, tensile stresses, at the top of the approach slab around the construction joint. Continuing the bottom layer of longitudinal reinforcing caused the joint to act as a hinge eliminating the stresses at the construction joint but increased the nominal positive moment at the midpoint of the approach slab. Given the later situation, bottom layer of continuity steel was preferred (Aktan et al. 2008).

Miller and Jahren (2015) agreed with this conclusion as cracking can be allowed on the bottom side of the slab. The design for the additional midspan moment is more achievable than designing for negative moment capacity at the top of the deck where cracking should be prevented. A waterstop could be included in the construction joint to prevent the passage of water and mitigate additional cracking (Miller and Jahren 2015).

The research team made direct contact with MDOT to gain more information about their experiences with bridge extension. A summary of the key takeaways is shown below:

- Implemented deck extensions for MDOT achieved the objectives Iowa DOT is seeking to accomplish
- Future detailing will provide continue bottom reinforcement
- Approach slab will be poured after the deck to provide a cold joint in the abutment interface
- Settlements issues of sleeper slab cause a ‘bump’ at the transition from the approach slab to the highway pavement

2.2 Use Of Ultra-High Performance Concrete On Bridge Joints

2.2.1 Background

Thirty years ago, a new technology called Ultra-High Performance Concrete (UHPC) started being researched for use in bridge design and construction. This new material offered very durable solutions, but required, new shapes, new design codes and standards, new precast fabrication methods and formworks (Perry and Corvez 2016). The lack of design codes and standards increased risk on its implementation for owners and designers. These limitations held the material back from growing at a faster pace. Nonetheless, as a very young material, 30 years into research and 20 years into development, acceptance has been growing as more research has been realized. The industry has been noticing the advantageous properties that the material processes (Perry and Corvez 2016).

2.2.2 Mechanical Properties

"Ultra-High Performance Concrete (UHPC) is a cementitious, concrete material that has a minimum specified compressive strength of 150 MPa (21.6 ksi) with specified durability, tensile ductility and toughness requirements; fibers are generally included to achieve specified requirements" (ACI-239 2012). UHPC exhibits very high compression strength, an improved tensile behavior and a sustained post cracking strength (Ronanki et al. 2016). This high compression strength and improved tensile behavior facilitate high bond strength and as a result a short development length of steel reinforcement. This is fully explained in the Federal Highway Administration (FHWA) Technical Note publication *Design and Construction of Field-Cast UHPC Connections* (Graybeal 2014).

Additionally, “compared with conventional normal- and highstrength concretes with their capillary porosity, UHPC exhibits a much denser microstructure. It has virtually no capillary pores and is therefore so impervious to liquids and gases that its corrosion is practically zero; it can serve as the wearing course of a bridge deck without any additional protection against chlorides, alkalis or de-icing salts” (Fehling et al. 2015). The low permeability is attributed to the fine powders and chemical reactivity which create an extremely compact matrix and small, discontinuous pore structure (Perry and Royce 2010). UHPC formulations often consist of a combination of portland cement, fine sand, silica fume, high-range water-reducing admixture (HRWR), fibers (usually steel), and water. Small aggregates are sometimes used, as well as a variety of chemical admixtures (Russell and Graybeal 2013). The improved properties of UHPC provide benefits of simplified construction techniques, speed of construction, improved durability, reduced maintenance, reduced out-of-service, minimum interruption, reduced element size and complexity, extended usage life and improved resiliency (Perry and Corvez 2016).

2.2.3 Implementation Of UHPC In Bridges

The first use of UHPC in a North American bridge was in 1997, for construction of the Sherbrooke Pedestrian Bridge Quebec, Canada (Perry and Seibert 2013). This 197 ft clear span bridge shown in Figure 2.7 was constructed from six precast 3-D Space Truss UHPC elements, post-tensioned together on site. “The structural concept consists of a space truss with a top UHPC chord that serves as the riding surface, two UHPC bottom chords, and truss diagonals that slope in two directions.” (Russell and Graybeal 2013)

Source: Russell and Graybeal (2013)

Figure 2.7: Sherbrooke Pedestrian Bridge, Quebec, Canada (1997)

In 2001, the US Federal Highway Administration (FHWA) initiated a research program to evaluate and introduce UHPC into the US Highway program (Graybeal 2008). The first UHPC highway bridge completed in North America was the Mars Hill Bridge in Wapello County, Iowa (Bierwagen et al. 2006). The simple single-span bridge, shown in Figure 2.8, comprises three 110-ft long precast, prestressed concrete modified 45-inch deep Iowa bulb-tee beams topped with a CIP concrete bridge deck. Each beam contained forty-seven 0.6-inch diameter, low-relaxation prestressing strands and no shear reinforcement (Russell and Graybeal 2013). The most significant aspect of this first UHPC highway bridge was the use of the three UHPC I-girders without any stirrups for shear reinforcing. This was a major milestone and a significant step towards the introduction of UHPC into the North American highway system (Perry and Corvez 2016).

Source: Russell and Graybeal (2013)

Figure 2.8: Mars Hill Bridge, Wapello County, IA (2006)

During this same period, the FHWA was working on an "optimized" precast bridge profile, named the "Pi-Girder" (π). The first generation of this girder was prototyped and installed at a test track in the FHWA's Turner-Fairbank Research Center near Washington, DC (Perry et al. 2010). In 2008, Buchanan County, Iowa completed the Jakway Park Bridge, shown in Figure 2.9, using the second generation precast UHPC Pi-girder (Graybeal 2004). The cross section, shown in Figure 2.10, is similar to a double-tee section but with bottom flanges on the outside of each web (Russell and Graybeal 2013).

Source: Russell and Graybeal (2013)

Figure 2.9: Jakway Park Bridge, Buchanan County, IA (2008)

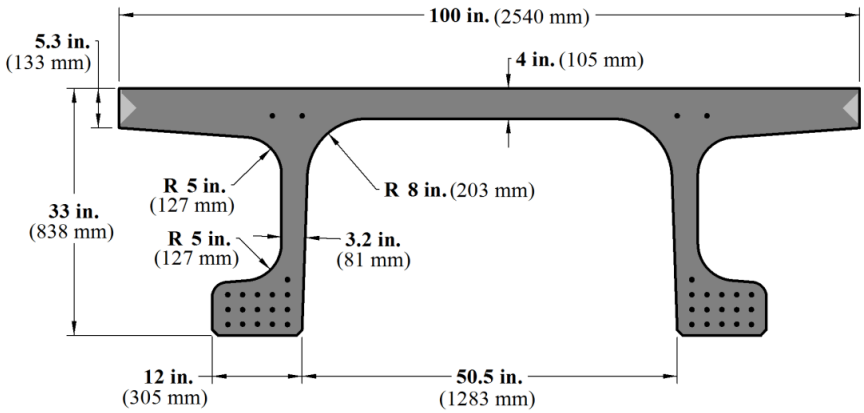

Source: Russell and Graybeal (2013)

Figure 2.10: Cross Section of Pi-shaped Girder

As of the end of 2016, over 200 bridges with UHPC elements would been completed in North America. These include either precast bridge elements or field-cast connections (for precast bridge elements) or, in some cases, both precast and field-cast UHPC solutions (Perry and Corvez 2016).

2.2.3.1 Utilization of UHPC joints and connections

While it is recognized that precast bridge components can provide high durability, conventional joints are often the weakest link in a bridge deck system. During the period of 2006 and 2016, more than 200 precast bridges have been completed utilizing UHPC field-cast connections (Perry and Corvez 2016). The UHPC joints are filled with UHPC and reinforcing steel is lapped across the joint. The lap length of reinforcing steel is based on the reference from Design and Construction of Field-Cast UHPC Connections (Graybeal 2014). UHPC field-cast connections have been used to connect bridge precast elements such as: full depth precast deck panels (shown in Figure 2.11), side-by-side box girders, side-by-side Deck Bulb-Tees, live-load continuity connections, precast approach slabs to abutments, curbs to decks, piles to abutments and in the haunches (to provide horizontal shear for composite construction) (Perry and Seibert 2013).

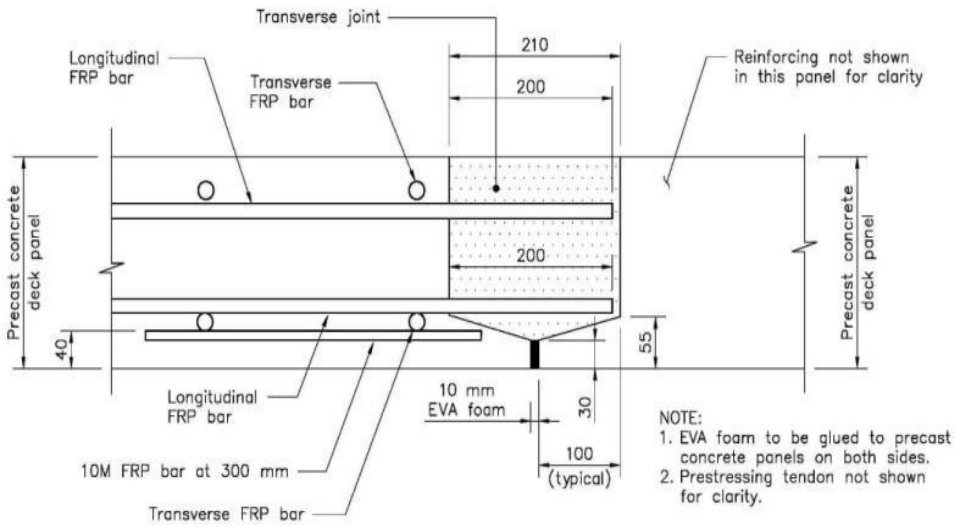

Source: Perry and Seibert (2013)

Figure 2.11: Typical Section through a Transverse, Full-Depth Precast Panel Joint

In 2009, the first highway bridge using UHPC joints between full-depth deck panels was constructed in the United States. Since then, 17 bridges of its kind have been built in US. As of 2013, there are about six states that have built precast deck panel bridges with UHPC joints (Liu and Schiff 2016). In 2012, 13 bridges were completed using this technology and in 2013, more than 30 bridges with UHPC elements were completed in multiple state and provincial jurisdictions in the USA and Canada (Perry and Corvez 2016).

The following pages will detail the first highway bridge using UHPC joints in 2009 and, in addition, the application of UHPC joints in different projects on three different states; New York, Illinois, and New Jersey.

2.2.3.1.1 UHPC in New York

New York's extensive state and local highway network that annually handles over 130 billion vehicle miles driven on the system is often in need of repair or replacement of bridge deck and bridge superstructure. It has a long history of using Prefabricated Bridge Elements and Systems (PBES) for accelerating bridge construction to maintain acceptable levels of mobility. Starting from 2008, NYSDOT has been deeply involved in the development, testing, trial application and utilization of field-cast UHPC joints between prefabricated elements for ABC (Royce 2016). As of now NYSDOT has successfully completed the construction of 30 bridges utilizing UHPC connections of prefabricated elements. Royce (2016) presents the NYSDOT's experience with ABC using PBES with field-cast UHPC joints. In this paper, four case studies are mentioned and detailed. These case studies alongside the development of an innovative link slab design utilizing UHPC will be discussed and summarized in the following pages.

Case Study 1, 2009, deals with the first field application of UHPC joints in bridge construction in New York as well as in the country, the superstructure replacement of Route 31 over Canandaigua Outlet. An 85 feet single span bridge with limited available beam depth shown in Figure 2.12.

Source: Royce (2016)

Figure 2.12: NYSDOT - Case Study 1: Route 31 over Canandaigua Outlet

DBT in Place before UHPC Placement

Longitudinal UHPC connections joints were used with Deck Bulb-Tees (DBT). Royce (2016) explains that this was implemented to shorten construction times and make the system even more durable than CIP systems. The material supplier educated the contractor about the importance of leak-proof forms before placing UHPC. The top quarter inch of the

UHPC joint fill has a tendency to have a low quality material which needs to be removed; therefore, joints were overfilled to ensure that the entire finished joint was filled with high quality material. The success of this experience led to design and construction of several bridge superstructures with prefabricated deck beam elements with UHPC joints.

Case Study 2, 2009, details the second application which was a construction of a 127-ft. single span steel girder bridge precast concrete deck with UHPC joints near Oneonta, NY, Figure 2.13. UHPC placement operation was completed in two days without any major problems. Royce (2016) says it could have been completed in a day if the contractor had provided sufficient labor and had larger UHPC mixers. Careful storage of the UHPC pre-mix through the storage period was observed because any moisture penetration into the premix powder will result in the formation of silica balls the UHPC mix (Royce 2016). To reduce or eliminate this problem, supplier made improvements in the packaging and storage of the material as well as the mixing process. During the placement of UHPC in the joints a few areas of leakage were noticed and corrected during construction. NYSDOT contract documents currently alert the contractors about the need for water-tight forms (Royce 2016).

Both case studies utilized prefabricated components and obtained considerable reduction of construction time compared to conventional methods. After these projects were completed, needs for further improvements in this technology were identified to achieve acceleration of construction. Among them were, firstly, the use of overlays over the precast components. These were problematic when concrete overlays were used due to the needed cure time and their avoidance was a desirable improvement. As a solution NYSDOT developed precast deck systems that have ½ inch sacrificial thickness for diamond grinding after the completion of the deck to obtain a smooth riding surface. Two types of composite

connections were developed in order to avoid the overlays. UHPC haunches with open stud pockets in addition to the joints and hidden haunches with two types of fill material, cementitious grout or UHPC. Cementitious grout fill material needed 6 inch studs penetrating above the bottom layer of the deck reinforcement. UHPC filled haunches were designed with 3 inch studs. The idea behind this approach is that shorter development is achievable in the UHPC due to its high sustained tensile strength. UHPC filled haunches with 3 inch studs was the most efficient way of construction though the material cost is bit higher. Secondly, acceleration of compressive strength gain of the UHPC joints was identified as another desirable improvement. 14 KSI was determined to be adequate for the performance of UHPC joints under live traffic. The available cure time for UHPC was determined to be 12 to 14 hours in order to complete a deck removal and replacement during one weekend closure.

Source: Royce (2016)

Figure 2.13: NYSDOT - Case Study 2: Route 23 over Otego Creek in Oneonta Precast Deck Placement in Progress

Case Study 3 details the construction of two bridges on Route 42 over West Kill on Lexington, NY. A 120-ft. single span precast deck over new multi-girder steel superstructure with UHPC joints over the steel girders is shown in Figure 2.14.

Source: Royce (2016)

Figure 2.14: NYSDOT - Case Study 3: Route 42 over Westkill

Panel Joint Placement in Progress

These were constructed during the winter of 2011 under an emergency contract. In August of 2011, the original bridges were washed out during Hurricane Irene. Stud sheer connectors were installed through openings in the deck panel with UHPC filled haunches and stud pockets. A diamond ground deck surface with no overlay was used for these bridges. Curing of UHPC under artificial heating was used since the ambient temperature during the curing time was mostly below freezing. The Department is now confident that construction during wintertime is feasible with the use of precast elements with UHPC. Even though curing of UHPC joints needs artificial heating, the heating set up is significantly less

complex and the duration is shorter compared to what would be needed for a CIP operation. In addition, based on the Department's past experience, artificial heating of CIP decks often results in deck cracking. That problem was obviously avoided with these bridges (Royce 2016).

Case Study 4 involves many bridges done under various contracts in different parts of the state. This group of bridges included a number of single span bridges, a two-span steel curve girder bridge and four three span bridges. Ten of these bridges are located in urban areas carrying interstate traffic while seven are on state highways in rural settings. The degree of construction acceleration was decided based on the needs of the specific location. About half of these bridges required deck replacement within a window of 72 hours; Friday night closure to early Monday morning opening to traffic. Many of them used five to ten days of closure time. Cost of deck replacement increased along with the degree of acceleration. The Department allowed the longest window feasible to keep the cost to the lowest possible. A typical example of one of these bridges can be observed in Figure 2.15. A 120-ft. single span precast deck without overlay over existing multi-girder steel superstructure with UHPC joints over the steel girders and hidden haunches with non-shrink grout and studs penetrating above the bottoms of precast panels (Royce 2016).

Source: Royce (2016)

Figure 2.15: NYSDOT - Case Study 4: I-81 over East Castle St.

Precast Deck Placement in Progress

In addition to the four case studies previously detailed, the NYSDOT Office of Structures has also developed an innovative link slab design utilizing UHPC to eliminate transverse deck joints wherever feasible. The link slab design assumes that the UHPC section is subject to bending. The link slab also acts as a semi-rigid link between spans transferring compressive, tensile, and shear stresses due to various loads (Royce 2016). The design of the link slab is influenced by variables such as span arrangement, bearing type and arrangement, girder end rotation due to live load, and bridge skew. A conceptual design of this link slab is shown in Figure 2.16. Several rehabilitation projects are being progressed within the Department utilizing UHPC link slabs to eliminate joints. Based on NYSDOT's experience to date, link slabs are performing well with no visible cracks within the UHPC slab (Royce 2016). A finished link slab can be seen in Figure 2.17.

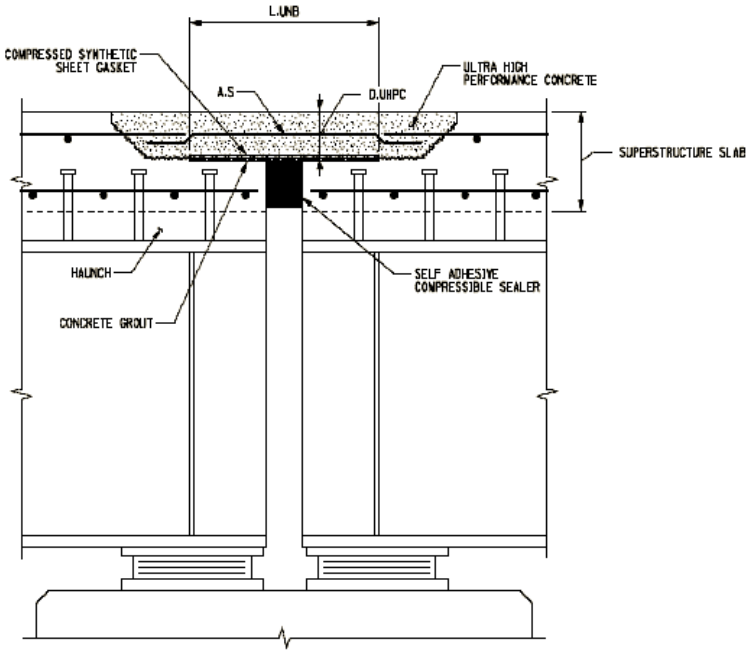

Source: Royce (2016)

Figure 2.16: NYSDOT - Link Slab Cross Section

Source: Royce (2016)

Figure 2.17: NYSDOT - Finished Link Slab

2.2.3.1.2 UHPC in Illinois

Liu and Schiff (2016) present the design and construction of Illinois's first precast deck Panel Bridge with UHPC joints, a $450 million Circle Interchange Project in Chicago. This project involves the replacement of the Peoria Street Bridge over I-290 and the Chicago Transit Authority (CTA) with a 3-span, continuous, steel plate girder bridge with a total length of 273'-0" and a bridge width of 56'-4". Three alternatives were proposed to the Illinois DOT (IDOT) for consideration: 1) Precast deck panels with internal post-tensioning; 2) AccelBridge System; and 3) Precast deck panels with UHPC joints. The IDOT decided to select the new generation deck system: precast deck panels with UHPC joints.

There are 52 deck panels in total and a longitudinal UHPC joint is provided to accommodate the 56-ft wide bridge. Twenty different deck panels are required due to the complex bridge layout such as CTA train station entrance to the west, CTA staircase to the east, and light poles and drainage scuppers. All the transverse and longitudinal joints are filled with UHPC. The design of UHPC joints is based on pull out research. The UHPC transverse joint and longitudinal joint details are shown in Figure 2.18 and Figure 2.19, respectively. The shear stud pockets are filled with non-shrink grout. The shear stud pocket detail is presented in Figure 2.20. Shear stud pockets utilizing UHPC will be presented in the next subsection. Deck construction started in May, 2015. It took about 10 days to complete deck panel construction.

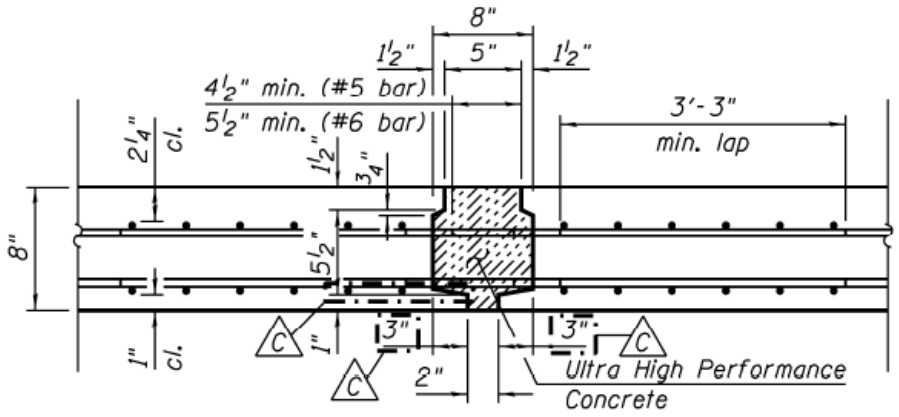

Source: Liu and Schiff (2016)

Figure 2.18: Circle Interchange Project - UHPC Transverse Joint

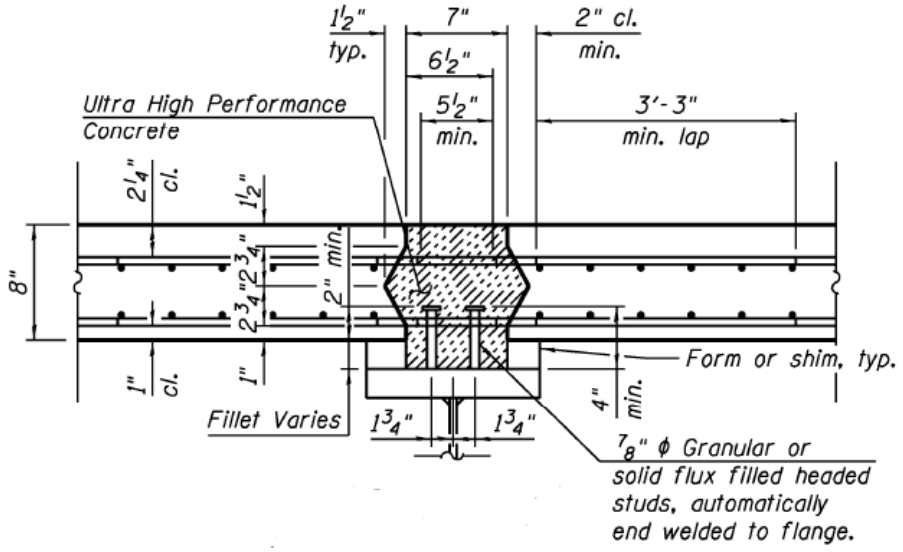

Source: Liu and Schiff (2016)

Figure 2.19: Circle Interchange Project - UHPC Longitudinal Joint

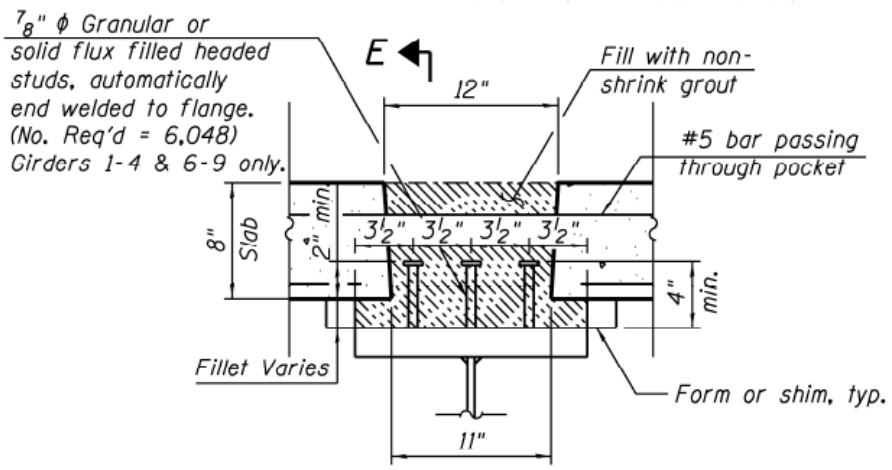

Source: Liu and Schiff (2016)

Figure 2.20: Circle Interchange Project - Shear Stud Pocket

2.2.3.1.3 UHPC in New Jersey

The Pulaski Skyway is a three and one-half mile long viaduct located in northern New Jersey that serves as a direct link to New York City via the Holland Tunnel. Because of the critical nature of the Skyway to the region's transportation, and the narrowness of the structure making it difficult to perform maintenance without impacting traffic, the New Jersey DOT (NJDOT) desired to ensure that the new bridge deck would have a service life of 75-years with little maintenance required during that time period. Consequently, plant-cast concrete deck panels with stainless steel reinforcing bars and field-cast UHPC panel closure joints were selected as the redecking system. McDonagh and Foden (2016) details the benefits of UHPC for the rehabilitation of the four-lane, 3.5-mile long Pulaski Skyway. This is discussed and summarized in the following pages.

UHPC is being used in three specific situations on the Pulaski Skyway. For the transverse panel-to-panel joints throughout the project, to fill the shear connections and haunches between the panels and the steel framing, and to fill the longitudinal joint at the median of the bridge. Each of these uses will be described and the benefits will be detailed.

The majority of transverse panel-to-panel joints on the project are 8 inches wide, as shown in Figure 2.21. The high strength of UHPC results in short reinforcing bar development and lap splice lengths, which enables the use of very narrow panel joints. This maximizes the amount of precast concrete deck and minimizes the amount of CIP material, which results in time savings. The fast cure time means that in as little as 24 hours after pouring the joints, the panels can be put in service, either for construction or service loads. The high flowability of UHPC means that there is a very low risk of unconsolidated material or air pockets in the joints. Finally, the deck panels are more likely to crack and see reinforcing bar corrosion than the joints because of high durability of UHPC combined with the high strength. This ensures that all of the durability measures incorporated into the precast panels themselves will be fully realized and not compromised by the panel joints.

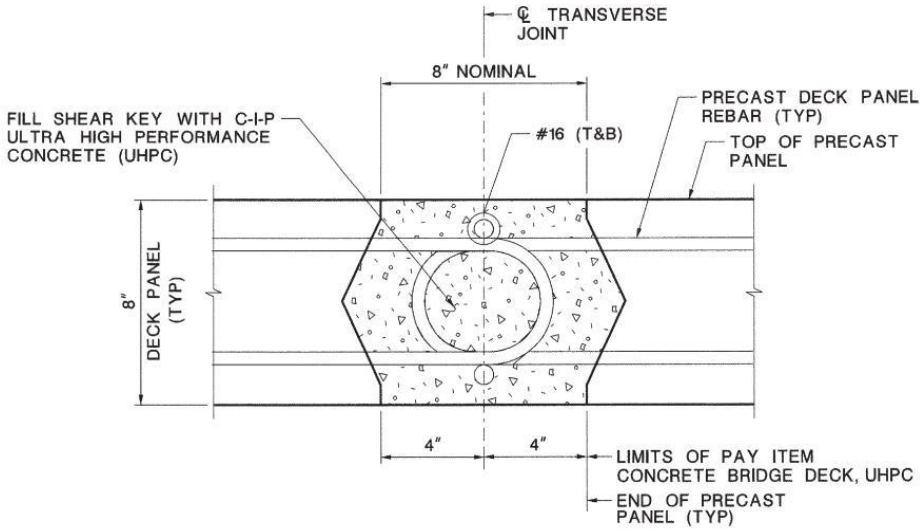

Source: McDonagh and Foden (2016)

Figure 2.21: Pulaski Skyway - Typical Transverse Joint

The typical full-depth precast concrete panel used for the new Pulaski Skyway deck has rectangular shear pockets to facilitate the connection between the panels and the shear studs, so that the panels will act compositely with the underlying steel framing. The panels are also connected to the stringers and floor beams, although rather than using rectangular block-outs, the entire length of underlying stringers and floor beams are blocked out. The haunches are beneath the panel between the pockets for the typical precast panel but integral with the continuous block-outs for the panels. These haunches and shear pockets were not originally designed to be UHPC, as can be seen in Figure 2.22 which indicates two different grouts, Type A and Type B. However, the contractor elected to use UHPC in order to combine the pocket with the haunch as well as with the transverse joints into a single pour. The high strength of UHPC in the pockets gave the designers and contractor some added flexibility over shear stud placement. Since minimum shear stud spacing criteria are typically

based on local failure of the concrete around the stud, the extremely high strength of the UHPC meant that the designers could accept tighter spacing of shear studs when conditions required it.

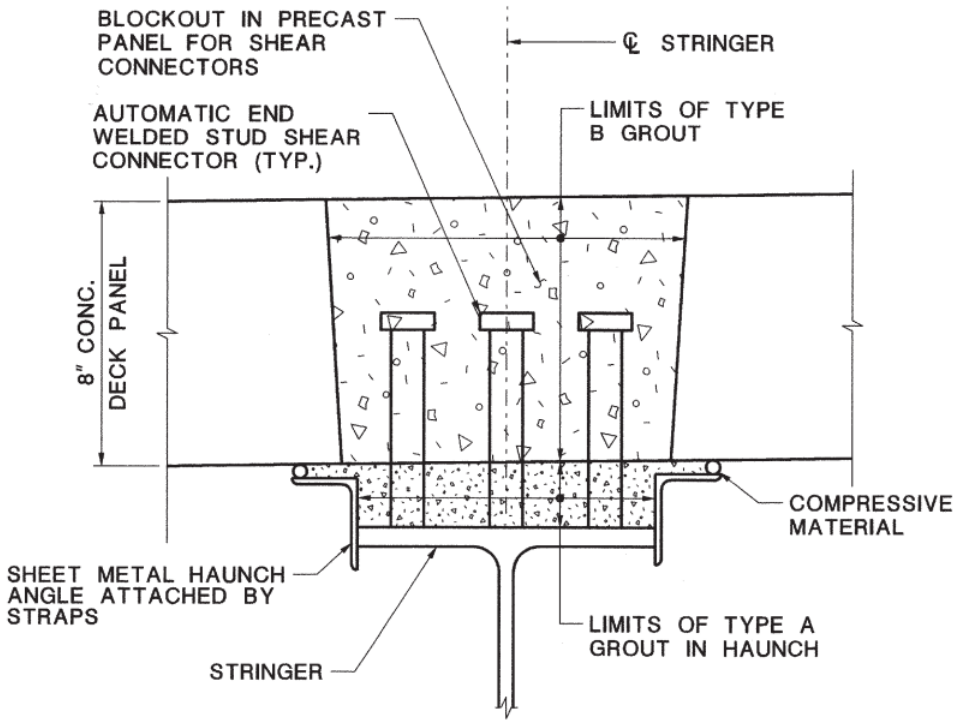

Source: McDonagh and Foden (2016)

Figure 2.22: Pulaski Skyway - Typical Shear Pocket Detail

Like the transverse joints, the fast curing time means that the panels can be put in service in as little as 24 hours. The high flowability of the UHPC was critical for the haunches, which were as thin as 5/8 inch. The high durability and low permeability of the UHPC ensures that the shear pockets and block-outs, as the transverse joints, will never become weak points in the precast deck systems (McDonagh and Foden 2016).

In order to maintain partial traffic during the redecking operation, only half of the Skyway was permitted to be closed at any time. Therefore, the presence of the existing southbound roadway carrying two lanes of traffic was a restriction for construction of the new northbound deck, which also had to be configured to carry two lanes of traffic when completed so that the existing southbound deck could be replaced with traffic on the northbound side. This arrangement meant that very little open space was available between the existing southbound deck and the new northbound deck for the extension of rebar necessary to make the two halves continuous in the final condition. This open space was typically only 10 inches to 12 inches wide. As a result, the high strength of UHPC was critical for this application. The designers detailed 6 inch long rebar hooks extending out of the edge of the northbound precast panels along the median. This provided more than enough extension to ensure that these bars would be fully developed in the UHPC median concrete. Later, the southbound precast panels, which will have the advantage of a 3 feet typical open median, will have straight rebar extending out of the panels along the median with a typical 12 inch extension. Lastly, a set of straight reinforcing bars, 2'-8" long will be placed in the median, lapping the rebar extending from both northbound and southbound panels, as shown in Figure 2.23. Thanks to the high strength of the UHPC, this rebar will have fully developed lap splices to the rebar extending from each panel, thereby ensuring that the rebar that extends transversely across the bridge is continuous between both edges of the bridge and across the median.

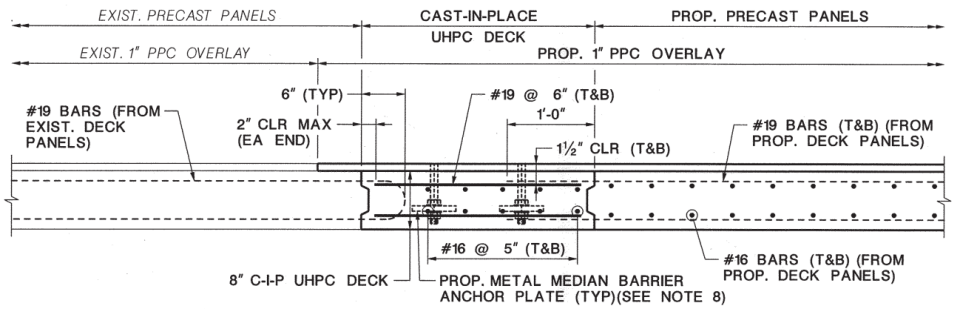

Source: McDonagh and Foden (2016)

Figure 2.23: Pulaski Skyway - Typical Median Detail

Once again, with the UHPC curing in as little as 24 hours, construction can continue and the median can be loaded rather rapidly. Furthermore, the fluidity of the UHPC eliminates any concern for air pockets or unconsolidated concrete that could be caused by the anchors for the metal median barrier that are to be cast in the median. Finally, as with the transverse panel joints, this continuous longitudinal panel joint will be stronger and more durable than the panels it is connecting, thereby ensuring the long-term durability of the entire deck system.

In conclusion, with UHPC employed for nearly all precast panel connections, the connections are no longer the weak points as they traditionally are, both in terms of strength and durability. Instead, the connections are the strongest and most durable points of the deck system, stronger and more durable than the precast deck panels with shop-cast concrete and corrosion-resistant rebar, all of which is expected to eliminate the need for major deck maintenance over the next 75 years (McDonagh and Foden 2016).

2.2.4 Current Situation

Several examples of UHPC joints were presented in this thesis and many more can be found in the literature and in the field. These completed projects prove to the industry that the technology is working and meets the needs of the users and owners. With this, codes and standards are required. Currently, structural design guides have been written in countries on every continent, except Africa and North America. In 2013, the American Concrete Institute (ACI) established committee ACI-239 'UHPC'. In 2015, the American Society of Testing and Materials (ASTM) began to write standards that recognize UHPC. In Canada, the Canadian Standards Association is writing standards on UHPC. All of these organizations are in the early stages of developing codes and standards for UHPC (Perry and Corvez 2016). With more applications and research realized with the material, more experience will be gained with the technology and with it, acceptance in the bridge design and construction industry should grow.

2.3 Modeling And Analysis Of Bridges

Various bridge components needed to be modeled and analyzed using Finite Element (FE) models to further develop the research. A review of the literature was realized to provide the research team the necessary tools to comply with these needs and requirements.

2.3.1 Modeling of Bridge Components

Different modeling practices for concrete decks and steel girders were reviewed in the literature. With this information comes different forms of the consideration of boundary conditions and constraints between the concrete deck and steel girders. These factors have to be included in the FE models to properly analyze the structures. Four papers were compared in terms of their modeling practices. The similarities and differences between the four papers will be highlighted in the discussion presented in the following pages.

2.3.1.1 Concrete and steel elements

Biggs et al. (2000) detailed the development of FE models used in order to analyze the composite action and global response of the reinforced-concrete deck and steel girders. In this model, concrete deck elements were modeled as shell elements S4R. A 4-node doubly curved thin or thick shell, reduced integration, hourglass control, finite membrane strains. Steel girder elements were modeled as three-dimensional, first order, beam elements B31OS. A 2-node linear open-section beam in space. Similarly, Klein (2006) developed separate FE models of composite bridge deck bridges with reinforced concrete slabs and longitudinal steel girders. The models varied in girder spacing to find the optimum case with the response obtained from the FE results. For both the concrete deck and the steel girders, shell elements S4R were utilized. The model is shown in Figure 2.24 in the results stage of the modeling.

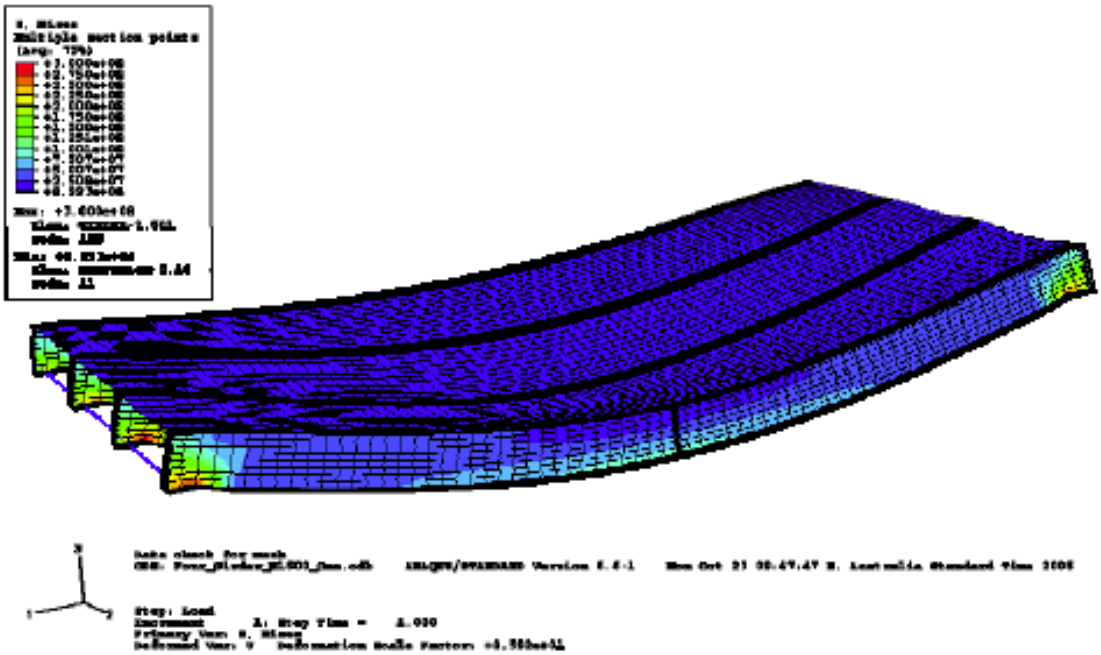

Source: Klein (2006)

Figure 2.24: Klein (2006) - Full 3-D FE Model

Bengtsson and Widén (2010) discussed the development of FE models that were realized to investigate fatigue cracks observed in the Vårby Bridge near Stockholm, Sweden. The Vårby Bridge is modeled with 3-D deformable shell elements for all elements including both the concrete deck and the steel girders. The composite bridge model is build up from four different parts for the steel details and one part representing the concrete deck. The deck is divided into a number of different strips along the bridge in order to simulate the different thicknesses of the concrete deck (Bengtsson and Widén 2010). These can be seen in Figure 2.25 and Figure 2.26. A full view of the model can be seen in Figure 2.27.

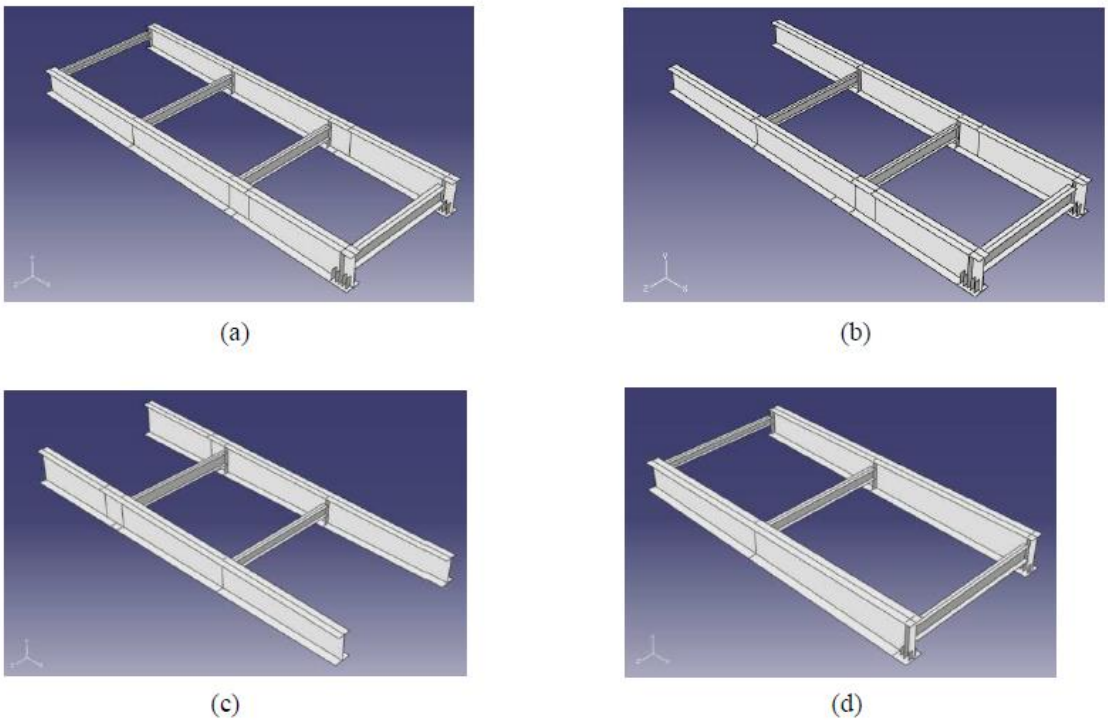

Source: Bengtsson and Widén (2010)

Figure 2.25: Vårby Bridge 2010 - Steel Girders

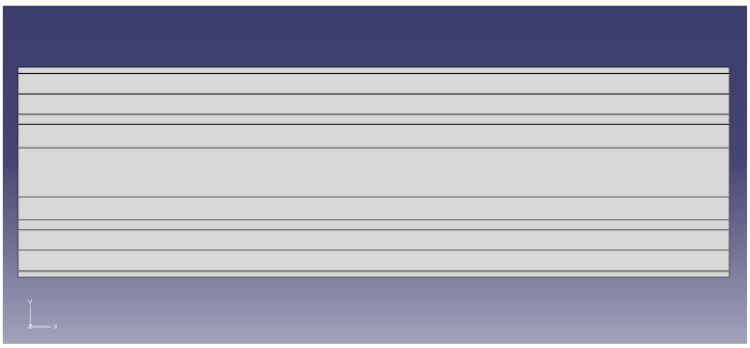

Source: Bengtsson and Widén (2010)

Figure 2.26: Vårby Bridge 2010 - Concrete Deck

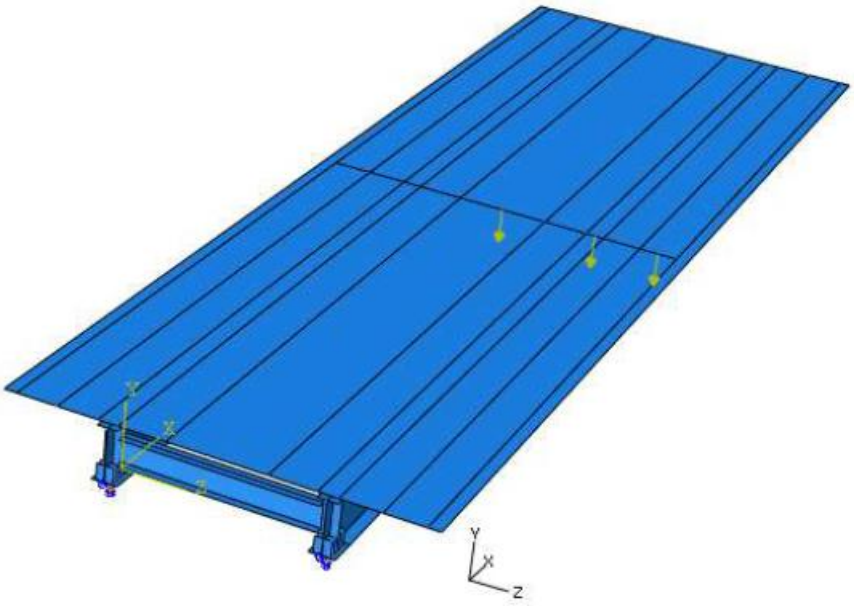

Source: Bengtsson and Widén (2010)

Figure 2.27: Vårby Bridge 2010 - Full 3-D FE Model

In further developments of the Vårby Bridge investigation, numerical analysis and model updating was in order. Keiwan and Fadi (2015) developed FE models with a wide range of parameter combinations. In these models, the concrete deck was modeled as shell elements while beam elements were used in most of the steel girders and crossbeams. Shell elements were used in the main girders. The main girders were identified as the girders that were monitored with strain gages during previous phases of the investigation. Beam elements can be seen in Figure 2.28 while the main girders can be seen in Figure 2.29.

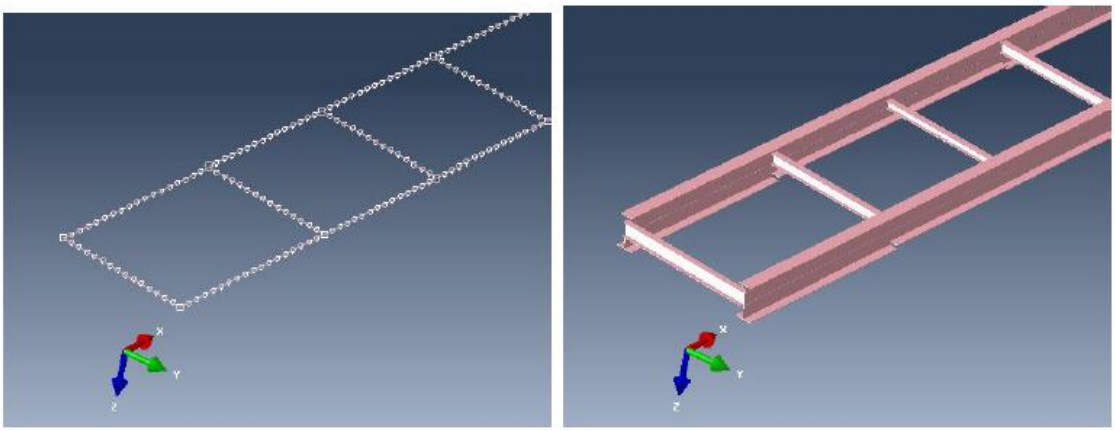

(a) *The longitudinal beams and the cross-beams modeled with beam elements with a mesh size of 500mm*

(b) *The longitudinal beams and the cross-beams modeled with beam elements and with rendered profiles.*

Source: Keiwan and Fadi (2015)

Figure 2.28: Vårby Bridge 2015 - Beam Elements

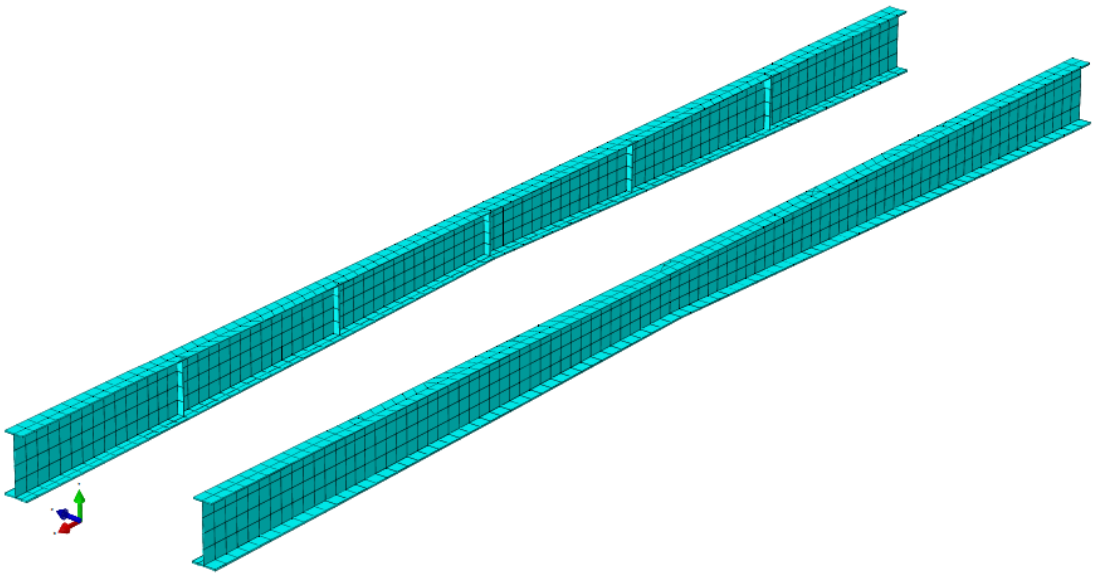

Source: Keiwan and Fadi (2015)

Figure 2.29: Vårby Bridge 2015 - Main Girders

2.3.1.2 Boundary conditions

Both Biggs et al. (2000) and Klein (2006) modeled the steel girders of the FE models as simply supported structures. One end of the structure is to be pinned while the opposite end is a pinned/sliding restraint. The nodes chosen for the boundary condition allocation were located at each end of the bottom side of the girders. One end is restrained for the three displacement directions. The opposite end is restrained in two directions instead. The nodes are not supported on the longitudinal direction of the bridge. This condition results in a sliding behavior for the simply supported condition being modeled (Klein 2006).

In the Vårby Bridge investigation, Bengtsson and Widén (2010) detailed the boundary conditions for the two main girders. There are 7 supports for the two main girders, C and D. The bridge is free to move in the longitudinal axis (x-axis) for both girders, but only for girder C in the transversal direction (z-axis). This applies for all supports, except the mid supports where the bearings are fixed for main girder D and partially fixed for main girder C (Bengtsson and Widén 2010). This is summarized in Table 2.1.

Table 2.1: Vårby Bridge 2010 - Boundary Conditions

Source: Bengtsson and Widén (2010)

	-x	-z	-y	Rotations		
C	Free	Free	Fixed	Free	Free	Free
C;mid support	Fixed	Free	Fixed	Free	Free	Free
D	Free	Fixed	Fixed	Free	Free	Free
D; mid support	Fixed	Fixed	Fixed	Free	Free	Free

Just like Klein (2006), the boundary conditions are attached to one node located directly under the web in the main girders and in line with the vertical web stiffeners. To represent the bearings in a reasonable way the horizontal plate under the vertical support stiffeners in the bottom flange are free to rotate around the node using a Multi-point constraint (MPC) (Bengtsson and Widén 2010). This is shown in Figure 2.30.

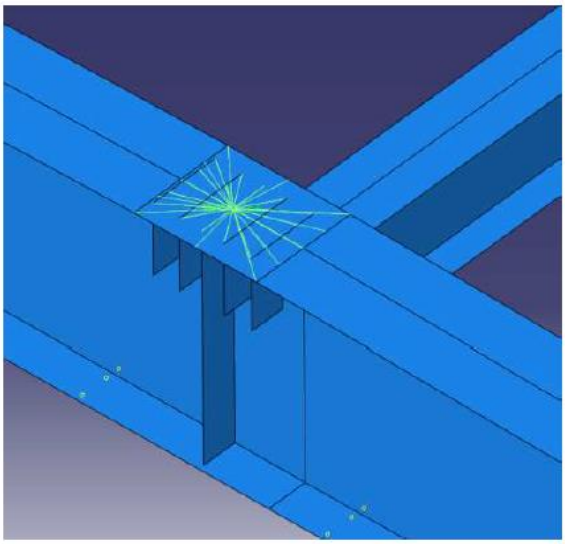

Source: Bengtsson and Widén (2010)

Figure 2.30: Vårby Bridge 2010 - Boundary Conditions MPC Link

Keiwan and Fadi (2015) detailed the boundary conditions in further developments of the Vårby Bridge investigation. It can be noticed that boundary conditions were kept intact from the previously discussed. The boundary conditions depend mostly on the bearing pads used in a particular bridge. Since it is the same bridge under investigation, bearing pads remained constant during the time of both research stages. Therefore, boundary conditions stayed the same.

2.3.1.3 Constrains

Different constraints between the concrete deck and steel girders were used across the four papers. Even the two papers on the Vårby Bridge investigation implemented different constraints. Shear studs are presented in most, if not all, steel girders bridges. Elongation of these studs may happen during uplift loads of the bridge deck since the shear studs are embedded into the concrete. The studs would prevent the lift of the deck from the top flange of the girders. Different ways of modeling this constraint were seen across the papers. These are detailed below.

Biggs et al. (2000) modeled the constraints between the concrete deck and steel girders by employing MPCs similar to the one shown in Figure 2.30. On the other hand, Klein (2006) used tie constraints assuming full interaction between the two elements and transference of all degrees of freedom.

Similarly to Klein (2006), Bengtsson and Widén (2010) also used tie constraints between the concrete deck and the steel girders in the FE models of the Vårby Bridge investigation. In future phases, Keiwan and Fadi (2015) employed very different constraints on multiple elements of the FE model. Since the main girders were modeled as a combination of beam elements and shell elements, these different elements had to be connected for a continuous beam behavior. MPCs were employed to connect the two. MPCs were also used to connect the crossbeams to the main girders. Web stiffeners were modeled in the main girders and were used as the source of the MPCs. Both applications of MPCs can be seen in Figure 2.31 and Figure 2.32.

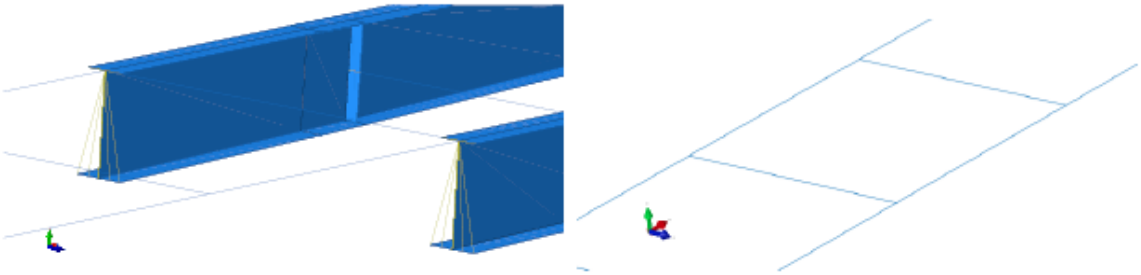

(a) *Showing the multiple point constraint connecting the beam elements to the shell elements of the longitudinal beams.*

(b) *Beam elements where main girders and crossbeams are modelled in the same part, ensuring full constraint.*

Source: Keiwan and Fadi (2015)

Figure 2.31: Vårby Bridge 2015 - Main Girders Constraints

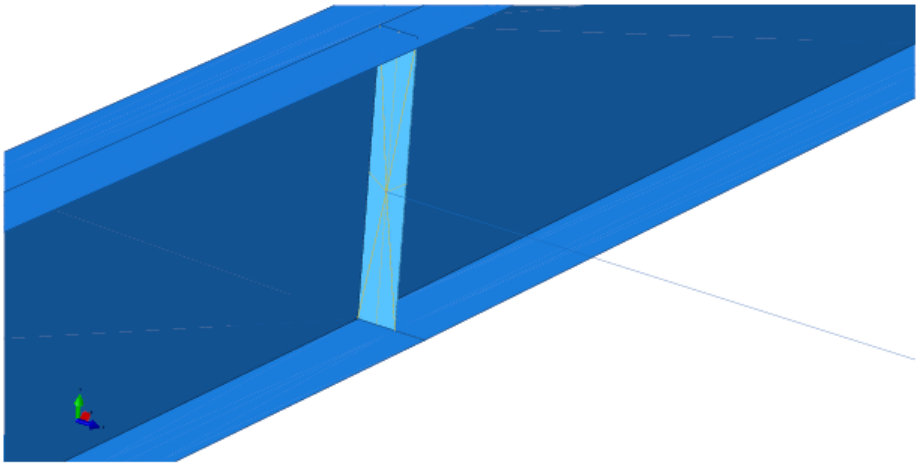

Source: Keiwan and Fadi (2015)

Figure 2.32: Vårby Bridge 2015 - Crossbeam Constraints

The interaction between the concrete deck and the steel girders was modified from the previous phase of the Vårby Bridge investigation. Previously, these two elements were connected with a tie constraint between the bottom surface of the concrete deck and the top face of the top flanges of the main steel girders. In this phase of the investigation, the connection was modeled with linear axial springs. These linear axial springs connect the main steel girder and the concrete deck. The springs are modeled by using two different approaches; Connectors (CONN3D2) and Engineering Springs (SPRING2). The springs can be seen alongside the connectors (CONN3D2) approach in Figure 2.33.

Keiwan and Fadi (2015) provides an overview of both approaches. This explanation is shown below.

"When using the SPRING2 approach in Abaqus, the springs are modeled in such a way that they are very stiff in the y and z direction so that the only action that is active is the slip action between the steel and concrete, i.e. the stiffness of the spring in the x direction." (Keiwan and Fadi 2015)

"The other approach is to use connector elements, CONN3D2, where wires are created between the mesh-nodes of the bridge deck and the longitudinal beams. The wires are then assigned different properties, having rigid connections in the y and z direction and a defined stiffness in the x direction." (Keiwan and Fadi 2015).

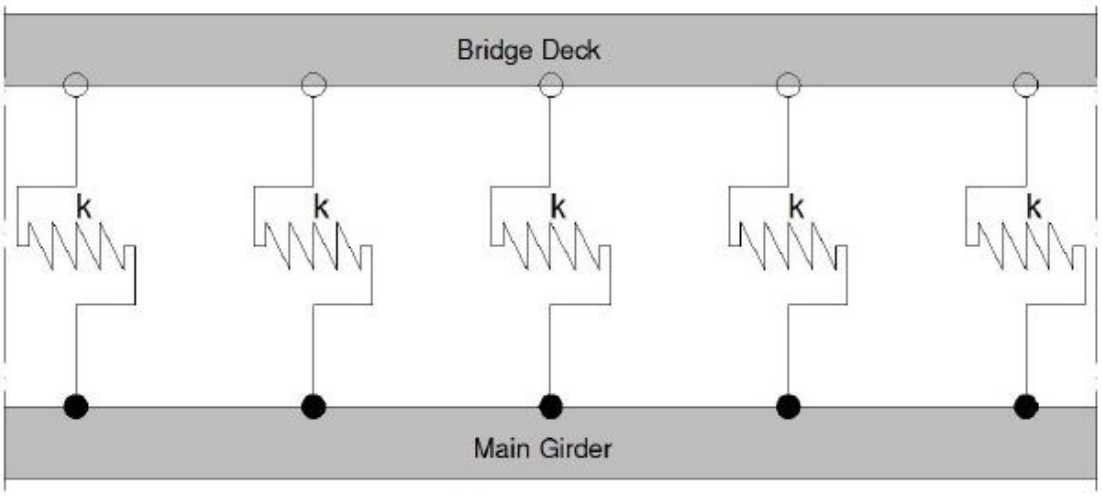

(a) *Axial springs in theory.*

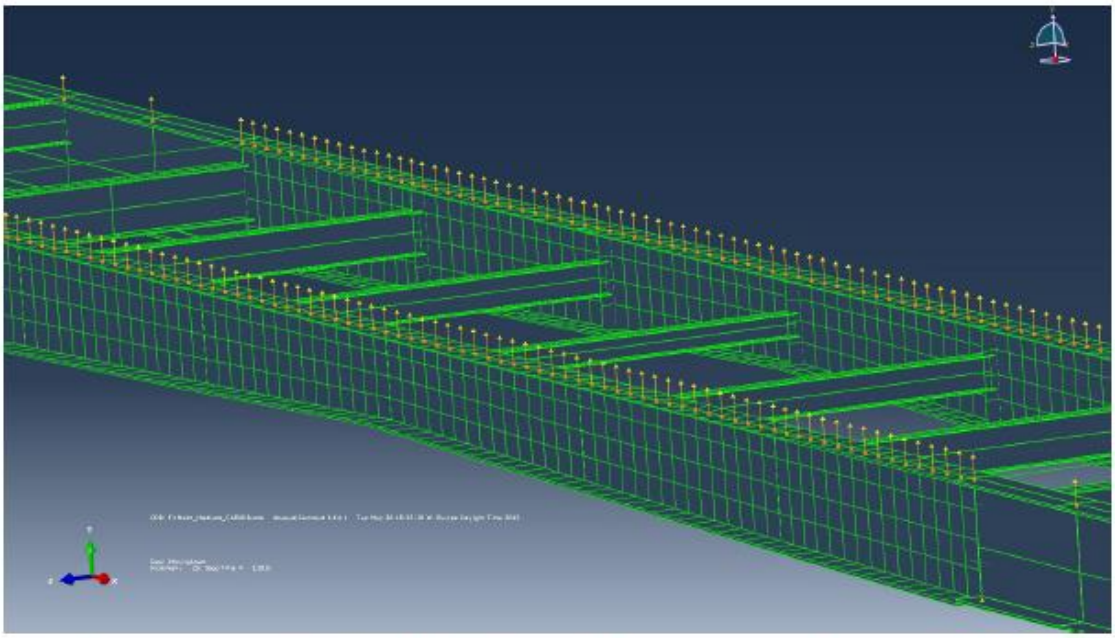

(b) *Spring connectors (CONN3D2) assigned to mesh nodes along the bridge deck.*

Source: Keiwan and Fadi (2015)

Figure 2.33: Vårby Bridge 2015 - Deck and Main Girder Constraints

2.3.2 Modeling of Approach Slab and Soil Support

To further develop the deck over backwall concept, FE models of full-scale bridges had to be modified to factor in the possible effects of the concept on the existing structures. The concept includes an approach slab extending from the existing bridge deck on one end to the roadway pavement on the other. A review on the literature of approach slab modeling was realized.

Rajek (2010) used FE models for the analysis of possible causes of approach slab deterioration. The model included the bridge roadway, approach slab, abutment, and fill as they all related to approach slab deterioration. Parametric studies were performed to determine the influential parameters that contribute to the deterioration of the approach slab. Rajek (2010) lists the parameters as void geometry, abutment height, approach slab length, soil stiffness, concrete stiffness, and joint restrictions (the joint between the roadway and approach slab).

The approach slab incorporated in the model was made to conform to Wisconsin DOT (WisDOT) standard specifications. WisDOT specifies a length of 15'-8" and a thickness of 1 foot for their standard approach slabs (Rajek 2010). The width of the approach slab was the minimum lane width (12 feet) as defined by the 2007 AASHTO Specifications. Rajek (2010) explains that friction was the primary constraint utilized in the model to control all concrete to concrete and soil-to-concrete interactions. The coefficient of friction used to define all concrete-to-concrete interactions was taken from section 11.6.4.3 of ACI 318-08

Plane strain and plane stress elements were used in the model. Plane strain quadrilateral quadratic elements with reduced integration were used for the soil region (Helwany 2007). Plane stress quadrilateral quadratic elements with reduced integration were used for all concrete parts.

A section view of the model is shown in Figure 2.34 with all the pertinent elements denominated.

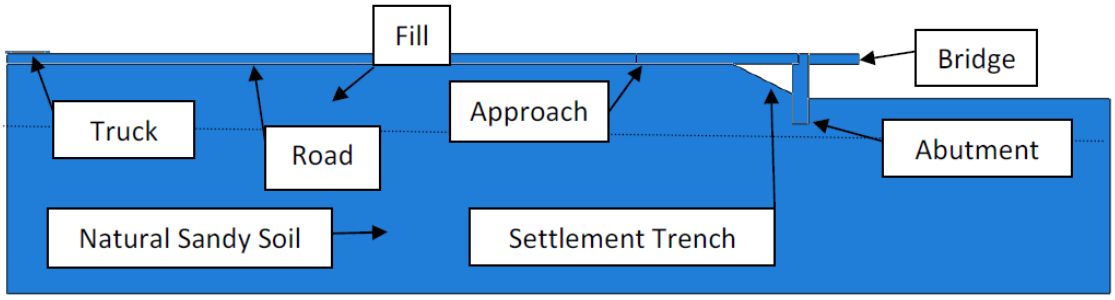

Source: Rajek (2010)

Figure 2.34: Rajek (2010) - Section View

A vertical displacement restraint was implemented at the bottom of the soil to simulate very stiff natural soils or bedrock at depth. Horizontal displacement restraints were placed at the sides of the soil. The bottom of the abutment was fixed to simulate a rigid pile and pile connection (Rajek 2010). These can be seen in Figure 2.35.

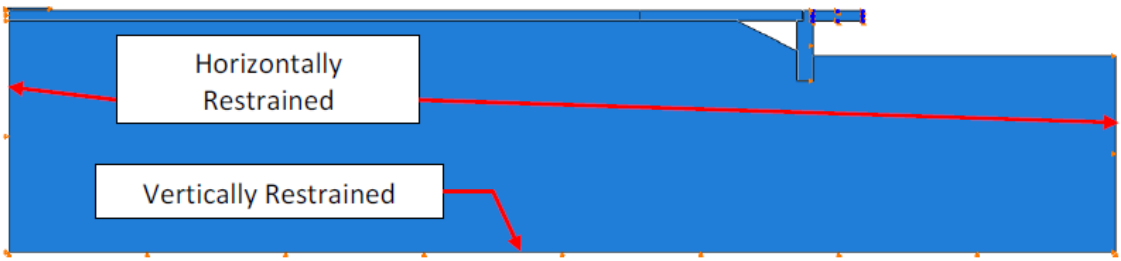

Source: Rajek (2010)

Figure 2.35: Rajek (2010) - Boundary Conditions

The soil was modeled as a compacted sandy soil using the elastoplastic Mohr-Coulomb material model within Abaqus. The sand emulated in the model was modeled after Portage Sand, as discussed by Schuettpelz et al. (2010). Soil properties are shown in Table 2.2.

Table 2.2: Rajek (2010) - Soil Properties

Source: Rajek (2010)

Classification	Mass Density (lbm/ft^3)	Young's Modulus (psi)	Poisson's Ratio	Friction Angle (deg)	Dilation Angle (deg)	ϕ'_{cv} (deg)	Meridional Eccentricity	Cohesion (psi)
Stiff	129	14500	0.3	45	12	35	0.1	0.145
Moderately Stiff	124	8700	0.3	37	5.6	32.5	0.1	0.145
Loose	121	1450	0.3	30	0	30	0.1	0.145

The geometry of the settlement trench formed under the approach slab was varied in the parametric study. The settlement trench geometries throughout the parametric study are shown in Figure 2.36. These are in general agreement with observations of Cosgrove and Lehane (2003).

It is explained that “while standard practice dictates that the angle of the settlement trench be equal to the constant volume friction angle (32.5 degrees), the model utilized for this study set the angle of the settlement trench at approximately 26.5 degrees. This was assumed accurate as the saturation of the soil and water pressure buildup within the soil would cause an increase in pore pressures. The effective stress of the soil would decrease as a result of the increase in pore pressure.” (Rajek 2010)

X (ft)	Y (ft)
0	0
2	1
4	2
6	3
8	4

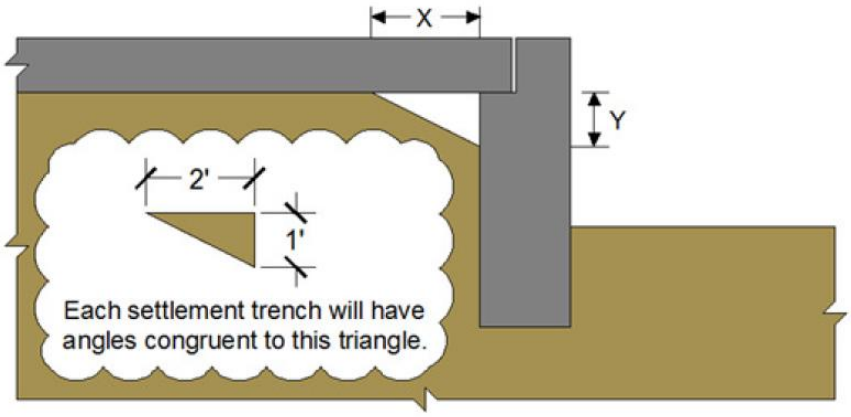

Source: Rajek (2010)

Figure 2.36: Rajek (2010) - Trench Geometry

CHAPTER 3. JOINT DETAILING

Further development of the deck over backwall concept will be presented in this chapter. The Iowa DOT realized a joint detailing taking into account the various options proposed by the research team and other factors.

The research team assisted the Iowa DOT in developing a plan that conforms to the deck over backwall concept and the Iowa DOT Bridge Approach Standards. The research team proposed various options to the Iowa DOT with numerous factors and variations being taken into account.

3.1 Research Team Options

The research team identified numerous factors that were considered while developing their options. These factors included the reinforcing steel continuity requirements, connection between new precast or CIP panel and the existing bridge deck, joint between new precast or CIP panel and backwall, concrete materials for new approach slab and sleeper slab, etc.

For all approach slab details in the proposed options, the research team used the Iowa DOT Bridge Approach Standards. The corresponding approach slab BR-205, a double reinforced 12” approach slab, can be seen in Figure 3.1.

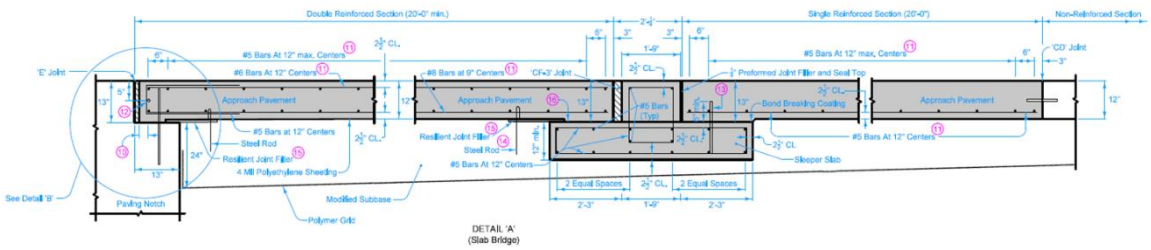

Source: Iowa DOT Office of Design (2018)

Figure 3.1: Iowa DOT Bridge Approach Standards

Double Reinforced 12" Approach - Slab Bridge

Three main options were developed by the research team. A CIP approach slab with a dowel reinforcement joint between the new approach slab and the existing bridge deck. A precast approach slab with a UHPC joint and a dowel reinforcement joint between the new approach slab and the existing bridge deck. The third option is a hybrid of the first and second options. A precast form slab rests on the supporting soil with a CIP approach slab. Just as the first option, it includes a dowel reinforcement joint between the new approach slab and the existing bridge deck. All three options are supported by a sleeper slab in the opposite end of the abutment interface. A full view of the abutment interface with the CIP options is shown in Figure 3.2. All three options are shown in Figure 3.3.

In discussions between the research team and the Iowa DOT, various elements of these options saw the possibility of alteration. For example, the dowel reinforcement joint in the first and third options could be replaced by continuity of the reinforcing steel of the exiting bridge deck. The concrete in the bridge deck area could be removed through hydrodemolition while preserving both the top and bottom longitudinal reinforcement bars of the existing bridge deck.

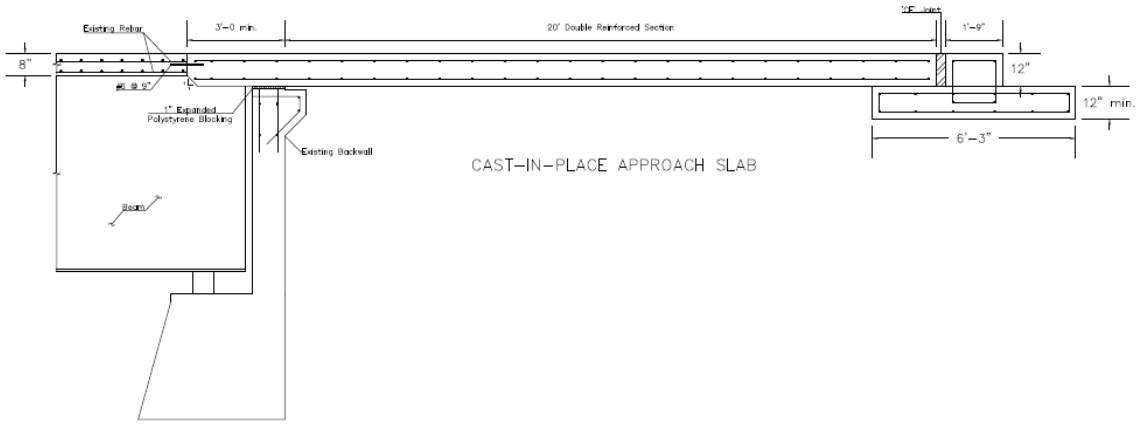

Figure 3.2: Detailing Options - Full View of Cast-In-Place Option

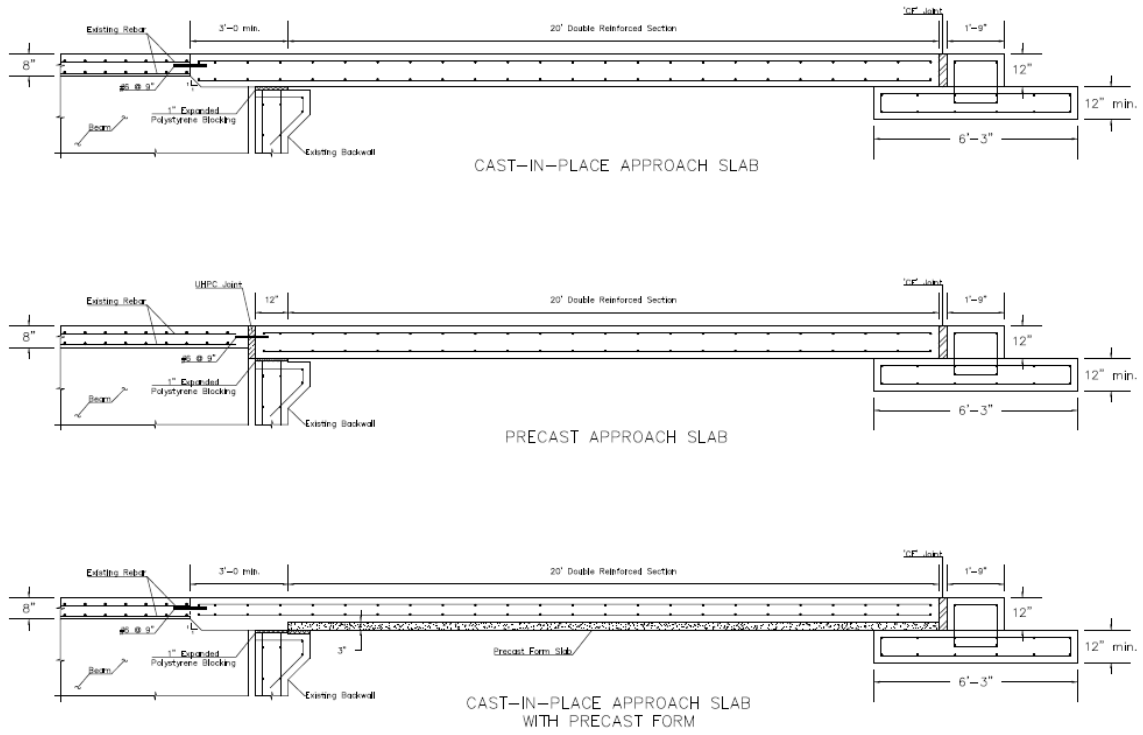

Figure 3.3: Detailing Options

In discussions between the research team and the Iowa DOT, the option of using micropiles in the sleeper slab was brought up and considered. The reasoning behind the possibility of implementing micropiles in the sleeper slab is that if settlement occurs in the sleeper slab interface, the approach slab will undergo unwanted deflection. With this deflection, negative moment and rotation will be transferred to the abutment interface and the existing bridge deck. The use of micropiles to support the sleeper slab would combat these concerns by minimizing the settlement of the sleeper slab and, therefore, the possible deflection of the approach slab. A joint detailing was developed by the research team for this option using the CIP option shown in Figure 3.3. The micropiles option can be seen in Figure 3.4. Further soil study would have to be conducted if this option is to be implemented to provide the necessary micropile detailing in terms of which sections to be used and for how deep the micropiles would be driven. In addition, the number of micropiles and their arrangements would have to be studied and not necessarily as shown in the figure.

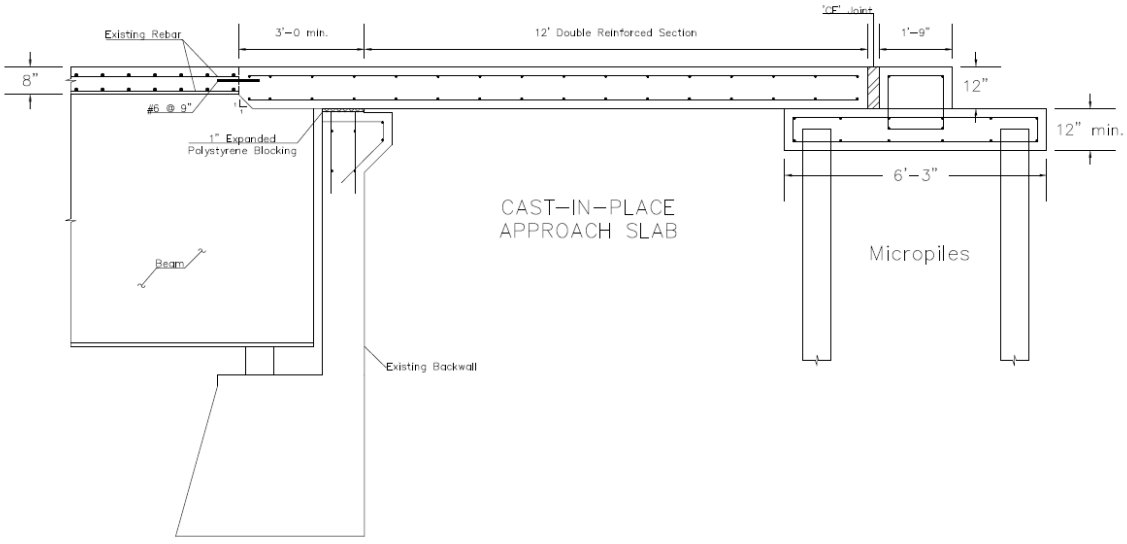

Figure 3.4: Detailing Options - Micropiles Option

3.2 Iowa Department of Transportation Joint Detailing

The Iowa DOT developed their own joint detailing of the deck over backwall concept considering the various options presented by the research team, the discussions that took place with the research team over early development of their joint, as shown in Figure 3.5. The Iowa DOT considered their own construction practices, and their own experiences and preferences to further develop their joint. The joint detailing is shown in Figure 3.6, Figure 3.7, Figure 3.8, and Figure 3.9. These figures show the concrete removal process, a section view, the saw cut and seal detailing, and a plan view respectively.

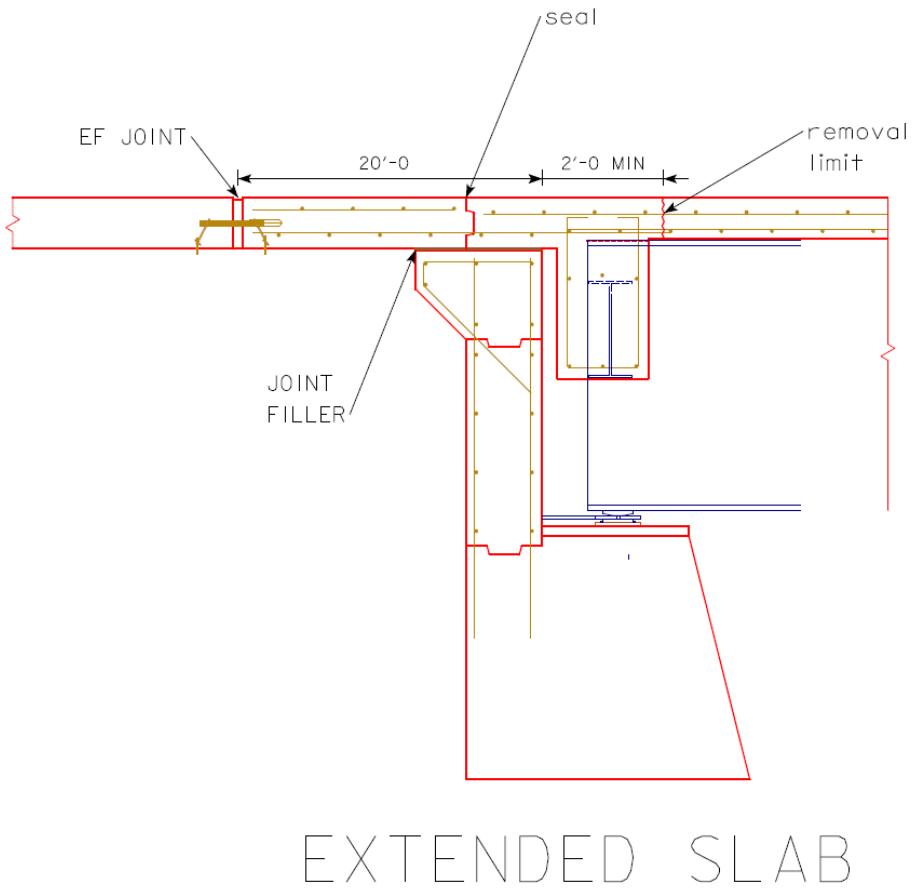

Source: Iowa DOT

Figure 3.5: Iowa DOT Joint - Preliminary Detailing

It can be seen in the figure below that the Iowa DOT chose to go with the option of having steel continuity of the reinforcing steel of the exiting bridge deck. The concrete in the bridge deck area should be removed while preserving both the top and bottom longitudinal reinforcement bars of the existing bridge deck. This is clearly stated in the figure.

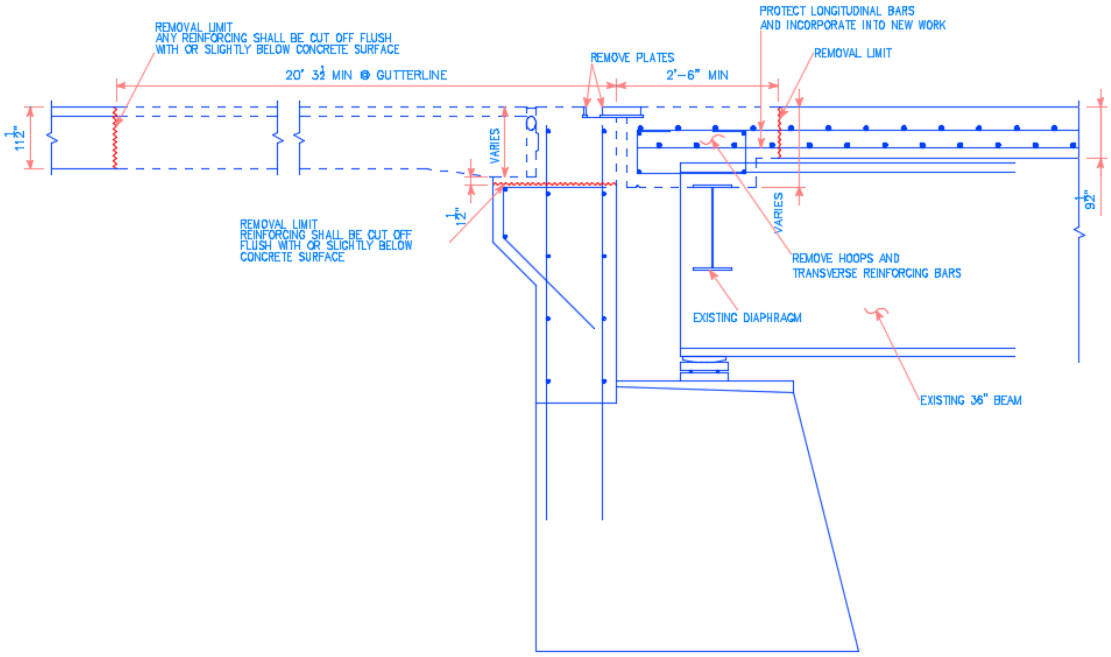

Source: Iowa DOT

Figure 3.6: Iowa DOT Joint - Concrete Removal Process

The detailing of the reinforcement bars is provided in Figure 3.7. Detailing of the curb and the new approach slab is also shown. A joint is provided 15 feet from the abutment stud wall. In addition, no sleeper slab or connection is provided at the opposite end of the abutment interface. Possible options for these two joints include the sleeper slab shown in the research team options, a subdrain, or Iowa DOT's own EF joint, CF joint, or CD joint. A combination of those previously mentioned can also be implemented, for example a CF joint and a sleeper slab.

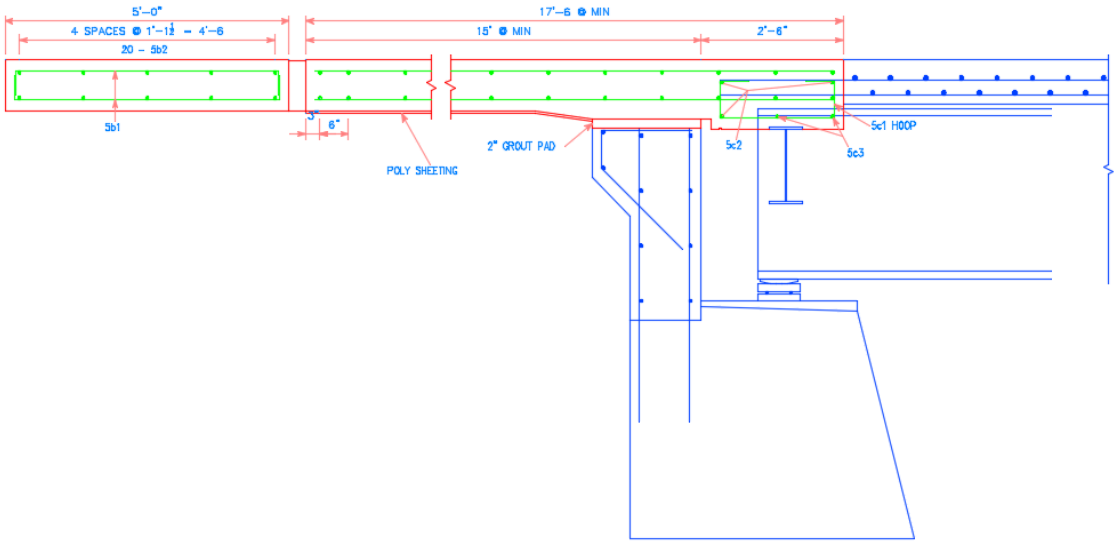

Source: Iowa DOT

Figure 3.7: Iowa DOT Joint - Section View

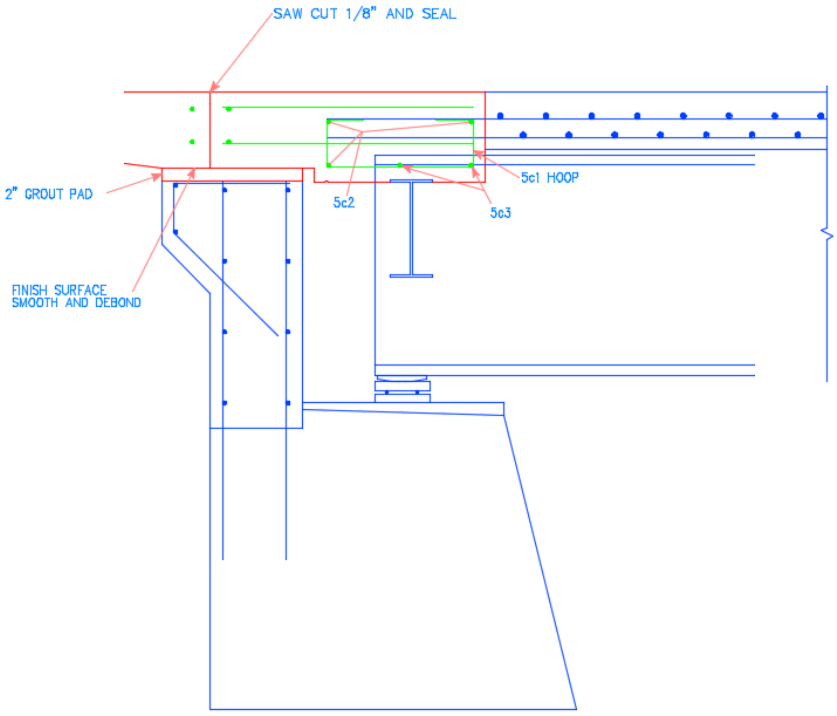

Source: Iowa DOT

Figure 3.8: Iowa DOT Joint - Saw Cut and Seal Detailing

Figure 3.8 details the option of a saw cut and seal joint at the abutment interface. This joint would aid the performance of the deck over backwall concept should the approach slab deflect a considerable amount. This deflection would transfer negative moments and rotation into the existing bridge deck. The saw cut and seal joint would prevent these moments from fully transferring into the existing bridge deck and prevent rotation from affecting driving comfort.

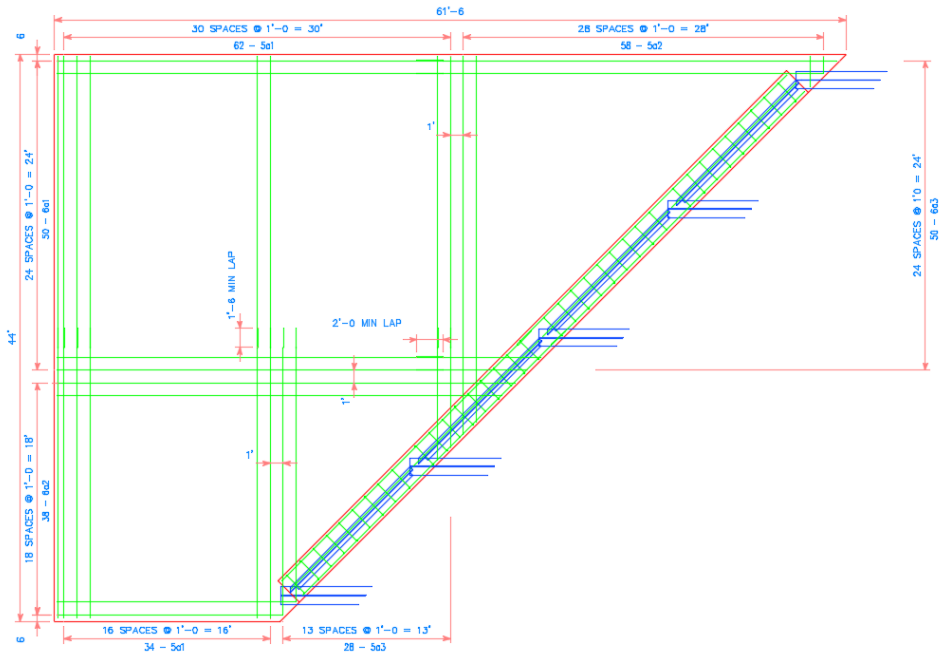

Source: Iowa DOT

Figure 3.9: Iowa DOT Joint - Plan View

The figure above shows a plan view of the joint developed by the Iowa DOT. Reinforcement bars details can be seen in the figure. All reinforcement bars in both the longitudinal and transverse direction are shown in the detailing. Spacing between reinforcement bars is shown as 1 foot for all directions. Splice lengths are specified in both the longitudinal and transverse directions.

CHAPTER 4. FINITE ELEMENT MODELING AND ANALYSIS

Two case study bridges were worked on throughout the course of the research. The first bridge is located on I-35 (Northbound, 049310) and I-35 (Southbound, 049320) 3.3 miles South of SR E-18, over Bear Creek, Story County. The second bridge is located in IA-330/Marshalltown Blvd 2.5 miles Southwest of Melbourne, over North Skunk River, Marshall County. Here in after, these bridges will be denoted as the Story County bridge and the Marshall County bridge.

The selected bridges were analyzed using FE models that were developed to model the conditions of the bridges presented in the original drawing plans. The information for the FE analyses was obtained from as-built drawing, design documents and expansion joint specifications shown in Appendix A and Appendix B for the Story County bridge and the Marshall County bridge respectively.

For the analysis, AASHTO Specifications were followed to evaluate the behavior of the bridges. The analysis results will eventually be used to identify critical conditions to guide the development of a plan for post-construction testing of the structures, and to correlate field responses and predictions. Subsequently, the models may be calibrated using the future field test results in order to increase their accuracy. The verification of the models will permit their confident use for designing expansion joints in the future.

4.1 Story County Bridge

A full 3-D model was realized in Abaqus FEA for the bridge under investigation. This model includes a concrete bridge deck supported by welded plate steel girders and diaphragms that rest on abutments at the ends and piers. A full 3-D model can be seen in Figure 4.1 with a sectional view in Figure 4.2. Constraints, boundary conditions, and other elements had to be assigned in the model. Also, loading conditions were also incorporated in the model from self-weight to surface weathering to truck loading.

An 8 inch by 338 feet bridge deck was modeled as a C3D8R element, which is an 8-nodeelement with linear brick, reduced integration, hourglass control. In addition, C3D8R was utilized for all concrete parts in the model, including the abutments and piers with their corresponding column and beam dimensions. The steel superstructure is composed of welded plate steel girders and transversal diaphragms at the ends and over the piers. The web and flanges of the welded plate girders as well as the diaphragms were modeled as S4R, 4-node doubly curved thin or thick shell with reduced integration, hourglass control, and finite membrane strains. For the flanges of the welded plate girders, width and thickness were modeled per the drawing plans. All steel superstructure was merged together. This can be appreciated in Figure 4.3.

This model underwent an elastic analysis. Only mass density and elastic properties like Young's modulus and Poisson's ratio were needed for to realize the analysis successfully. The mass density utilized for the concrete and steel derived from their specific weight of 150 lb/ft^3 and 490 lb/ft^3 respectively. As for the Young's modulus and Poisson's ratio, 3,718 ksi and 0.15 was utilized for concrete and 29,000 ksi and 0.3 for the steel. In addition, the coefficient of thermal expansion for both concrete and steel was determined to be 5.5E-6 1/°F and 6.5E-6 1/°F respectively.

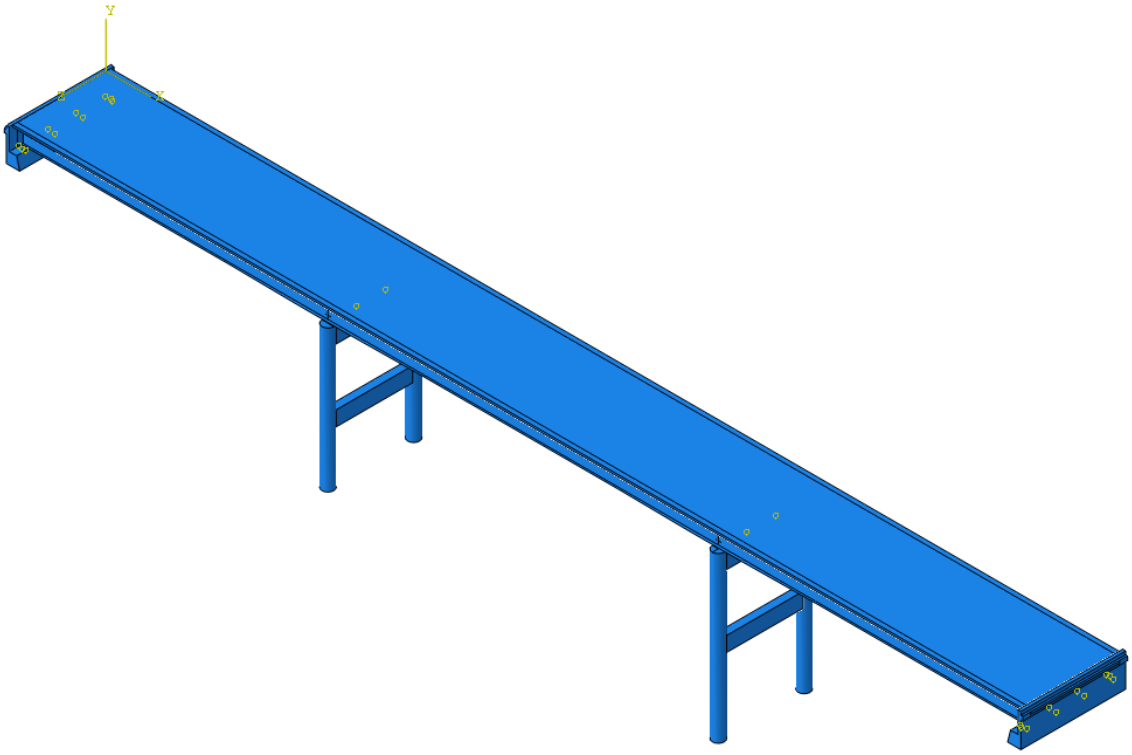

Figure 4.1: Story - Full 3-D FE Model

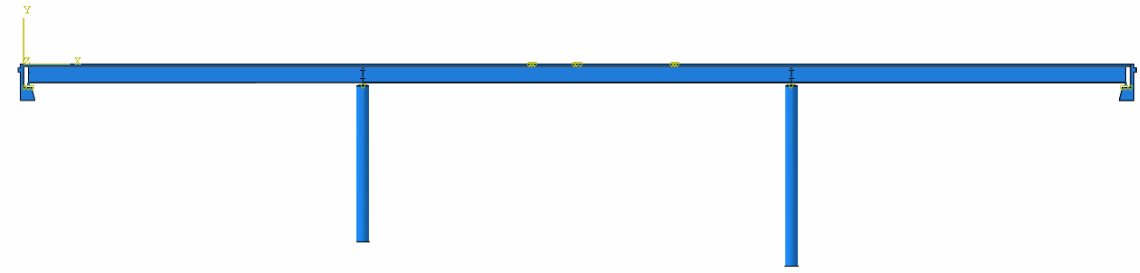

Figure 4.2: Story - Section View

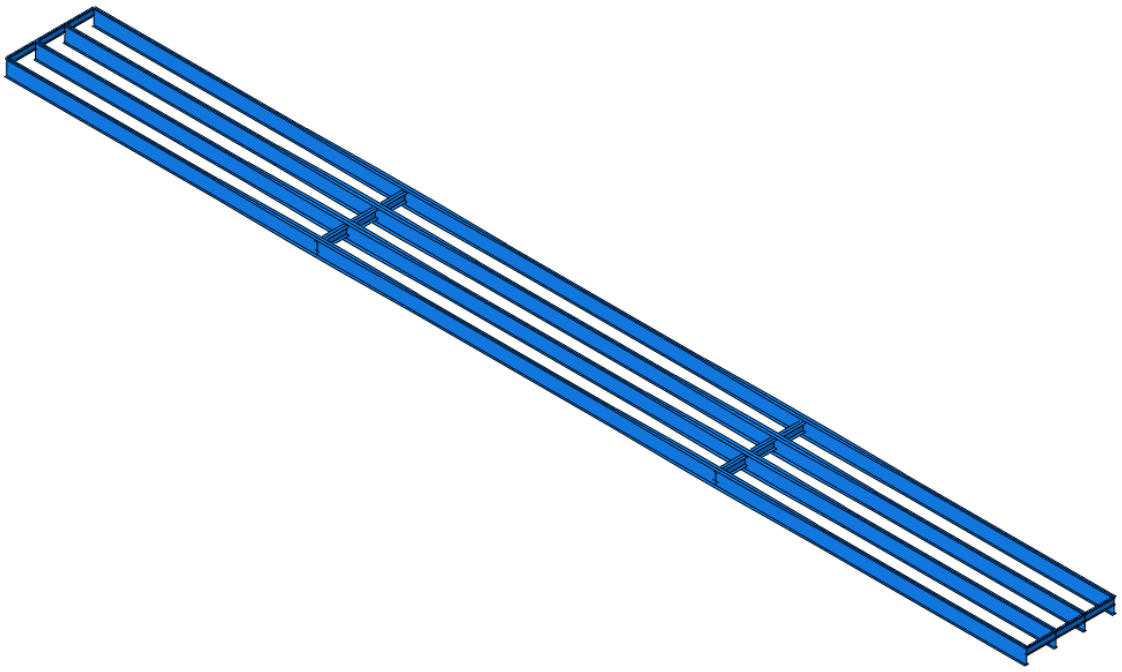

Figure 4.3: Story - Steel Superstructure

Boundary conditions were assigned on the abutment's vertical and horizontal faces that are in the direction of the supporting soil. Vertical faces have horizontal constraints and, vice versa, horizontal faces have vertical constraints. A fixed boundary condition was assigned to the bottom face of the pier columns simulating the foundations that rest under the top soil. Boundary conditions can be seen in Figure 4.4 marked in red at the abutment and on the bottom face of the pier. Tie constraints were assigned between the beams and columns of the piers. Tie constraints were also assigned between the top flanges of all the welded plate girders and the bottom surface of the bridge deck. Connection wires were utilized between the steel girders and the abutments and piers to simulate the rocker and fixed bearings at the points of interest. All reaction values presented in the following pages correspond to these connection wires.

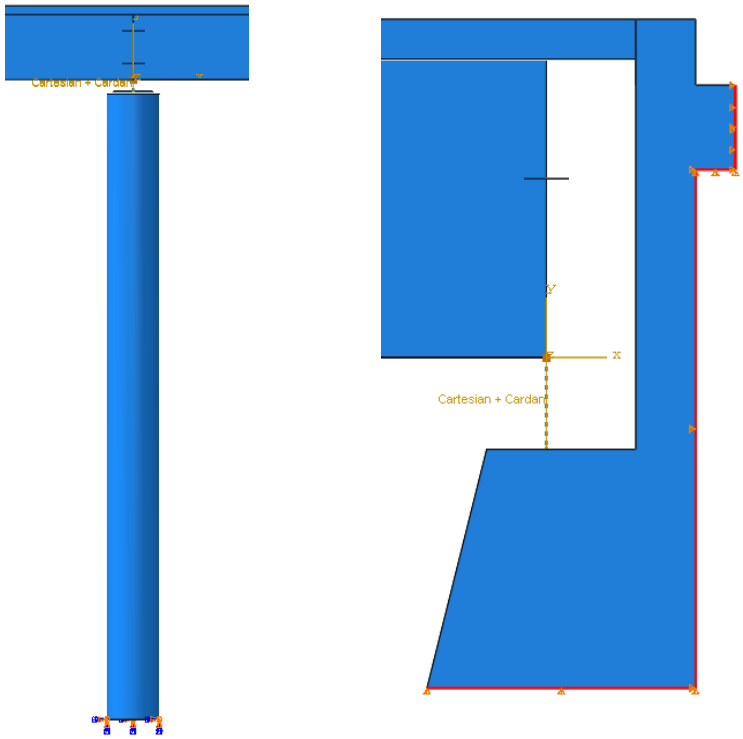

Figure 4.4: Story - Boundary Conditions

4.1.1 Convergence Study

The model was trialed on numerous occasions with different meshing sizes. Results stabilized at an approximate meshing size of 5 inches. A meshing size of 4 inches was determined to be the most effective for the model at this point. The time elapsed to complete the analysis for a meshing size of 3 inches was almost five times as much as the time elapsed for a meshing size of 4 inches. This can be recognized in Table 4.1. The time elapsed for each trial in shown for all mesh sizes along with their deflection values. A graph of the different values that were trialed with their results can be observed in Figure 4.5. With a mesh size of 4 inches, the structure was modeled using 332,627 elements, 437,973 nodes, and 1,663,341 variables.

Table 4.1: Story - Mesh Convergence Study

Mesh Size (in)	Max Deflection at Midspan (in)	Time Elapsed (s)
8	1.242	108.4
6	1.248	178.6
5	1.035	416.1
4.5	1.031	552
4	1.032	785.2
3.5	1.031	1056.6
3	1.031	4641

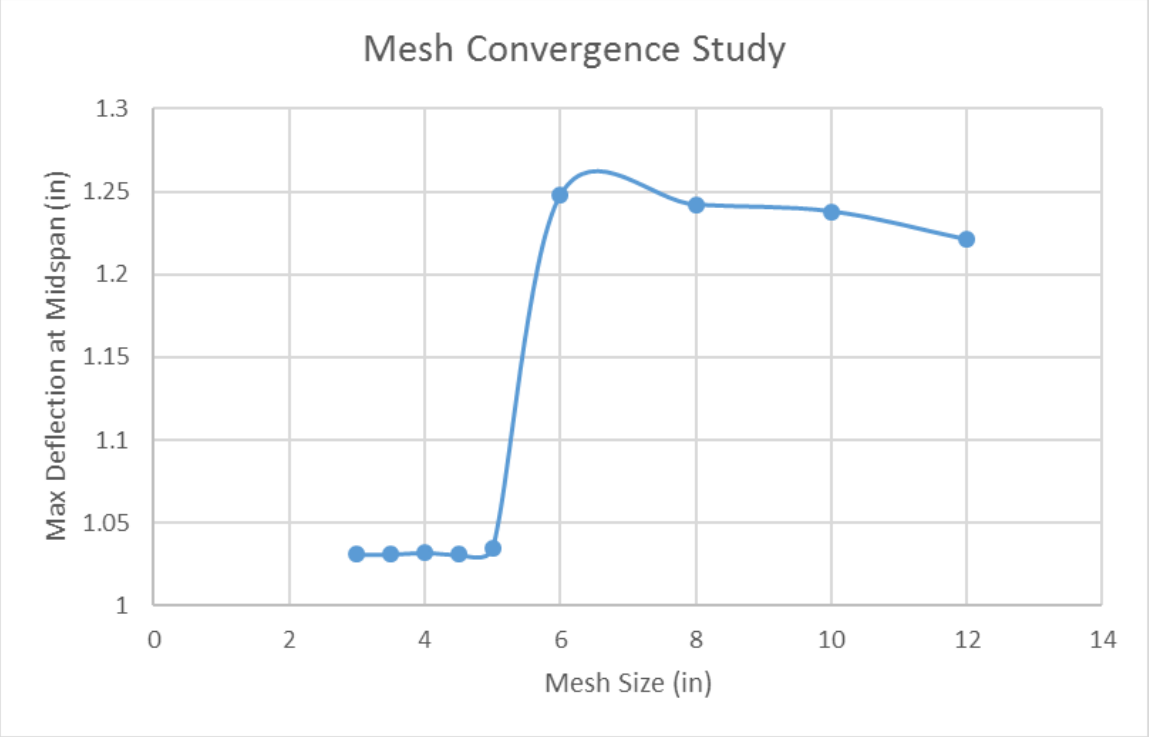

Figure 4.5: Story - Mesh Convergence Study

4.1.2 Validation With Original Plans

The information needed to realize the FE model and analysis for the Story County bridge was obtained from its original drawing plans. Abutment and pier reactions can be observed in such plans and in Table 4.2. These reactions were the source of comparison for the results obtained from the FE analysis shown in the next section. It is important to mention that the FE model does not fully incorporate all the elements shown in the plans but includes the most pertinent ones.

Table 4.2: Story - Abutment and Pier Reactions from the Drawing Plans

Source: Story County Bridge Plans

	Abutment Reactions (kips)		Pier Reactions (kips)	
	Exterior	Interior	Exterior	Interior
DL #1	31	47.1	113.4	172.1
DL #2	21.5	4.5	74.5	15.5
ULL	-	-	67	78
CLL	-	-	19.6	22.8
HS-20-16	48.2	56.3	-	-
Impact	10.6	12.3	17.9	20.8
Total	111.3	120.2	292.4	309.2

Dead load #1 includes weight of slab, girders, and diaphragms.

Dead Load #2 includes weight of curbs, rail, and future wearing surface.

Notice that an HS-20-16 truck load is shown in the table above. References to this truck load were not found in the literature. Therefore, the truck load was assumed to be an HS-20-44 truck loading condition and it was allocated in the same manner as the rest in the FE model. Even though this truck load was assumed to be HS-20-44, it is referred to as HS-20-16 in the discussion.

4.1.2.1 Dead load reactions and deflection

Self-weight was included in the whole model. A surface weathering loading condition of 19 lb/ft^2 over the roadway was also added. Curb loading on 1.5 feet of the edges was added as a surface area simulating a 2'8" by 1 feet area of concrete by the entire length of the bridge deck. Results for dead load deflection and a comparative loading conditions table can be appreciated in Figure 5 and Table 2.

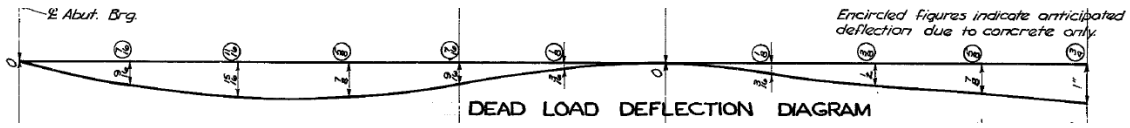

Source: Story County Bridge Plans

Figure 4.6: Story - Anticipated Dead Load Deflection

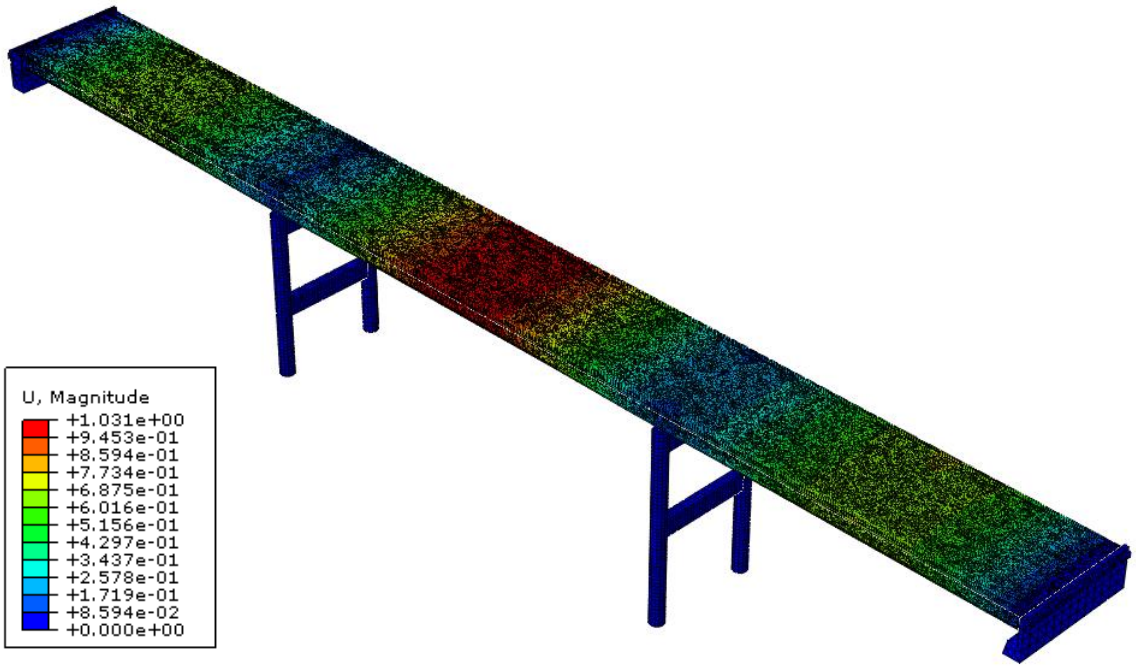

Figure 4.7: Story - Deformation Contour Plot for Dead Load

Table 4.3: Story - Dead Load Abutment and Pier Reactions

	Abutment Reactions (kips)				Pier Reactions (kips)			
	Ext	% diff	Int	% diff	Ext	% diff	Int	% diff
DL #1	33.08	6.71	44.54	5.44	124.87	10.11	154.39	10.29
DL #2	18.01	16.24	6.95	54.47	58.43	21.57	22.94	48.00
Total	51.09	2.69	51.49	0.22	183.30	2.45	177.33	5.48

The maximum deflection obtained was approximately 1 inch at the center of the bridge. This value correlates with the value obtained from the original drawing plans. The resulting abutment and pier reactions were tabulated and compared with the values obtained from the drawing plans. Two dead load loading conditions were considered for the pier and abutment reactions. Lower percentages of difference were achieved in the exterior reactions than in the interior reactions mainly due to oversimplification used on the original drawing regarding the curb and railing load. Both pier reactions show low percentages in the total reaction, 2.45% for the exterior support and 5.48% for the interior support. Abutment reactions also show low percentages of difference for the total reaction, 2.69% and 0.22% for the exterior and interior reactions respectively.

4.1.2.2 Temperature loading

Temperature loading was also modeled. Rocker and expansion plate settings from the original drawing plans can be seen in Table 4.4. A shrinkage and expansion of 0.5 inches can be seen at 10 degrees F and 90 degrees F respectively with a base temperature of 50 degrees F. Results from the FE modeling can be seen in Figure 4.8.

Table 4.4: Story - Expansion Plate Settings

Source: Story County Bridge Plans

ROCKER & EXPANSION PLATE SETTINGS

	S. Abut.		Pier #1	Pier #2	N. Abut.	
Temp. at time of setting	"D"					"D"
10°	3"	½	0	0	½	3"
50°	2½	0	0	0	0	2½
90°	2"	½	0	0	½	2"

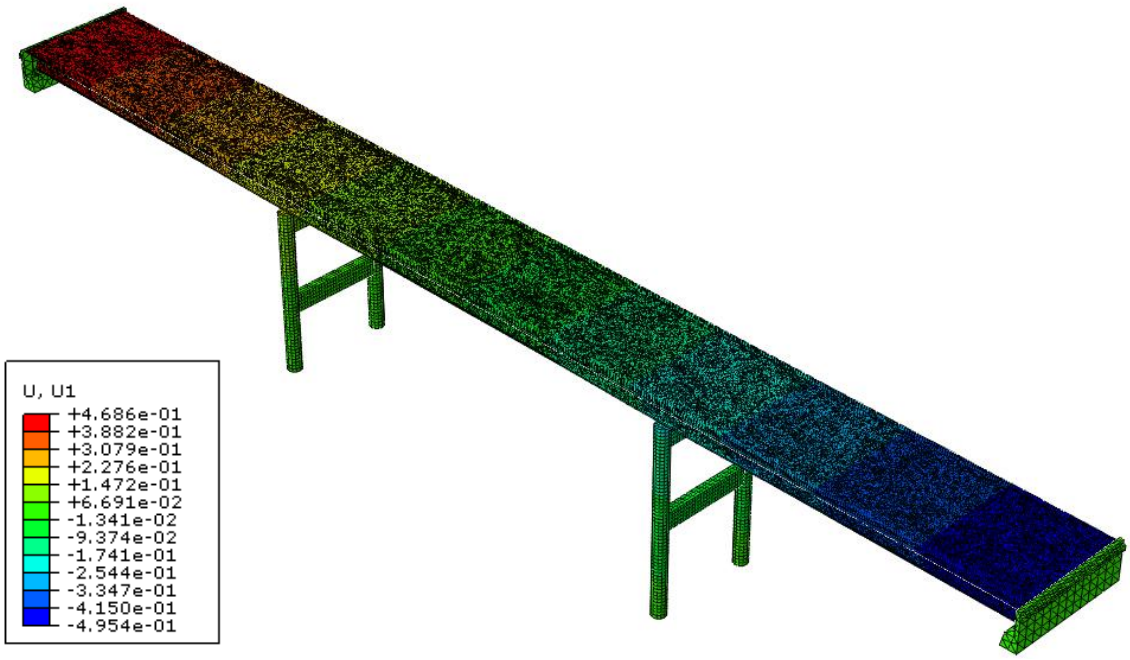

Figure 4.8: Story - Deformation Contour Plot for Temperature Loading

A maximum deformation of approximately 0.5 inches was obtained from the FE modeling. This value matches the original plan value previously shown. The result obtained from the FE modeling was also compared to the value obtained with Equation (1).

$$\Delta L = \alpha \Delta T L \tag{1}$$

where ΔL is the change in length, α is the coefficient of thermal expansion of the material, ΔT is the change in temperature, and L is the original length.

For the Story County bridge, the original length is taken as half of the total length of the bridge deck, 169 feet or 2028 inches, resulting in a change in length of approximately 0.45 inches when the change of temperature equals 40 degrees F and the coefficient of thermal expansion of concrete is used, 5.5E-6 1/°F. The value obtained results in a percentage of difference of 10% from the original plan value and the FE results.

4.1.2.3 Live load reactions and deflection

HS-20-44 AASHTO Specifications truck loading conditions were modeled and placed on top of the bridge deck. According to the AASHTO Specifications, the wheel loads were assumed as uniformly distributed over an area of 20 inches by 10 inches. The wheel spacing and loading is shown in Figure 4.9. A linear load of 0.640 kips per linear foot of lane over a 10 feet width was also included in the truck loading conditions. This was modeled as a surface area over the length of the bridge. Concentrated loads and linear load can be seen in Figure 4.10.

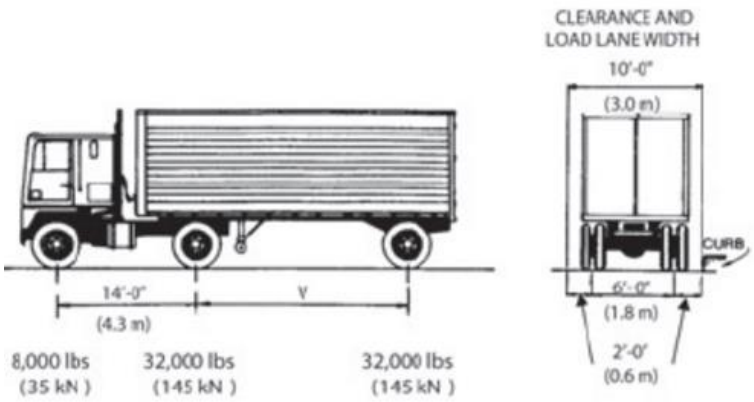

Source: Ryan et al. (2012)

Figure 4.9: HS-20-44 Loading Conditions and Tire Spacing

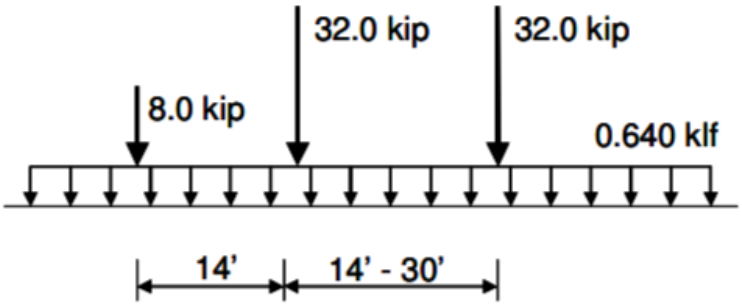

Source: Ryan et al. (2012)

Figure 4.10: HS-20-44 Loading Conditions and Uniform Live Load

Impact loads were also considered. A 20% impact load of the concentrated load from the tires was modeled. This impact load is derived from Equation (2).

$$I = \frac{50}{L + 125} \leq 0.3 \tag{2}$$

where L is the longest span of the bridge in feet.

For the Story County bridge, the longest span is equal to 132 feet therefore resulting in an impact load of approximately 19.46%. Because of this, a 20% impact load was used.

4.1.2.3.1 Controlling truck loading conditions

A 3-D model was created in VBridge. This program was used to verify the controlling truck loading conditions to maximize the desired result (deflection, pier reactions, abutment reactions). The 3-D model can be seen in Figure 4.11. HS-20-44 AASHTO Specifications truck loading conditions were modeled and placed on top of the bridge deck. Controlling truck loading conditions for abutment reactions, pier reactions, and deflection can be seen in Figure 4.12, Figure 4.13, and Figure 4.14 respectively. Lane load allocation can be seen in Figure 4.15, Figure 4.16, and Figure 4.17 as well.

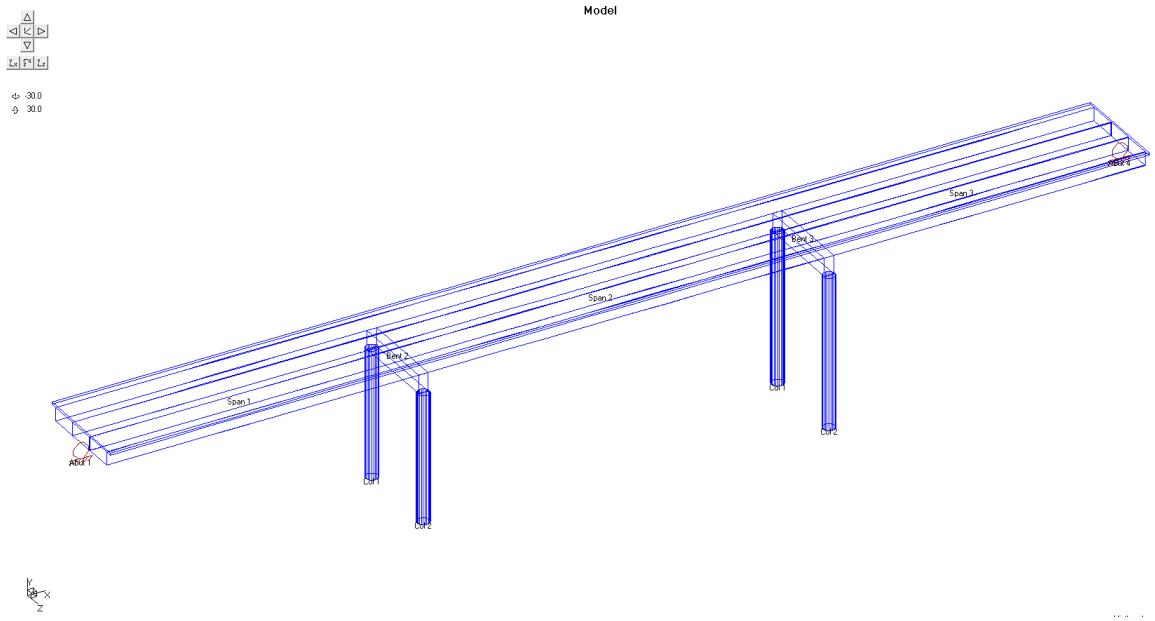

Figure 4.11: Story - Full 3-D VBridge Model

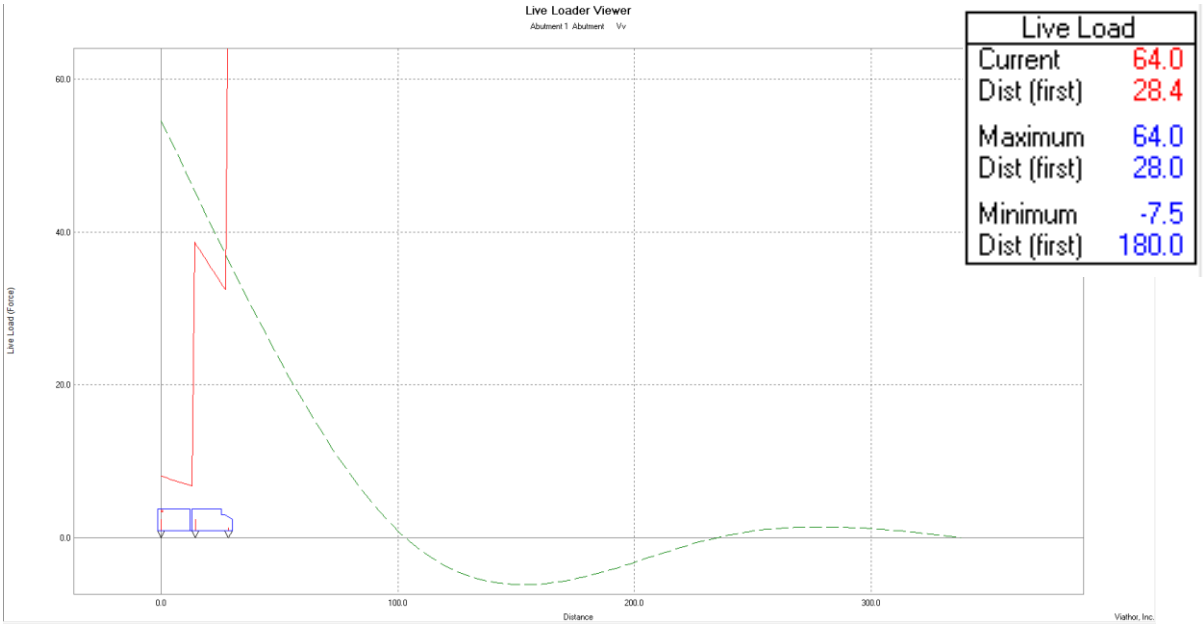

Figure 4.12: Story - Controlling Truck Loading Conditions for Abutment Reactions

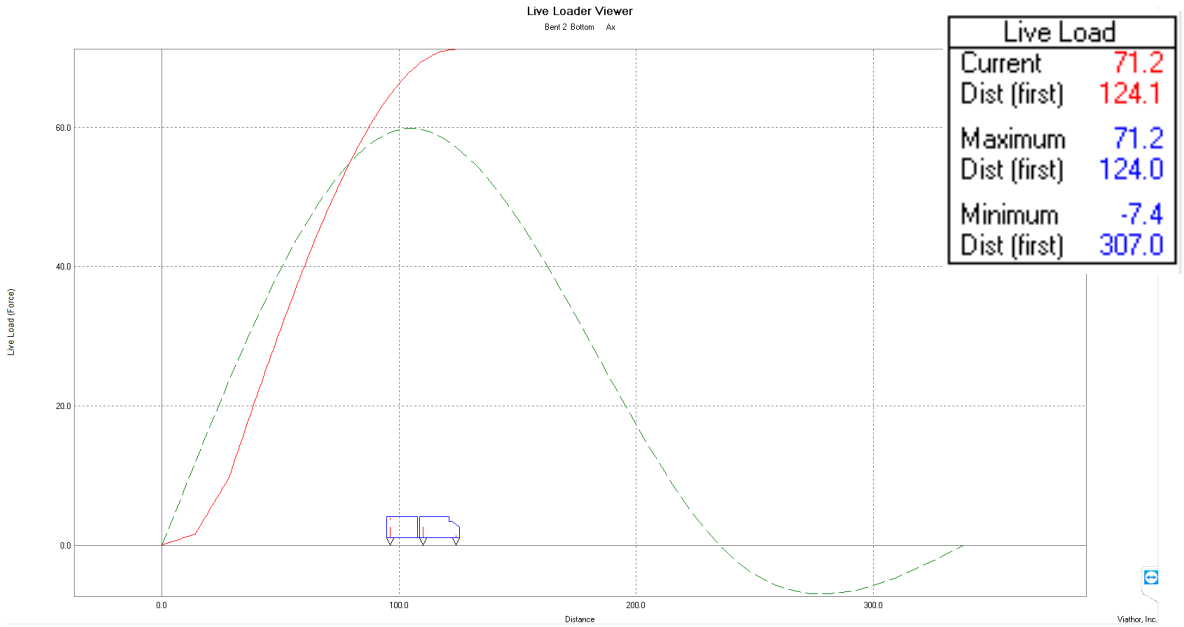

Figure 4.13: Story - Controlling Truck Loading Conditions for Pier Reactions

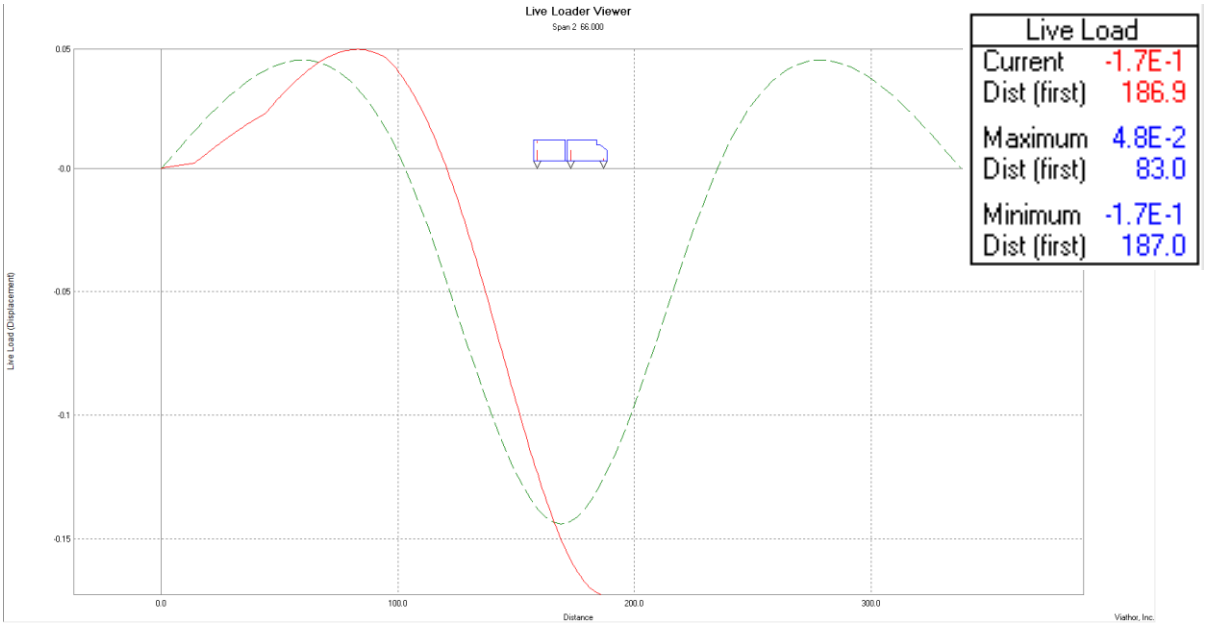

Figure 4.14: Story - Controlling Truck Loading Conditions for Deflection

Figure 4.15: Controlling Lane Load for Abutment Reactions

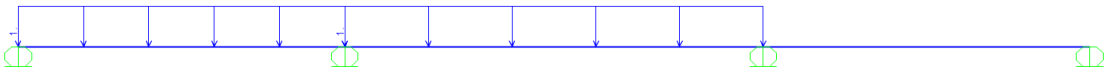

Figure 4.16: Controlling Lane Load for Pier Reactions

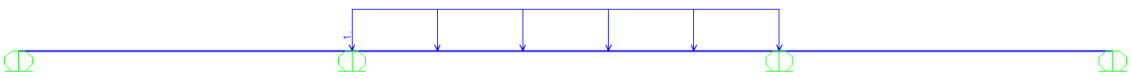

Figure 4.17: Controlling Lane Load for Deflection

4.1.2.3.2 Truck loading deflection

The Story County bridge model was loaded with the truck loading conditions discussed previously. The load allocation that corresponds with maximizing deflection at the midspan of the bridge can be seen in Figure 4.14 for the truck load and Figure 4.17 for the lane load. The load in the model can be seen in Figure 4.18. Lane load can clearly be seen marked in red in the interior span. Two concurrent 10 feet wide pressure loads were modeled in the center of the roadway. The truck load can also be seen with orange. Two HS-20-44 trucks were modeled acting over each lane load location. Results for these loading conditions can be seen in Figure 4.19.

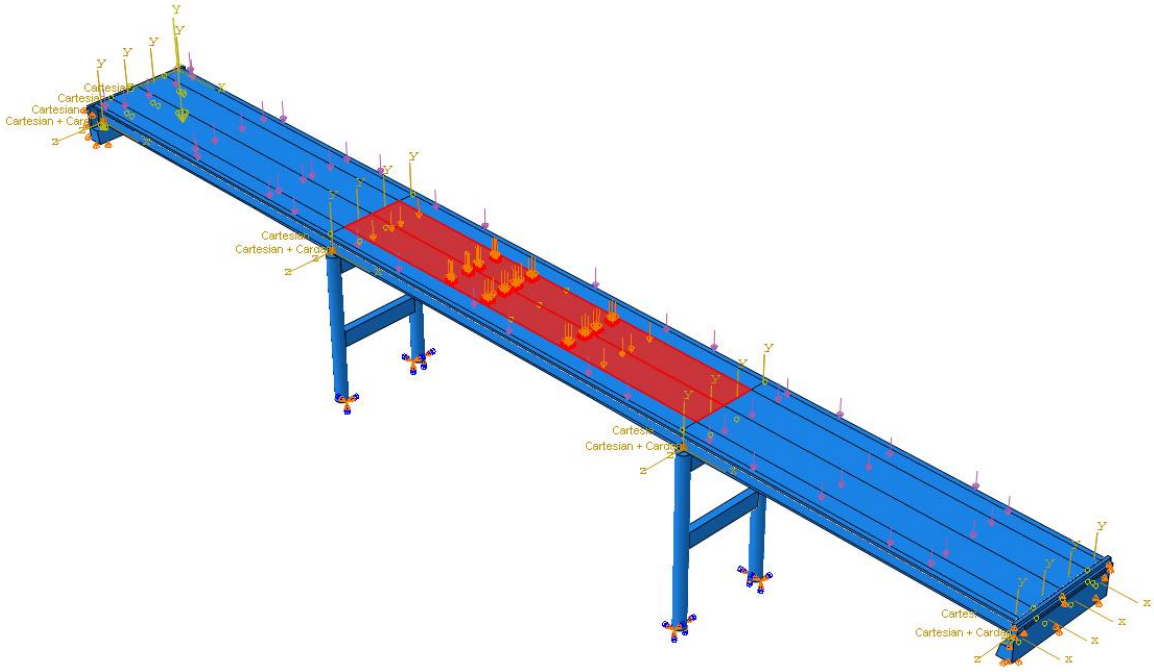

Figure 4.18: Story - Load Allocation for Deflection

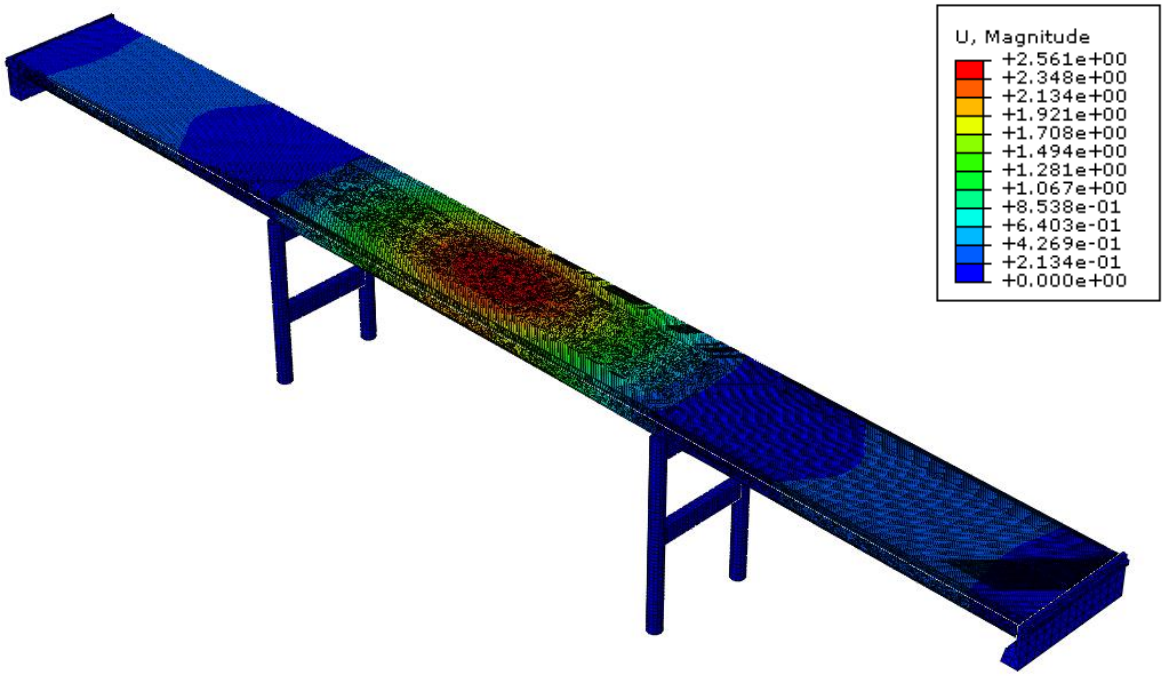

Figure 4.19: Story - Deformation Contour Plot for Deflection Truck Load

From the results of the FE model, a maximum deflection at midspan of approximately 2.5 inches was obtained. AASHTO Specifications provides certain deflection limits for vehicular bridges in the absence of other criteria. These limits are set as L/800 for general vehicular load and L/1000 for vehicular and pedestrian loads where L is the span where the deflection is being questioned. Since the Story County bridge does not have pedestrian loads, L/800 is applicable. Using the center span of the Story County bridge with L of 132 feet or 1584 inches, the L/800 design limit come out as approximately 1.98 inches. Accounting for the dead load deflection shown previously, the live load resulted in a deflection of approximately 1.53 inches which is lower than the L/800 deflection limit.

4.1.2.3.3 Truck loading reactions

To maximize abutment and pier reactions, different truck loading allocation were needed. The load allocation that corresponds with maximizing abutment reactions can be seen in Figure 4.12 for the truck load and Figure 4.15 for the lane load. Also, the load allocation that corresponds with maximizing pier reactions can be seen in Figure 4.13 for the truck load and Figure 4.16 for the lane load.

Firstly, the abutment reactions results will be discussed. The load in the model can be seen in Figure 4.20 marked in red. The lane load can be clearly seen in the exterior spans with the rear axle of the concentrated truck load at the edge of the bridge deck. Two HS-20-44 trucks were modeled side by side with the one side of the truck axle 2 feet from the curb. The lane loads were modeled as two concurrent 10 feet wide pressure loads starting from the curb. A deformation contour plot is provided in Figure 4.21. Maximum deformation can be clearly seen in the exterior span where the concentrated truck load is applied. Results for dead load and abutment reactions can be seen in Table 4.5. A comparison between the results obtained from the FE model with the original plans is shown.

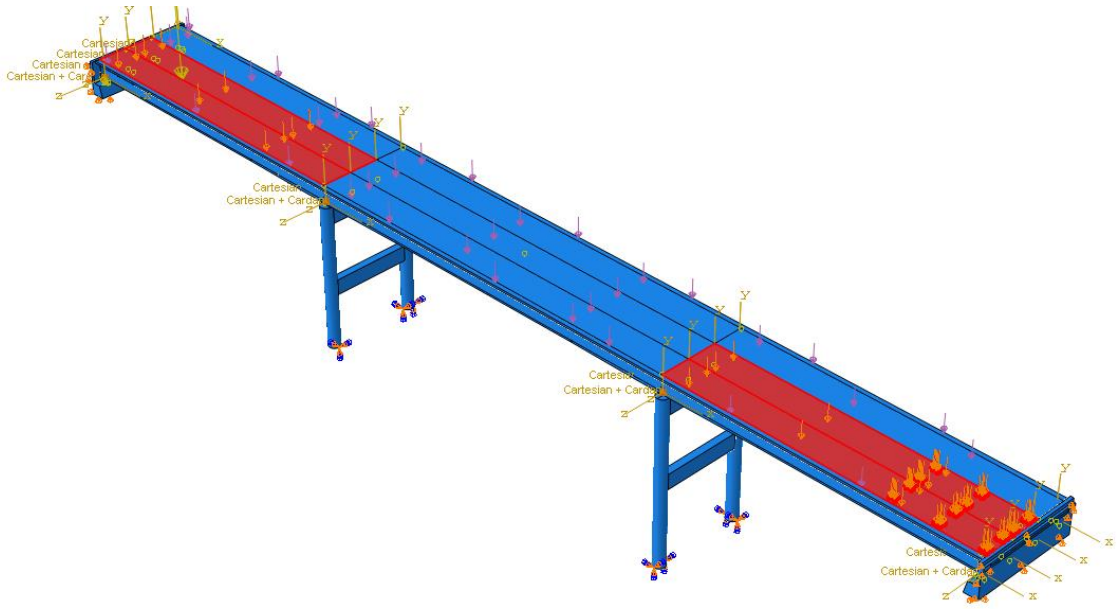

Figure 4.20: Story - Load Allocation for Abutment Reactions

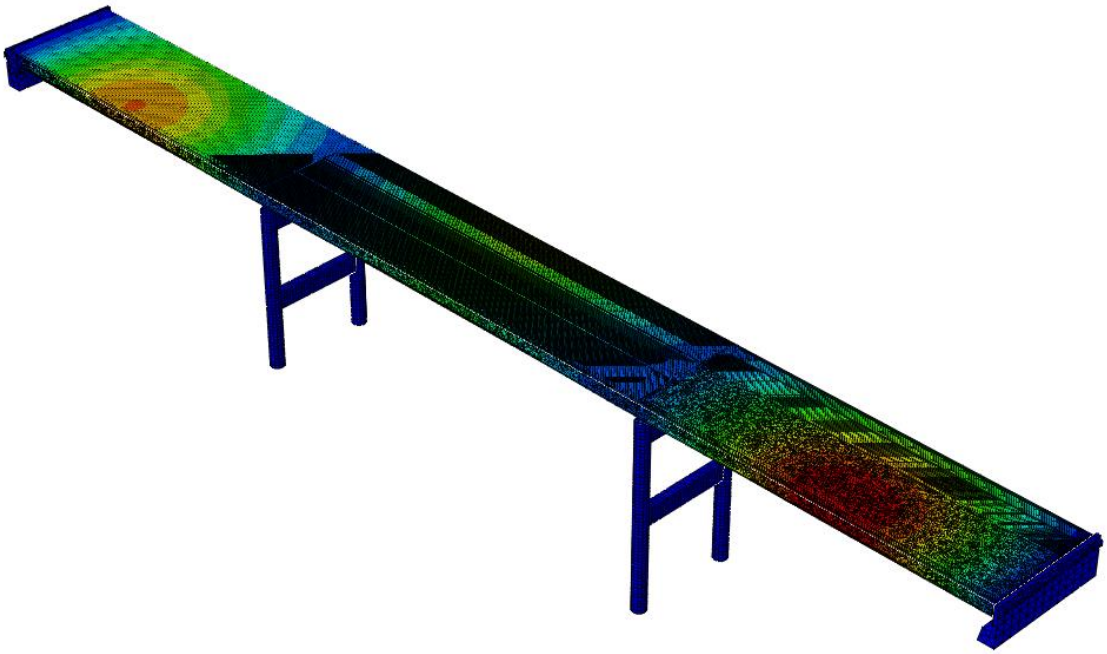

Figure 4.21: Story - Deformation Contour Plot for Abutment Reactions Truck Load

Table 4.5: Story - Dead Load and Live Load Abutment Reactions

	Abutment Reactions (kips)			
	Ext	% diff	Int	% diff
DL #1	33.11	6.80	44.50	5.52
DL #2	18.03	16.14	6.95	54.35
ULL	-	-	-	-
CLL	-	-	-	-
HS-20-16	55.03	14.17	83.30	47.96
Impact	7.07	33.27	11.68	5.04
Total	113.24	1.74	146.43	21.82

High percentages of difference were obtained in the truck loading values. The highest percentage of difference was almost 48% in the interior support for the HS-20-16 load. This difference attributes to the percentage of difference of 21.82% obtained in the total load for the interior support. The exterior support also shows high percentages as well with 14.17% for the HS-20-16 load and 33.27% for the impact load. The total load however only amounts to a percentage of difference of 1.74%.

After careful inspection of the original plan values, it was decided that it was necessary to alter the truck loading conditions in the FE model to try to improve its accuracy when compared with the original plan values. This is due to the fact that the loads in the plans are calculated based on a one-dimensional bridge analysis.

From the literature (Ryan et al. 2012), it was discovered that a 26 kip load was used instead of the current HS-20-44 truck loading conditions for the drawing plan values. This loading condition is shown in Figure 4.22.

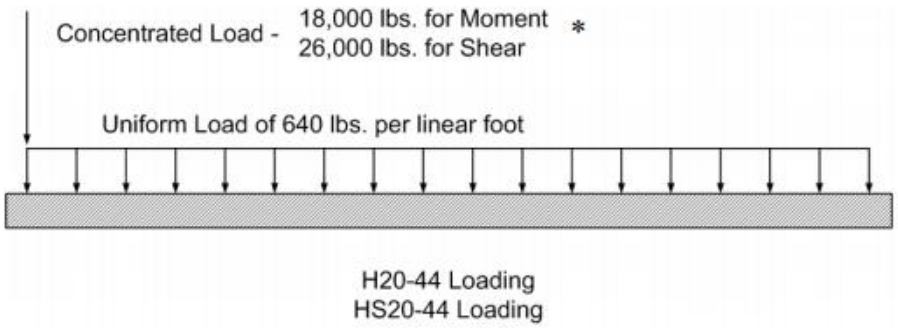

* Use two concentrated loads for negative moment in continuous spans (Refer to *AASHTO LRFD Bridge Design Specifications 5th edition*, 2010 Interim; Article 3.6.1.2)

Source: Ryan et al. (2012)

Figure 4.22: Truck Loading Conditions from the Drawing Plans

To get the drawing plan values, the 26 kip load is divided into two axles of the truck and multiplied by various factors. For interior girders, it should be multiplied by the load distribution factor (LDF) obtained with Equation (3)

$$LDF = \frac{S}{5.5} \tag{3}$$

where LDF is the load distribution factor and S is the girder spacing in feet.

For exterior girders, Equation (4) is used with the factor calculated on Equation (5).

$$g = e g_{interior} \tag{4}$$

$$e = 0.6 + \frac{d_e}{10} \tag{5}$$

where g is the LDF for exterior girders, $g_{interior}$ is the LDF for interior girders, e is a conversion factor from interior girder to exterior girder, and d_e is the distance between the exterior girders to the center of the curb in feet.

An additional factor for skewed bridges is also added and relevant for the Marshall County bridge yet it will not be discussed.

In addition, judging by the magnitudes of the original plan values, it was determined that an impact load was applied on the lane load as well as the concentrated live load from the tire loads. This is contrary to the current AASHTO Specifications.

Truck loading conditions were altered to attempt to match the drawing plan values. One truck was modeled instead of two with the impact load applied on the lane load as well. This new load allocation can be seen in Figure 4.23 with one truck in one of the exterior spans instead of two. Results for dead load and abutment reactions can be seen in Table 4.6. A comparison between the results obtained from the updated FE model with the original plans is shown.

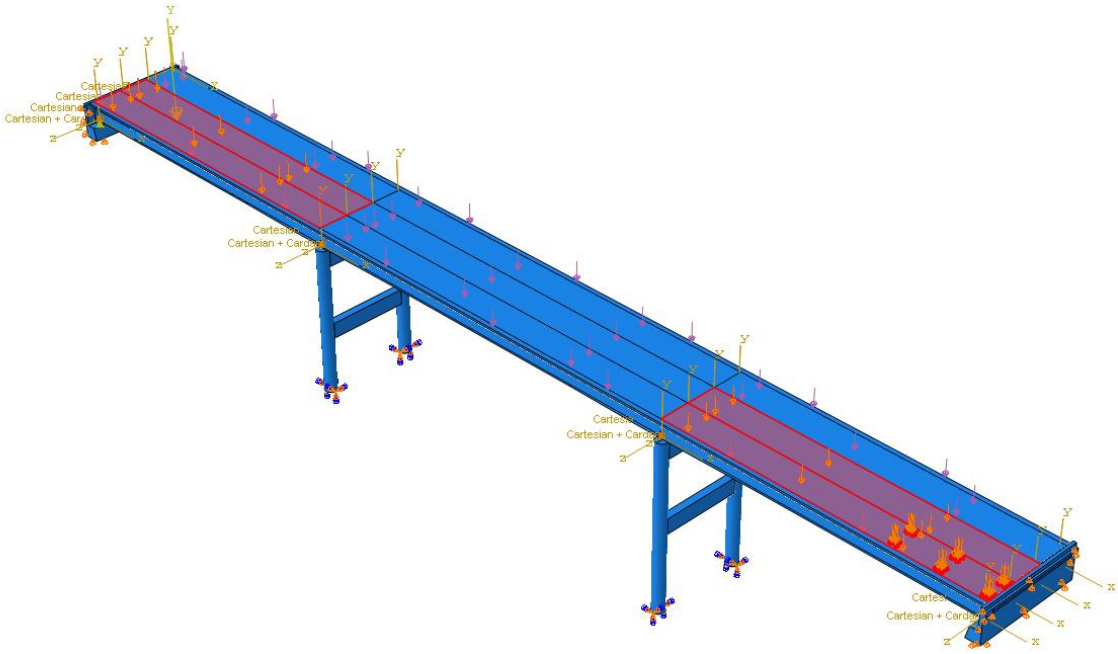

Figure 4.23: Story - Updated Load Allocation for Abutment Reactions

Table 4.6: Story - Dead Load and Updated Live Load Abutment Reactions

	Abutment Reactions (kips)			
	Ext	% diff	Int	% diff
DL #1	33.12	6.84	44.53	5.45
DL #2	18.08	15.93	6.96	54.56
ULL	-	-	-	-
CLL	-	-	-	-
HS-20-16	53.34	10.66	53.13	5.64
Impact	10.67	0.64	10.63	13.61
Total	115.20	3.50	115.24	4.12

Percentages of difference lowered in the interior support after the truck loading conditions were altered. The HS-20-16 which had a percentage of difference of 47.96% in the previous discussion, now resulted in a percentage of difference of 5.64%. The total load of the interior support lowered from 146.43 kips to 115.24 kips. The percentage of difference lowered from 21.82% to 4.12%. This difference is because the interior support is now taking only one side of the axle from the truck. Previously, the interior support took the same axle plus another axle. The exterior support did not suffer major differences. The HS-20-16 load went from 55.03 kips to 53.34 kips and the impact load went from 7.07 kips to 10.67 kips. The percentage of difference for the total load on the exterior support went from 1.74% to 3.50%. This low difference can be due to the exterior support already taking the same axle of the truck nearest to the curb. The HS-20-16 load decreases because there is no truck load in the concurrent span transversely.

The pier reactions will be discussed in the following pages. The load in the model can be seen in Figure 4.24 marked in red. The lane load can be clearly seen in the exterior spans with the rear axle of the concentrated truck load at the edge of the bridge deck. Two HS-20-44 trucks were modeled side by side with the one side of the truck axle 2 feet from the curb. The lane loads were modeled as two concurrent 10 feet wide pressure loads starting from the curb. A deformation contour plot is provided in Figure 4.25. The maximum deformation can be clearly seen in the exterior span where the concentrated truck load is applied. Results for dead load and pier reactions can be seen in Table 4.7. A comparison between the results obtained from the FE model with the original plans is shown.

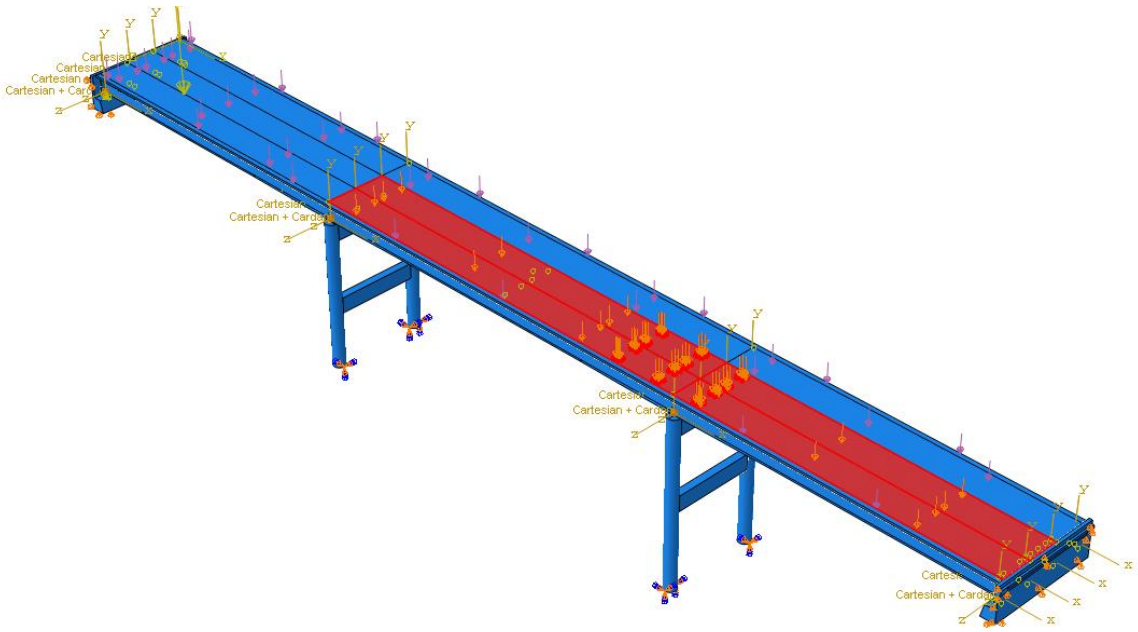

Figure 4.24: Story - Load Allocation for Pier Reactions

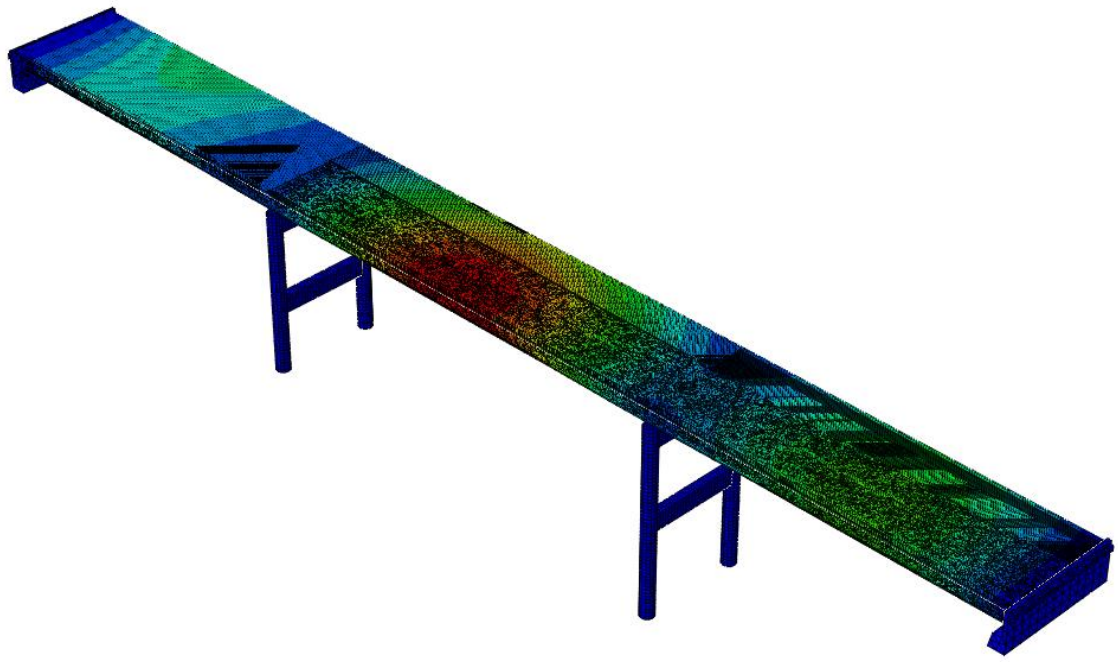

Figure 4.25: Story - Deformation Contour Plot for Pier Reactions Truck Load

Table 4.7: Story - Dead Load and Live Load Pier Reactions

	Pier Reactions (kips)			
	Ext	% diff	Int	% diff
DL #1	126.23	11.31	150.29	12.68
DL #2	58.95	20.88	22.40	44.48
ULL	58.05	13.36	71.52	8.31
CLL	40.05	104.36	64.55	183.09
HS-20-16	-	-	-	-
Impact	8.01	55.25	12.91	37.94
Total	291.29	0.38	321.66	4.03

High percentages of difference were obtained in the truck loading values. The highest percentage of difference was almost 183.09% in the interior support for the concentrated live load. This difference attributes to the percentage of difference of 4.03% obtained in the total load for the interior support. The exterior support also shows high percentages as well with 104.36% for the concentrated live load and 55.25% for the impact load. The total load however only amounts to a percentage of difference of 0.38%.

For the reasons explained previously, truck loading conditions were altered to attempt to match the drawing plan values. One truck was modeled instead of two with the impact load applied on the lane load as well. This new load allocation can be seen in Figure 4.26 with one truck in one of the exterior spans instead of two. Results for dead load and pier reactions can be seen in Table 4.8. A comparison between the results obtained from the updated FE model with the original plans is shown.

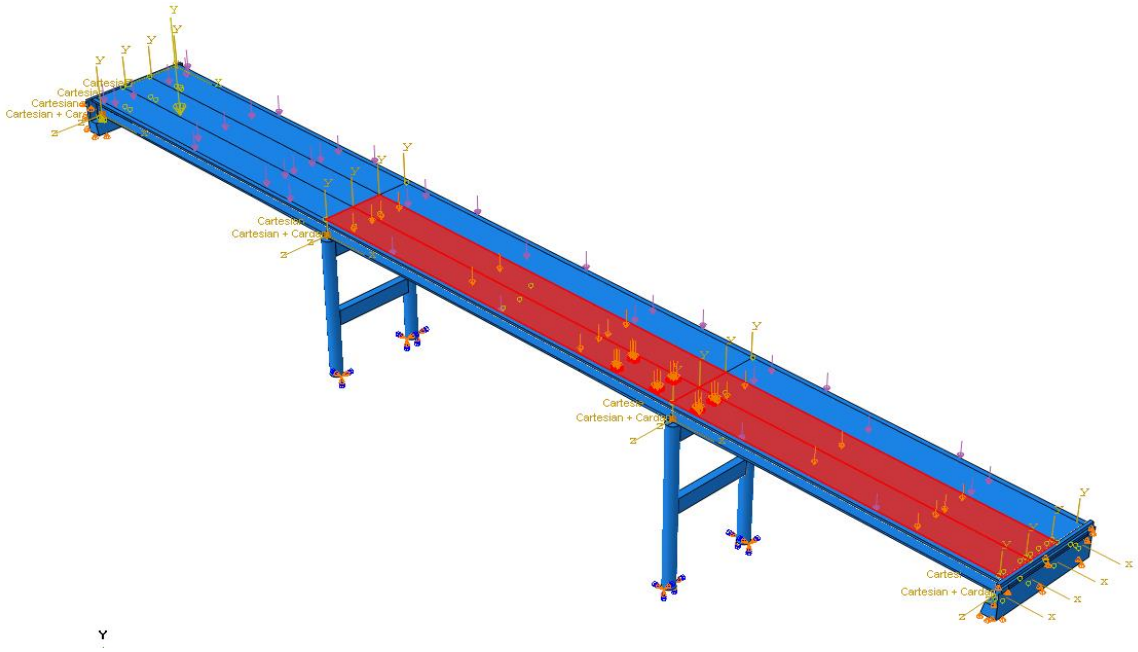

Figure 4.26: Story - Updated Load Allocation for Pier Reactions

Table 4.8: Story - Dead Load and Updated Live Load Pier Reactions

	Pier Reactions (kips)			
	Ext	% diff	Int	% diff
DL #1	126.24	11.32	150.29	12.68
DL #2	58.95	20.88	22.40	44.48
ULL	58.05	13.35	71.51	8.32
CLL	37.03	88.91	32.51	42.60
HS-20-16	-	-	-	-
Impact	19.02	6.24	20.81	0.03
Total	299.28	2.35	297.51	3.78

Percentages of difference lowered in the interior support after the truck loading conditions were altered. The concentrated live load which had a percentage of difference of 183.09% in the previous discussion, now resulted in a percentage of difference of 42.60%. The percentage of difference for the impact load lowered from 37.94% to 0.03%. The total load of the interior support lowered from 321.66 kips to 297.51 kips. The percentage of difference lowered from 4.03% to 3.78%. This difference is because the interior support is now taking only one side of the axle from the truck. Previously, the interior support took the same axle plus another axle. The exterior support did not suffer major differences. The concentrated live load went from 40.05 kips to 37.03 kips and the impact load went from 8.01 kips to 19.02 kips. The percentage of difference for the total load on the exterior support went from 0.38% to 2.35%. This low difference can be due to the exterior support already taking the same axle of the truck nearest to the curb. The concentrated live load decreases because there is no truck load in the concurrent span transversely.

4.2 Marshall County Bridge

A full 3-D model was realized in Abaqus FEA for the bridge under investigation. This model includes a concrete bridge deck supported by welded plate steel girders and diaphragms that rest on abutments at the ends and piers. A skew of 45 degrees is also modeled. A full 3-D model can be seen in Figure 4.27 with a plan view in Figure 4.28, in which the skew can be appreciated. Constraints, boundary conditions, and other elements had to be assigned in the model. Also, loading conditions were incorporated in the model from self-weight, surface weathering, to truck loading.

An 8 inch by 210 feet bridge deck was modeled as a C3D8R element, which is an 8-node linear brick element with reduced integration and hourglass control. In addition, C3D8R was utilized for all concrete parts in the model, this includes the abutments and the pier caps. The steel superstructure is composed of welded plate steel girders and transversal diaphragms at the ends and over the piers. The web and flanges of the welded plate girders as well as the diaphragms were modeled as S4R, 4-node doubly curved thin or thick shell element with reduced integration, hourglass control, and finite membrane strains. For the flanges of the welded plate girders, width and thickness were modeled per the drawing plans. All steel superstructure was merged together. This can be appreciated in Figure 4.29.

This model underwent an elastic analysis. Only mass density and elastic properties such as Young's modulus and Poisson's ratio were needed for to realize the analysis successfully. The mass density utilized for the concrete and steel derived from their specific weight of 150 lb/ft^3 and 490 lb/ft^3 respectively. As for the Young's modulus and Poisson's ratio, 3,718 ksi and 0.15 was utilized for concrete and 29,000 ksi and 0.3 for the steel. In addition, the coefficient of thermal expansion for both concrete and steel was determined to be 5.5E-6 1/°F and 6.5E-6 1/°F respectively.

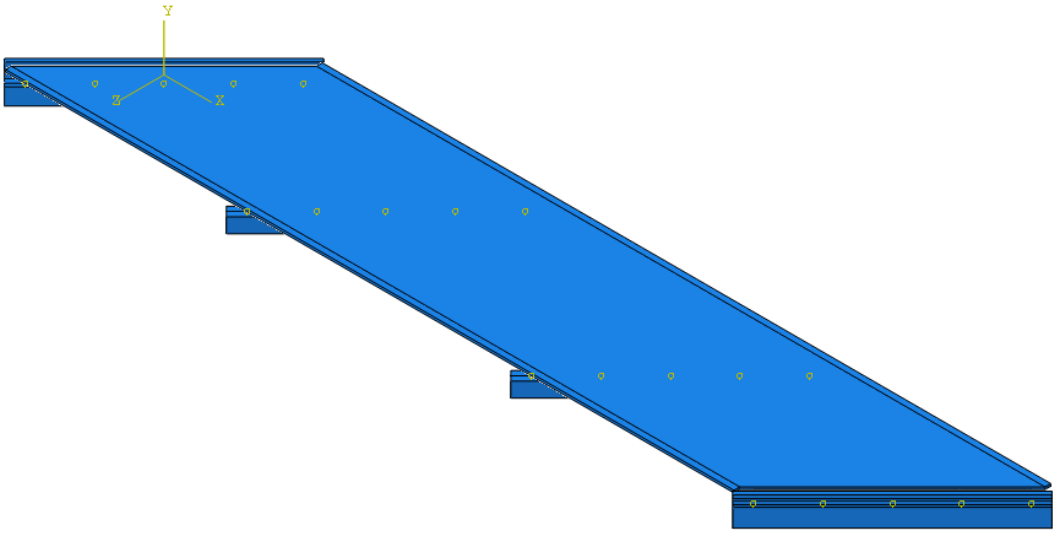

Figure 4.27: Marshall - Full 3-D FE Model

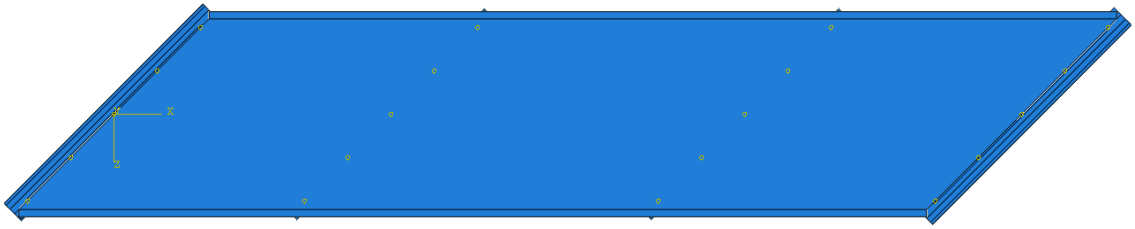

Figure 4.28: Marshall - Plan View

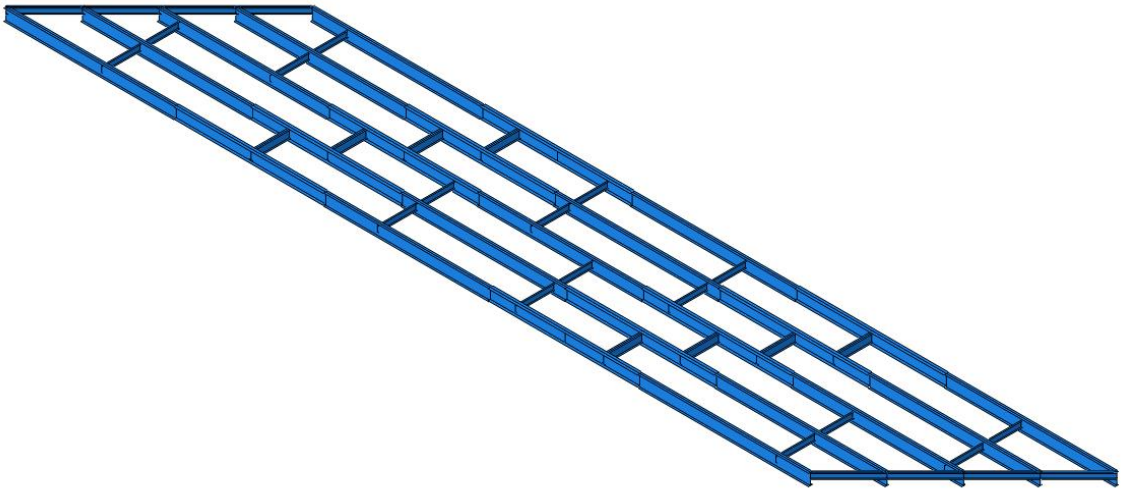

Figure 4.29: Marshall - Steel Superstructure

Boundary conditions were assigned on the abutment's vertical and horizontal faces that are in the direction of supporting soil. Vertical faces have horizontal constraints and, vice versa, horizontal faces have vertical constraints. A fixed boundary condition was assigned to the bottom face of the pier caps simulating the foundations that rest under the top soil. Boundary conditions can be seen in Figure 4.30 marked in red at the abutment and on the bottom face of the pier cap. Tie constraints were assigned between the top flanges of all the welded plate girders with the bottom surface of the bridge deck. Connection wires were utilized between the steel girders and the abutments and piers to simulate the rocker bearings at the points of interest. All reaction values presented in the following pages corresponds to these connection wires.

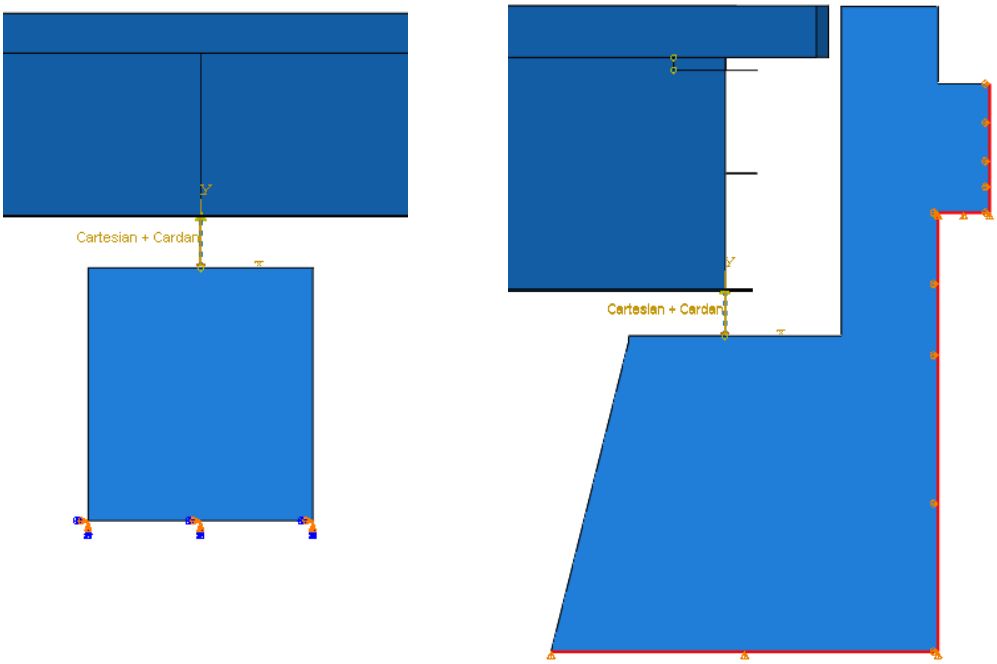

Figure 4.30: Marshall - Boundary Conditions

4.2.1 Convergence Study

The model was trialed on numerous occasions with different meshing sizes. Results stabilized at an approximate meshing size of 5 inches. A meshing of 4 inches was determined to be the most effective for the model at this point. Just for reference, the time elapsed to complete the analysis for a meshing size of 3 inches was almost six times as large as the time elapsed for a meshing size of 4 inches. This can be recognized in Table 4.9. The time elapsed for each trial in shown for all mesh sizes along with their deflection values. A graph of the different values that were trialed with their results can be observed in Figure 4.31. With a mesh size of 4 inches, the structure was modeled using 318,380 elements, 450,396 nodes, and 1,562,961 variables.

Table 4.9: Marshall - Mesh Convergence Study

Mesh Size (in)	Max Deflection at Midspan (in)	Time Elapsed (s)
12	0.7187	77.7
10	0.7103	100.9
8	0.7513	144.5
6	0.7381	243.7
5	0.5261	654.7
4.5	0.5247	835
4	0.5272	1125.9
3.5	0.5375	1777.9
3	0.5213	11924.8

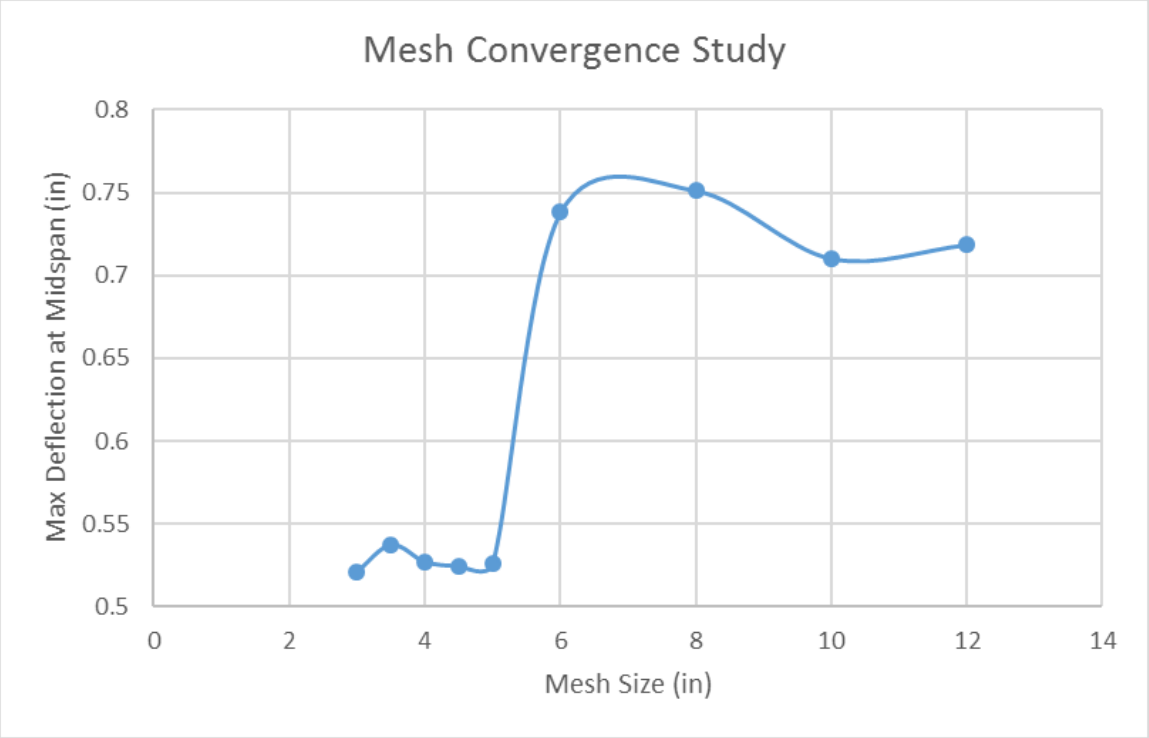

Figure 4.31: Marshall - Mesh Convergence Study

4.2.2 Validation With Original Plans

The information needed to realize the FE model and analysis for the Marshall County bridge was obtained from its original drawing plans. Abutment and pier reactions can be observed in such plans and in Table 4.10. These reactions were the source of comparison for the results obtained from the FE analysis shown in the next section. It is important to mention that the FE model does not fully incorporate all the elements shown in the plans but includes the most pertinent ones.

Table 4.10: Marshall - Abutment and Pier Reactions from the Drawing Plans

Source: Marshall County Bridge Plans

	Abutment Reactions (kips)		Pier Reactions (kips)	
	Exterior	Interior	Exterior	Interior
DL #1	24.5	27.8	90.1	102.0
DL #2	10.0	4.7	34.6	16.3
ULL	-	-	42.5	50.3
CLL	-	-	20.0	23.7
HS-20-44	45.6	53.9	-	-
Impact	12.0	14.2	15.8	18.7
Total	92.1	100.6	203.0	211.0

Dead load #1 includes weight of slab, girders, and diaphragms.

Dead Load #2 includes weight of curbs, rail, and future wearing surface.

4.2.2.1 Dead load reactions and deflection

Self-weight was included in the whole model. A surface weathering loading condition of 20 lb/ft^2 over the roadway was also added. Curb loading on 1'8" of the edges was added as a surface area simulating a 1'8" by 1 foot area of concrete by the entire length of the bridge deck. Results for dead load deflection and a comparative loading conditions table can be appreciated in Figure 4.33 and Table 4.11.

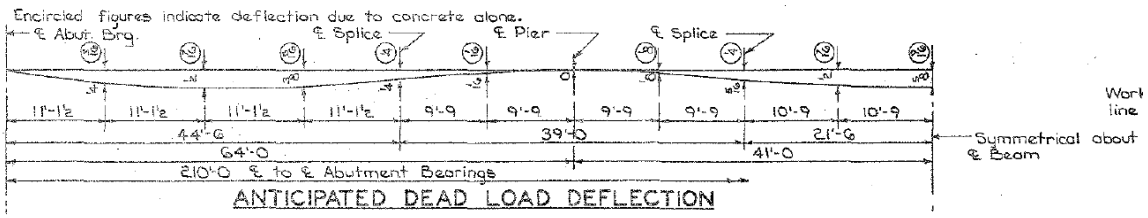

Source: Marshall County Bridge Plans

Figure 4.32: Marshall - Anticipated Dead Load Deflection

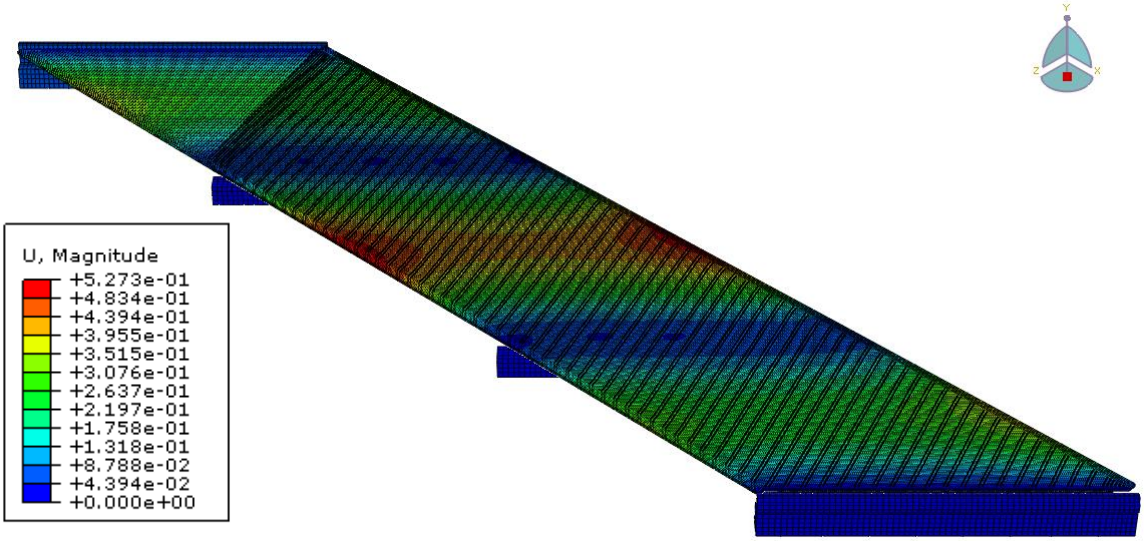

Figure 4.33: Marshall - Deformation Contour Plot for Dead Load

Table 4.11: Marshall - Dead Load Abutment and Pier Reactions

	Abutment Reactions (kips)				Pier Reactions (kips)			
	Ext	% diff	Int	% diff	Ext	% diff	Int	% diff
DL #1	25.01	2.07	28.13	1.19	86.36	4.15	100.35	1.61
DL #2	10.17	1.67	4.75	1.10	33.99	1.76	16.68	2.35

The maximum deflection obtained was approximately 0.53 inches at the center of the bridge. This value presents approximately a percentage of difference of 15% from the value obtained from the original drawing plans of 5/8".

The resulting abutment and pier reactions were tabulated and compared with the values obtained from the drawing plans. Two dead load loading conditions were considered for the pier and abutment reactions. Both pier and abutment reactions show low percentages of difference ranging from a maximum of 4.15% to a minimum of 1.10%.

4.2.2.2 Temperature loading

Temperature loading was also modeled. Expansion plate settings from the original drawing plans can be seen in Table 4.12. A shrinkage and expansion of 0.25 inches can be seen at 10 and 90 °F respectively with a base temperature of 50 °F. Results from the FE modeling can be seen in Figure 4.34.

Table 4.12: Marshall - Expansion Plate Settings

Source: Marshall County Bridge Plans

EXPANSION PLATE SETTINGS

Temp. at time of setting	South Abut.		Pier 1	Pier 2	North Abut.	
	D					D
10°	2¼	− 5/16	—	—	− 5/16	2¼
50°	2	0	—	—	0	2
90°	1¾	+ 5/16	—	—	+ 5/16	1¾

NOTE: Settings for other temperatures are proportional

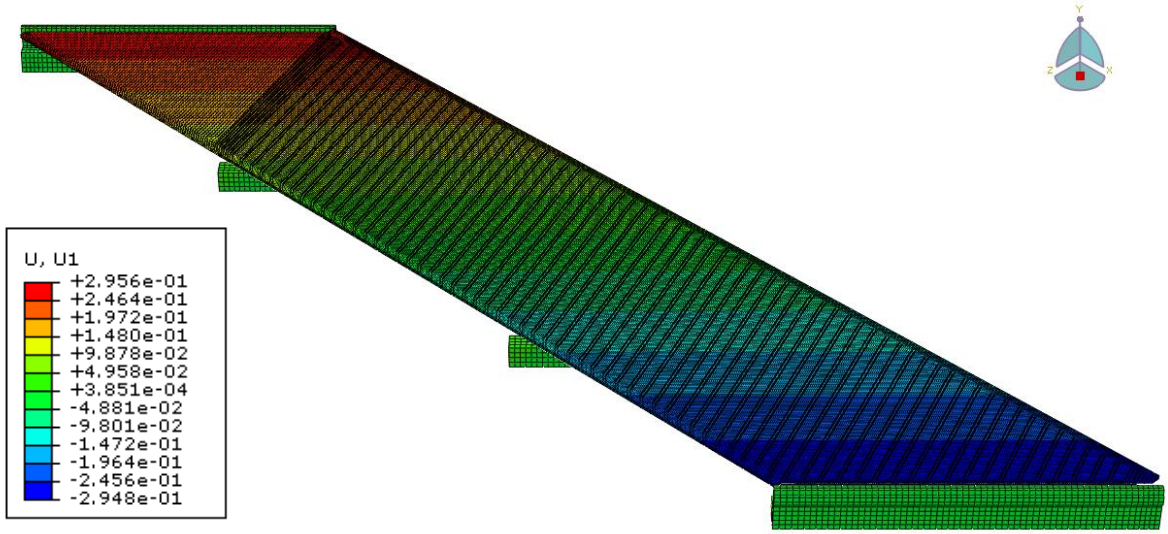

Figure 4.34: Marshall - Deformation Contour Plot for Temperature Loading

A maximum deformation of approximately 0.3 inches was obtained from the FE modeling. This value presents a percentage of difference of 20% from the original plan value previously shown. The result obtained from the FE modeling was also compared to the value obtained with Equation (1).

For the Marshall County bridge, the original length is taken as half of the total length of the bridge deck, 105 feet or 1260 inches, resulting in a change in length of approximately 0.28 inches when the change of temperature equals 40 degrees F and the coefficient of thermal expansion of concrete is used, 5.5E-6 1/°F. The value obtained results in a percentage of difference of 6.22% from the result obtained from the FE modeling.

4.2.2.3 Live load reactions and deflection

Same loading conditions were applied as 4.1.2.3, Figure 4.9 and Figure 4.10.

Impact loads were also considered. A 25% impact load of the concentrated load from the tires was modeled. This impact load is derived from Equation (2). For the Marshall County bridge, the longest span is equal to 82 feet therefore resulting in an impact load of approximately 24.15%. Because of this, a 25% impact load was used.

4.2.2.3.1 Controlling truck loading conditions

A 3-D model was created in VBridge. This program was used to verify the controlling truck loading conditions to maximize the desired result (deflection, pier reaction, abutment reaction). The 3-D model can be seen in Figure 4.35 with a top view on Figure 4.36. HS-20-44 AASHTO Specifications truck loading conditions were modeled and placed on top of the bridge deck. Controlling truck loading conditions for abutment reactions, pier reactions, and deflection can be seen in Figure 4.37, Figure 4.38, and Figure 4.39 respectively.

The controlling lane loads are the same as the ones shown in 4.1.2.3.1, Figure 4.15, Figure 4.16, and Figure 4.17. These conditions can be summarized as the lane load being applied on exterior spans to maximize abutment reactions, on continuous spans to for the reactions of the pier in-between, and on the center span for deflection at midspan.

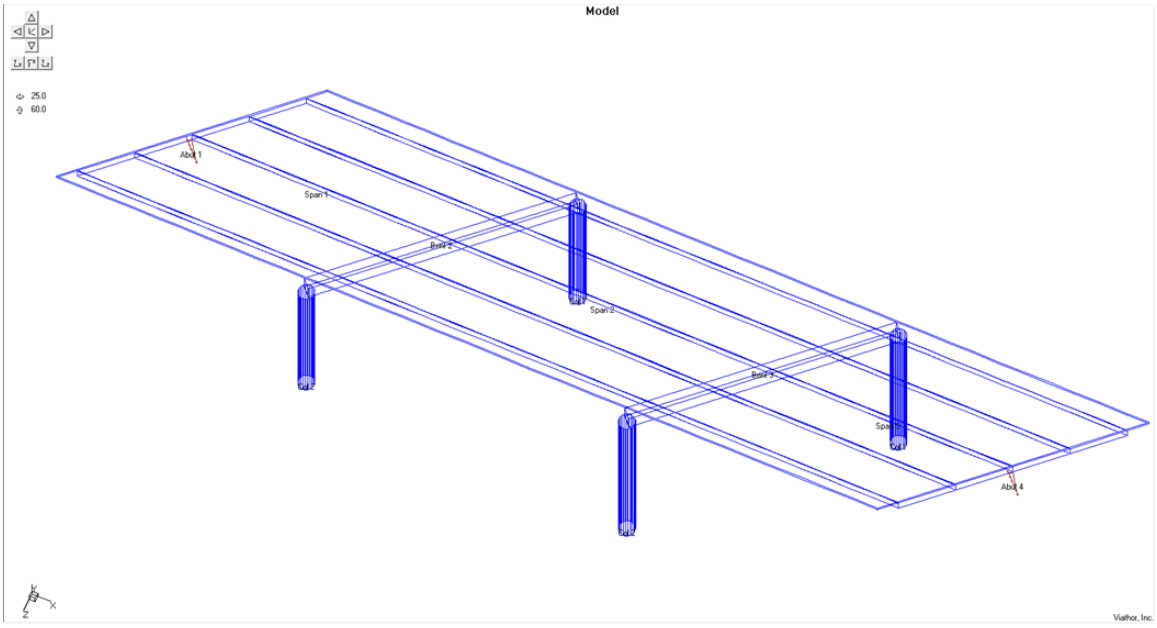

Figure 4.35: Marshall - Full 3-D VBridge Model

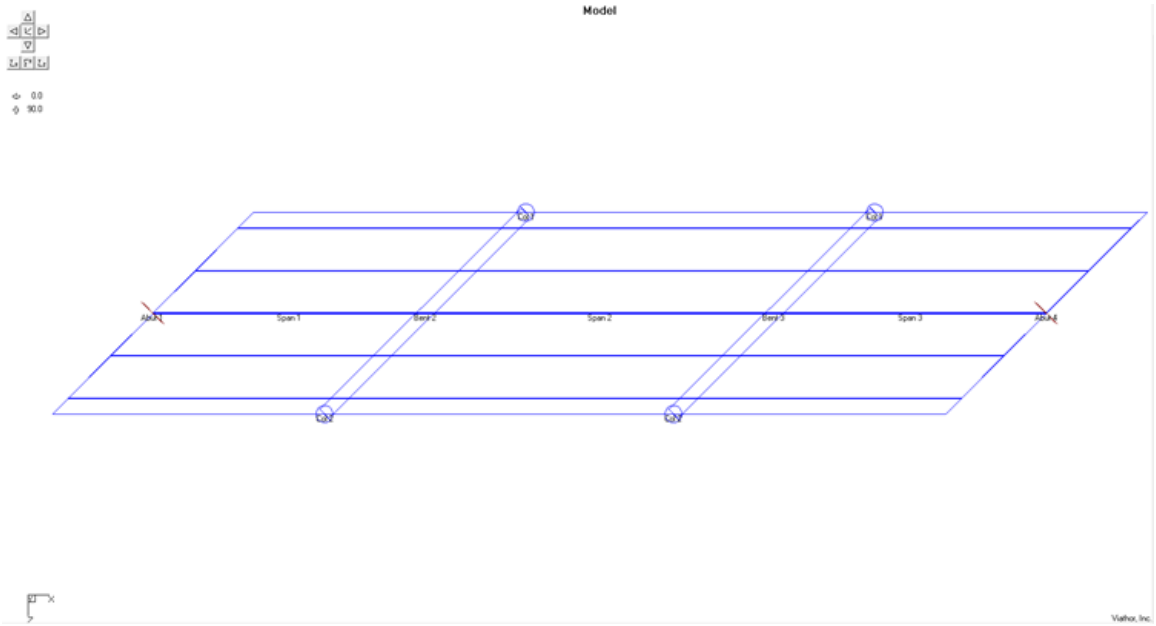

Figure 4.36: Marshall - Plan View of VBridge Model

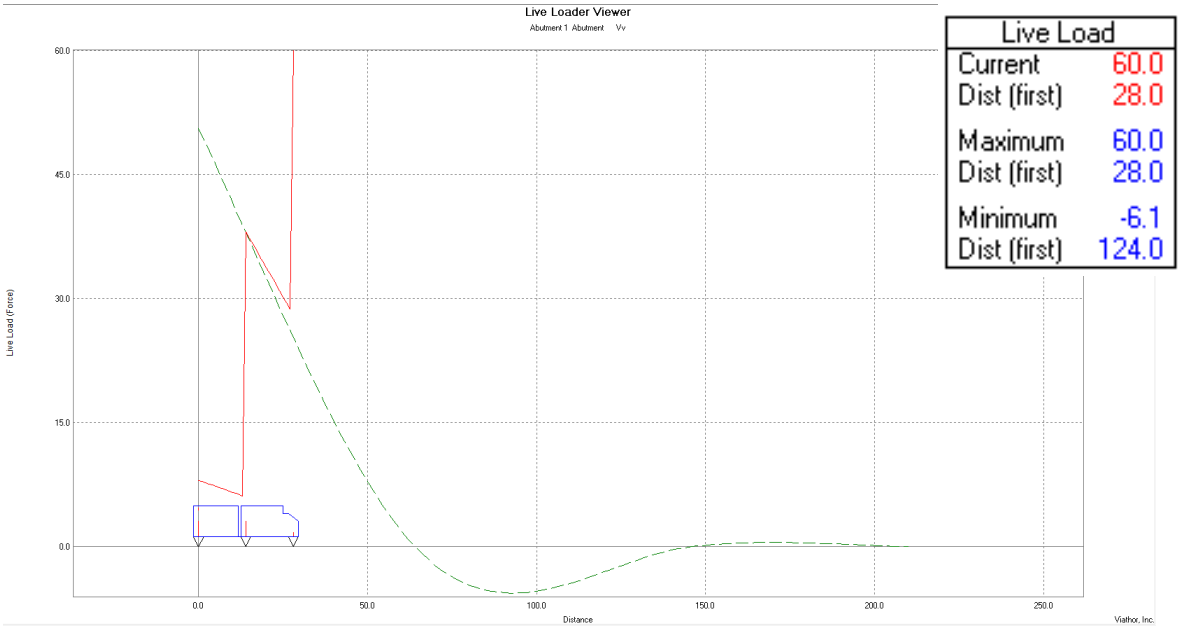

Figure 4.37: Marshall - Controlling Truck Loading Conditions for Abutment Reactions

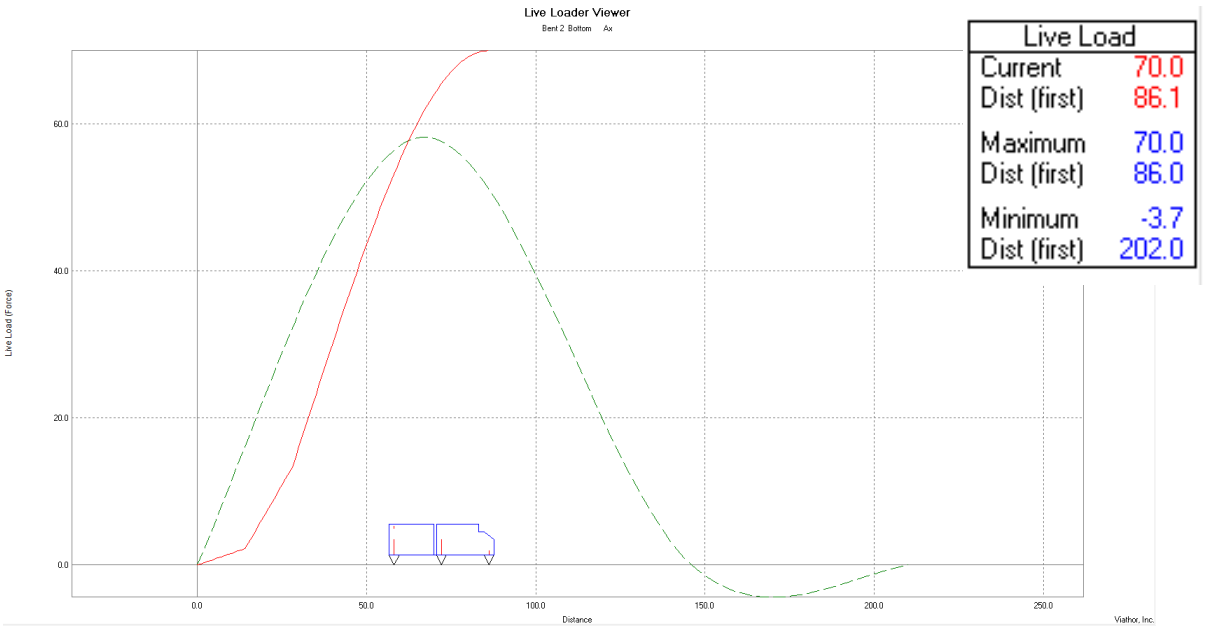

Figure 4.38: Marshall - Controlling Truck Loading Conditions for Pier Reactions

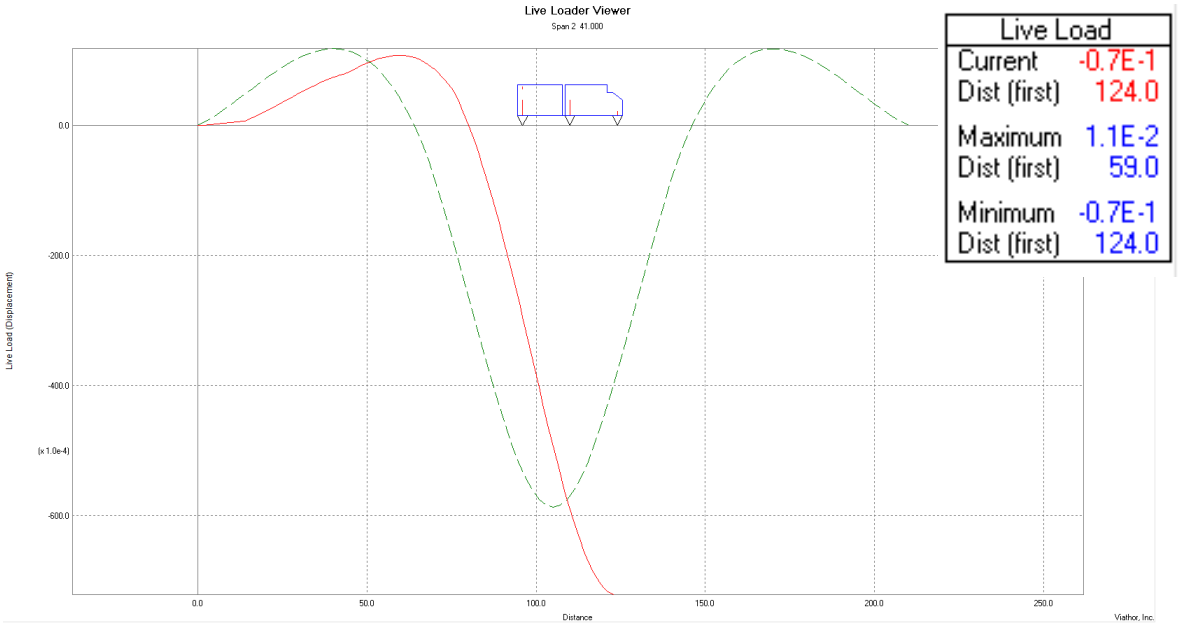

Figure 4.39: Marshall - Controlling Truck Loading Conditions for Deflection

4.2.2.3.2 Truck loading deflection

The Marshall County bridge model was loaded with the truck loading conditions discussed previously. The load allocation that corresponds with maximizing deflection at the midspan of the bridge can be seen in Figure 4.39 for the truck load and Figure 4.17 for the lane load. The load in the model can be seen in Figure 4.40. Lane load can clearly be seen marked in red in the interior span. Two concurrent 10 feet wide pressure loads were modeled in the center of the roadway. The truck load can also be seen with orange arrows indicating the location and direction. Two HS-20-44 trucks were modeled acting over each lane load location. Results for these loading conditions can be seen in Figure 4.41.

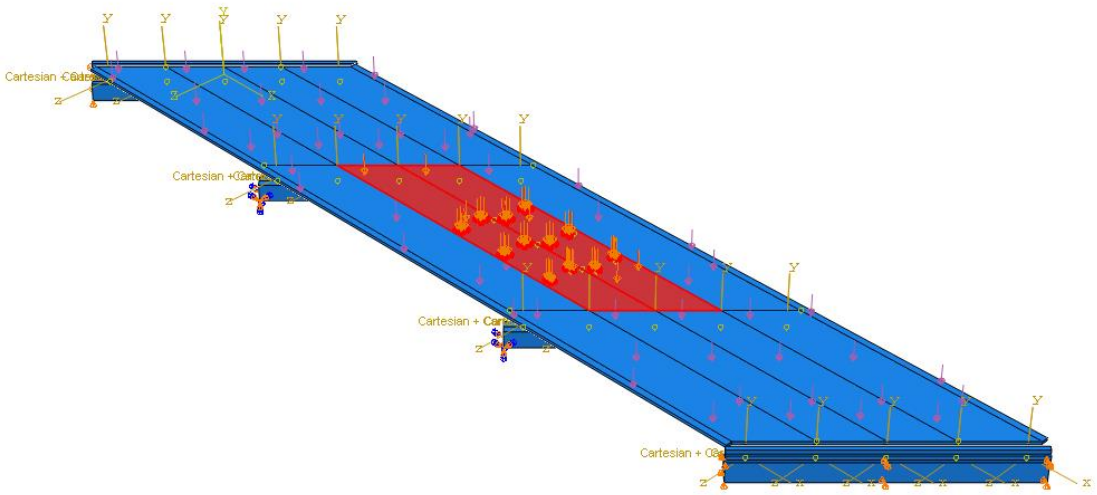

Figure 4.40: Marshall - Load Allocation for Deflection

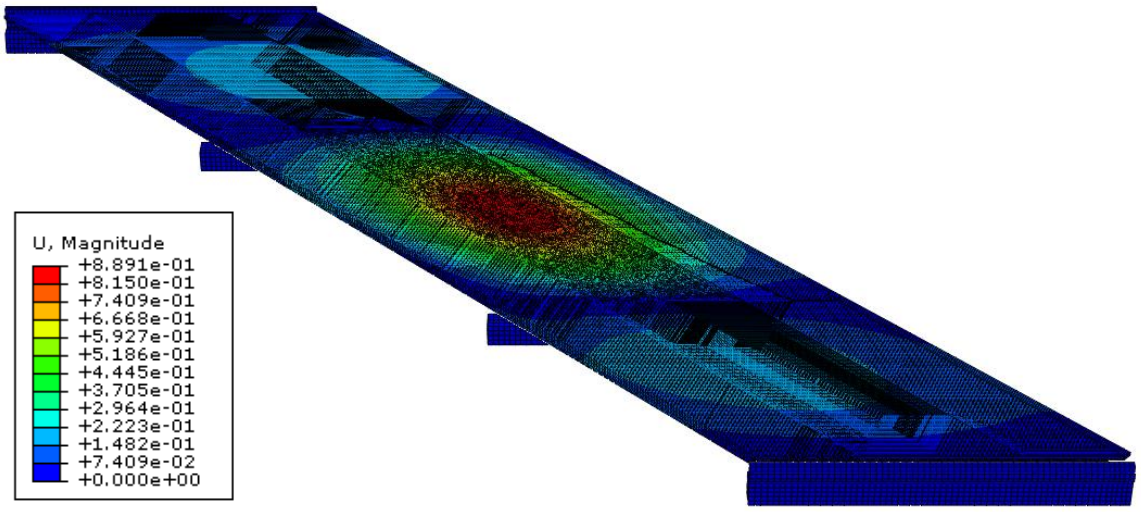

Figure 4.41: Marshall - Deformation Contour Plot for Deflection Truck Load

From the results of the FE model, a maximum deflection at midspan of approximately 1.3 inches was obtained. AASHTO Specifications provides certain deflection limits for vehicular bridges in the absence of other criteria. These limits are set as L/800 for general vehicular load and L/1000 for vehicular and pedestrian loads where L is the span where the deflection is being questioned. Since the Marshall County bridge does not have pedestrian loads, L/800 is applicable. Using the center span of the Marshall County bridge with L of 82 feet or 984 inches, the L/800 design limit come out as approximately 1.23 inches. Accounting for the dead load deflection shown previously, the live load resulted in a deflection of approximately 0.89 inches which is lower than the L/800 deflection limit.

4.2.2.3.3 Truck loading reactions

To maximize abutment and pier reactions, different truck loading allocation were needed. The load allocation that corresponds with maximizing abutment reactions can be seen in Figure 4.37 for the truck load and Figure 4.15 for the lane load. The load allocation that corresponds with maximizing pier reactions can be seen in Figure 4.38 for the truck load and Figure 4.16 for the lane load.

Firstly, the abutment reactions results will be discussed. The load in the model can be seen in Figure 4.42 marked in red. The lane load can be clearly seen in the exterior spans with the rear axle of the concentrated truck load at the edge of the bridge deck. Two HS-20-44 trucks were modeled side by side with the one side of the truck axle 2 feet from the curb. The lane loads were modeled as two concurrent 10 feet wide pressure loads starting from the curb. A deformation contour plot is provided in Figure 4.43. Maximum deformation can be clearly seen in the exterior span where the concentrated truck load is applied. Results for dead load and abutment reactions can be seen in Table 4.13. A comparison between the results obtained from the FE model with the original plans is shown.

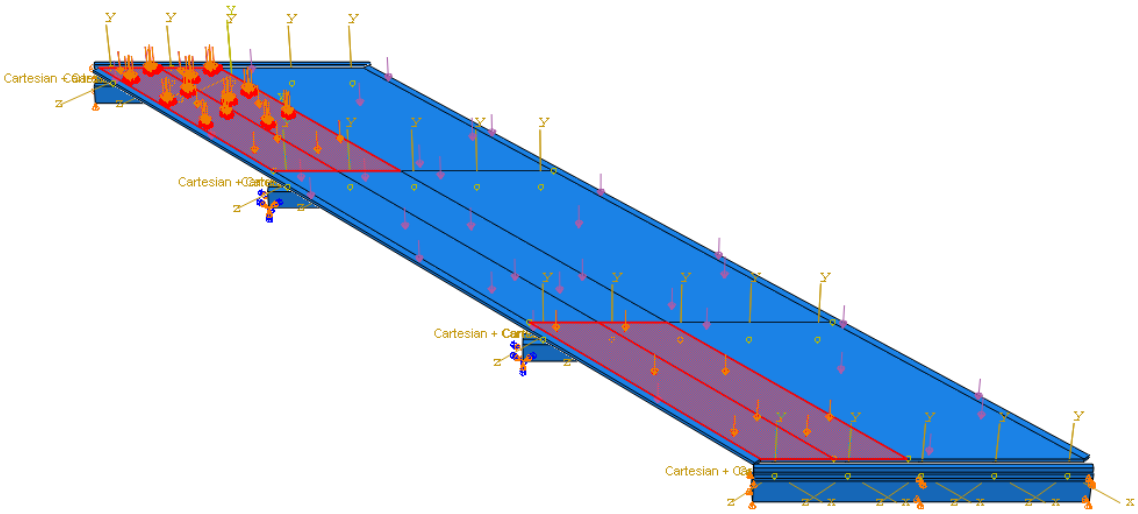

Figure 4.42: Marshall - Load Allocation for Abutment Reactions

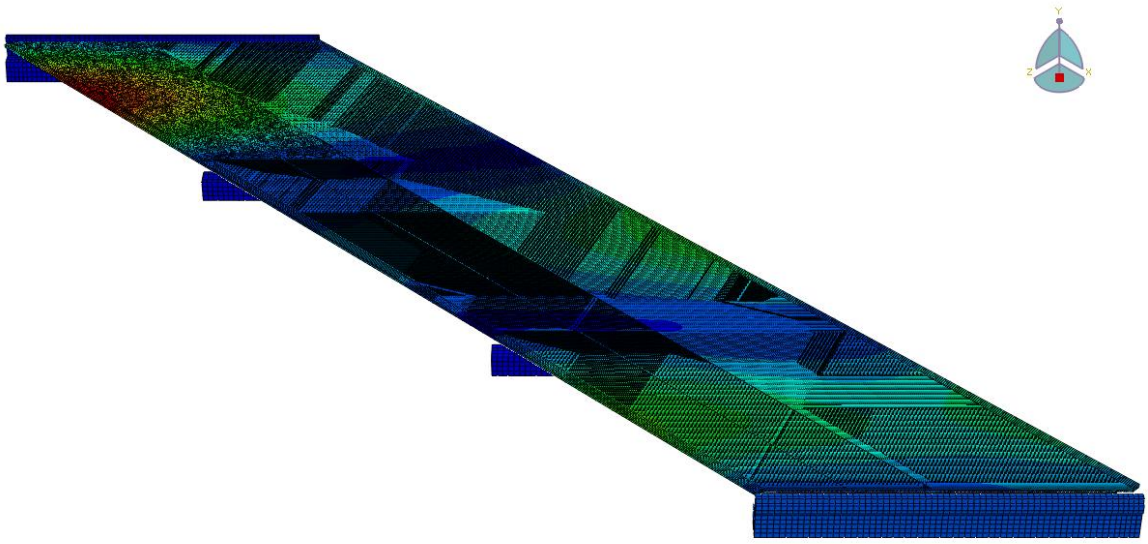

Figure 4.43: Marshall - Deformation Contour Plot for Abutment Reactions Truck Load

Table 4.13: Marshall - Dead Load and Live Load Abutment Reactions

	Abutment Reactions (kips)			
	Ext	% diff	Int	% diff
DL #1	24.10	1.65	27.90	0.36
DL #2	10.30	3.00	4.60	2.23
ULL	-	-	-	-
CLL	-	-	-	-
HS-20-44	44.50	2.41	68.49	27.07
Impact	8.12	32.32	12.98	8.62
Total	87.02	5.52	113.96	13.28

High percentages of difference were obtained in the truck loading values. The highest percentage of difference was 32.32% in the exterior support for the impact load and 27.07% in the interior support for the HS-20-44 load. These differences attribute to the percentage of difference of 5.52% and 13.28% obtained in the total load for the exterior and interior support respectively.

For the same reasons explained in the Story County bridge discussion, truck loading conditions were altered to attempt to match the drawing plan values. One truck was modeled instead of two with the impact load applied on the lane load as well. This new load allocation can be seen in Figure 4.44 with only one truck in one of the exterior spans instead of two.

Results for dead load and abutment reactions can be seen in Table 4.14. A comparison between the results obtained from the updated FE model with the original plans is shown.

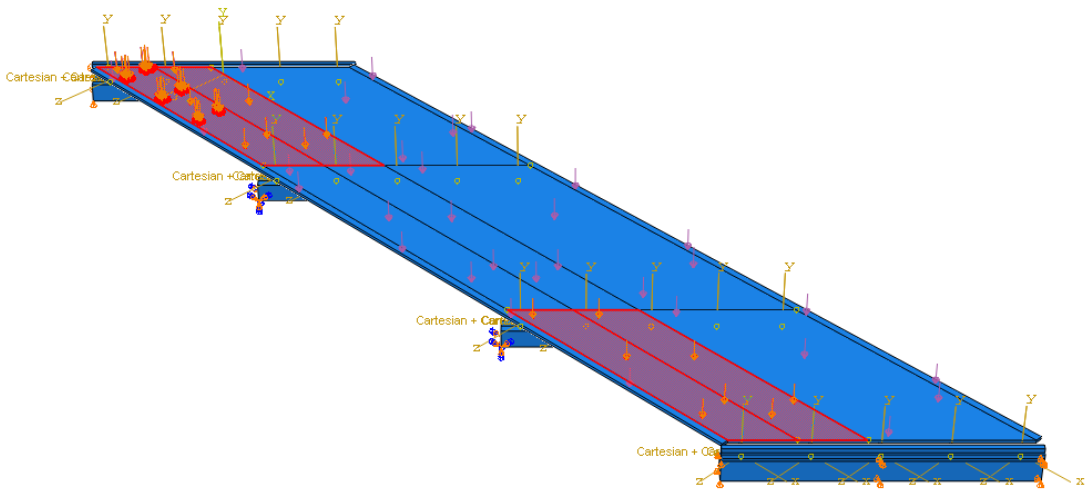

Figure 4.44: Marshall - Updated Load Allocation for Abutment Reactions

Table 4.14: Marshall - Dead Load and Updated Live Load Abutment Reactions

	Abutment Reactions (kips)			
	Ext	% diff	Int	% diff
DL #1	24.10	1.65	27.90	0.36
DL #2	10.30	3.01	4.60	2.22
ULL	-	-	-	-
CLL	-	-	-	-
HS-20-44	42.33	7.17	43.54	19.21
Impact	10.58	11.81	10.89	23.34
Total	87.31	5.20	86.93	13.59

Percentages of difference remained almost constant for the total abutment reaction of both the interior and exterior support after the truck loading conditions were altered. The total load of the interior support lowered from 113.96 kips to 86.93 kips, yet the percentage of difference increased from 13.28 % to 13.59%. Previously the load was 13.28% higher than the original plan values while with the altered truck loading the load is 13.59% lower. The total load of the exterior support remained almost constant as well. 87.02 kips in the previous model to 87.31 kips with the altered truck loading. The percentage of difference went from 5.52% to 5.20%.

The pier reactions will be discussed in the following sections. The load in the model can be seen in Figure 4.45 marked in red. The lane load can be clearly seen in the exterior spans with the rear axle of the concentrated truck load at the edge of the bridge deck. Two HS-20-44 trucks were modeled side by side with the one side of the truck axle 2 feet from the curb. The lane loads were modeled as two concurrent 10 feet wide pressure loads starting from the curb. A deformation contour plot is provided in Figure 4.46. Maximum deformation can be clearly seen in the exterior span where the concentrated truck load is applied. Results for dead load and pier reactions can be seen in Table 4.15. A comparison between the results obtained from the FE model with the original plans is shown.

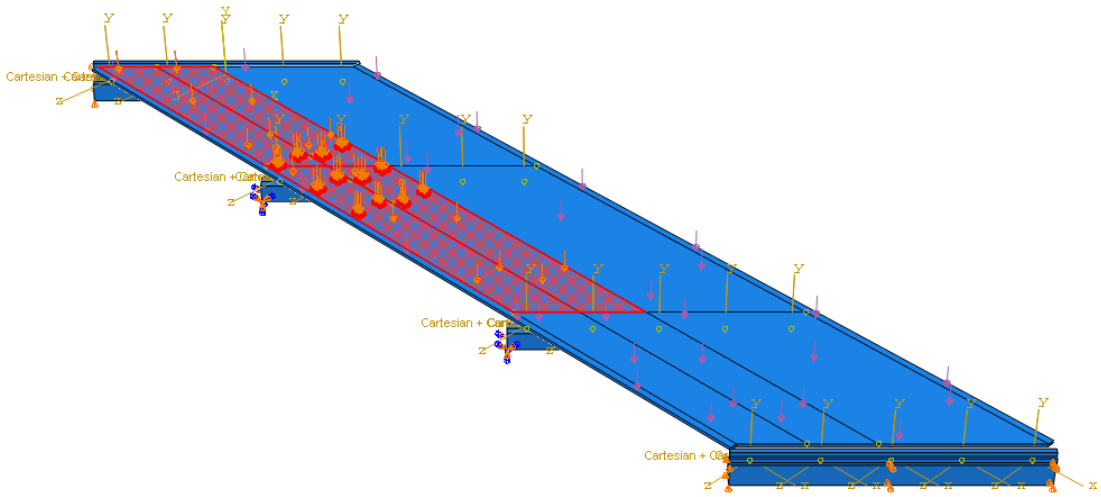

Figure 4.45: Marshall - Load Allocation for Pier Reactions

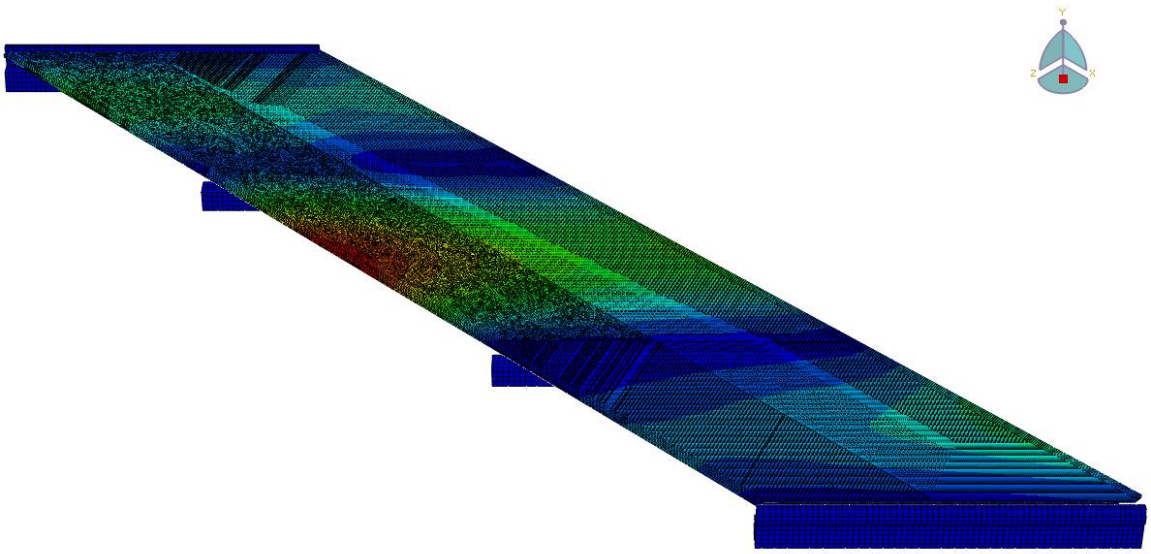

Figure 4.46: Marshall - Deformation Contour Plot for Pier Reactions Truck Load

Table 4.15: Marshall - Dead Load and Live Load Pier Reactions

	Pier Reactions (kips)			
	Ext	% diff	Int	% diff
DL #1	86.96	3.48	101.42	0.56
DL #2	33.96	1.85	16.65	2.17
ULL	39.20	7.77	49.46	1.67
CLL	43.33	116.64	76.17	221.37
HS-20-44	-	-	-	-
Impact	10.83	31.45	19.04	1.82
Total	214.28	5.56	262.74	24.52

High percentages of difference were obtained in the truck loading values. The highest percentage of difference was 221.37% in the interior support for the concentrated live load. This difference attributes to the percentage of difference of 24.52% obtained in the total load for the interior support. The exterior support also shows high percentages as well with 116.64% for the concentrated live load and 31.45% for the impact load. The total load however only amounts to a percentage of difference of 5.56%.

For the reasons explained previously, truck loading conditions were altered to attempt to match the drawing plan values. One truck was modeled instead of two with the impact load applied on the lane load as well. This new load allocation can be seen in Figure 4.47 with one truck in one of the exterior spans instead of two.

Results for dead load and pier reactions can be seen in Table 4.16. A comparison between the results obtained from the updated FE model with the original plans is shown.

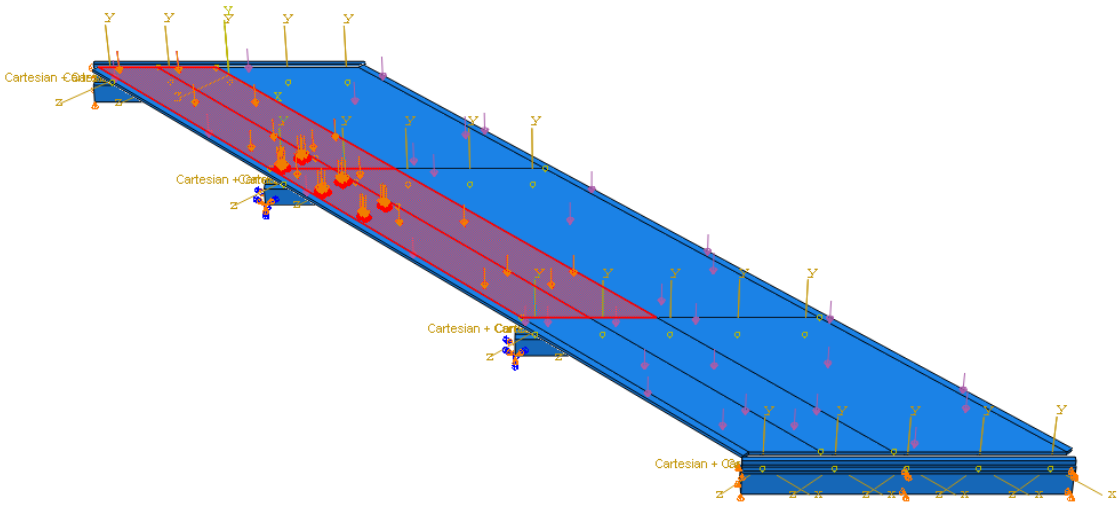

Figure 4.47: Marshall - Updated Load Allocation for Pier Reactions

Table 4.16: Marshall - Dead Load and Updated Live Load Pier Reactions

	Pier Reactions (kips)			
	Ext	% diff	Int	% diff
DL #1	87.04	3.39	101.22	0.76
DL #2	33.98	1.79	16.62	1.95
ULL	39.24	7.68	49.38	1.83
CLL	42.68	113.39	31.18	31.57
HS-20-44	-	-	-	-
Impact	20.48	29.61	20.14	7.70
Total	223.41	10.06	218.54	3.57

Percentages of difference lowered in the interior support after the truck loading conditions were altered. The concentrated live load which had a percentage of difference of 221.37% in the previous discussion, now resulted in a percentage of difference of 31.57%. The total load of the interior support lowered from 262.74 kips to 218.54 kips. The percentage of difference lowered from 24.52% to 3.57%. This difference is because the interior support is now taking only one side of the axle from the truck. Previously, the interior support took the same axle plus another axle. The exterior support did not suffer major differences. The concentrated live load went from 43.33 kips to 42.68 kips and the impact load went from 10.83 kips to 20.48 kips. The percentage of difference for the total load on the exterior support actually increased from 5.56% to 10.06%. This low difference can be due to the exterior support already taking the same axle of the truck nearest to the curb.

4.2.3 Joint And Approach Slab Modeling

The Marshall County bridge model was updated with the deck over backwall concept developed in Chapter 3. A 20 feet section was taken from the farthest abutment end in the longitudinal direction. Since the bridge is skewed 45 degrees, the other end would span a total of 64 feet. The bridge deck was extended over the abutment interface while the top of the abutment was cut off. Soil was added as a C3D8R element, an 8-node linear brick element with reduced integration and hourglass control. Three soil compositions were taken into consideration denominated as loose, moderately stiff, and stiff. Soil properties for each one are shown in Chapter 2, Table 2.2. Pertinent results are shown for all three compositions in the following pages. A 12 feet void was assumed from the abutment backwall according to Iowa DOT Office of Bridges and Structures (2018a). A 2 to 1 ratio was used for the horizontal to vertical distance of this void as shown in Chapter 2, Figure 2.36.

A full-scale view of this model can be seen in Figure 4.48. A section view of the abutment interface can be seen in Figure 4.49 and Figure 4.50. In early developments of the detailing shown in Chapter 3, Figure 3.5, options included an end span beam that encases the diaphragms. While the Marshall County bridge does not have this end span beam, the effect of it on the different points of interest across the joint and approach slab can be appreciated.

The webs of the girders were embedded into the curb and end span beam. Top flanges of the girders were also embedded into the curb. The end diaphragms were embedded into the end span beam. Tie constraints between the top flanges of all the welded plate girders and the bottom face of the bridge deck were kept from the previous model. The top flanges of the end diaphragms were constrained with the bottom face of the curb. Tie constraints were also used between the bottom face of the bridge deck and the top face of the curb. Tie constraints were also used between the bottom face of the curb and the top face of the end span beam.

Boundary conditions were kept identical to the model detailed previously for the abutment and piers. New boundary conditions were assigned to the approach slab and soil. A vertical constraint was assigned at the far edge of the approach slab. Horizontal constraints were assigned to the vertical faces of the soil. Vertical constraints were assigned to the bottom face of the soil. An additional constraint in the third direction was assigned to the skewed face of the soil. These boundary conditions can be seen in Figure 4.51 and Figure 4.52 marked in red.

A contact interaction was provided between the bottom face of the bridge deck (approach slab) and the top face of the soil. This interaction is shown in Figure 4.53. In addition, connection wires were kept between the steel girders and the abutments/piers. All reaction values presented in the following pages corresponds to these connection wires.

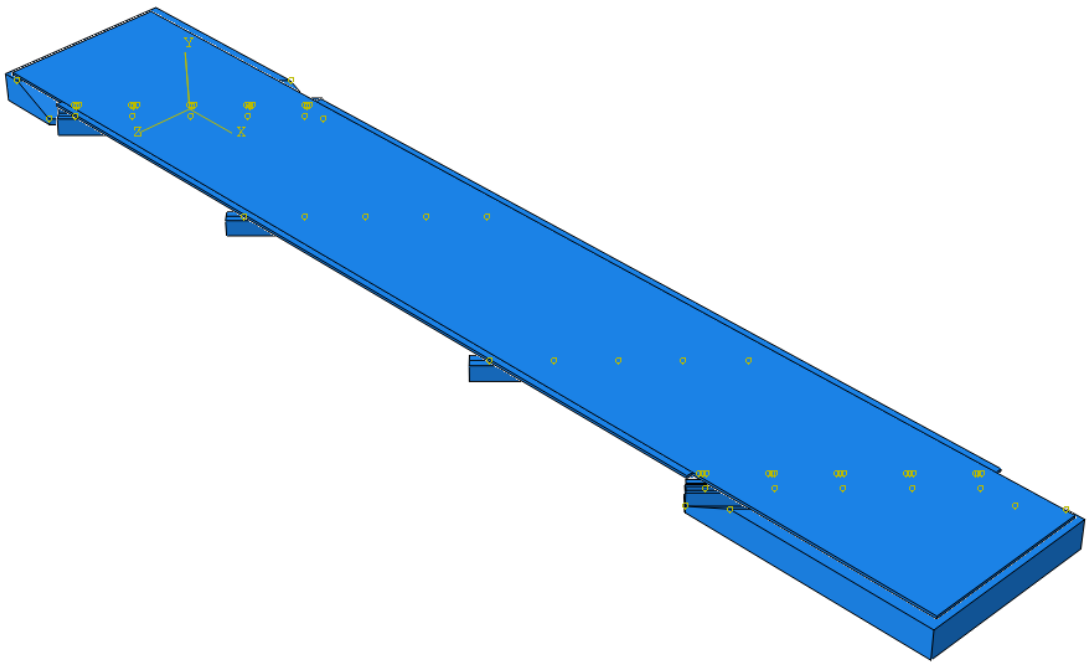

Figure 4.48: Full 3-D FE Model with Approach Slab

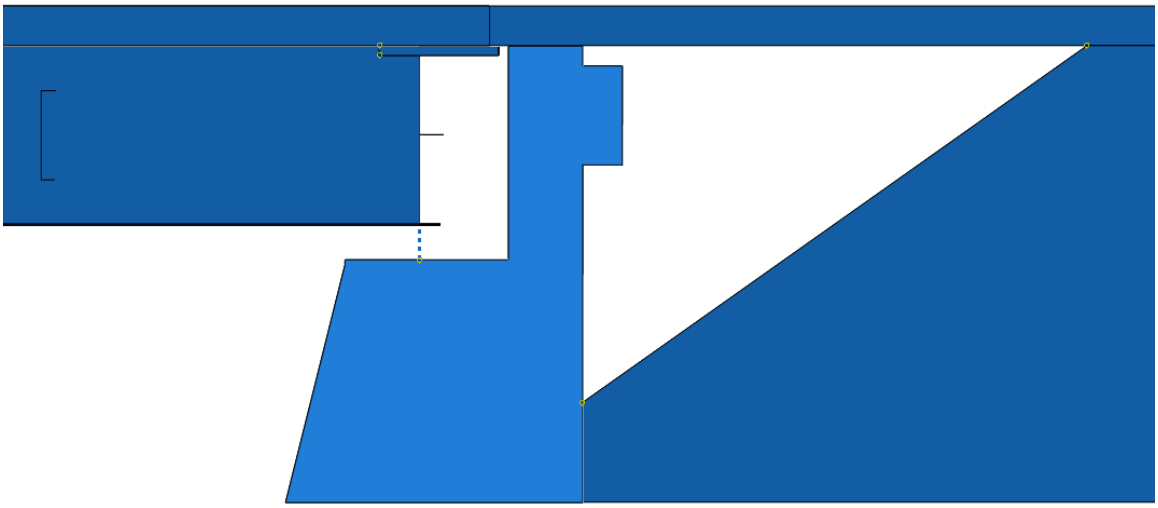

Figure 4.49: Section View without End Span Beam

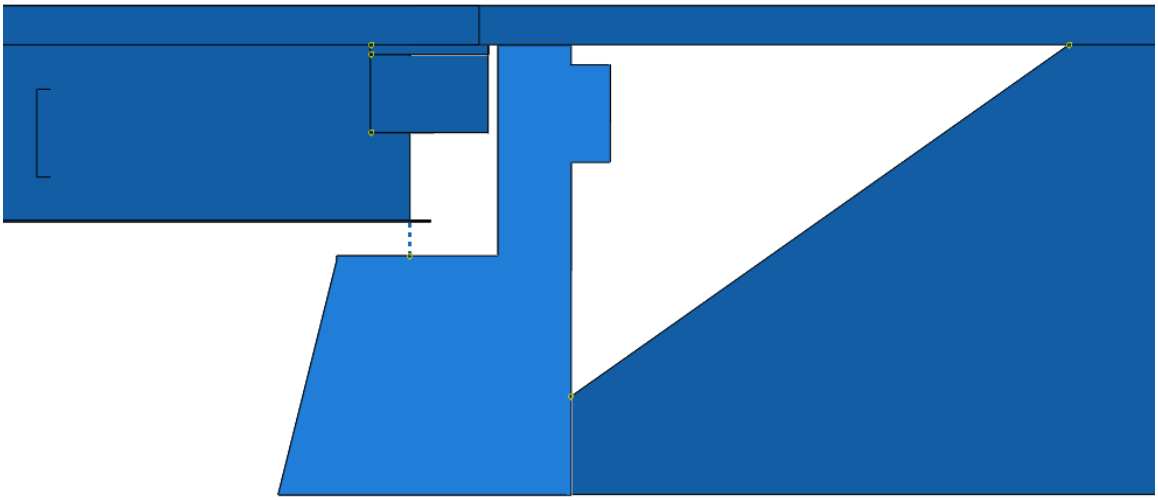

Figure 4.50: Section View with End Span Beam

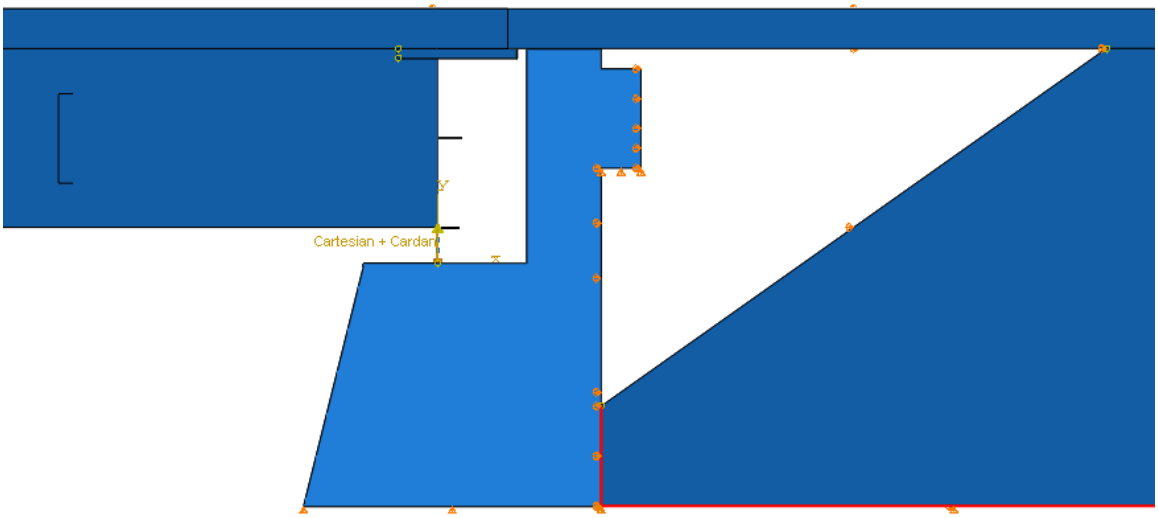

Figure 4.51: Boundary Conditions Section View

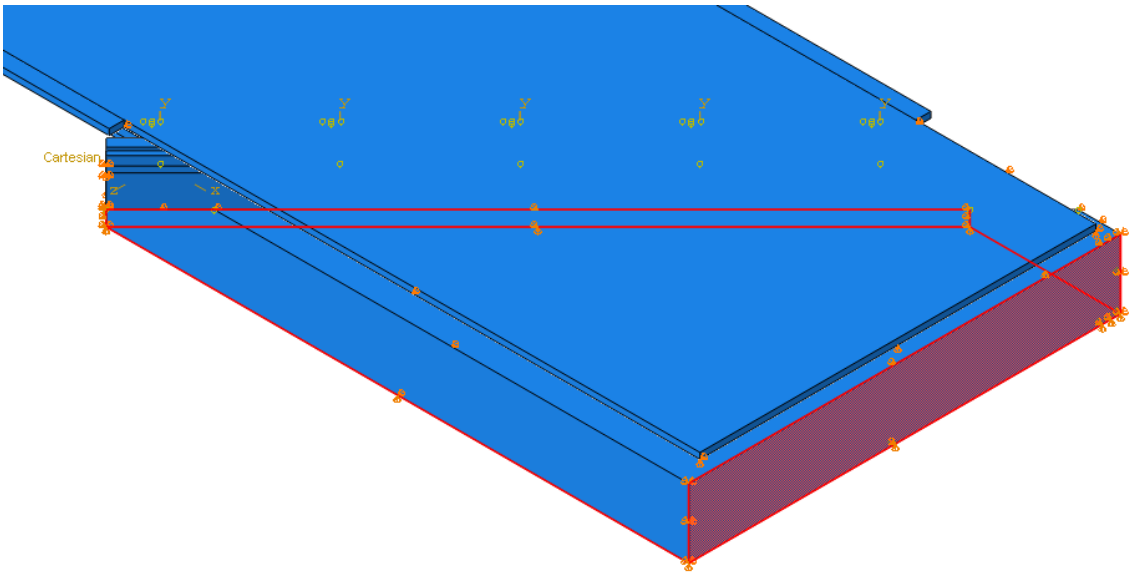

Figure 4.52: Boundary Conditions 3-D View

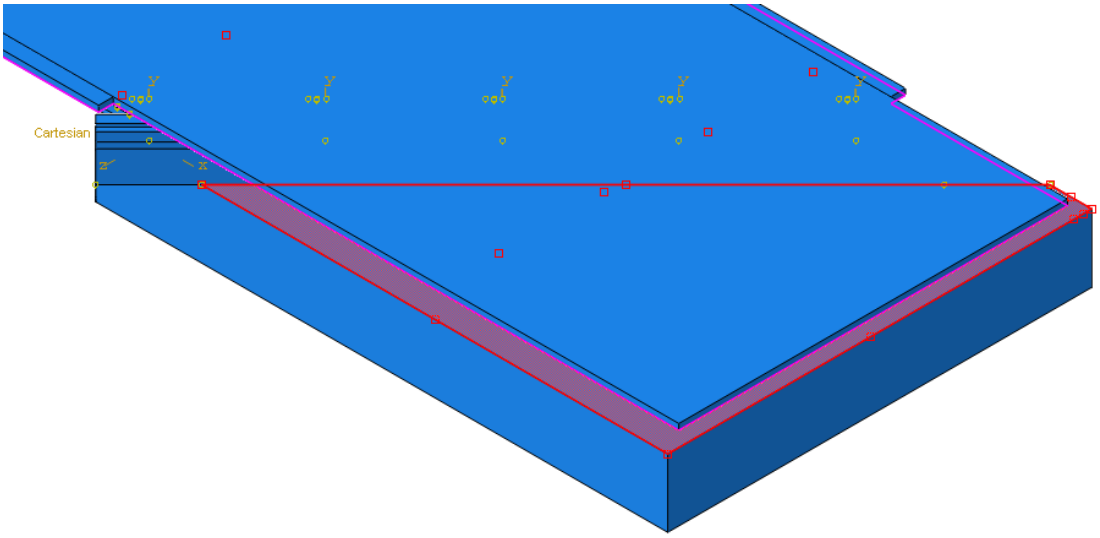

Figure 4.53: Contact Interaction

With this model, the impact of the deck over backwall concept on the existing structure can be predicted. Certain points of interest were identified for the results of the model. First and foremost, the increase in bearing loads due to the new dead load of the bridge deck will be studied. Additional load will also be taken by the bearings due to live load in the approach slab that was previously not considered. Abutment reactions from the connection wires will be studied under different dead load and live load conditions to study the bearing loads. Additionally, deformation due to temperature loading with the additional 20 feet in one end and 64 feet in the other end will also be shown. Deflection values at the abutment interface and in the midspan of the approach slab will also be discussed. In this discussion, midspan does not refer to exactly the midspan of the approach slab, but mainly the region between abutment interface and the edge support. Stress levels at the abutment interface and the midspan were also identified as points of interest. Both the top and bottom faces of the bridge deck (approach slab) will be studied.

Firstly, the dead load reactions results from the FE model will be discussed. Table 4.17 shows abutment reactions in kips for different dead loads. The first two columns, corresponding to the dead loads with no end span beam, show the original dead loads that are being transferred to the bearings on each support. The columns show the values for DL#1 and DL#2 as it has been done previously. The remaining columns show the increase in dead load for that specific element. For example, when the bridge was modeled with the end span beam, 3.53 kips, 6.06 kips, 5.93 kips, 6.33 kips, and 3.33 kips were added to the DL#1 abutment reactions for the first exterior, first interior, second interior, third interior, and second exterior supports respectively. Notice that only DL#1 is shown for the column with the end span beam section because adding this element does not affect DL#2. However, DL#2 is shown in all other columns since a larger area for FWS is provided by the top face of the approach slab.

When the approach slab was modeled with no soil, the supports showed the largest increase in dead load as expected since the bearings are taking most of the self-weight of the approach slab with only an edge support at the other end. The largest increase was seen at the middle interior support with 48.51 kips and 9.69 kips for DL#1 and DL#2. As expected, when the soil was modeled these values lowered considerably. With each increase in the soil composition, the load taken by the bearings lowered. Though the difference is minimal in some cases between a moderately stiff and a stiff soil. This relationship between the moderately stiff and stiff soil is seen constantly throughout the results presented in the following pages. The truck load might not be large enough to deform and impact a moderately stiff or stiff soil to the degree that it would affect the support the soil provides the approach slab.

The first exterior support from top to bottom of the table refers to the support closest to the 20 feet section of the approach slab. Each support consequently follows in the transversal direction until the remaining exterior support which corresponds to the 64 feet section of the approach slab.

Table 4.17: Dead Load Abutment Reactions

Support	No Beam		Beam	Approach Slab							
				No Soil		Soil					
						Loose		Moderately Stiff		Stiff	
	DL#1	DL#2	DL#1	DL#1	DL#2	DL#1	DL#2	DL#1	DL#2	DL#1	DL#2
Exterior	26.03	11.09	3.53	10.15	1.17	10.51	0.69	5.72	0.41	5.19	0.38
Interior	30.73	5.00	6.06	40.59	7.88	19.65	2.68	14.89	2.42	14.40	2.37
Interior	31.16	5.32	5.93	48.51	9.69	18.22	2.57	13.26	2.31	12.73	2.27
Interior	30.83	5.17	6.33	37.07	7.46	18.20	2.61	12.76	2.18	12.11	2.13
Exterior	27.82	10.70	3.33	7.53	1.04	8.30	1.13	7.80	1.06	7.71	1.06

All possible combinations of dead load scenarios can be seen in Figure 4.54. It can be seen in the figure that most combinations would fall on a range of approximately 40 kips to 60 kips. Most of the lower values would correspond to exterior reactions while the higher values would correspond to interior reactions. The highest values, over 80 kips, correspond to scenarios with no soil supporting. The realistic values would fall under the 40 kips to 60 kips range mentioned previously. Two steps can be seen in the horizontal axis where each step corresponds to a different loading case. The first step corresponds to combinations of DL#1 and the second step corresponds to the additional load from the combinations of DL#2.

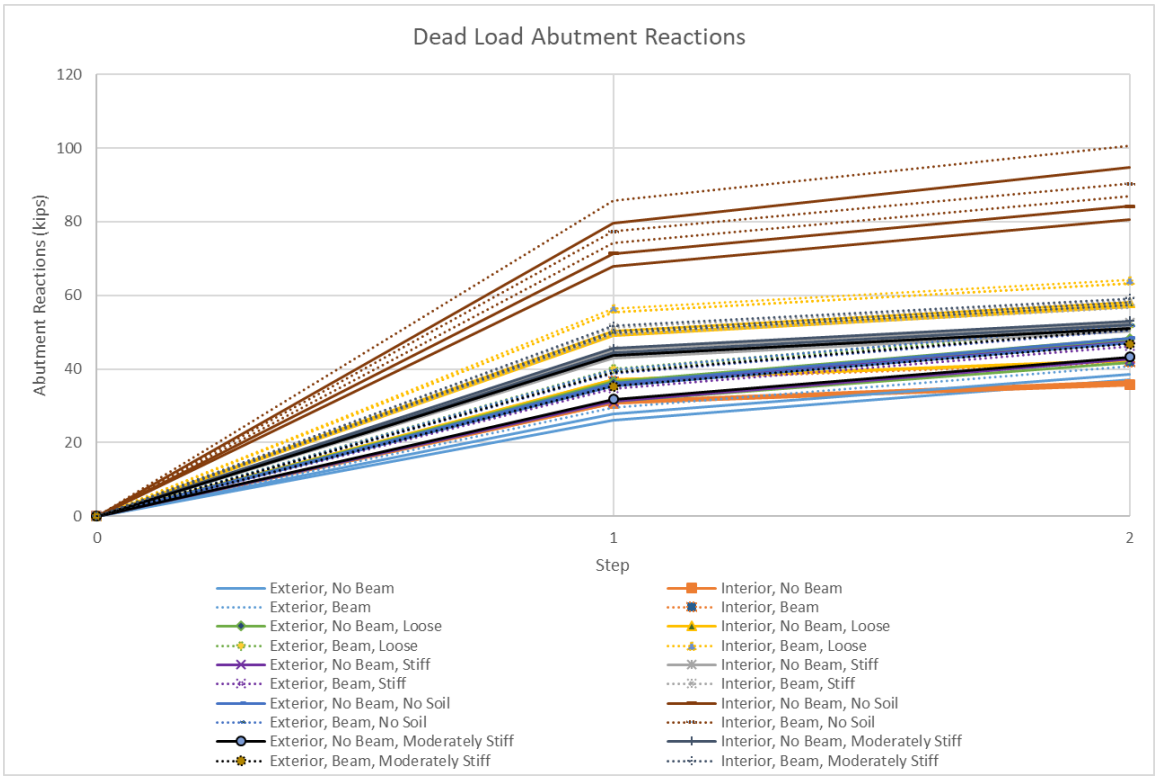

Figure 4.54: Dead Load Abutment Reactions

Temperature loading was also included in this FE model. Results from the previous FE model can be seen in Figure 4.34. A maximum deformation of approximately 0.3 inches was obtained from that model. Results for the model with the approach slab are shown in Figure 4.55. As it can be seen in the figure, a maximum deformation of approximately 0.46 inches was obtained. This presents an increment of approximately 0.16 inches. Comparing this value of 0.16 inches to the value obtained from Equation (1), approximately 0.17 inches, the FE result closely match the one obtained from the equation. A percentage of difference of approximately 4% can be obtained from the exact value using the result from the equation as the base value.

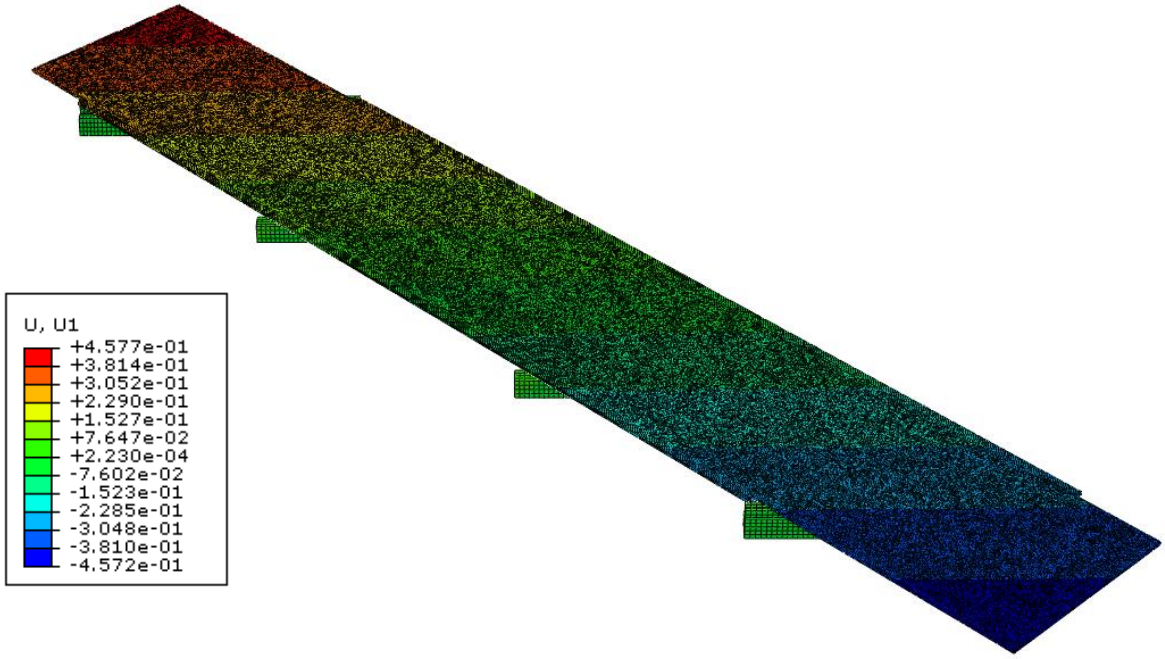

Figure 4.55: Deformation Contour Plot for Temperature Loading

To study the additional bearing loads due to live loads in the approach slab, different live load configurations were modeled acting in the top face of the approach slab. Different live load configurations were modeled as different truck loading allocations. The different truck cases are detailed in Chapter 7, Figure 7.5, Figure 7.6, Figure 7.7, and Figure 7.8. In total, four cases were considered. Figure 4.56, Figure 4.57, Figure 4.58, and Figure 4.59 show the truck load allocation in the FE model for Case 1, Case 2, Case 3, and Case 4 respectively. The truck load can clearly be seen marked in red in the various figures. Truck loading conditions were modeled as they were previously and detailed in 4.1.2.3, Figure 4.9 and Figure 4.10. Only the concentrated live load from the tires was considered in this study. Though, impact values can be calculated based on a fraction of the results obtained. This would apply not only for live load reactions but for deflection and stress values as well.

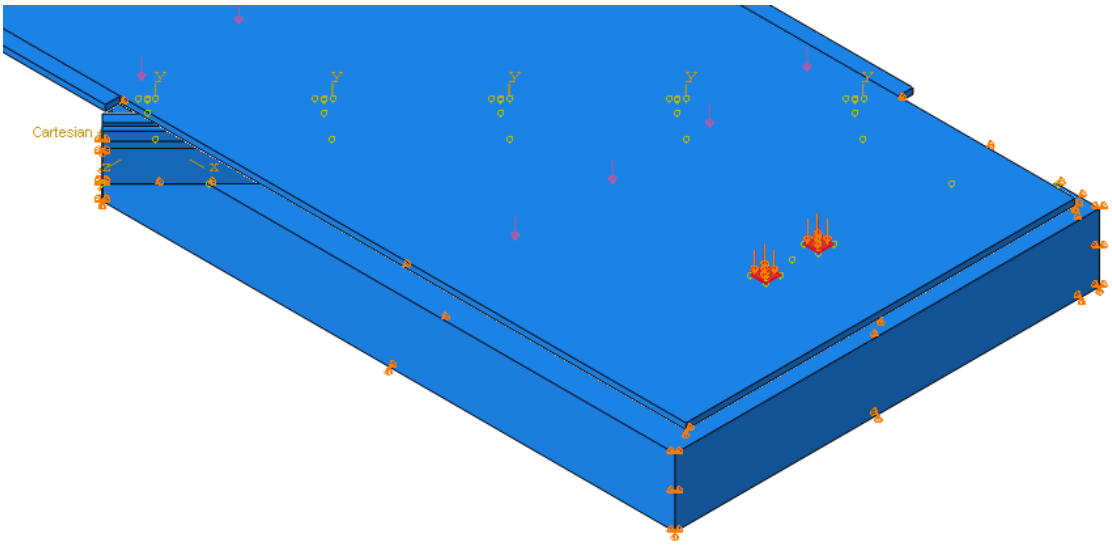

Figure 4.56: Case 1 - Truck Load Allocation

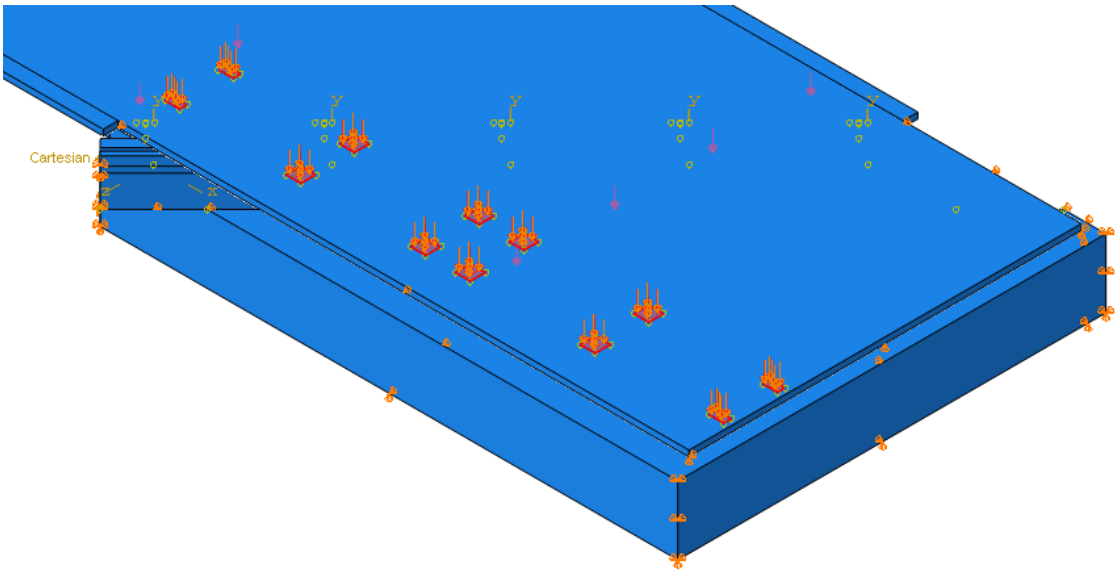

Figure 4.57: Case 2 - Truck Load Allocation

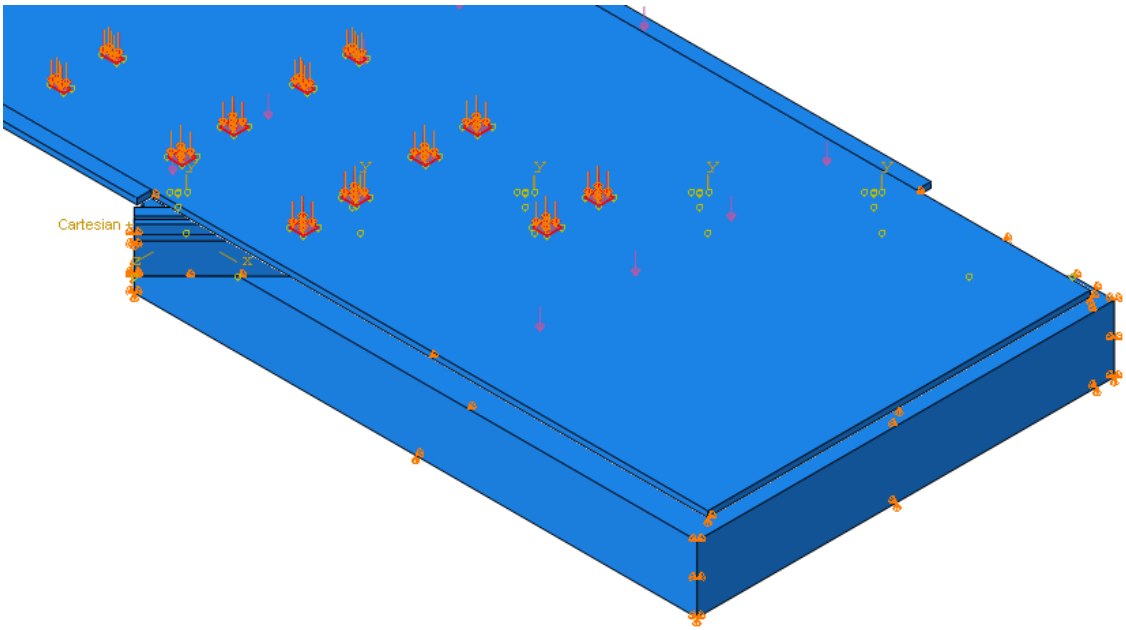

Figure 4.58: Case 3 - Truck Load Allocation

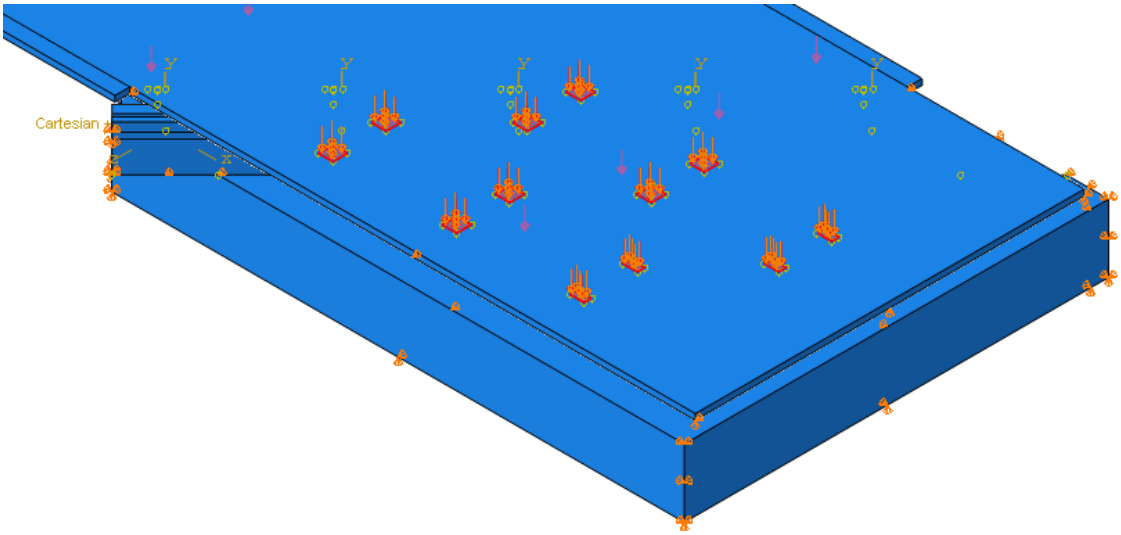

Figure 4.59: Case 4 - Truck Load Allocation

Results for live load abutment reactions in kips are shown in Table 4.18, Table 4.19, Table 4.20, and Table 4.21 for Case 1, Case 2, Case 3, and Case 4 respectively. Figure 4.60 shows a bar graph with all the values being compared.

Table 4.18: Case 1 - Live Load Abutment Reactions

Support	No Beam				Beam			
	Soil			No Soil	Soil			No Soil
	Loose	Moderately Stiff	Stiff		Loose	Moderately Stiff	Stiff	
Exterior	-0.25	-0.13	-0.07	3.08	-0.26	-0.16	-0.09	4.33
Interior	-0.31	-0.12	-0.07	8.41	-0.30	-0.12	-0.07	7.45
Interior	-0.19	-0.01	-0.01	4.71	-0.20	-0.02	-0.01	4.74
Interior	-0.01	-0.01	0.00	1.41	-0.03	0.00	0.00	1.54
Exterior	0.00	0.00	0.00	-0.11	0.00	0.00	0.00	0.14

Table 4.19: Case 2 - Live Load Abutment Reactions

Support	No Beam				Beam			
	Soil			No Soil	Soil			No Soil
	Loose	Moderately Stiff	Stiff		Loose	Moderately Stiff	Stiff	
Exterior	-0.34	-0.01	0.00	-8.08	-0.80	-0.24	-0.20	-7.89
Interior	-2.07	-1.03	-0.87	15.03	-1.92	-1.22	-1.10	17.10
Interior	4.02	1.69	1.48	54.56	5.73	3.24	2.98	53.76
Interior	24.15	20.38	19.76	69.65	23.23	19.46	18.90	63.70
Exterior	7.02	6.41	6.24	8.30	8.97	7.93	7.72	14.32

Table 4.20: Case 3 - Live Load Abutment Reactions

Support	No Beam				Beam			
	Soil			No Soil	Soil			No Soil
	Loose	Moderately Stiff	Stiff		Loose	Moderately Stiff	Stiff	
Exterior	-1.55	-1.36	-1.31	-2.11	-1.82	-1.60	-1.56	-2.30
Interior	10.33	10.08	10.02	11.27	11.46	11.35	11.31	12.11
Interior	41.56	40.61	40.36	44.88	41.58	40.82	40.62	43.91
Interior	47.44	45.78	45.46	51.62	47.84	46.31	46.05	50.25
Exterior	24.20	23.65	23.53	24.67	26.41	25.72	25.59	26.84

Table 4.21: Case 4 - Live Load Abutment Reactions

Support	No Beam				Beam			
	Soil			No Soil	Soil			No Soil
	Loose	Moderately Stiff	Stiff		Loose	Moderately Stiff	Stiff	
Exterior	-2.28	-1.49	-1.36	-5.73	-2.51	-1.79	-1.67	-4.46
Interior	11.31	8.27	7.74	33.82	12.45	9.31	8.76	34.73
Interior	26.44	22.38	21.76	67.83	26.84	22.62	21.97	65.72
Interior	17.00	12.96	12.25	51.72	18.28	14.05	13.36	48.91
Exterior	1.17	0.47	0.33	2.58	2.54	1.30	1.09	6.97

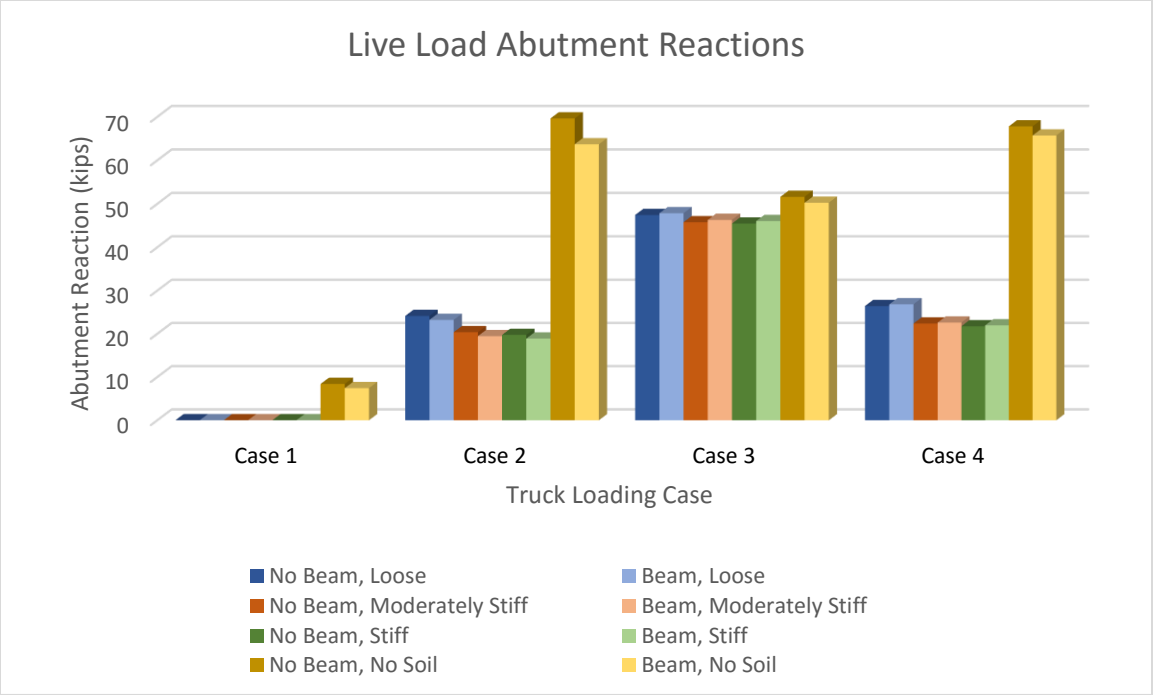

Figure 4.60: Live Load Abutment Reactions

When modeled with soil, Case 1 did not increase the live load abutment reaction of any support. This is due to the load being supported by the soil directly. In all other cases modeled with soil, the live load abutment reaction increased significantly in some of the supports. Case 3 showed the highest live load abutment reactions, with 47.84 kips and 26.41 kips for the third interior support and second exterior support respectively. This is expected since this truck allocation is the closest to the abutment interface. This case is similar to the controlling load case for abutment reactions shown in 4.2.2.3.1, Figure 4.37. It can clearly be seen how the live load reactions lowers as the soil composition increases. Also, no major difference can be seen from the models with and without an end span beam. The largest difference was seen for Case 3 on the third interior support with no soil, approximately 6 kips of difference. For the most part, values changed by less than 2 kips on cases with soil with higher values for cases without soil.

Results for deflection values in inches are shown in Table 4.22, Table 4.23, Table 4.24, and Table 4.25 for Case 1, Case 2, Case 3, and Case 4 respectively. Figure 4.61, Figure 4.62, Figure 4.63, and Figure 4.64 show bar graphs with all the values being compared.

Table 4.22: Case 1 - Deflection Values

Location	No Beam				Beam			
	Soil			No Soil	Soil			No Soil
	Loose	Moderately Stiff	Stiff		Loose	Moderately Stiff	Stiff	
Midspan	-0.28	-0.06	-0.04	-3.46	-0.28	-0.06	-0.04	-3.19
Abutment	-0.09	-0.03	-0.03	-0.27	-0.05	-0.02	-0.02	-0.17

Table 4.23: Case 2 - Deflection Values

Location	No Beam				Beam			
	Soil			No Soil	Soil			No Soil
	Loose	Moderately Stiff	Stiff		Loose	Moderately Stiff	Stiff	
Midspan	-0.32	-0.07	-0.06	-6.50	-0.32	-0.06	-0.04	-6.01
Abutment	-0.09	-0.04	-0.04	-0.51	-0.05	-0.03	-0.02	-0.31

Table 4.24: Case 3 - Deflection Values

Location	No Beam				Beam			
	Soil			No Soil	Soil			No Soil
	Loose	Moderately Stiff	Stiff		Loose	Moderately Stiff	Stiff	
Midspan	-0.21	-0.04	-0.03	-3.15	-0.21	-0.04	-0.03	-2.87
Abutment	-0.09	-0.05	-0.05	-0.28	-0.05	-0.03	-0.03	-0.17

Table 4.25: Case 4 - Deflection Values

Location	No Beam				Beam			
	Soil			No Soil	Soil			No Soil
	Loose	Moderately Stiff	Stiff		Loose	Moderately Stiff	Stiff	
Midspan	-0.28	-0.07	-0.06	-5.32	-0.28	-0.06	-0.05	-4.85
Abutment	-0.09	-0.05	-0.05	-0.51	-0.06	-0.03	-0.03	-0.31

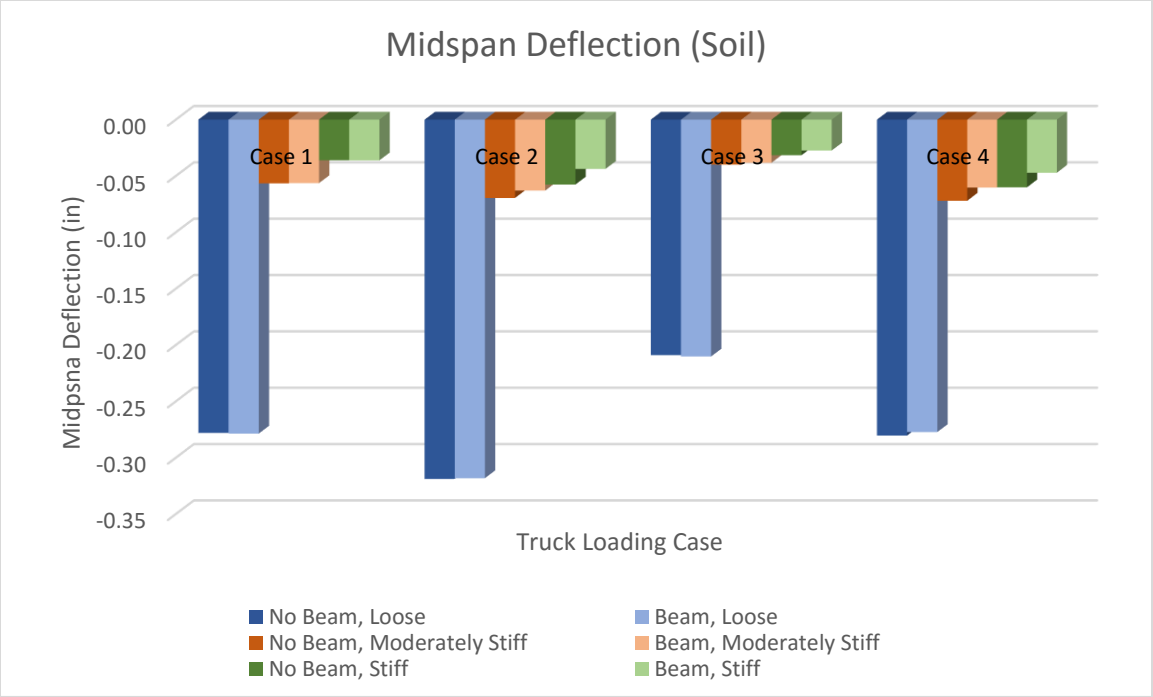

Figure 4.61: Midspan Deflection Values with Soil

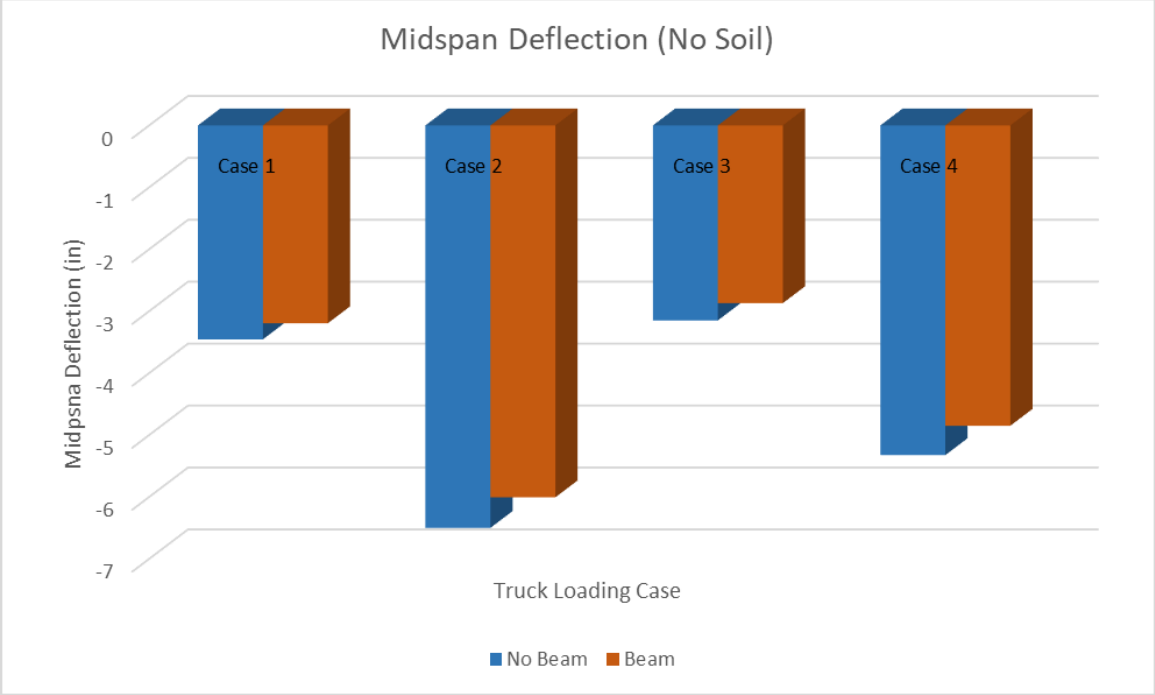

Figure 4.62: Midspan Deflection Values without Soil

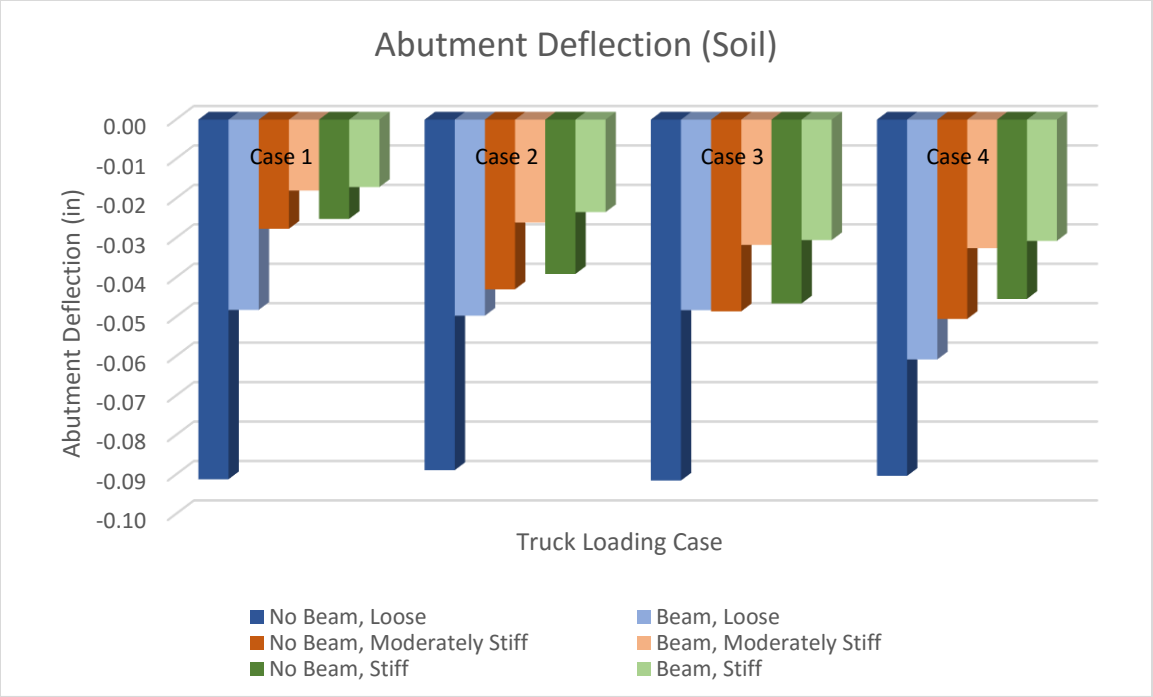

Figure 4.63: Abutment Deflection Values with Soil

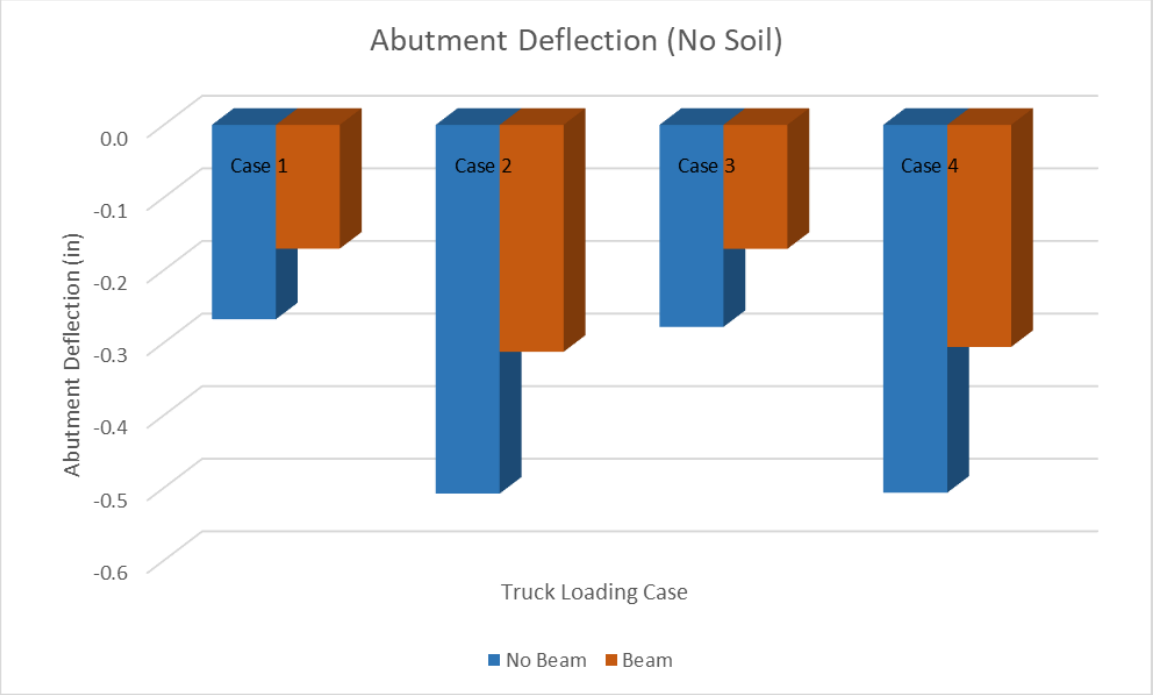

Figure 4.64: Abutment Deflection Values without Soil

Similar behavior was followed across all values obtained for deflection values at the abutment interface and at the midspan of the approach slab. The highest midspan deflection for loose soil was obtained for Case 2 with a value of 0.32 inches. For moderately stiff and stiff soil the highest value dropped to 0.07 inches and 0.06 inches respectively. As for the abutment interface deflection, the highest value for loose soil was 0.09 inches across all truck loading cases. Values differed when modeled with moderately stiff and stiff soil from 0.03 inches to 0.05 inches.

Models with no soil resulted in values 10 and 20 times over the loose soil results and in some cases 100 times over the moderately stiff and stiff soil results. Models with an end span beam resulted in equal or lower deflections values than models without the element at both the abutment interface and midspan of the approach slab. Though the difference is minimal for values obtained at the midspan of the approach slab, where only four of the 24 results for midspan deflections with soil being modeled changed. The effect of the end span beam can be seen on deflection values in the abutment interface however. Some values dropped by 40% when modeled with the end span beam. For example, the deflection at the abutment interface for all truck loading cases with the exception of Case 4 lowered from 0.09 inches to 0.05 inches.

With these values, the 2-inch grout pad in the Iowa DOT joint discussed in Chapter 3, Figure 3.7, between the approach slab and the top face of the abutment is more than enough to confidently implement the deck over backwall concept. The abutment was not designed to support the excess dead load and live load that comes with this design. Ideally, a 2-inch grout pad should prevent most of the dead and live load and stress levels to be transferred from one element to another.

Results for stress levels in psi are shown in Table 4.26, Table 4.27, Table 4.28, and Table 4.29 for Case 1, Case 2, Case 3, and Case 4 respectively. Figure 4.65, Figure 4.66, Figure 4.67, Figure 4.68, Figure 4.69, Figure 4.70, Figure 4.71, and Figure 4.72 show bar graphs with all the values being compared. The values shown correspond to von Mises stress levels on the different points of interest across the joint and approach slab.

Table 4.26: Case 1 - Stress Values (psi)

Location		No Beam				Beam			
		Soil			No Soil	Soil			No Soil
		Loose	Moderately Stiff	Stiff		Loose	Moderately Stiff	Stiff	
Midspan	Top	285.4	132.7	132.5	1125.0	289.9	157.4	158.8	1047.0
	Bottom	332.5	176.7	176.6	1125.0	361.5	157.4	158.8	1047.0
Abutment	Top	568.1	396.7	397.0	1499.0	433.0	392.9	317.3	1569.0
	Bottom	473.8	308.7	308.8	1499.0	433.0	314.4	317.3	1569.0

Table 4.27: Case 2 - Stress Values (psi)

Location		No Beam				Beam			
		Soil			No Soil	Soil			No Soil
		Loose	Moderately Stiff	Stiff		Loose	Moderately Stiff	Stiff	
Midspan	Top	245.9	132.7	132.5	1706.0	227.5	169.6	172.1	1507.0
	Bottom	245.9	176.6	132.5	1706.0	302.1	169.6	172.1	1507.0
Abutment	Top	586.4	484.5	440.9	2680.0	600.7	423.4	429.8	3013.0
	Bottom	586.4	440.5	440.9	2923.0	675.4	423.4	429.8	3013.0

Table 4.28: Case 3 - Stress Values (psi)

Location		No Beam				Beam			
		Soil			No Soil	Soil			No Soil
		Loose	Moderately Stiff	Stiff		Loose	Moderately Stiff	Stiff	
Midspan	Top	222.4	78.5	79.0	810.1	236.9	126.5	127.4	704.2
	Bottom	222.4	78.5	79.0	810.1	236.9	126.5	127.4	704.2
Abutment	Top	589.9	469.8	473.2	1617.0	588.7	504.7	508.8	1687.0
	Bottom	589.9	469.8	473.2	1617.0	588.7	504.7	508.8	1687.0

Table 4.29: Case 4 - Stress Values (psi)

Location		No Beam				Beam			
		Soil			No Soil	Soil			No Soil
		Loose	Moderately Stiff	Stiff		Loose	Moderately Stiff	Stiff	
Midspan	Top	254.9	176.9	176.8	1301.0	292.2	238.5	240.7	1129.0
	Bottom	305.3	176.9	176.8	1301.0	292.2	238.5	240.7	1129.0
Abutment	Top	607.8	441.1	397.3	2382.0	652.9	397.2	401.0	2481.0
	Bottom	607.8	397.0	397.3	2599.0	652.9	476.5	401.0	2706.0

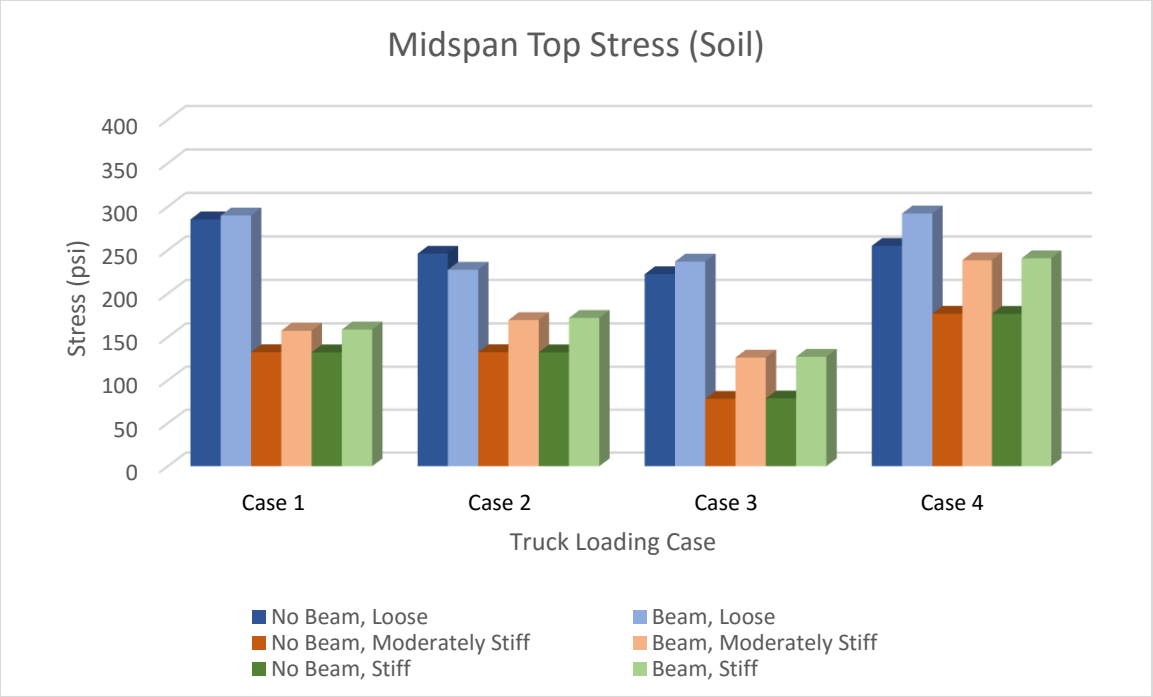

Figure 4.65: Midspan Top Stress Values with Soil

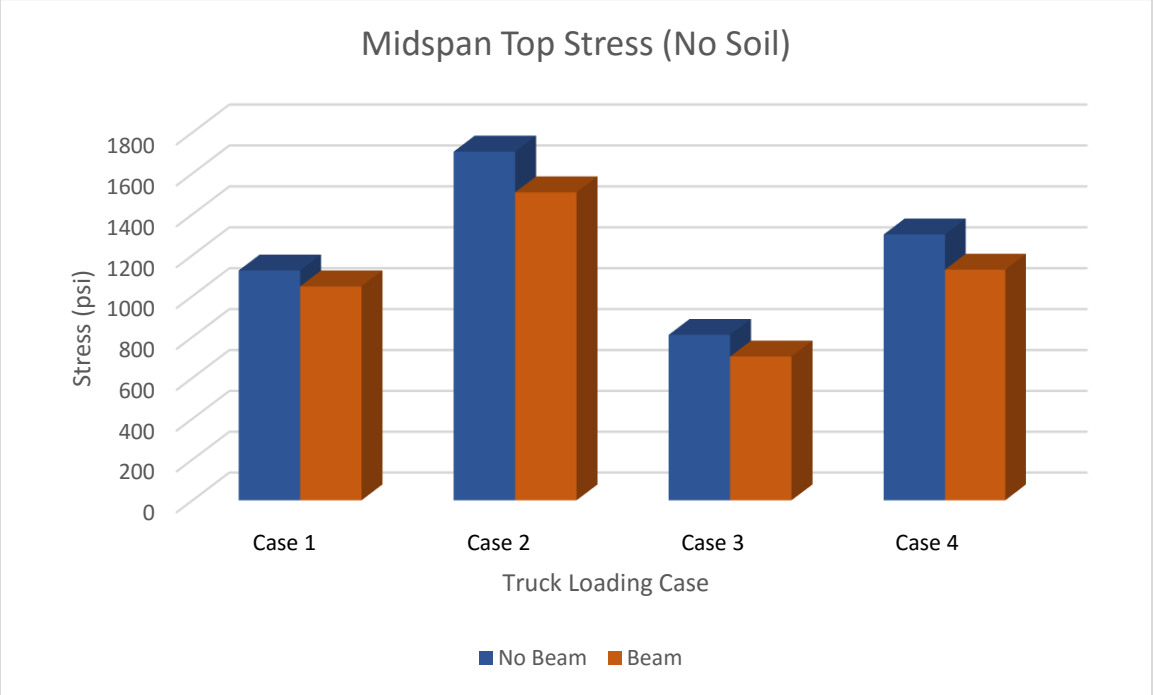

Figure 4.66: Midspan Top Stress Values without Soil

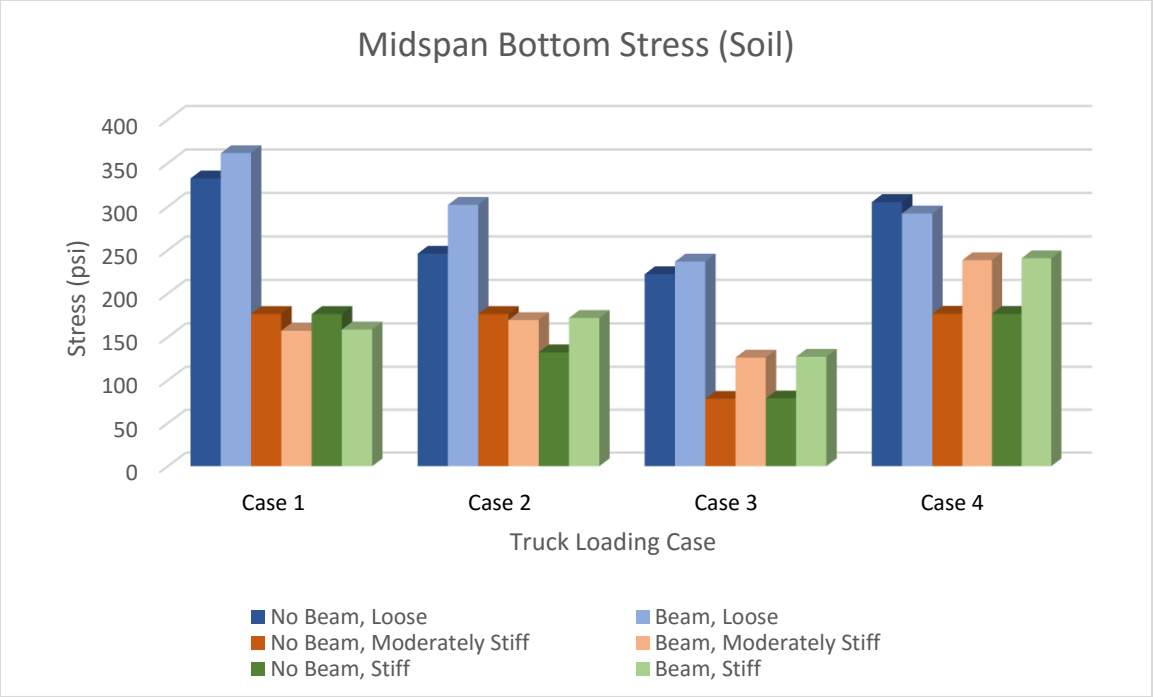

Figure 4.67: Midspan Bottom Stress Values with Soil

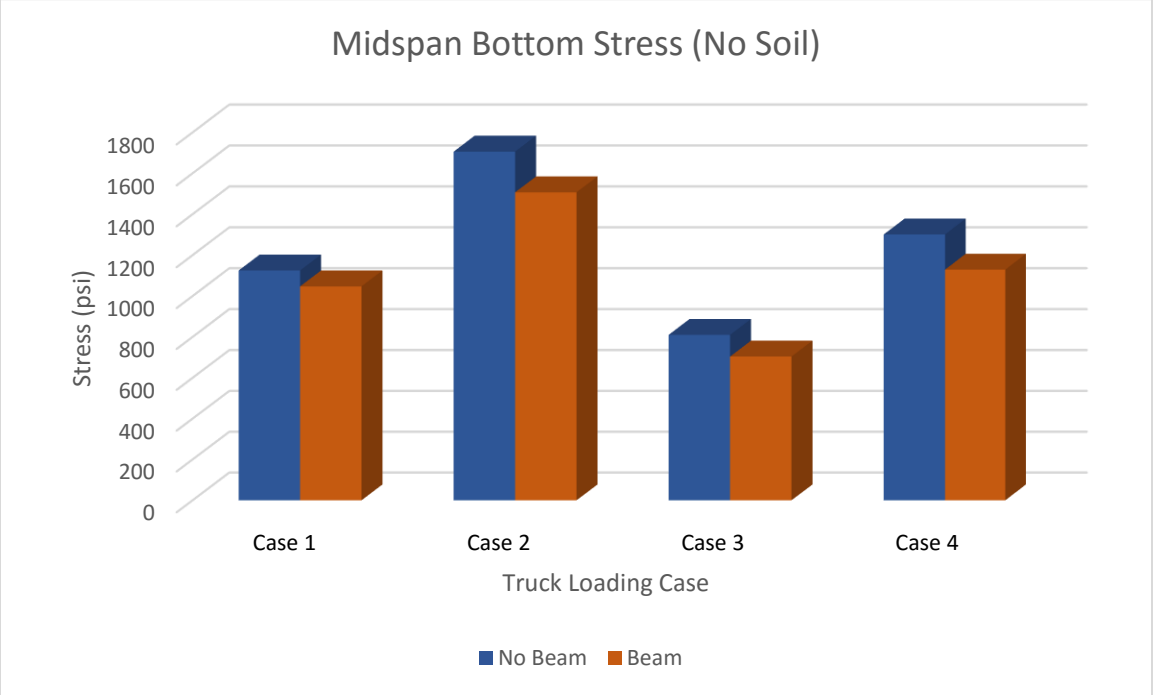

Figure 4.68: Midspan Bottom Stress Values without Soil

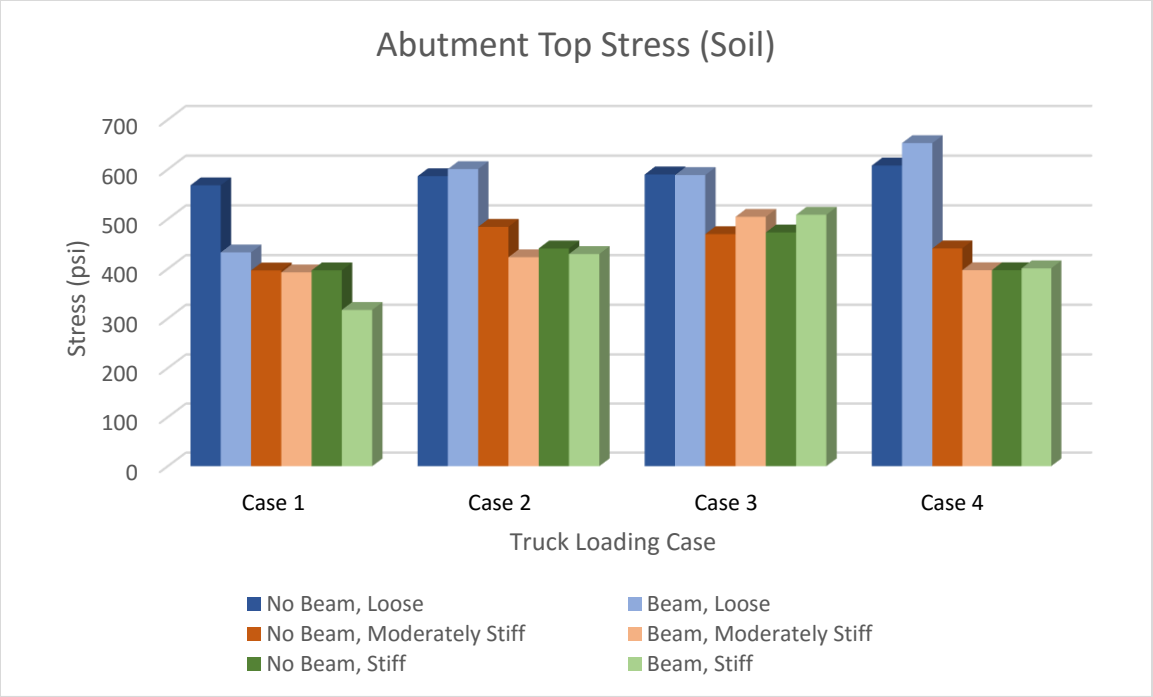

Figure 4.69: Abutment Top Stress Values with Soil

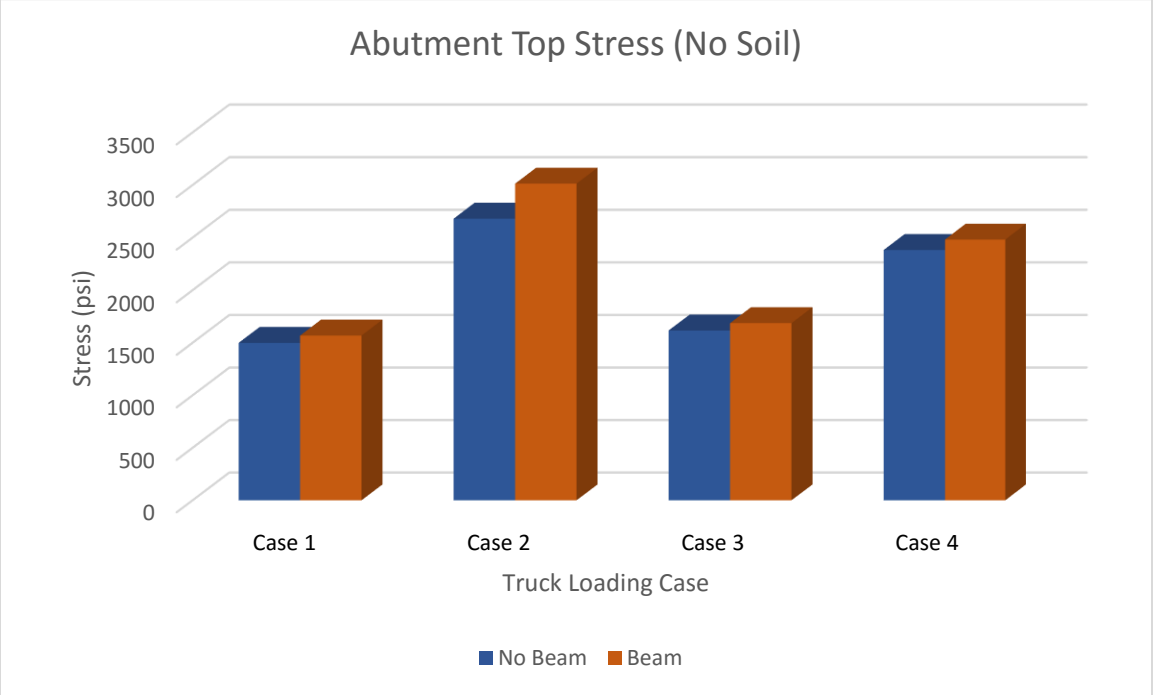

Figure 4.70: Abutment Top Stress Values without Soil

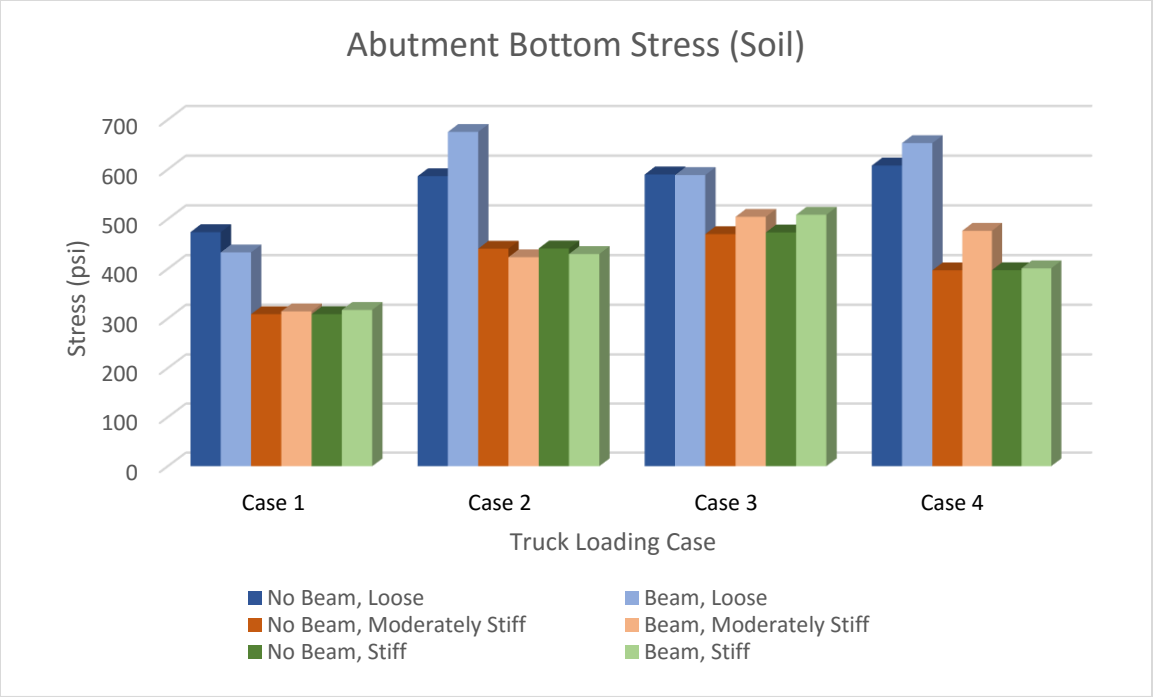

Figure 4.71: Abutment Bottom Stress Values with Soil

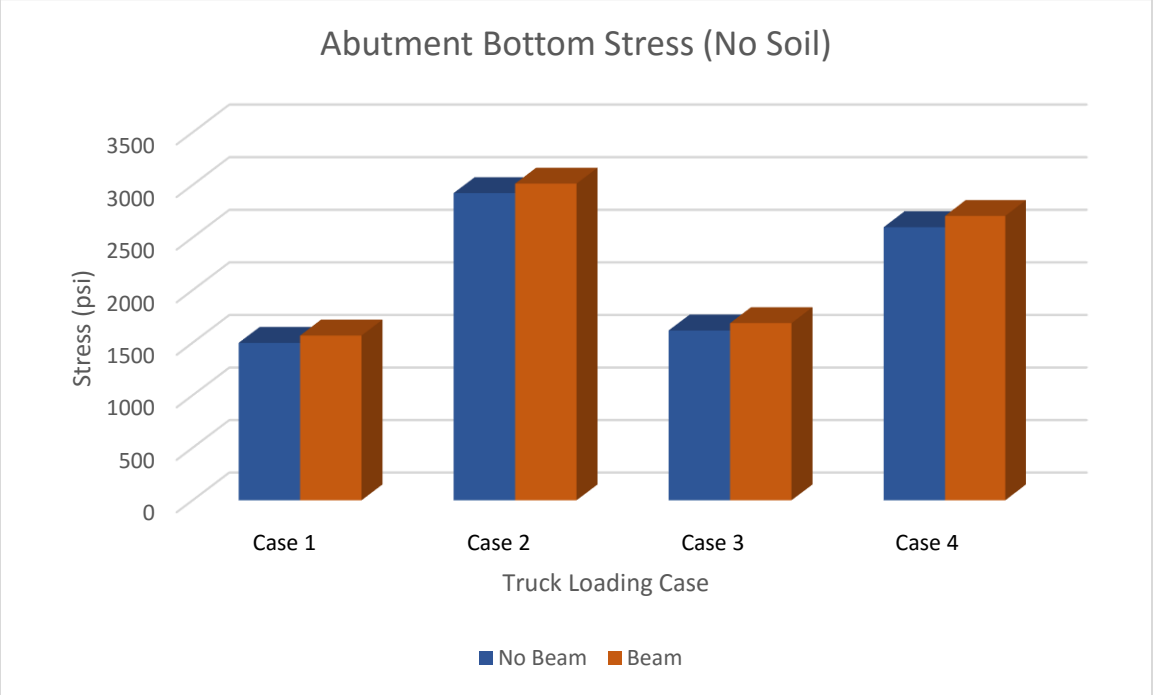

Figure 4.72: Abutment Bottom Stress Values without Soil

More deviation in the results for the stress levels can be seen in comparison to the deflection values detailed previously. The stress values will be rounded to the nearest tenth throughout the discussion. The highest midspan stress at the top face of the approach slab for models with loose soil was obtained for Case 4 with a value of 290 psi for models with an end span beam. For models without an end span beam, Case 1 controlled with 290 psi as well. As the loose soil is changed to moderately stiff, the values dropped to 240 psi and 130 psi respectively. However, Case 1 no longer controls for models without an end span beam with moderately stiff soils. Instead, Case 4 controls with a stress value of 180 psi. The highest midspan stress at the bottom face of the approach slab for models with loose soil was obtained for Case 1 with a value of 360 psi for models with an end span beam. For models without an end span beam, Case 1 also controlled with 330 psi. As the loose soil is changed to moderately stiff, the values dropped to 160 psi and 180 psi respectively. Again, Case 4 also controls for models without an end span beam with moderately stiff soil with a stress value of 180 psi as well.

The same analysis was realized for the abutment interface stress levels. The highest stress at the top face of the approach slab for models with loose soil was obtained for Case 4 with a value of 650 psi for models with an end span beam. For models without an end span beam, Case 4 also controlled with 600 psi. As the loose soil is changed to moderately stiff, the values dropped to 400 psi and 440 psi respectively. However, Case 4 no longer controls for both models with moderately stiff soils. Instead, Case 3 controls for models with an end span beam and Case 2 for models without the element. Stress values are 500 psi 480 psi respectively. The highest abutment interface stress at the bottom face of the approach slab for models with loose soil was obtained for Case 2 with a value of 680 psi for models with an

end span beam. For models without an end span beam, Case 4 controlled as well with 610 psi. As the loose soil is changed to moderately stiff, the values dropped to 420 psi and 400 psi respectively. However, Case 3 controls for models with and without an end span beam with moderately stiff soil. The stress values are 500 psi and 470 psi respectively.

Models with no soil resulted in values 5 or 6 times over the loose, moderately stiff, and stiff soil results. Midspan stresses did not change from top face to bottom face of the approach slab for models without soil. This can be seen in Figure 4.66 and Figure 4.68 as they are exactly the same bar graphs. However, abutment interface stresses showed more variance than midspan stresses from top face to bottom face of the approach slab for models without soil. As it can be seen, Figure 4.70 and Figure 4.72 are not exactly the same though very similar with only differing for Case 2 and Case 4.

While the results for models with an end span beam were slightly higher in most cases than models without an end span beam, a direct correlation could not be established like the deflection values presented previously. The increase or decrease of stress levels was not a constant value and varied over the different truck loading cases and the different soil compositions.

4.2.4 Parametric Study Of Skew Angle

The Marshall County bridge model was used to study the effects of various bridge skew angles on different points of interest across the joint and approach slab. In addition to the values obtained previously for the Marshall County bridge model with a skew angle of 45 degrees, the model was altered to match skew angles of 30 degrees and 60 degrees in addition to a non-skewed version of the model. The same modeling procedures from the previously discussed models were followed in terms of material properties, element types, constraints, and boundary conditions. In discussions with the Iowa DOT, a loose soil composition was considered to be too conservative producing higher results that the expected while moderately stiff and stiff soil presented similar results. For these reasons, one soil composition was used throughout this parametric study, a moderately stiff soil composition. A plan view of each model can be seen in Figure 4.73, Figure 4.74, and Figure 4.75 for the non-skewed, 30 degrees, and 60 degrees models respectively. The plan view for the 45 degree skew model, the original Marshall County bridge model, has been shown previously in Figure 4.28.

Figure 4.73: Parametric Study - Non-Skewed Model

Figure 4.74: Parametric Study - 30 degree Skew Model

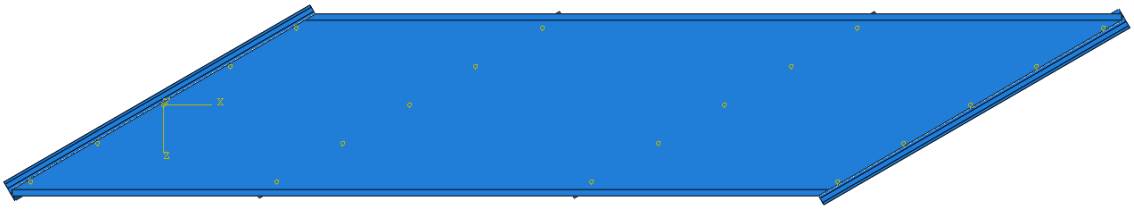

Figure 4.75: Parametric Study - 60 degree Skew Model

In this parametric study, certain points of interest will be compared between the models. These were identified as the dead load abutment reactions and temperature deformation of the bridges with and without the approach slab, live load abutment reactions due to various truck loading cases, deflection values and stress levels at the abutment interface and in the midspan of the approach slab. Both the top and bottom faces of the bridge deck (approach slab) will be studied.

Firstly, the dead load reactions results from the FE models will be discussed. Table 4.30 shows dead load abutment reactions in kips for the different skew angles. The columns show the values for DL#1 and DL#2 as it has been done previously. Table 4.31 and Table 4.32 show the increase in dead load in the correspond support due to the approach slab for models with and without soil respectively. The first exterior support from top to bottom of

the table refers to the support farthest to the 20 feet section of the approach slab. Each support consequently follows in the transversal direction until the remaining exterior support which corresponds to the 20 feet section of the approach slab. This explanation is not applicable to the non-skewed model since both sections of the approach slab are 20 feet long.

Table 4.30: Parametric Study - Dead Load Abutment Reactions

Support	No Skew		30		45		60	
	DL#1	DL#2	DL#1	DL#2	DL#1	DL#2	DL#1	DL#2
Exterior	25.65	10.57	26.12	10.64	27.82	10.70	28.06	10.13
Interior	30.13	5.06	30.22	5.11	30.83	5.17	30.86	5.08
Interior	30.31	5.16	30.46	5.18	31.16	5.32	29.77	5.08
Interior	30.13	5.06	30.24	5.03	30.73	5.00	29.98	5.01
Exterior	25.65	10.57	25.39	10.87	26.03	11.09	25.22	11.45

Table 4.31: Parametric Study - Dead Load Abutment Reactions without Soil

Support	No Skew		30		45		60	
	DL#1	DL#2	DL#1	DL#2	DL#1	DL#2	DL#1	DL#2
Exterior	8.57	1.77	13.84	2.75	7.53	1.04	9.96	1.83
Interior	14.40	2.81	30.06	5.98	37.07	7.46	57.61	11.53
Interior	13.92	2.72	28.00	5.57	48.51	9.69	86.70	17.32
Interior	14.38	2.80	25.82	5.04	40.59	7.88	100.60	19.81
Exterior	8.58	1.77	8.83	1.75	10.15	1.17	-0.62	-0.58

Table 4.32: Parametric Study - Dead Load Abutment Reactions with Soil

Support	No Skew		30		45		60	
	DL#1	DL#2	DL#1	DL#2	DL#1	DL#2	DL#1	DL#2
Exterior	6.70	1.30	6.87	1.19	7.80	1.06	8.50	1.27
Interior	11.41	1.93	11.18	2.00	12.76	2.18	16.66	2.75
Interior	11.02	1.88	11.36	2.07	13.26	2.31	17.37	2.94
Interior	11.40	1.93	12.14	2.09	14.89	2.42	19.57	2.95
Exterior	6.71	1.30	6.70	1.15	5.72	0.41	6.11	0.84

A general trend can be seen in the tables presented previously with the additional dead load from the approach slab being c. This can be seen more clearly when the approach slab was modeled with no soil. The additional DL#1 from the approach slab increases by a maximum of 14.4 kips for the non-skewed model, 30.06 kips for the 30 degree skew model, 48.51 kips for the 45 degree skew model, and 100.6 kips for the 60 degree skew model. Similar increases in terms of magnitude can be seen for DL#2. For models with soil, the dead load abutment reactions still increased as the bridge skew angle was increased. However, the increase was lower in magnitude from model to model with values of 11.41 kips for the non-skewed model, 12.14 kips for the 30 degree skew model, 14.89 kips for the 45 degree skew model, and 19.57 kips for the 60 degree skew model. This is expected due to the additional support that the soil provides the approach slab.

Temperature loading was also included in the FE models. Table 4.33 shows the temperature deformation results for the different skew angles. A general increase in temperature deformation can be seen in the table as the bridge skew angle was increased. However, the 45 degree model presents some interesting results. It shows the lowest deformation for models without the approach slab yet the highest deformation for models with the approach slab. This may be due to the symmetry that exists between both bridge ends in the 45 degree model versus the 30 degree skew model and the 60 degree skew model.

Table 4.33: Parametric Study - Temperature Deformation

Temperature Deformation (in)							
No Skew	Approach	30	Approach	45	Approach	60	Approach
0.30	0.35	0.33	0.38	0.30	0.46	0.39	0.45

To compare the live load abutment reactions for the various bridge skew models, different live load configurations were modeled acting in the top face of the approach slab. These live load configurations correspond to different truck loading cases. Two cases were considered for this parametric study, Case 1 and Case 2. Interestingly, Case 2 presented some difficulties in modeling. For the non-skewed model, the middle and front axles of one of the trucks were not considered in the non-skewed since they were located beyond the approach slab. Similarly, for the 30 degree skew model, the front axle of one of the trucks was not considered. These can be seen in Figure 4.76 and Figure 4.77 for the non-skewed model and the 30 degree skew model respectively. Figure 4.78 shows the Case 2 truck loading allocation for the 60 degree skew model. The truck load can clearly be seen marked in red in the various figures. Truck loading conditions were modeled as they were previously and detailed. Only the concentrated live load from the tires was considered in this study.

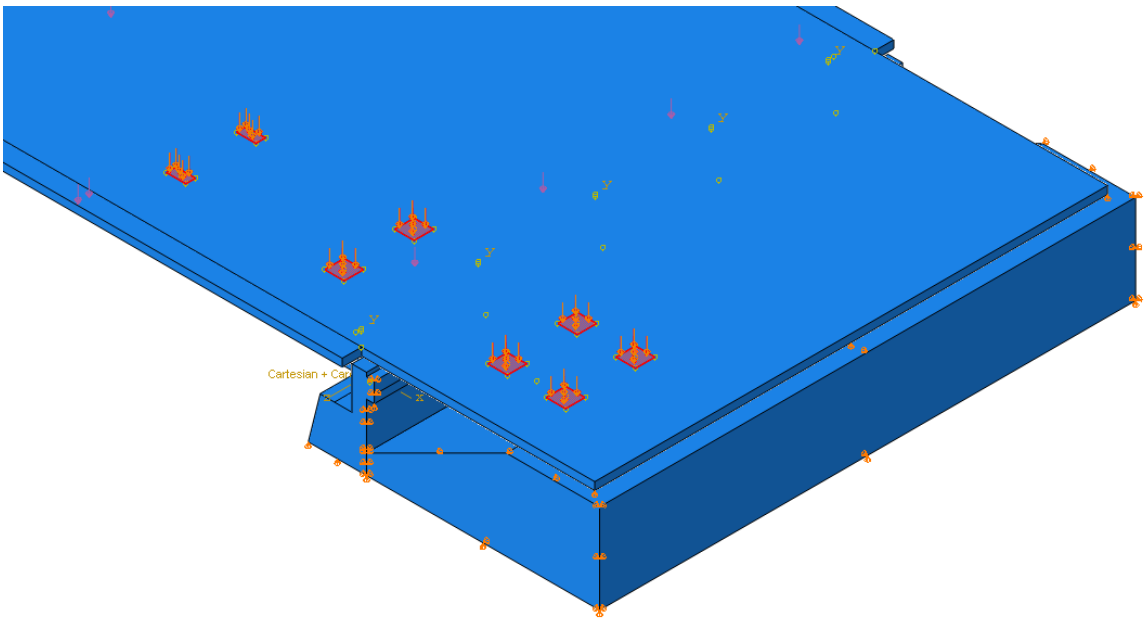

Figure 4.76: Case 2 - Non-Skewed Model

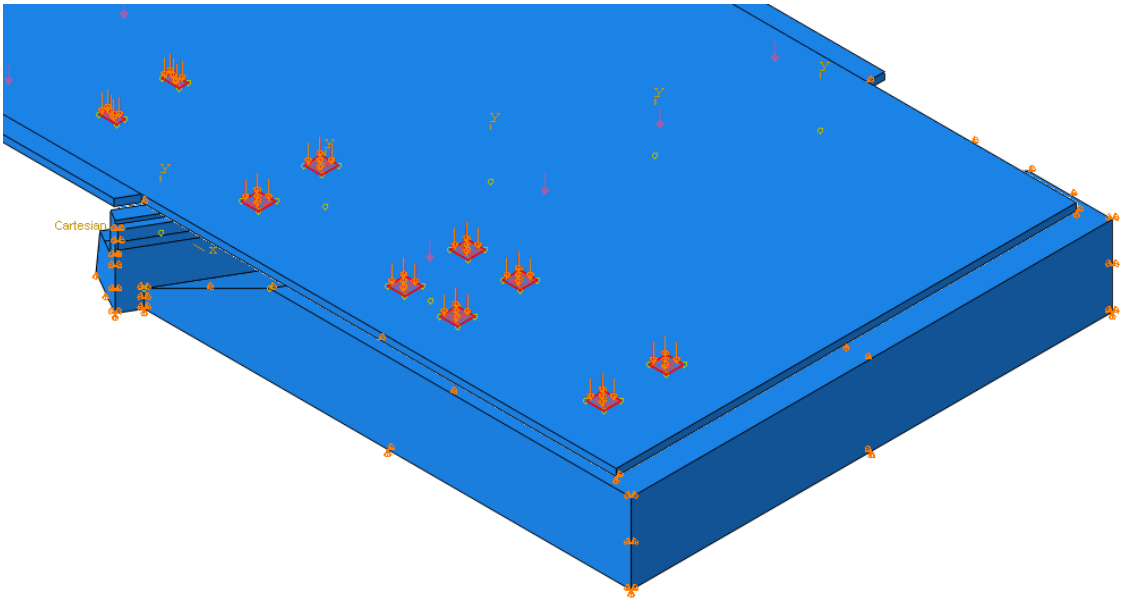

Figure 4.77: Case 2 - 30 degree Skew Model

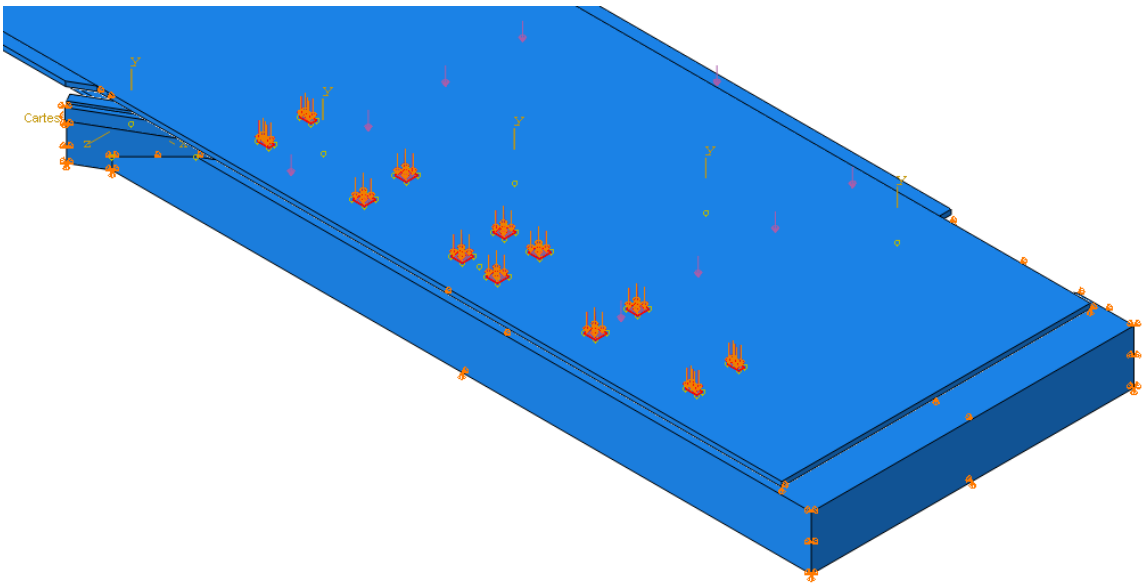

Figure 4.78: Case 2 - 60 degree Skew Model

Results for live load abutment reactions in kips are shown in Table 4.34 and Table 4.35 for Case 1 and Case 2 respectively. Figure 4.79 and Figure 4.80 show bar graphs with all the values being compared for models with soil and without soil, respectively.

Table 4.34: Parametric Study - Case 1 - Live Load Abutment Reactions

Support	Soil				No Soil			
	No Skew	30	45	60	No Skew	30	45	60
Exterior	-0.56	0.00	0.00	0.00	-0.48	0.30	-0.11	0.15
Interior	2.36	-0.02	-0.01	-0.01	5.97	2.53	1.41	0.58
Interior	6.06	-0.12	-0.01	-0.01	11.50	5.98	4.71	2.63
Interior	2.35	-0.19	-0.12	-0.01	5.96	8.64	8.41	10.64
Exterior	-0.56	-0.10	-0.13	-0.06	-0.48	0.19	3.08	2.58

Table 4.35: Parametric Study - Case 2 - Live Load Abutment Reactions

Support	Soil				No Soil			
	No Skew	30	45	60	No Skew	30	45	60
Exterior	22.47	12.21	6.41	0.36	31.84	28.40	8.30	6.68
Interior	31.61	23.87	20.38	7.03	42.02	60.89	69.65	68.74
Interior	3.17	1.64	1.69	1.71	6.68	24.43	54.56	98.32
Interior	-1.17	-0.96	-1.03	-0.81	-1.06	3.86	15.03	46.85
Exterior	-0.36	-0.07	-0.01	0.04	-0.60	-5.09	-8.08	-26.56

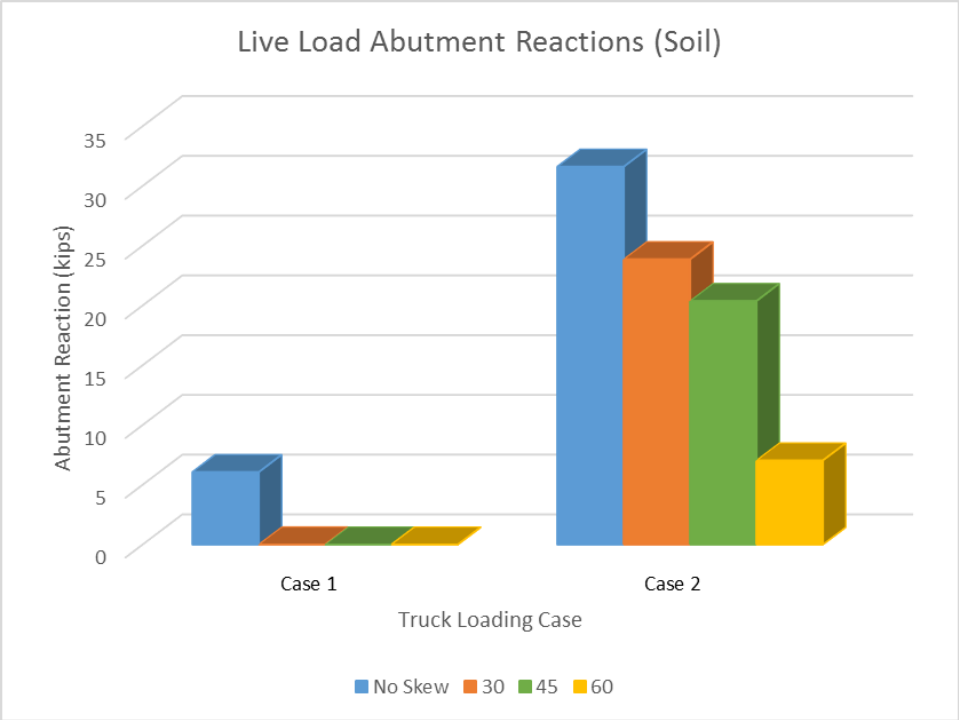

Figure 4.79: Parametric Study - Live Load Abutment Reactions with Soil

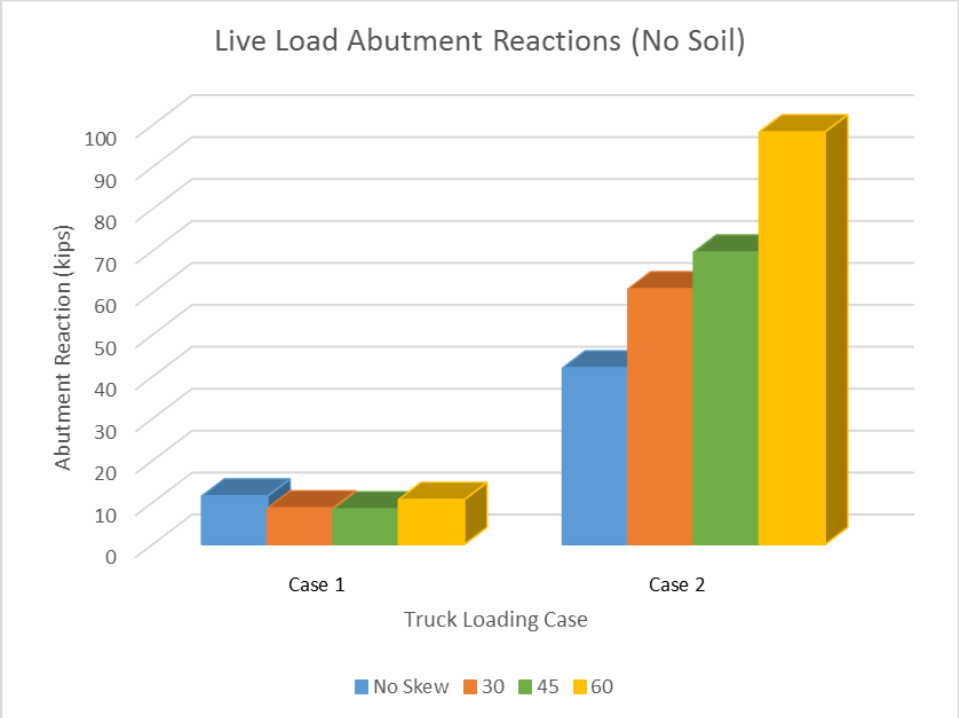

Figure 4.80: Parametric Study - Live Load Abutment Reactions without Soil

A general trend can also be seen in the tables presented previously. For models without soil, live load abutment reactions for Case 2 increase as the bridge skew angle was increased. This is expected since, without a soil support, the applied load will have to transfer to the abutment supports and the edge support at the opposite end of the abutment interface. For models with soil, the live load abutment reactions decreased as the bridge skew angle was increased. This difference is due to the 12 feet void incorporated in the soil. For models with a lower skew angle, the applied load will be applied closer or on top of the void. In models with a higher skew angle, the load will be applied farther from the void. For these reasons, the live load abutment reactions for Case 2 on models with soil decrease as the bridge skew angle was increased.

No clear trend could be recognized with Case 1 since the live load abutment reactions varied as the bridge skew angle was changed. For skewed models with soil, the abutment reaction was 0 kips or uplift as expected. The soil and the edge support at the opposite end of the abutment interface are supporting all the truck load in these cases. Some live load abutment reaction can be seen for the non-skewed model since the load is applied on top of the 12 feet void in contrast with the other models.

Results for deflection values in inches are shown in Table 4.36 and Table 4.37 for Case 1 and Case 2 respectively. Figure 4.81, Figure 4.82, Figure 4.83, and Figure 4.84 show bar graphs with all the values being compared for midspan deflections and abutment interface deflections.

Table 4.36: Parametric Study - Case 1 - Deflection Values

Location	Soil				No Soil			
	No Skew	30	45	60	No Skew	30	45	60
Midspan	-0.12	-0.06	-0.06	-0.06	-0.31	-2.32	-3.46	-12.32
Abutment	-0.03	-0.02	-0.03	-0.05	-0.07	-0.17	-0.27	-0.74

Table 4.37: Parametric Study - Case 2 - Deflection Values

Location	Soil				No Soil			
	No Skew	30	45	60	No Skew	30	45	60
Midspan	-0.17	-0.07	-0.07	-0.06	-0.53	-5.02	-6.50	-20.92
Abutment	-0.06	-0.05	-0.04	-0.05	-0.12	-0.34	-0.51	-1.22

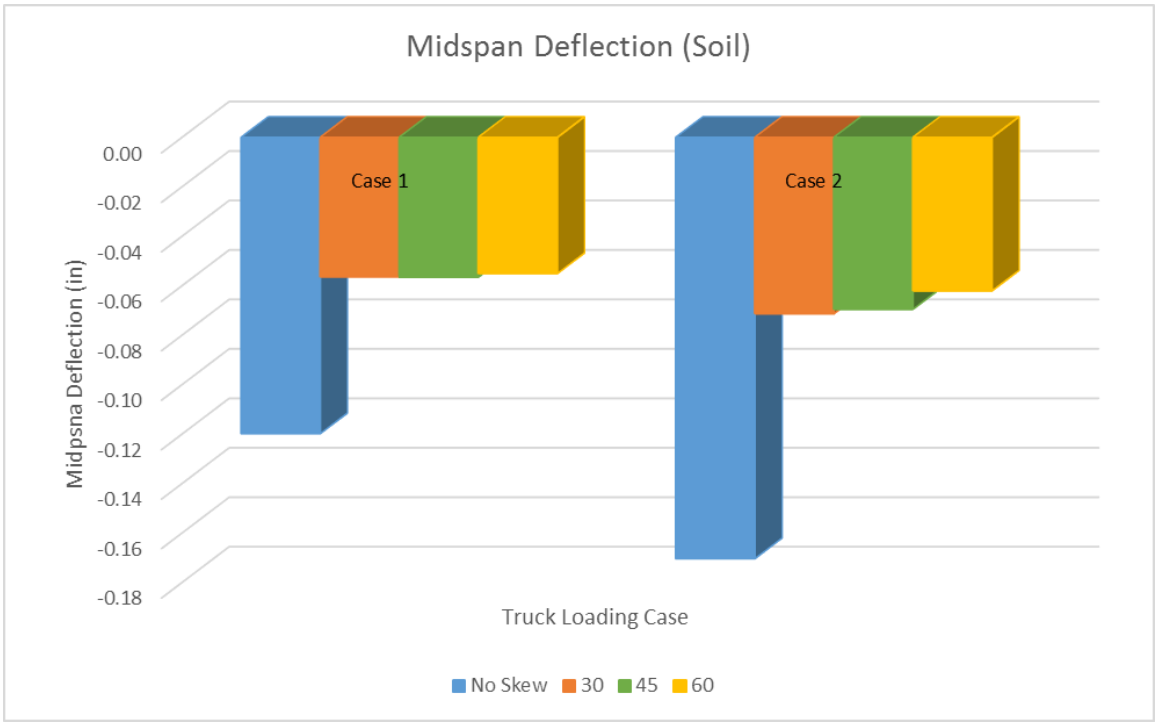

Figure 4.81: Parametric Study - Midspan Deflection Values with Soil

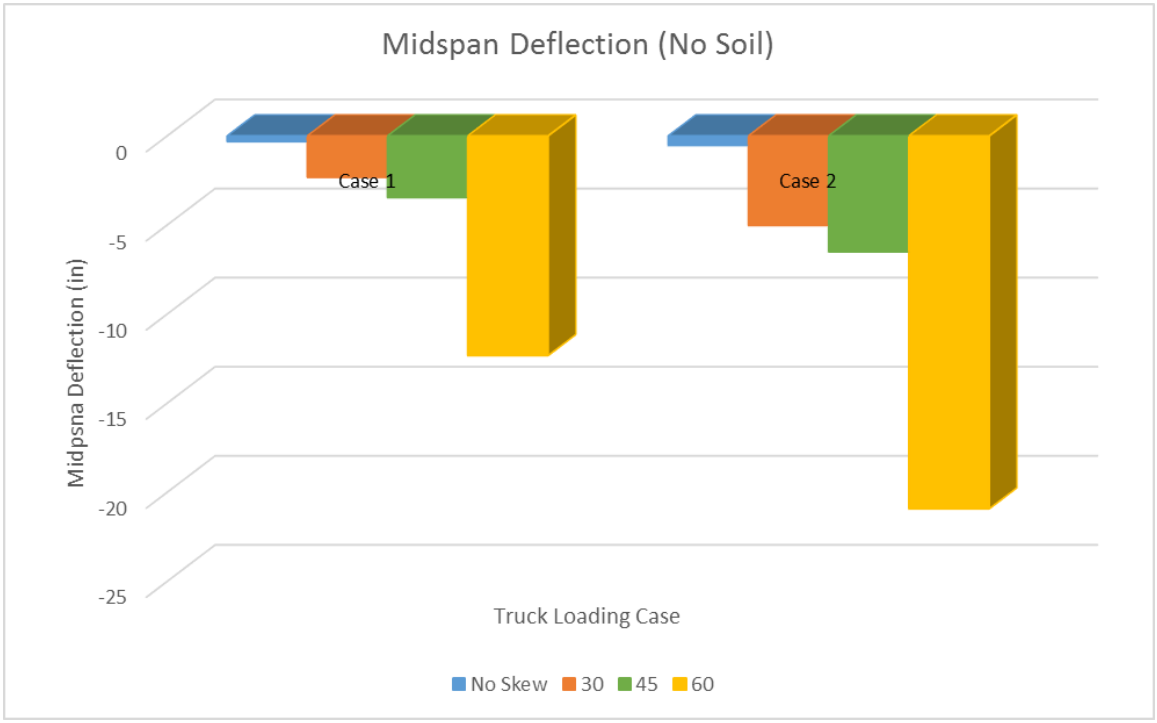

Figure 4.82: Parametric Study - Midspan Deflection Values without Soil

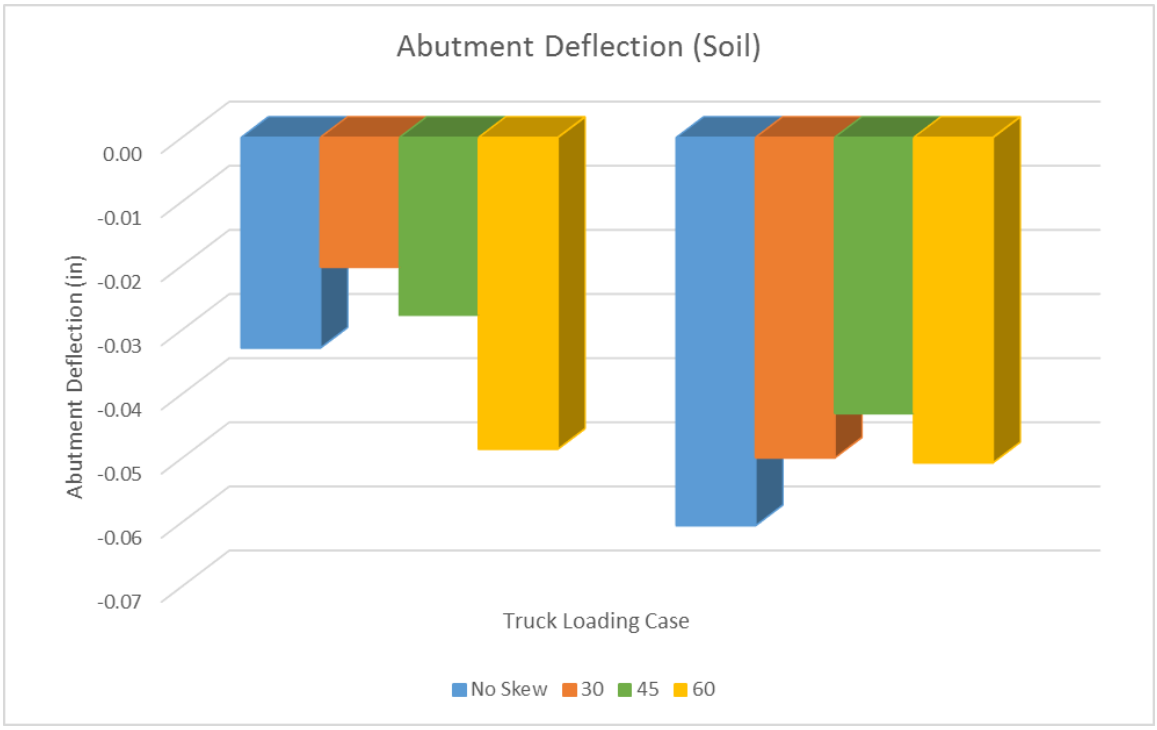

Figure 4.83: Parametric Study - Abutment Deflection Values with Soil

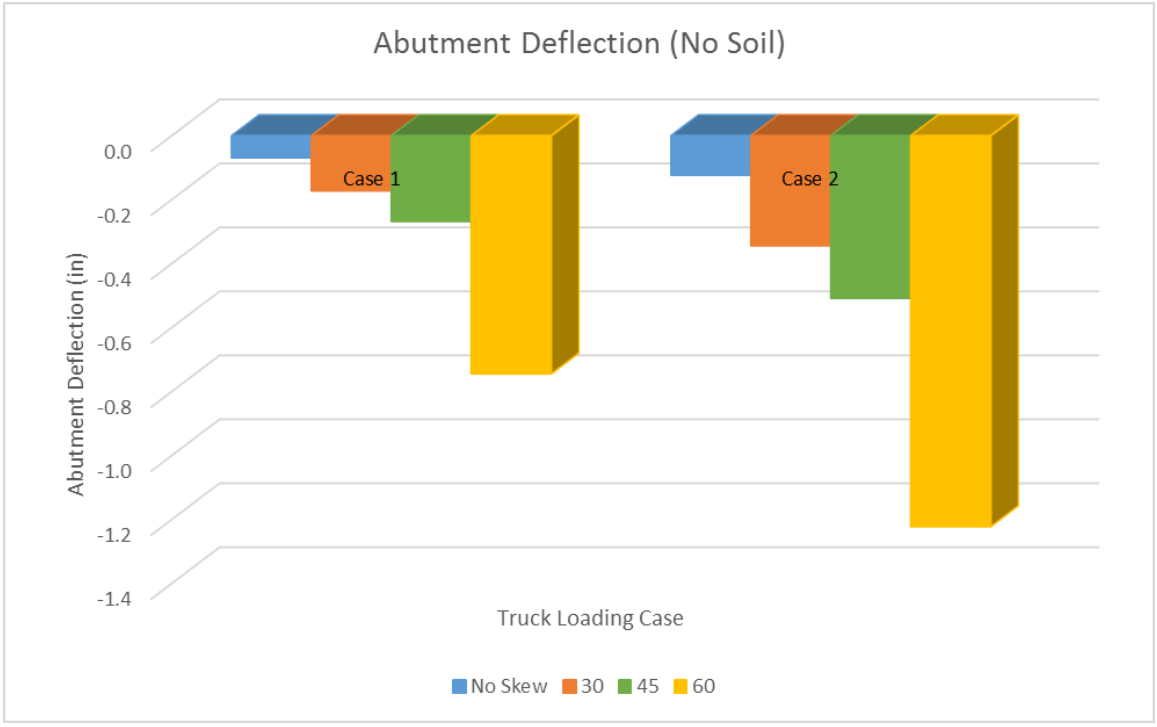

Figure 4.84: Parametric Study - Abutment Deflection Values without Soil

A general trend can also be seen in the tables presented previously. As expected, for models without soil, the deflection at the midspan of the approach slab and at the abutment interface increased as the bridge skew angle was increased. This was seen for both Case 1 and Case 2 truck loading conditions. For models with soil, the midspan deflection values decreased as the bridge skew angle was increased. As explained before, this difference is due to the 12 feet void incorporated in the soil. No clear trend could be recognized for abutment deflection values in models with soil. The results varied without a pattern as the bridge skew angle was changed.

Results for stress levels in psi are shown in Table 4.38 and Table 4.39 for Case 1 and Case 2 respectively. Figure 4.85, Figure 4.86, Figure 4.87, and Figure 4.88 show bar graphs with all the values being compared. The values shown correspond to von Mises stress levels on the different points of interest across the joint and approach slab.

Table 4.38: Parametric Study - Case 1 - Stress Values

Location		Soil				No Soil			
		No Skew	30	45	60	No Skew	30	45	60
Midspan	Top	299.0	129.6	132.7	117.7	528.0	940.2	1125.0	1125.0
	Bottom	341.0	172.8	176.7	156.8	528.0	940.2	1125.0	1125.0
Abutment	Top	425.1	388.5	396.7	391.4	632.2	1252.0	1499.0	2801.0
	Bottom	383.1	302.2	308.7	430.5	632.2	1252.0	1499.0	3055.0

Table 4.39: Parametric Study - Case 2 - Stress Values

Location		Soil				No Soil			
		No Skew	30	45	60	No Skew	30	45	60
Midspan	Top	355.0	175.5	132.7	156.6	818.0	1829.0	1706.0	2620.0
	Bottom	405.4	219.3	176.6	195.6	818.0	1829.0	1706.0	2620.0
Abutment	Top	607.0	482.2	484.5	468.6	1224.0	2438.0	2680.0	4799.0
	Bottom	506.2	394.6	440.5	468.6	1021.0	2438.0	2923.0	5235.0

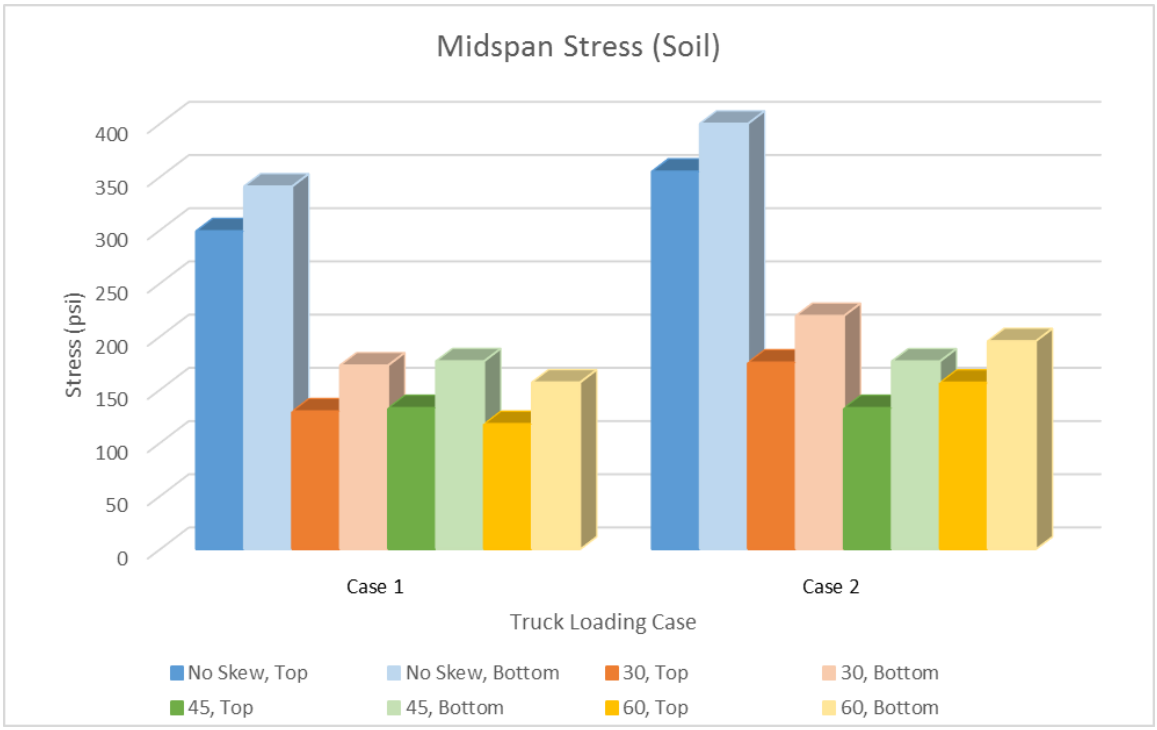

Figure 4.85: Parametric Study - Midspan Stress Values with Soil

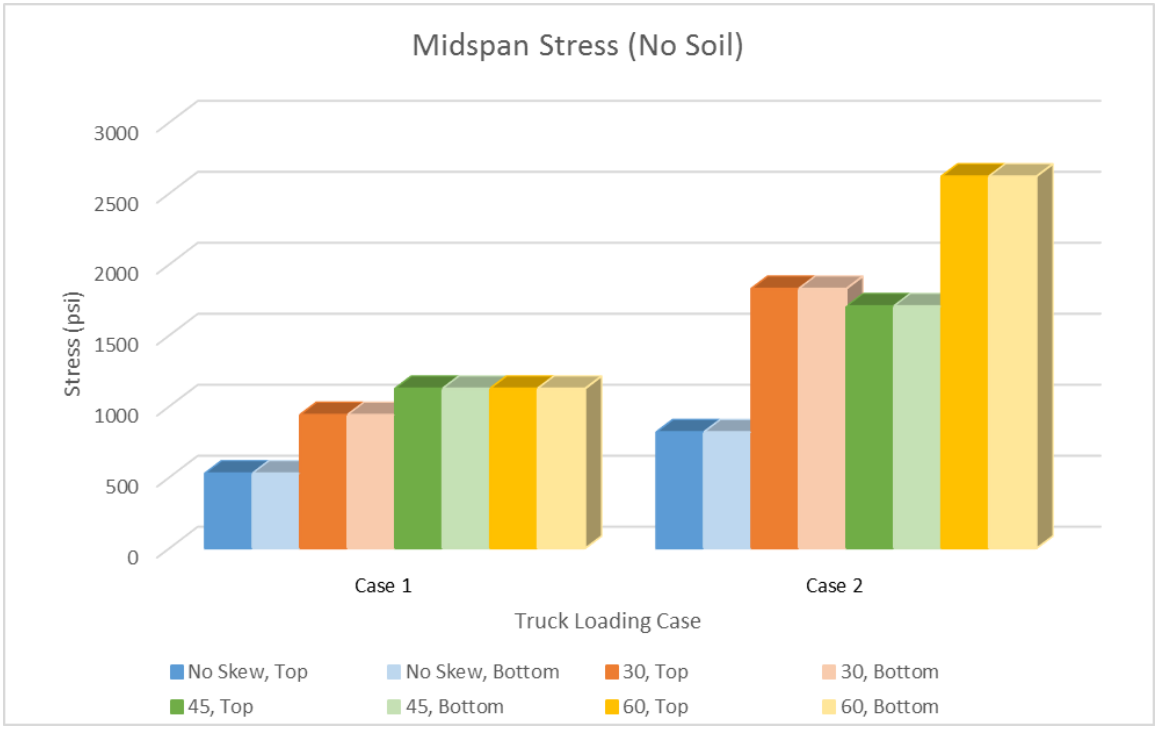

Figure 4.86: Parametric Study - Midspan Stress Values without Soil

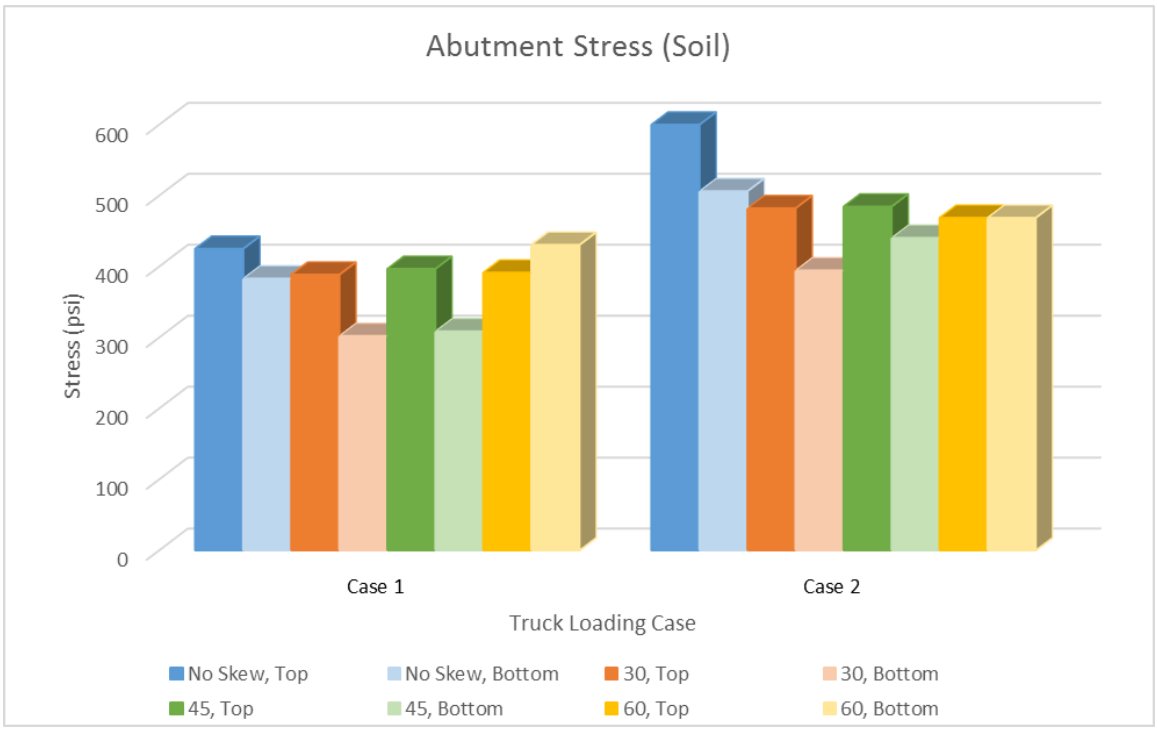

Figure 4.87: Parametric Study - Abutment Stress Values with Soil

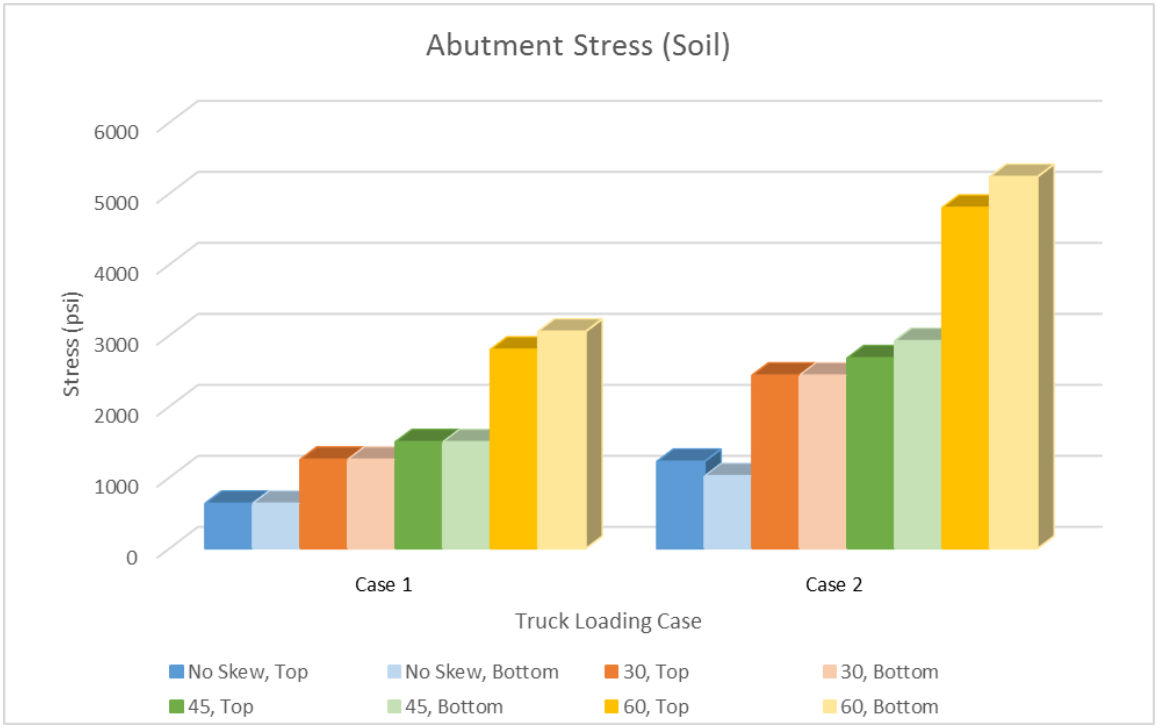

Figure 4.88: Parametric Study - Abutment Stress Values without Soil

As expected, for models without soil, the stress values at the midspan of the approach slab and at the abutment interface increased as the bridge skew angle was increased. This is true for both the top face and the bottom face of the bridge deck (approach slab). This was also seen for both Case 1 and Case 2. For models with soil, stress values of all skewed model lowered when compared to the non-skewed model. As explained before, this difference is due to the 12 feet void incorporated in the soil. However, no clear trend could be recognized when comparing the values between the skewed models. The results varied without a pattern as the bridge skew angle was changed. This inconsistency might be due to the difference in modeling the Case 2 truck loading conditions with missing axles for two of the models, the non-skewed model and the 30 degree skew model. The 12 feet void incorporated in the soil also impact these results.

4.3 Summary And Discussion

Full-scale FE models were realized of the selected candidate bridges during the course of this research. The two distinct bridges were denominated the Story County bridge and the Marshall County bridge. Both bridges are welded plate steel girder bridges with three spans and stud abutments. The details that differ from each other are shown below.

The Story County bridge is 338 feet long bridge, 343 feet face to face of paving notches, with a roadway of 30 feet. This bridge is a non-skewed bridge with four girders the bridge deck. Interior span is 132 feet long while exterior spans are 103 feet long. The Marshall County bridge is a 210 feet long bridge, 217 feet 9-3/8 inches face to face of paving notches, with a roadway of 44 feet. This bridge is skewed 45 degrees with five girders supporting the bridge deck. Interior span is 82 feet long while exterior spans are 64 feet long. The detailing of the welded plate steel girders in terms of the height, width, and thickness of

the flanges and webs is also different. These can be seen in more detail in the original plans for each bridge, Appendix A and Appendix B for the Story County bridge and for the Marshall County bridge respectively.

To properly model the bridges, different types of elements were used. All concrete members were modeled as C3D8R elements, which is an 8-node linear brick element with reduced integration and hourglass control. All steel elements were modeled as S4R elements, 4-node doubly curved thin or thick shell, reduced integration, hourglass control, finite membrane strains. These elements are commonly used on members where one dimensions is much lower in magnitude than the other two. For all flanges and webs, the thickness of the member is much lower than the corresponding height or width. The concrete bridge deck could have been modeled as an S4R element as well since two dimensions are much higher than the other (length and width are much higher than the thickness). In early developments of the model, the concrete deck was modeled as a C3D8R element and since it did not add recognizable computation time. The concrete deck was kept that way throughout the research.

All steel members of the welded plate steel girders and diaphragms were merged together and assigned a uniform mesh size. Boundary conditions were assigned to all faces that corresponded with soil support. These faces are at the bottom of the piers and in the bottom of the abutments and their corresponding backwall as well. Tied constraints were modeled between the top flanges of the steel girders and the bottom face of the concrete deck. These tie constraints assume full interaction between the two elements and transference of all degrees of freedom. Connecting wires between the bottom of the welded plate steel girders and the piers and abutments we also modeled. These wires were used to model the

bearings at these locations. Dead load and live load reaction values were taken from these wires in the various sections of this chapter.

Both bridges were compared with the original plan values for dead load deflection and reactions, temperature expansion, and live load reactions. An additional verification was made with live load deflections values corresponding with AASHTO Specifications limits. Results for both bridges will be discussed below.

For the Story County bridge, dead load deflection results from the FE model matched with the original plan value of 1 inch at midspan of the interior span. Dead load reactions showed high percentages of difference for DL#2 yet the total load ranged from a percentage of difference of 0.22% to a 5.48%. The high difference in DL#2 may be due to various assumptions being made for that load in the original plan values. For temperature loading, the FE results matched the one from the original plans with 0.5 inches. These values also show a 10% percentage of difference from the value obtained by Equation (1).

For the live load results, deflection values were verified with the AASHTO Specifications limit of L/800. The value obtained from the FE results was lower than this limit. For live load reactions, various cases were analyzed depending on what value was being maximized. Also, reaction values show very high percentage of difference when analyzed with current loading conditions. Loading conditions were altered because of this to match the ones used in the original plans. The discussion that follows corresponds to those values. For the abutment reactions, low percentages of difference were obtained in the total load where percentages of difference ranged from 3.5% for the exterior supports to 4.12% for the interior supports. For the pier reactions, low percentages of error were obtained in the

total load where percentages of difference range from 2.35% for the exterior supports to 3.78% for the interior supports.

With low percentages of difference across all loading conditions (dead load, temperature loading, and live loads), this model can be confidently used to compare and correlate with the experimental investigation results that would be obtained in the future. This investigation is detailed in Chapter 6.

For the Marshall County bridge, dead load deflection results from the FE model resulted in a percentage of difference of 15% with the original plan value. This may be due to additional dead load members being taken into consideration in the original plan value. Dead load reactions showed low percentages of difference in all values with values ranging from 1.1% to 4.15%. For temperature loading, the FE results show percentages of difference of 20% with the original plan value and 6.22% with the value obtained from Equation (1). The original plan value might be calculated based on a different coefficient of thermal expansion than the one used across all models.

For the live load results, deflection values were verified with the AASHTO Specifications limit of L/800. The value obtained from the FE results was lower than this limit. For live load reactions, various cases were analyzed depending on what value was being maximized. Also, reaction values show very high percentage of difference when analyzed with current loading conditions. Loading conditions were altered because of this to match the ones used in the original plans. The discussion that follows corresponds to those values. For the abutment reactions, low percentages of difference were obtained in the total load where percentages of difference ranged from 5.2% for the exterior supports to 13.59% for the interior supports. For the pier reactions, low percentages of error were obtained in the

total load where percentages of difference range from 10.06% for the exterior supports to 3.57% for the interior supports.

With low percentages of difference across all loading conditions (dead load, temperature loading, and live loads), this model can be confidently used to study the impact of the deck over backwall concept in existing bridge elements, discussed in the following pages. This model can also be used to compare and correlate with the post-construction testing results that would be obtained in the future. This testing is detailed in Chapter 7.

The impact of the deck over backwall concept was seen in Section 4.2.3. Additional members had to be modeled in the FE model that included the deck over backwall concept and the approach slab. The soil was modeled as a C3D8R element just like the concrete members. Tie constraints were added in the abutment interface between the curb and the end span beam with the concrete deck. Diaphragms were embedded into this curb and end span beam. Additionally, a contact interaction was imposed between the soil and the bottom face of the approach slab.

This model was analyzed under dead load, temperature loading, and various configurations of live loads. Abutment reactions were studied under the dead loads and live loads mentioned previously. Deflection and stress levels were taken in various points of interest across the joint in the abutment interface and the midpsan of the approach slab.

Result show an increase in bearing loads due to the additional dead loads from the approach slab and live loads corresponding to the different truck loading conditions. The deck over the backwall dead loads corresponded to approximately an additional 15 kips to 28 kips for interior supports and 5 kips to 11 kips for exterior supports. These values assume some form of soil support and the presence of an end span beam. For models without soil

support, dead load corresponded to approximately an additional 60 kips for interior supports and 11 kips for exterior supports.

The additional 64 foot section in one end of the approach slab accounted for an additional temperature deformation of 0.16 inches. This value showed a percentage of difference of 4% from the value calculated with Equation (1).

Live load corresponded to approximately a maximum of 48 kips for interior supports and 26 kips for exterior supports. These values assume some form of soil support. For models without soil support, live load corresponded to approximately a maximum of 70 kips for interior supports and 27 kips for exterior supports.

Deflection values were obtained in the abutment interface and the midspan of the approach slab. For the deflection values across the abutment interface, the maximum deflection for models with soil was 0.09 inches. For models without soil the value increased as expected to 0.51 inches. For the midpspan of the approach slab, the maximum for models with soil was 0.32 inches. For models without soil the value increased to 6.5 inches.

Stress values were obtained in the abutment interface and the midspan of the approach slab. For the stress values across the abutment interface, the maximum stress for models with soil was 675.4 psi. For models without soil the value increased as expected to 3013 psi. For the stress of the approach slab, the maximum stress for models with soil was 361.5 psi. For models without soil the value increased as expected to 1706 psi.

A parametric study of various bridge skew angles was also realized with the Marshall County bridge. The model was altered to match skew angles of 30 degrees and 60 degrees in addition to a non-skewed version of the model. These models and the original 45 degree model were compared. Results for models without soil show that generally an increase in the

bridge skew angle leads to an increase in all points of interest under study. These being the dead load abutment reactions and temperature deformation of the bridges with and without the approach slab, live load abutment reactions, deflection values and stress levels at the abutment interface and in the midspan of the approach slab. Results for models with soil show more variance due to the incorporation of a 12 feet void in the soil and difficulties with the Case 2 truck loading condition.

With these values, the Iowa DOT can confidently design the new joint and the approach slab for the deck over backwall concept. Reinforcement bars and concrete strength can be designed with the stress levels provided by the FE model at the abutment interface and in the midspan of the approach slab.

CHAPTER 5. COST ANALYSIS

An estimate of the installation, repair, or replacement costs over the service life of the bridge was developed for different types of joints including the deck over backwall concept. Construction costs of the Iowa DOT joint was also estimated using the Final Bridge Design Software, with a spreadsheet titled Prepare Cost Estimate last updated on 4/25/17 (Iowa DOT Office of Bridges and Structures 2018b). This spreadsheet stores historical cost data for bid items in state job estimates. Most items have cost data from 05-2016 through 04-2017. The remaining items have cost data within the past ten years. With the cost estimate and the construction cost of the concept, a comparison with the implementation of other types of joints was completed.

5.1 Background

To develop the cost estimate, a service life and a cost associated with each type of joint was needed. Civjan and Quinn (2016) researched the best practices for bridge expansion joints and headers in the Northeastern States of the Unites States. As part of the research for the Massachusetts DOT (MassDOT), the Massachusetts DOT and several neighboring DOTs were surveyed on their use of expansion joints and, more particularly for this research, the service life of each type of joint. The nine states surveyed were Connecticut, Maine, Massachusetts, New Hampshire, New Jersey, New York, Pennsylvania, Rhode Island, and Vermont. Table 5.1 shows the responses from the nine states in terms of the service life for the various types of joints. Civjan and Quinn (2016) compiled the service life of the various types of joints from the responses of the nine states and categorized them in ranges from 0 to 4 years, 5 to 8 years, 9 to 12 years, 13 to 16 years, and above 16 years.

Table 5.1: Typical Service Life of Joints

Source: Civjan and Quinn (2016)

All States: Typical Service Life of Joints												
Years	SS:D	SS:O	APJ	CS	SS	EM	PS	MJ	SPJ	FJ	OJ	LS
0-4	0	1	6	2	2	1	11	0	0	0	1	0
5-8	1	1	13	2	1	1	0	1	0	0	0	0
9-12	5	1	1	6	5	1	2	3	0	1	1	1
13-16	1	0	1	5	7	0	0	4	3	2	0	2
>16	4	0	0	2	4	1	0	8	3	16	3	4

Where SS:D stands for Saw and Seal Deck over Backwall, SS:O for Saw and Seal over EM-SEAL, APJ for Asphalt Plug Joint, CS for Compression Seal, SS for Strip Seal, EM for EM-SEAL, PS for Pourable Seal, MJ for Modular Joint, SPJ for Sliding Plate Joint, FJ for Finger Joint, OJ for Open Joint, and LS for Link-Slab.

Civjan and Quinn (2016) also provided typical costs in cost per linear foot, US dollars ($) per linear foot, for the installation of the different joint types. For the cost estimate developed in the following pages, the installation cost was assumed to be the same as a repair or replacement cost with the exception of Strip Seals were the installation cost was taken a $300-$800 while the repair or replacement cost was taken as $75. These costs alongside the different types of joints can be seen in Table 5.2. The cost for three types of joints was not provided. These joints are Sliding Plate Joint, Open Joint, and Link-Slab. In the service life study and the cost estimate detailed in the following pages, these types of joints were omitted since a direct comparison in terms of cost could not be established.

Table 5.2: Typical Cost of Joints

Source: Civjan and Quinn (2016)

Joint Type	Cost per Linear ft.
Finger Joints	$1375-$1750
Pourable Seal	$300 (including header)
Compression Seal	$450
Strip Seal	$300-$800, $75 to replace seal
Saw and Seal Deck over Backwall	$15-$25
Saw and Seal over EM-SEAL	$60
Asphalt Plug Joint	$120-$200
Modular Joint	$1750-$4600
EM-SEAL	$90

As it can be seen in the table above, the cost of the Saw and Seal Deck over Backwall is extremely low, $15-$25 per linear foot, compared to the rest of the joint types. The Saw and Seal detailing can be seen in the joint developed by the Iowa DOT detailed in Chapter 3, Figure 3.8. The highest cost can be recognized on Finger Joints with costs of $1375-$1750 per linear foot and on Modular Joints with costs of $1750-$4600 per linear foot.

To develop the cost estimate, these costs were taken as three different cost points. These cost points are Low, Average, and High (L, A, and H). The lowest cost of each type of joint corresponds to the L cost point, the average cost to the A cost point, and the highest cost to the H cost point. For example, for the Asphalt Plug Joint, the Low cost would be $20 per linear foot, Average cost would be $160 per linear foot, and High cost would be $200 per linear foot. Some of the types of joints have the same value for all three cost points like Pourable Seals, Compression Seals, Strip Seals to replace, Saw and Seal over EM-SEAL, and EM-SEAL.

5.2 Service Life Of Joints

As seen in Table 5.1, every type of joint in the table has different values for their service life. To develop the cost estimate, the service life of each type of joint was studied in relation with the bridge service life. This study aimed to find the number of times the joint has to be repaired or replaced in the service life of the bridge. A variable bridge service life of 25 years and 50 years was used.

The service life of each joint was categorized into three stages. The stages were denominated as Early, Average, and Late service life. For the Early service life of each joint, the lower value of each range of Table 5.1 was used to average the service life. For example, in the 5-8 range, 5 years of service was used for the Early stage. For the Average service life of each joint, the average of each range was used to average the service life. For the Late service life, the highest value was used to average the service life. Some adjustments were made in the process. For the above 16 range, 16 years was used across all three stages. For example, if the service life of particular joint was 20 years, the data for that joint would be capped at 16 years. For the 0-4 range, a minimum of 1 year was used for the Early service life since it is unrealistic for a joint to have a service life of 0 years.

Using the process detailed previously, the number of repair or replacements for each joint over a bridge service life of 25 years and 50 years was determined. Every joint type starts with an installation and that was assumed as a repair or replacement in the study with the exception of the Strip Seal joints. Table 5.3 and Table 5.4 show the number of times the joint has to be repaired or replaced for the bridge service life of 25 years and 50 years respectively. Each table has the three stages (Early, Average, and Late) detailed previously for each type of joint.

Table 5.3: Repair or Replacements over 25 Years

Joint Type	Repair or Replacements		
	Early	Average	Late
Finger Joints	2	2	2
Pourable Seal	14	8	5
Compression Seal	3	3	3
Strip Seal	3	3	2
Saw and Seal Deck over Backwall	3	3	2
Saw and Seal over EM-SEAL	6	4	4
Asphalt Plug Joint	6	5	4
Modular Joint	2	2	2
EM-SEAL	4	3	3

Table 5.4: Repair or Replacements over 50 Years

Joint Type	Repair or Replacements		
	Early	Average	Late
Finger Joints	4	4	4
Pourable Seal	28	16	10
Compression Seal	6	5	5
Strip Seal	5	5	4
Saw and Seal Deck over Backwall	5	5	4
Saw and Seal over EM-SEAL	11	8	7
Asphalt Plug Joint	12	9	7
Modular Joint	4	4	4
EM-SEAL	7	6	6

From the results presented above, it can be recognized that the number of repair or replacements for the Saw and Seal Deck over Backwall ranks among the lowest of the nine joint types being studied. On the other hand, it is quite clear that the Pourable Seal joint has the highest number of repair or replacements. Generally, the ascending order of each type of joint in number of repair or replacements could be ranked as Finger Joint and Modular Joint, Strip Seal and Saw and Seal deck over Backwall, Compression Seal, EM-SEAL, Saw and Seal over EM-SEAL, Asphalt Plug Joint, and Pourable Seal. These numbers are used in the cost estimate realized and detailed in the next pages.

5.3 Cost Estimate Over Bridge Service Life

A cost estimate of the repair or replacement cost of various types of joints over a design service life of a bridge of 25 years and 50 years was developed. Various factors were taken into account for this analysis. The bridge in question would change the joint length, therefore, influencing the cost of each repair or replacement. The analysis was realized for the two case study bridges, the Story County bridge and the Marshall County bridge. Story County has a roadway width of 30 feet while being a non-skewed bridge, therefore, the joint is taken as 30 feet as well. On the other hand, the Marshall County bridge has a roadway of 44 feet transversely and approximately 62.225 feet diagonally in the skew of the joint.

Another factor that was taken into account was the inflation rate. The inflation rate was assumed as 2%, 3%, and 4% during the course of this analysis. Another factor that was considered was the service life of each joint. As previously discussed, each joint has a different service life and three different stages were determines for each as an Early, Average, and Late service life. The last factor that was taken into account was the service life of the bridge itself. 25 years and 50 years was used for this variable.

Throughout the discussion, the indicators LE, LA, LL, AE, AA, AL, HE, HA, and HL are used. The first letter means the cost of repair or replacement (Low, Average, and High) and the second letter means the stage of the service life (Early, Average, and Late). For example, the designation AE would mean an Average Cost with an Early Service Life for the different types of joints.

The future cost of repair or replacement of each joint at the end of its service life, was determined with Equation (6).

$$FV = PV \times (1 + i)^N \tag{6}$$

Where FV is the future value, PV is the present value, i is the inflation rate, and N is the number of periods.

To develop the cost estimate, the FV of repair or replacements of the different types of joints was calculated using PV as the cost of each type of joint shown in 5.1, Table 5.2, and N as the service life of each type of joint discussed in 5.2, Table 5.3 and Table 5.4.

Results for the Marshall County bridge with an inflation rate of 2% for a bridge service life of 25 years are shown in Figure 5.1 for AE, Figure 5.2 for AA, Figure 5.3 for AL. In addition, results for a bridge service life of 50 years are shown in Figure 5.4 for AE, Figure 5.5 for AA, and Figure 5.6 for AL. Figures were not shown for the rest of the cases (Story County bridge, other cost and service life combinations, and other inflation rates). Each step in the graph means a repair or replacement cost. Every joint type starts with an installation cost in the present or year 0. This installation cost is assumed to be the same as the repair or replacement cost for all types of joints except Strip Seals.

The costs for the Story County bridge are shown in Table 5.5, Table 5.6, Table 5.7, Table 5.8, Table 5.9, and Table 5.10 varying the bridge service life between 25 years and 50 years and the inflation rate between 2%, 3%, and 4%. The costs for the Marshall County bridge are shown in Table 5.11, Table 5.12, Table 5.13, Table 5.14, Table 5.15, and Table 5.16 varying the same factors. Each table shows the different cost and service life combinations (LE, LA, LL, etc.). The tables are color coded with red cells representing the higher values of costs and green cells representing the lower values of costs.

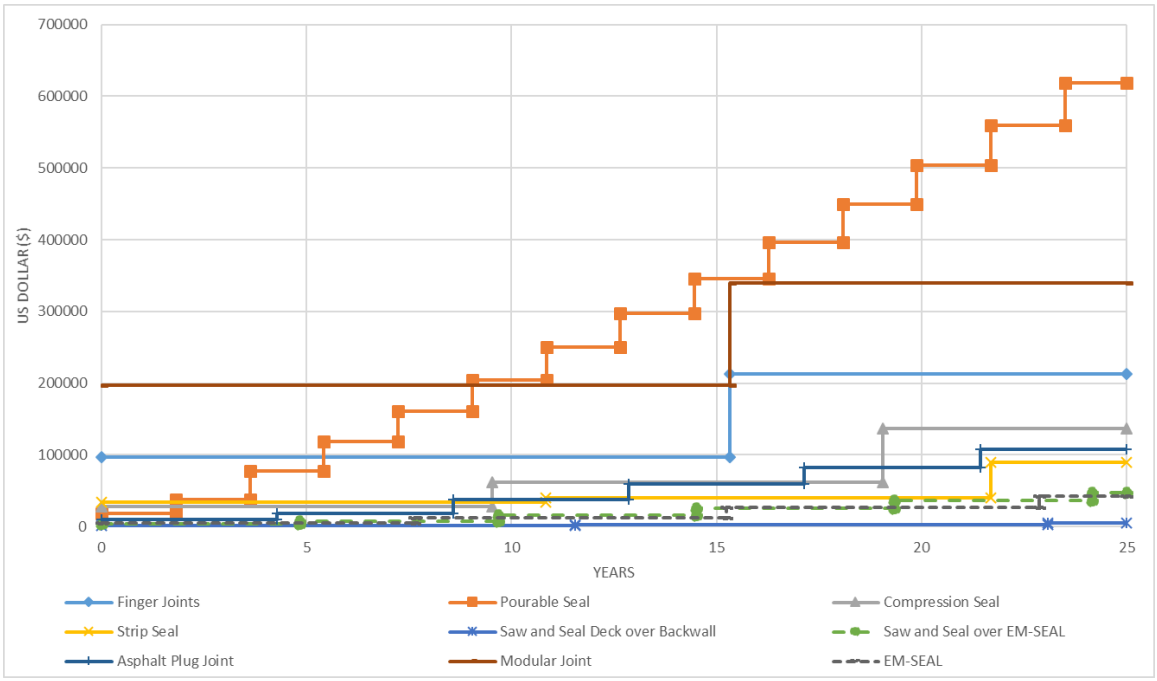

Figure 5.1: 25 Years - Average Cost, Early Service Life

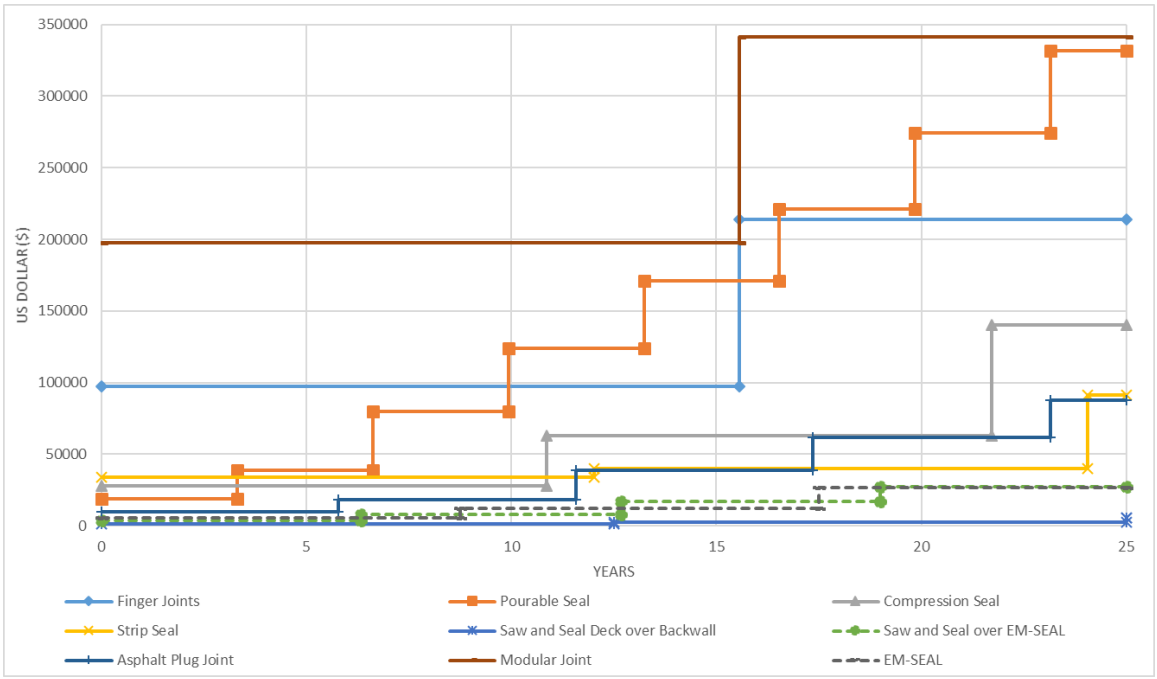

Figure 5.2: 25 Years - Average Cost, Average Service Life

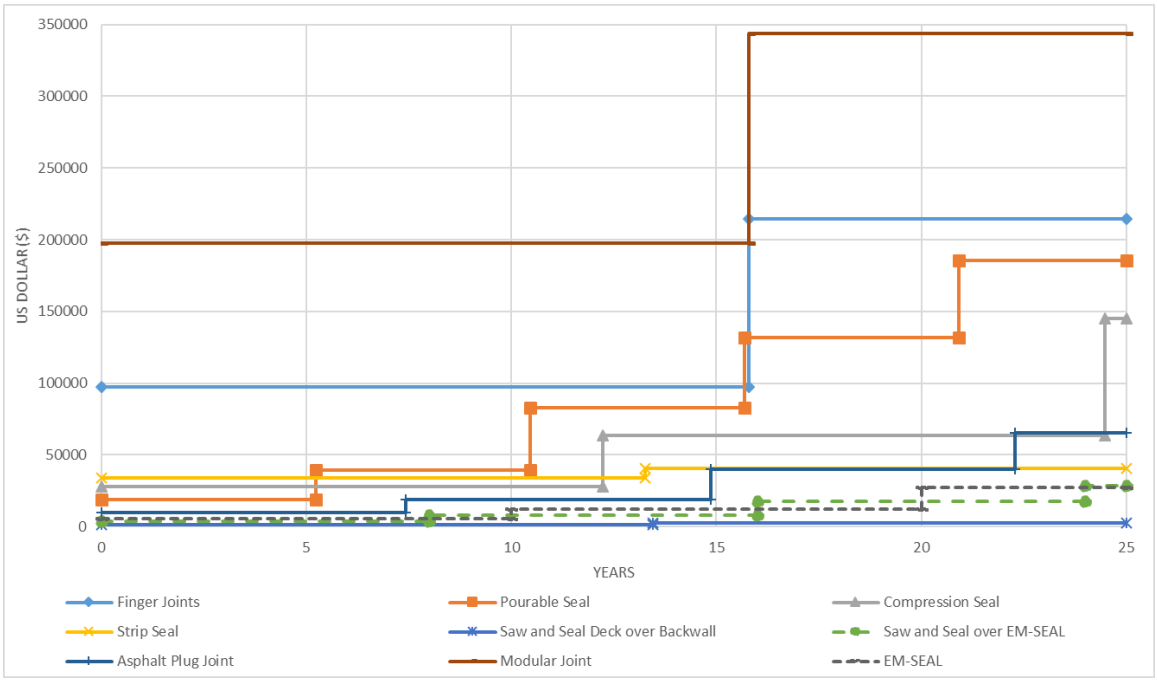

Figure 5.3: 25 Years - Average Cost, Late Service Life

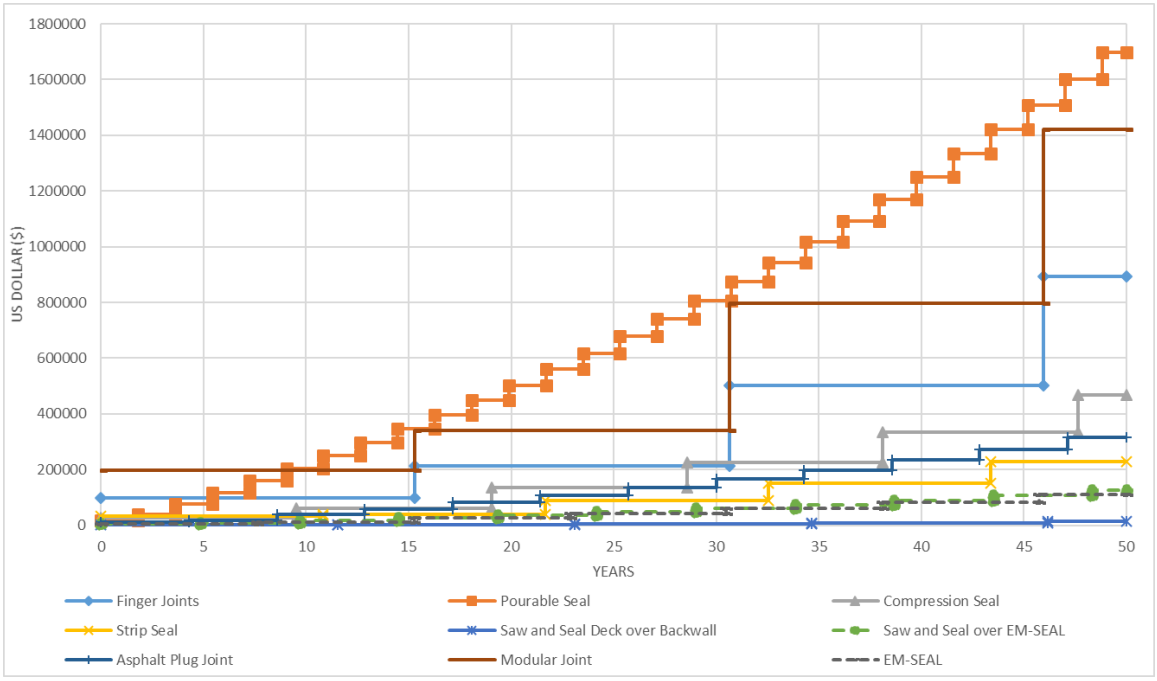

Figure 5.4: 50 Years - Average Cost, Early Service Life

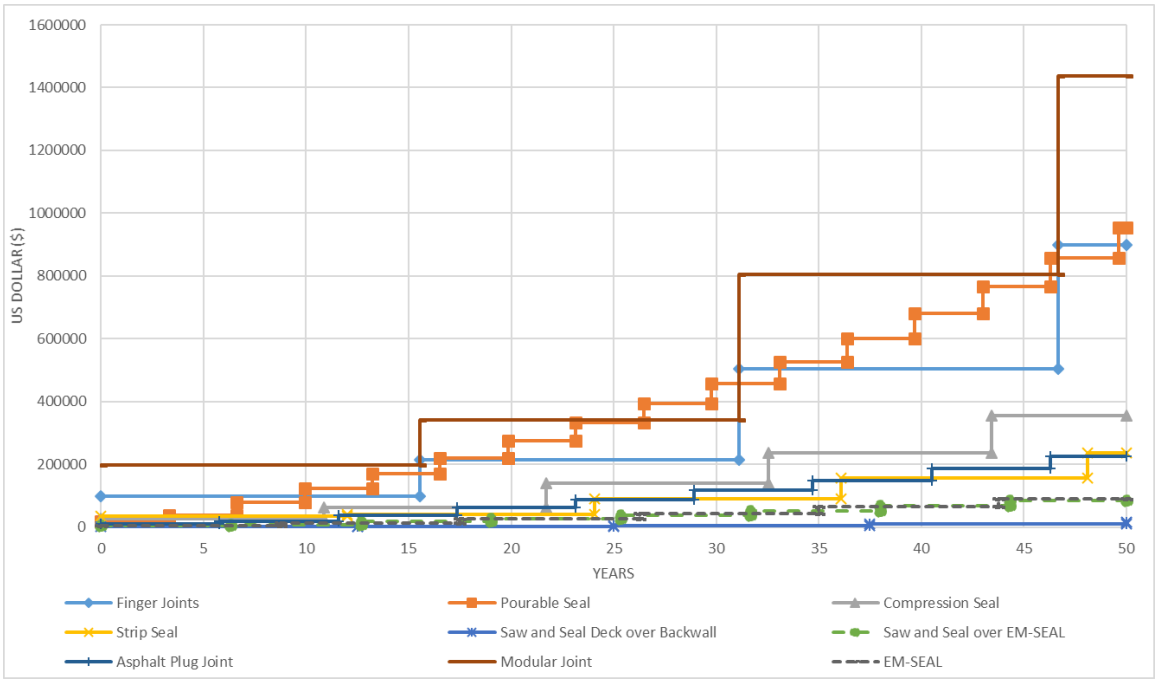

Figure 5.5: 50 Years - Average Cost, Average Service Life

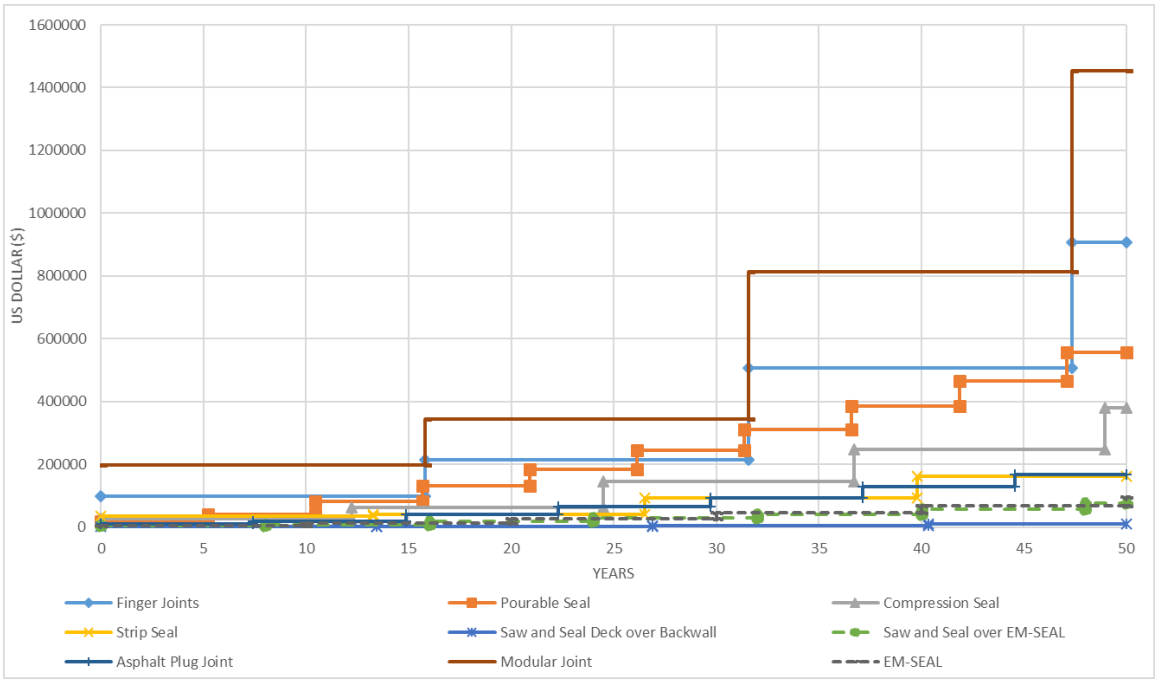

Figure 5.6: 50 Years - Average Cost, Late Service Life

Table 5.5: Story - 25 Years Service Life, 2% Inflation Rate

Joint Type	US Dollar ($)								
	LE	LA	LL	AE	AA	AL	HE	HA	HL
Finger Joints	97115	97378	97642	102740	103003	103267	108365	108628	108892
Pourable Seal	298007	159914	89288	298007	159914	89288	298007	159914	89288
Compression Seal	65797	67723	69820	65797	67723	69820	65797	67723	69820
Strip Seal	26401	26898	11926	43197	43915	19426	59993	60931	26926
Saw and Seal Deck over Backwall	2292	2341	1037	2631	2683	1187	2969	3025	1337
Saw and Seal over EM-SEAL	23103	13130	13855	23103	13130	13855	23103	13130	13855
Asphalt Plug Joint	44871	36574	27201	52032	42321	31402	59193	48068	35602
Modular Joint	120751	121773	122809	163501	164523	165559	206251	207273	208309
EM-SEAL	20531	12940	13295	20531	12940	13295	20531	12940	13295

Table 5.6: Story - 50 Years Service Life, 2% Inflation Rate

Joint Type	US Dollar ($)								
	LE	LA	LL	AE	AA	AL	HE	HA	HL
Finger Joints	406765	410168	413608	430325	433861	437435	453885	457554	461262
Pourable Seal	819095	459409	267887	819095	459409	267887	819095	459409	267887
Compression Seal	225164	171813	183172	225164	171813	183172	225164	171813	183172
Strip Seal	66962	70207	47600	109563	114622	77535	152164	159038	107469
Saw and Seal Deck over Backwall	5913	6182	4159	6786	7085	4760	7660	7989	5362
Saw and Seal over EM-SEAL	60384	40408	36140	60384	40408	36140	60384	40408	36140
Asphalt Plug Joint	131027	94412	69492	151939	109247	80223	172851	124082	90955
Modular Joint	505764	512921	520216	684821	692989	701303	863878	873058	882391
EM-SEAL	52826	43060	46279	52826	43060	46279	52826	43060	46279

Table 5.7: Story - 25 Years Service Life, 3% Inflation Rate

Joint Type	US Dollar ($)								
	LE	LA	LL	AE	AA	AL	HE	HA	HL
Finger Joints	106119	106575	107033	111744	112200	112658	117369	117825	118283
Pourable Seal	337950	181040	99860	337950	181040	99860	337950	181040	99860
Compression Seal	72998	76356	80091	72998	76356	80091	72998	76356	80091
Strip Seal	28771	29633	12330	46605	47835	19830	64438	66036	27330
Saw and Seal Deck over Backwall	2607	2694	1120	2968	3062	1270	3329	3429	1420
Saw and Seal over EM-SEAL	26322	14532	15796	26322	14532	15796	26322	14532	15796
Asphalt Plug Joint	50311	41441	30695	58165	47759	35251	66020	54076	39807
Modular Joint	130170	131911	133691	172920	174661	176441	215670	217411	219191
EM-SEAL	23250	14223	14834	23250	14223	14834	23250	14223	14834

Table 5.8: Story - 50 Years Service Life, 3% Inflation Rate

Joint Type	US Dollar ($)								
	LE	LA	LL	AE	AA	AL	HE	HA	HL
Finger Joints	535431	542624	549936	563813	571264	578838	592194	599904	607739
Pourable Seal	1089052	614352	352402	1089052	614352	352402	1089052	614352	352402
Compression Seal	298084	221395	245181	298084	221395	245181	298084	221395	245181
Strip Seal	83388	89965	57586	135074	145224	92614	186761	200483	127642
Saw and Seal Deck over Backwall	7765	8336	5267	8840	9472	5973	9916	10607	6678
Saw and Seal over EM-SEAL	80094	52224	47907	80094	52224	47907	80094	52224	47907
Asphalt Plug Joint	172379	123574	90007	199291	142413	103368	226204	161252	116729
Modular Joint	656782	671624	686903	872481	889286	906551	1088180	1106947	1126200
EM-SEAL	68965	55519	62269	68965	55519	62269	68965	55519	62269

Table 5.9: Story - 25 Years Service Life, 4% Inflation Rate

Joint Type	US Dollar ($)								
	LE	LA	LL	AE	AA	AL	HE	HA	HL
Finger Joints	116465	117167	117875	122090	122792	123500	127715	128417	129125
Pourable Seal	337950	181040	99860	337950	181040	99860	337950	181040	99860
Compression Seal	72998	76356	80091	72998	76356	80091	72998	76356	80091
Strip Seal	28771	29633	12330	46605	47835	19830	64438	66036	27330
Saw and Seal Deck over Backwall	2607	2694	1120	2968	3062	1270	3329	3429	1420
Saw and Seal over EM-SEAL	26322	14532	15796	26322	14532	15796	26322	14532	15796
Asphalt Plug Joint	50311	41441	30695	58165	47759	35251	66020	54076	39807
Modular Joint	130170	131911	133691	172920	174661	176441	215670	217411	219191
EM-SEAL	23250	14223	14834	23250	14223	14834	23250	14223	14834

Table 5.10: Story - 50 Years Service Life, 4% Inflation Rate

Joint Type	US Dollar ($)								
	LE	LA	LL	AE	AA	AL	HE	HA	HL
Finger Joints	716040	729655	743578	750624	764684	779062	785207	799714	814545
Pourable Seal	1468563	833705	469895	1468563	833705	469895	1468563	833705	469895
Compression Seal	400492	288990	333581	400492	288990	333581	400492	288990	333581
Strip Seal	105162	117084	70481	168552	186744	111826	231941	256403	153170
Saw and Seal Deck over Backwall	10346	11434	6753	11687	12882	7588	13027	14329	8423
Saw and Seal over EM-SEAL	107752	68327	64437	107752	68327	64437	107752	68327	64437
Asphalt Plug Joint	229846	163892	118058	264942	188122	134888	300038	212351	151718
Modular Joint	865520	893103	921796	1128352	1159329	1191470	1391185	1425554	1461145
EM-SEAL	91238	72482	85153	91238	72482	85153	91238	72482	85153

Table 5.11: Marshall - 25 Years Service Life, 2% Inflation Rate

Joint Type	US Dollar ($)								
	LE	LA	LL	AE	AA	AL	HE	HA	HL
Finger Joints	201435	201979	202527	213102	213647	214194	224769	225314	225861
Pourable Seal	618119	331691	185200	618119	331691	185200	618119	331691	185200
Compression Seal	136476	140470	144819	136476	140470	144819	136476	140470	144819
Strip Seal	54761	55791	24736	89599	91087	40293	124437	126383	55849
Saw and Seal Deck over Backwall	4754	4856	2152	5456	5565	2463	6159	6275	2774
Saw and Seal over EM-SEAL	47919	27233	28738	47919	27233	28738	47919	27233	28738
Asphalt Plug Joint	93070	75862	56420	107923	87782	65133	122777	99702	73846
Modular Joint	250460	252578	254728	339131	341250	343399	427803	429921	432071
EM-SEAL	42585	26840	27575	42585	26840	27575	42585	26840	27575

Table 5.12: Marshall - 50 Years Service Life, 2% Inflation Rate

Joint Type	US Dollar ($)								
	LE	LA	LL	AE	AA	AL	HE	HA	HL
Finger Joints	843703	850762	857896	892571	899906	907319	941439	949050	956741
Pourable Seal	1698951	952897	555646	1698951	952897	555646	1698951	952897	555646
Compression Seal	467030	356372	379931	467030	356372	379931	467030	356372	379931
Strip Seal	138891	145621	98730	227253	237747	160821	315615	329874	222911
Saw and Seal Deck over Backwall	12265	12822	8627	14076	14696	9874	15887	16570	11121
Saw and Seal over EM-SEAL	125248	83813	74962	125248	83813	74962	125248	83813	74962
Asphalt Plug Joint	271774	195827	144139	315149	226598	166398	358524	257368	188657
Modular Joint	1049045	1063891	1079021	1420441	1437385	1454629	1791838	1810879	1830237
EM-SEAL	109571	89315	95990	109571	89315	95990	109571	89315	95990

Table 5.13: Marshall - 25 Years Service Life, 3% Inflation Rate

Joint Type	US Dollar ($)								
	LE	LA	LL	AE	AA	AL	HE	HA	HL
Finger Joints	220110	221055	222007	231777	232722	233674	243444	244389	245341
Pourable Seal	700970	375510	207128	700970	375510	207128	700970	375510	207128
Compression Seal	151411	158375	166124	151411	158375	166124	151411	158375	166124
Strip Seal	59677	61465	25575	96667	99218	41131	133656	136971	56687
Saw and Seal Deck over Backwall	5406	5589	2323	6155	6350	2634	6904	7112	2945
Saw and Seal over EM-SEAL	54597	30143	32764	54597	30143	32764	54597	30143	32764
Asphalt Plug Joint	104353	85956	63666	120645	99060	73117	136938	112164	82567
Modular Joint	269996	273607	277299	358667	362278	365971	447338	450949	454642
EM-SEAL	48224	29501	30768	48224	29501	30768	48224	29501	30768

Table 5.14: Marshall - 50 Years Service Life, 3% Inflation Rate

Joint Type	US Dollar ($)								
	LE	LA	LL	AE	AA	AL	HE	HA	HL
Finger Joints	1110581	1125500	1140667	1169449	1184904	1200613	1228317	1244308	1260559
Pourable Seal	2258889	1274277	730946	2258889	1274277	730946	2258889	1274277	730946
Compression Seal	618280	459212	508550	618280	459212	508550	618280	459212	508550
Strip Seal	172961	186604	119444	280169	301221	192098	387376	415839	264753
Saw and Seal Deck over Backwall	16105	17291	10925	18336	19646	12388	20567	22001	13852
Saw and Seal over EM-SEAL	166129	108321	99368	166129	108321	99368	166129	108321	99368
Asphalt Plug Joint	357544	256315	186691	413366	295390	214404	469187	334466	242117
Modular Joint	1362285	1393070	1424760	1809683	1844539	1880351	2257080	2296008	2335942
EM-SEAL	143047	115156	129157	143047	115156	129157	143047	115156	129157

Table 5.15: Marshall - 25 Years Service Life, 4% Inflation Rate

Joint Type	US Dollar ($)								
	LE	LA	LL	AE	AA	AL	HE	HA	HL
Finger Joints	241569	243025	244494	253236	254692	256162	264903	266359	267829
Pourable Seal	797353	426423	232280	797353	426423	232280	797353	426423	232280
Compression Seal	168514	179319	191608	168514	179319	191608	168514	179319	191608
Strip Seal	65292	68053	26519	104649	108541	42075	144006	149030	57632
Saw and Seal Deck over Backwall	6178	6470	2515	6979	7289	2827	7779	8108	3138
Saw and Seal over EM-SEAL	62427	33444	37508	62427	33444	37508	62427	33444	37508
Asphalt Plug Joint	117321	97725	72093	135235	112172	82371	153149	126620	92648
Modular Joint	291998	297464	303094	380669	386136	391765	469341	474807	480436
EM-SEAL	54811	32511	34451	54811	32511	34451	54811	32511	34451

Table 5.16: Marshall - 50 Years Service Life, 4% Inflation Rate

Joint Type	US Dollar ($)								
	LE	LA	LL	AE	AA	AL	HE	HA	HL
Finger Joints	1485197	1513435	1542315	1556929	1586093	1615914	1628660	1658751	1689513
Pourable Seal	3046065	1729253	974646	3046065	1729253	974646	3046065	1729253	974646
Compression Seal	830692	599418	691908	830692	599418	691908	830692	599418	691908
Strip Seal	218125	242854	146190	349606	387340	231946	481087	531827	317703
Saw and Seal Deck over Backwall	21460	23716	14007	24240	26719	15739	27020	29722	17471
Saw and Seal over EM-SEAL	223496	141722	133654	223496	141722	133654	223496	141722	133654
Asphalt Plug Joint	476742	339942	244874	549537	390198	279783	622332	440454	314691
Modular Joint	1795244	1852457	1911970	2340406	2404656	2471324	2885568	2956856	3030678
EM-SEAL	189245	150341	176623	189245	150341	176623	189245	150341	176623

From the results presented in the previous pages, it is clear that the Saw and Seal Deck over Backwall has the lowest cost across all types of joints and in all combinations of cost and service life (LE, LA, LL, etc.). It also has the lowest cost over a bridge service life of 25 years and 50 years as well. This can be easily recognized in the color-coded tables as Saw and Seal Deck over Backwall presents the most green cells in each table. From the other types of joints, Modular Joint, Finger Joint, Pourable Seal were identified as having the highest cost by a wide margin for all of the cases shown. Saw and Seal over EM-SEAL, Asphalt Plug Joint, Strip Seal, and EM-SEAL ranked the lowest in terms of costs among the remaining types of joints.

5.4 Construction Cost Of Deck Over Backwall Concept

Various items were taken into consideration to develop an estimate of the construction cost of the deck over backwall concept. The Final Bridge Design Software (Iowa DOT Office of Bridges and Structures 2018b) was used to identify items that would pertain to the construction cost of the deck over backwall concept. Table 5.17 shows the items that were chosen in the software with the long bid and short bid descriptions, measuring unit, unit price for each one, and date of cost data.

Table 5.17: Deck over Backwall Concept Construction Items

Source: Iowa DOT Office of Bridges and Structures (2018)

Item Code	Long Bid Item Description	Unit	Unit Price ($)			Date of Cost Data	Short Bid Item Description
			Low	High	Average		
2102-2710070	EXCAVATION, CLASS 10, ROADWAY AND BORROW	CY	2	89.5	3.07	5-2016 thru 4-2017	EXCAVATION, CL 10, RDWY+BORROW
2115-0100000	MODIFIED SUBBASE	CY	17	135	40.36	5-2016 thru 4-2017	MODIFIED SUBBASE
2301-0690205	BRIDGE APPROACH, BR-205	SY	150	190	174.06	5-2016 thru 4-2017	BRIDGE APPROACH, BR-205
2401-7207020	REMOVAL OF CONCRETE	CY	267	267	267	12-2014 thru 10-2015	RMVL OF CONC

The first item shown in the table above is the excavation of Class 10 soil. According to Iowa DOT (2018), Class 10 soils include normal earth materials such as loam, silt, gumbo, peat, clay, soft shale, sand, and gravel. It was determined that this Class applied for most cases, therefore it was used in the estimate. The excavation consists 24 inches below the approach slab according to Iowa DOT Office of Design (2018). This can be seen in Chapter 3, Figure 3.1. Using this standard, the deck over backwall concept was estimated as having a similar cost to the BR-205 approach slab shown in the same figure. The new modified subbase was also considered in the cost estimate. It is to be placed in the same volume that was excavated supporting the new approach slab. Finally, the concrete removal of the current approach slab plus the abutment interface was assumed for the length of the deck over backwall concept and a 12 inch thickness.

Even though the Marshall County bridge was chosen as the test bridge that the deck over backwall concept would be implemented, calculations were done for both the Story County bridge and the Marshall County bridge. A substantial difference in the estimate can be seen from a non-skewed bridge to a skewed bridge since different units of area and volume lead to different cost estimates. The skew of the Marshall County bridge results in one end of the approach slab being a 20 feet section while the other being a 64 foot section. This increases the cost from non-skewed bridge counterparts like the Story County bridge. A summary of the costs associated with the deck over backwall concept is presented in Table 5.18 and Table 5.19 for the Story County bridge and the Marshall County bridge respectively. The average unit price from the Final Bridge Design Software was used for both estimates.

Table 5.18: Story - Construction Cost of Deck over Backwall Concept

Short Bid Item Description	Total Quantity	Unit	Total Cost ($)	Unit Price ($)		
				Low	High	Average
EXCAVATION, CL 10, RDWY+BORROW	44.44	CY	136.44	2	89.5	3.07
MODIFIED SUBBASE	44.44	CY	1,793.78	17	135	40.36
BRIDGE APPROACH, BR-205	66.67	SY	11,603.88	150	190	174.06
RMVL OF CONC	22.22	CY	5,933.33	267	267	267
	Total Cost ($)		19,467.44			

Table 5.19: Marshall - Construction Cost of Deck over Backwall Concept

Short Bid Item Description	Total Quantity	Unit	Total Cost ($)	Unit Price ($)		
				Low	High	Average
EXCAVATION, CL 10, RDWY+BORROW	136.89	CY	420.25	2	89.5	3.07
MODIFIED SUBBASE	136.89	CY	5,524.84	17	135	40.36
BRIDGE APPROACH, BR-205	205.33	SY	35,739.96	150	190	174.06
RMVL OF CONC	68.44	CY	18,274.67	267	267	267
	Total Cost ($)		59,959.71			

The total construction cost of the deck over backwall concept resulted in approximately $20,000 for the Story County bridge and $60,000 for the Marshall County bridge. The approach slab itself, which was assumed as the BR-205 approach slab from the Iowa DOT Bridge Approach Standards, accounts for more than half of the total construction cost of the deck over backwall concept. While the concrete removal accounts for almost a third of the cost and the remaining items in excavation and the modified subbase account for the other fractions of the construction cost.

From these total cost numbers, the impact of the skew on the approach slab costs can be recognized. An almost 50% increase in roadway length, 44 feet for the Marshall County bridge and 30 feet for the Story County bridge, with a 45-degree skew, triples the construction cost of the approach slab. This major difference is due to the higher area and volume requirements of an approach slab with a non-skewed end. In comparison, for other

types of joints, the skew and the roadway difference would more than double due to costs being calculated per foot (62.225 feet for Marshall County and 30 feet for Story County).

With this construction cost estimate, a better comparison can be realized with other types of joints combining the repair or replacement costs of the Saw and Seal Deck over Backwall and the construction cost of the deck over backwall concept calculated previously. Results are shown in Table 5.20 and Table 5.21 for the Marshall County bridge with an inflation rate of 2%. Table 5.22 and Table 5.23 correspond to an inflation rate of 3%. The tables correspond to a bridge service life of 25 years and 50 years respectively. Only the comparable types of joints in terms of costs are shown. Four types of joints (FJ, PS, CS, and MJ) were omitted since the cost resulted extremely high compared to the ones shown in the tables. The tables are also color coded in the same manner as the previously shown.

Table 5.20: Deck over Backwall Comparison, 25 Years Service Life, 2% Inflation Rate

Joint Type	US Dollar ($)								
	LE	LA	LL	AE	AA	AL	HE	HA	HL
Strip Seal	54761	55791	24736	89599	91087	40293	124437	126383	55849
Saw and Seal Deck over Backwall	64714	64815	62111	65416	65525	62423	66118	66235	62734
Saw and Seal over EM-SEAL	47919	27233	28738	47919	27233	28738	47919	27233	28738
Asphalt Plug Joint	93070	75862	56420	107923	87782	65133	122777	99702	73846
EM-SEAL	42585	26840	27575	42585	26840	27575	42585	26840	27575

Table 5.21: Deck over Backwall Comparison, 50 Years Service Life, 2% Inflation Rate

Joint Type	US Dollar ($)								
	LE	LA	LL	AE	AA	AL	HE	HA	HL
Strip Seal	138891	145621	98730	227253	237747	160821	315615	329874	222911
Saw and Seal Deck over Backwall	72224	72782	68586	74036	74656	69834	75847	76530	71081
Saw and Seal over EM-SEAL	125248	83813	74962	125248	83813	74962	125248	83813	74962
Asphalt Plug Joint	271774	195827	144139	315149	226598	166398	358524	257368	188657
EM-SEAL	109571	89315	95990	109571	89315	95990	109571	89315	95990

Table 5.22: Deck over Backwall Comparison, 25 Years Service Life, 3% Inflation Rate

Joint Type	US Dollar ($)								
	LE	LA	LL	AE	AA	AL	HE	HA	HL
Strip Seal	59677	61465	25575	96667	99218	41131	133656	136971	56687
Saw and Seal Deck over Backwall	65366	65549	62282	66115	66310	62593	66864	67071	62905
Saw and Seal over EM-SEAL	54597	30143	32764	54597	30143	32764	54597	30143	32764
Asphalt Plug Joint	104353	85956	63666	120645	99060	73117	136938	112164	82567
EM-SEAL	48224	29501	30768	48224	29501	30768	48224	29501	30768

Table 5.23: Deck over Backwall Comparison, 50 Years Service Life, 3% Inflation Rate

Joint Type	US Dollar ($)								
	LE	LA	LL	AE	AA	AL	HE	HA	HL
Strip Seal	172961	186604	119444	280169	301221	192098	387376	415839	264753
Saw and Seal Deck over Backwall	76065	77250	70885	78296	79606	72348	80526	81961	73812
Saw and Seal over EM-SEAL	166129	108321	99368	166129	108321	99368	166129	108321	99368
Asphalt Plug Joint	357544	256315	186691	413366	295390	214404	469187	334466	242117
EM-SEAL	143047	115156	129157	143047	115156	129157	143047	115156	129157

From the tables shown, it can be seen that for a bridge service life of 25 years, the deck over backwall concept has a higher cost than other comparable types of joints. The high initial cost accounts for most of the costs since the repair or replacement cost of Saw and Seal Deck over Backwall was the lowest of all types of joints by a wide margin. While the deck over backwall concept might not be the best option for a bridge service life of 25 years in terms of cost, for a bridge service life of 50 years, the deck over backwall concept has the lowest costs when compared to all other types of joints across all different combinations of cost points and service life stage (LE, LA, LL, etc.).

5.5 Break-Even Point Analysis

As it was detailed previously for the Marshall County bridge, the deck over backwall concept produced the lowest costs for a bridge service life of 50 years. In contrast, it did not rank as the best alternative for a bridge service life of 25 years. Because of this, a break-even point (BEP) between the 25 years and 50 years was identified. Beyond that point, the deck over backwall concept would produce the lowest costs among all other types of joints across all different combinations of cost points and service life stage. Figure 5.7, Figure 5.8, and Figure 5.9 show the cost estimate graphs presented previously for the Marshall County bridge with an interest rate of 2%. The vertical axis is limited to $100,000 so that the BEP can be appreciated. Table 5.24 presents the BEP for the Marshall County bridge across all different combinations of cost points and service life stage for interest rates of 2%, 3%, and 4%. The average BEP for each interest rate is also shown.

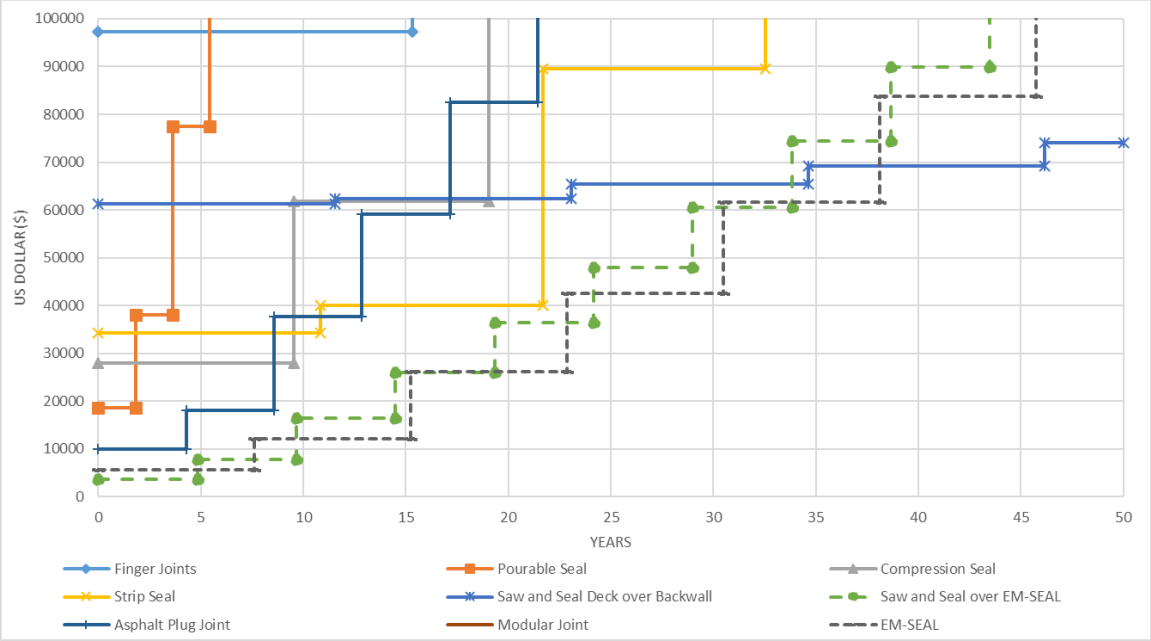

Figure 5.7: Break-Even Point - Average Cost, Early Service Life

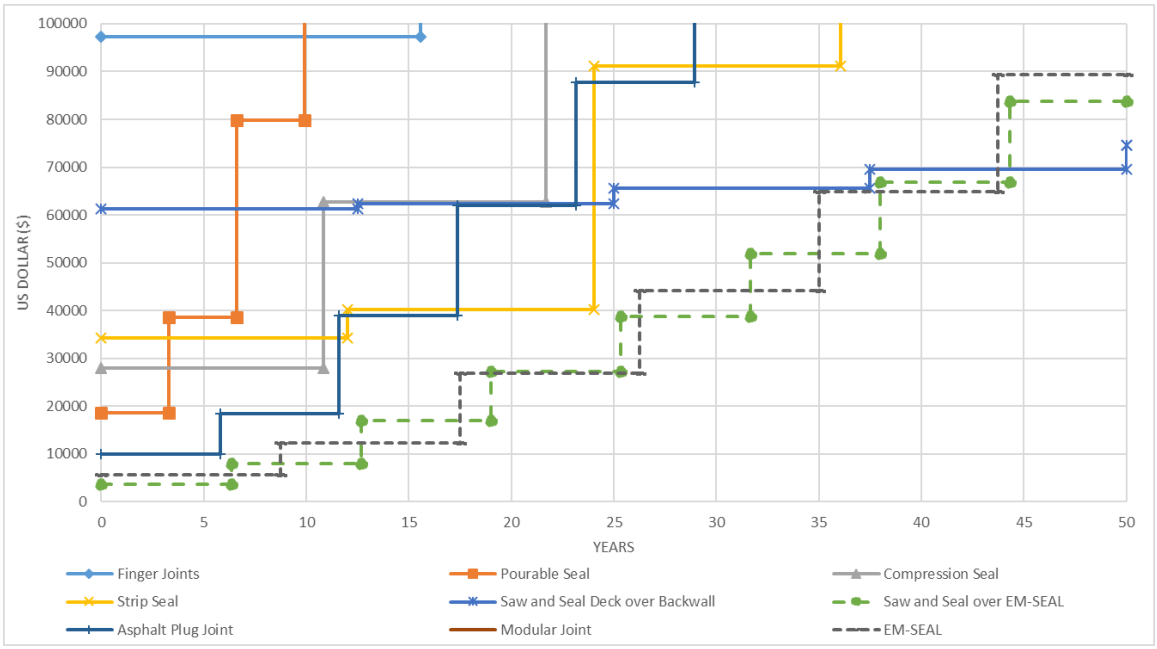

Figure 5.8: Break-Even Point - Average Cost, Average Service Life

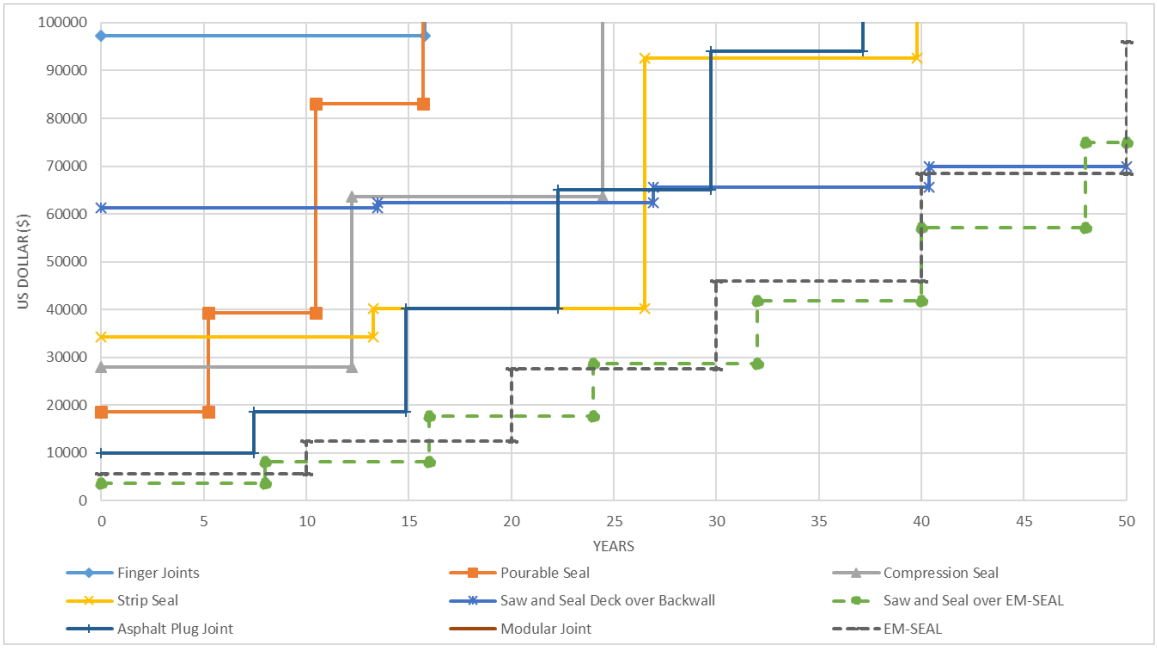

Figure 5.9: Break-Even Point - Average Cost, Late Service Life

Table 5.24: Break-Even Point of Deck over Backwall Concept

Break-Even Point (Years)										
Interest Rate	LE	LA	LL	AE	AA	AL	HE	HA	HL	Average
2%	38	44	50	38	44	50	38	44	50	44
3%	33	38	40	31	38	48	31	38	48	38
4%	33	35	40	31	38	40	31	38	40	36

As it can be seen in the table, the BEP for the deck over backwall concept ranges from 31 years to 50 years. Some BEPs end up at exactly 50 years since the particular type of joint that would be comparable to the deck over backwall concept would need a repair or replacement on that same year. The lowest BEP that was obtained in the study was 31 years on four of the 27 different cases considered. The average BEP is shown for all three interest rates used in the analysis. The average BEPs were 44 years, 38 years, and 36 years for interest rates of 2%, 3%, and 4% respectively. From these results, it can be concluded that as the interest rate increases, the BEP decreases. In this analysis, the interest rate does not affect the initial construction cost of the deck over backwall concept. Since the repair or replacement costs of Saw and Seal Deck over backwall were the lowest among all different types of joints, as the interest rate increases all repair or replacement costs for the remaining types of joints would increase more than the Saw and Seal Deck over Backwall.

5.6 Summary And Discussion

To develop a cost analysis comparing the deck over backwall concept and different types of joints, pertinent information was used from Civjan and Quinn (2016) with the service life and installation costs of types of joints. Both variables, service life and installation costs, were varied throughout the development of the cost estimate. From this information, various service life stages were determined for each type of joint. The service life of each joint was split into values for an Early, Average, or Late (E, A, or L) service life. The costs of each joint were also varied throughout the study with different cost points. The installation for the different types of joints ranged in cost value and three different cost points were determined for each one. These cost points were Low, Average, and High (L, A, and H). Other factors were also varied during the cost analysis. Interest rates were used as 2%, 3%, and 4% though results were only shown for 2% and 3%. In addition, the study was developed for both the Story County bridge and the Marshall County bridge even though the majority of the results shown correspond to the Marshall County bridge.

A cost estimate of nine different types of joints was developed based on the number of times the joint has to be repaired or replaced in the service life of the bridge. The installation costs of each joint were assumed to be the same as the repair or replacement costs with the exception of one type of joint, Strip Seal joints. A variable bridge service life of 25 years and 50 years was used throughout the study. Results from this estimate show that Saw and Seal Deck over Backwall produced the lowest repair or replacement cost among all nine joints across all different interest rates (2%, 3%, and 4%), both bridges under study (Story County bridge and Marshall County bridge), and combinations of cost points and service life stage (LE, LA, LL, etc.).

An initial construction cost of the deck over backwall concept was developed. Iowa DOT Final Fridge Design software was used to estimate the construction cost using the applicable bid items. The total construction cost of the deck over backwall concept resulted in approximately $20,000 for the Story County bridge and $60,000 for the Marshall County bridge. The impact of the skew was identified with the higher amounts of volume and area due to the approach slab having a non-skewed end.

The construction cost was incorporated in the repair or replacement cost estimate previously discussed. Result show that for a bridge service life of 25 years, the concept has a higher cost than other comparable types of joints. The high initial cost accounts for most of the cost since the repair or replacement cost of Saw and Seal Deck over Backwall was the lowest of all types of joints. For a bridge service life of 50 years, the concept has the lowest costs when compared to all other types of joints across all different combinations of cost points and service life stages. Because of this, a BEP between the 25 years and 50 years was identified. Beyond that point, the deck over backwall concept would produce the lowest costs among all other types of joints across all different combinations of cost points and service life stage. Results show that as the interest rate increases, the BEP decreases. The average BEPs were 44 years, 38 years, and 36 years for interest rates of 2%, 3%, and 4% respectively. The BEP for the deck over backwall concept ranges from 31 years to 50 years.

Many assumptions and simplifications were made to realize the cost estimate of the various types of joints. Numerous factors could have been incorporated to improve the accuracy of this analysis. Costs of maintenance of the interaction between abutment/bridge deck and approach slab was not taken into account. Maintenance of steel girders, bearings, reinforcement, etc. was not considered either. These, among many other factors, could affect

the cost of the different types of joints compared in this study. Ideally, all of these factors would increment the costs of all types of joints. However, since the deck over Backwall would not be composed of an expansion joint in the abutment interface, some of the costs associated with these factors could be greatly reduced, and, quite possibly, be eliminated in its entirety in terms of cost.

In conclusion, if these factors are all taken into account, the type of joint that would increase the least would likely be the Saw and Seal Deck over Backwall further expanding the cost difference between itself and the next lowest cost for any particular type of joint and any particular combination of cost and service life stage (LE, LA, LL, etc.).

While this cost analysis covered the most pertinent elements of the construction process, many other components could be factored into the analysis. Some of these components could be formwork costs, labor costs, work zone costs, lane closure costs, mobilization, etc. These can all be added in the construction cost of the deck over backwall. At the same time, these components and many others could also be added in the installation, repair, or replacement costs of all types of joints that were studied.

CHAPTER 6. EXPERIMENTAL INVESTIGATION PLAN

The research team realized a plan to conduct laboratory testing on the Iowa DOT joint detailing presented in Chapter 3. The test results will be compared and correlated with FE results obtained in Chapter 4. The FE models can be validated and confidently used for further advancements of the research.

6.1 Test Setup

The joint detailing developed by the Iowa DOT will be tested on a laboratory setting. Simplifications had to be realized to facilitate the framework and the casting of the concrete while not impacting the pertinent results that the experimental investigation would produce.

The full-scale test specimen can be seen in the laboratory testing plan shown in Figure 6.2. A more detailed look into the joint is shown below in Figure 6.1. The plan includes reference lines to separate each section, the approach slab, the bridge deck, and the curb. The abutment stud wall and backwall are represented as well even though these elements are not physically present in the test specimen or the laboratory. Load location can also be applied at the center of the 20 feet double reinforced section.

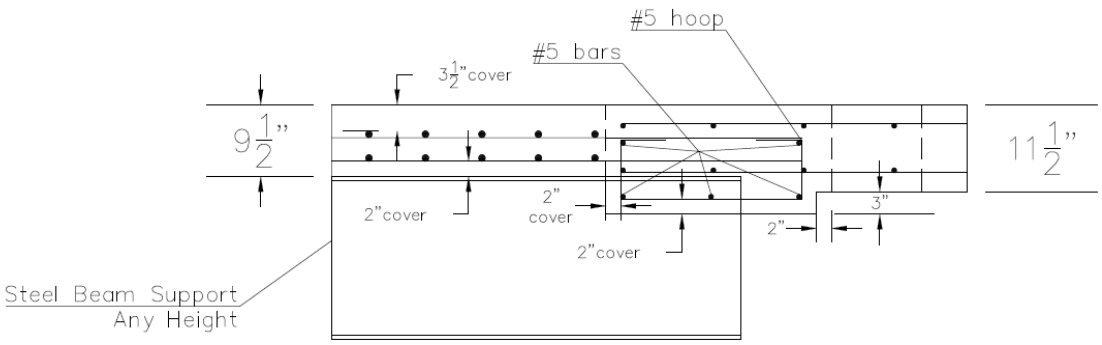

Figure 6.1: Laboratory Testing Joint

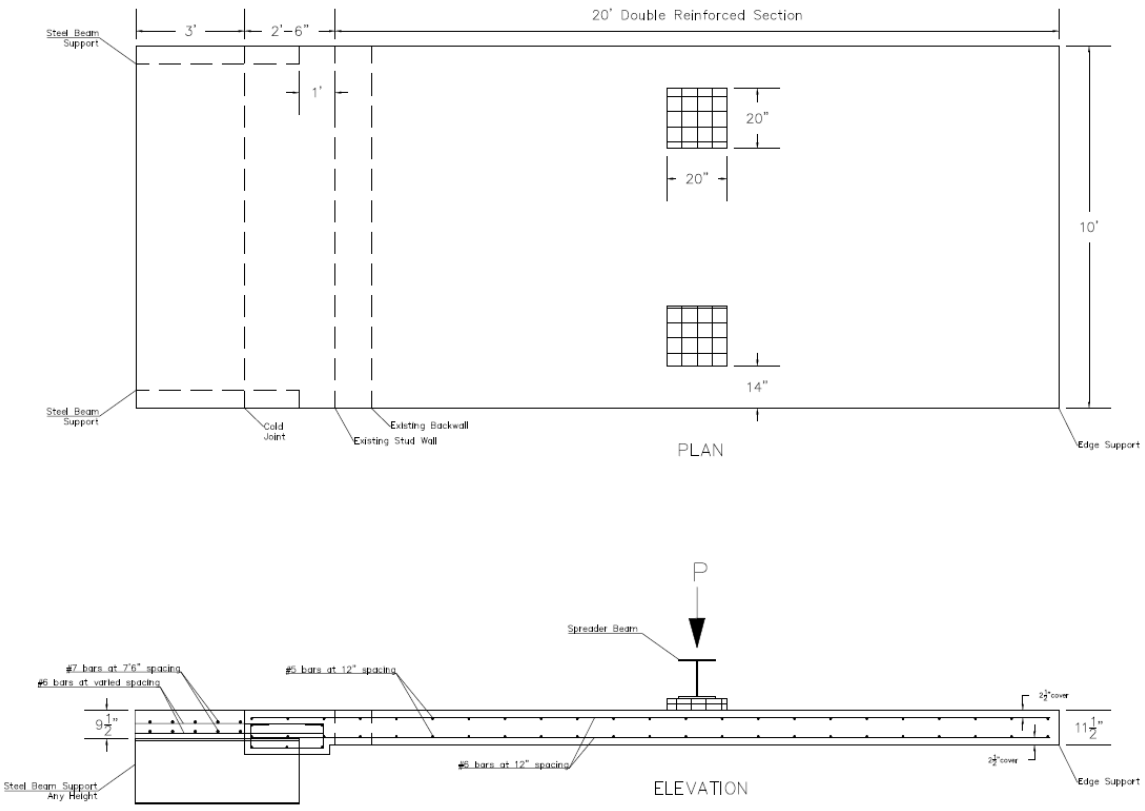

Figure 6.2: Laboratory Testing Plan

The test specimen was 25.5 feet long in total composed by three specific sections. The thickness varied in those three different sections. The thickness of each section were 9.5 inches, 11.5 inches, and 14.5 inches. The 9.5 inches section was 3 feet long and represented the existing bridge deck with its corresponding reinforcement. Reinforcement bars in this section were not coated with epoxy. A 14.5 inches section followed corresponding to the curb and its detailing. The 11.5 inches section corresponded to the approach slab. The reinforcement bars of both the curb section and the approach slab section will be coated with epoxy.

Various factors influenced the size of the test specimen. Room availability in the structures laboratory during the dates that the testing would be realized greatly influenced the size of the test specimen. In addition, the girder spacing for the Marshall County bridge is 10 feet. This length also correlates with the load allocation for a lane load according to the AASHTO Specifications (American Association of State Highway and Transportation Officials 2014). This is explained in detail in Chapter 4, Section 4.1.2.3. With these factors taken into account and a 10 ft width being feasible with the room availability in the structures laboratory, it was decided that a width of 10 feet was going to be used for the specimen.

The test specimen is to be supported at the opposite end of the abutment interface by a roller support. The roller support is not allocated in the edge but 6 inches into the approach slab. This would not affect the results obtained at the points of interest. On the other end, beams extend over the bridge deck section and into the curb section. The beams have stud shear connectors in the top flanges and would be embedded into the bridge deck section.

6.2 Load Allocation

A simulation of an HS-20-44 truck loading condition was used. This truck loading condition is detailed in Chapter 4, Figure 4.9 and Figure 4.10. Load would be applied at the center of the 20 feet double reinforced section over two areas simulating the rear axle of an HS-20-44 truck loading condition. According to the AASHTO Specifications, the wheel loads were assumed as uniformly distributed over an area of 20 inches by 20 inches spaced by 6 feet center to center. The test specimen will be tested until the load applied causes failure to occur. Though, data will be acquired throughout the test and, more pertinent, when the load on each area resulted 16,000 pounds. The rear axle of an HS-20-44 truck loading condition weights a total of 32,000 pounds.

6.3 Instrumentation

A total of 19 strain gages will be installed in the test specimen. With these strain gages, stress levels at desired locations of the approach slab can be monitored throughout the test. Three strain gages will be installed at the center of the 20 feet double reinforced section on the bottom longitudinal reinforcement bars below each load application area. Additionally, three strain gages will be installed on the bottom reinforcement bars in between the two load application areas at the center of the width of the slab. The remaining strain gages will be installed on the top and bottom longitudinal reinforcement bars at the center of the abutment interface, between the stud wall and the backwall reference lines. Two strain gages, one on the top and one on the bottom reinforcement bars, will be installed on the first line of reinforcement bars closest to each beam support. Six additional strain gages, three on the top and three on the bottom reinforcement bars, will be installed at the center of the width of the slab. The strain gage arrangement can be seen below in Figure 6.3 and Figure 6.4.

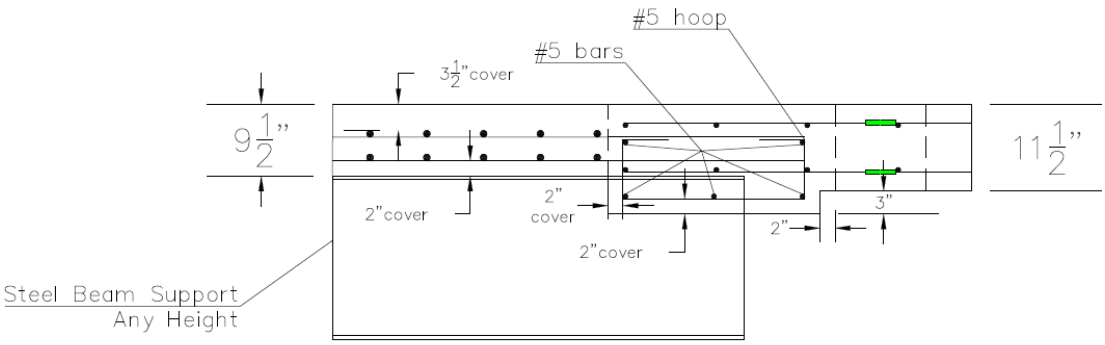

– Strain Gages

Figure 6.3: Joint Strain Gage Arrangement

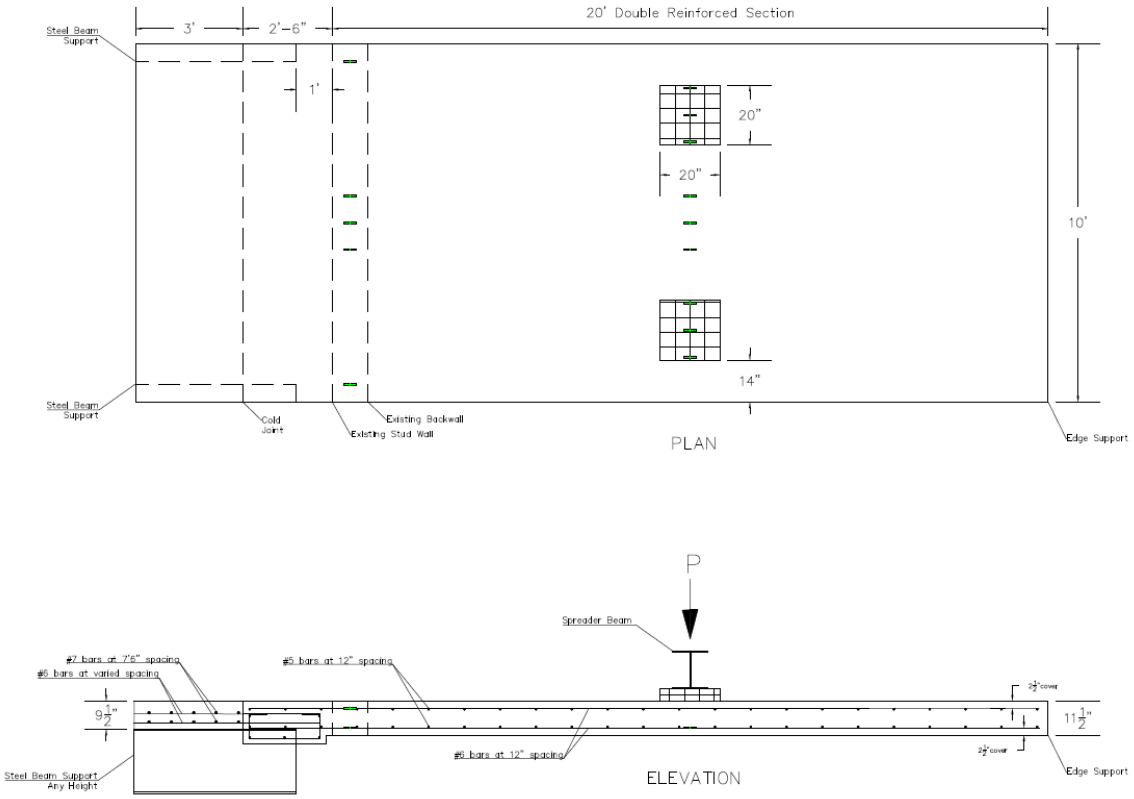

Figure 6.4: Strain Gage Arrangement

Visual inspection will also be realized throughout the test. Concrete cracking at different locations will be recorded. Close attention will be paid on the joint between the bridge deck and the approach slab. Additionally, any cracking on the bottom of the approach slab and its location will also be taken as a point of interest.

CHAPTER 7. CONSTRUCTION OBSERVATION AND POST-CONSTRUCTION TESTING PLAN

In this chapter, a construction observation and post-construction testing plan was developed according to the joint developed by the Iowa DOT. An instrumentation plan was developed with various types of sensors and equipment. A post-construction plan with different truck loading cases was developed as well. The correlations between the results from future field testing and predictions will serve to calibrate and improve the accuracy of the FE models. The test results will also provide vital information on the behavior of expansion joints and allow their efficient design.

7.1 Joint Detailing

The joint developed by the Iowa DOT detailed in Chapter 3, Figure 3.6, Figure 3.7, Figure 3.8, and Figure 3.9, was determined to be the deck over backwall concept that would be implemented in a future Iowa DOT construction season. This joint was used for the development of the instrumentation plan and post-construction testing discussed in the following pages.

7.2 Instrumentation

The instrumentation plan developed for the deck over backwall concept consists of various types of sensors and equipment. The instrumentation includes strain gages with temperature sensors, monitoring plates for surveying data, surveying equipment, and gapmeters. Each sensor and equipment serve a purpose to obtain real-life data to correlate with the FE results discussed in Chapter 4.

Thiagarajan et al. (2013) detailed Missouri DOT's (MoDOT) experience with the field performance of various types of bridge approach slab designs. Monitoring plates were incorporated in their approach slabs to provide a smooth and flat surface to collect accurate readings. The deflections of the approach slab can be monitored over time using surveying equipment over these monitoring plates. The equipment is shown in Figure 7.1. Detailed information on the monitoring plates is provided in Figure 7.2. In discussions between the research team and the Iowa DOT, the option of using vertical reinforcement bars embedded into the concrete was brought up. The main advantage from the use of the monitoring plates is that the plates would not be chipped away by snow plow strikes or traffic loads. However, that option could be implemented as well since surveying data can be taken at the same points. There are nine points of interest shown in Figure 7.3.

Gapmeters would also be incorporated between the girders and the abutment stud wall. These sensors would monitor the displacement of the girders at a certain height in the longitudinal direction. With this data, rotation of the girders can also be monitored.

A total of 13 strain gages locations have been recommended where their results would be of interest. There are nine strain gage locations across the abutment interface. Four at the midspan of the transverse spans and five across each girder support. Four additional strain gages locations were identified at the midspan of the approach slab. This arrangement can be appreciated in more detail in the instrumentation plan shown in Figure 7.4. Both top and bottom reinforcement bars can be allocated with strain gages. Multiple strain gages should be used in each location since there is the possibility that a certain number of strain gages do not work correctly because of a malfunction. With these strain gages, stress levels at the desired locations of the joint and approach slab can be monitored over time.

Source: Thiagarajan et al. (2013)

Figure 7.1: Surveying Prism (Left), Total Station (Right)

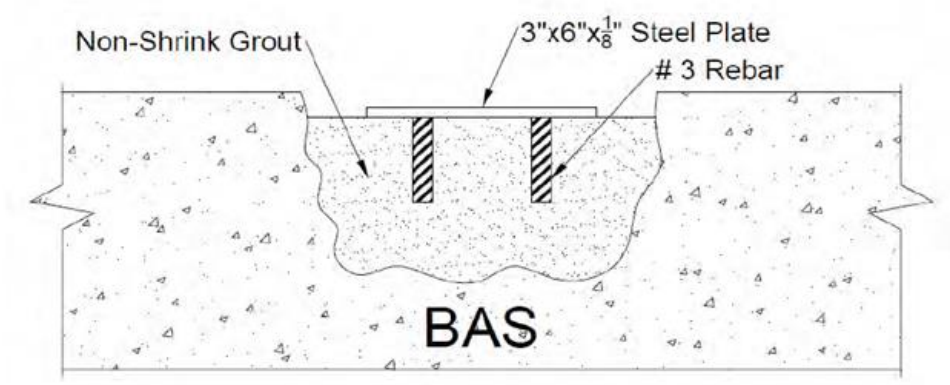

Source: Thiagarajan et al. (2013)

Figure 7.2: Monitoring Plates Details

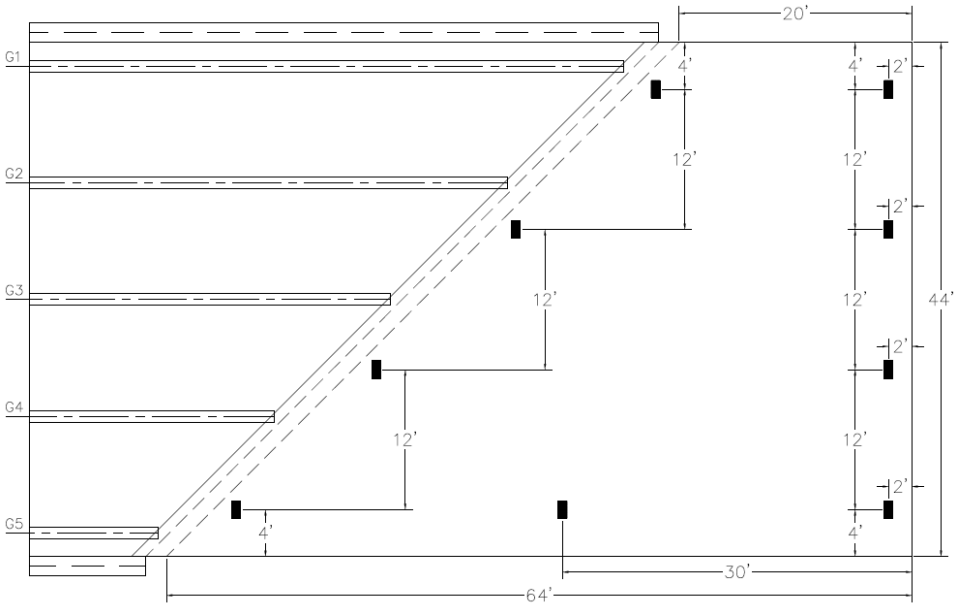

Figure 7.3: Monitoring Plates Distribution

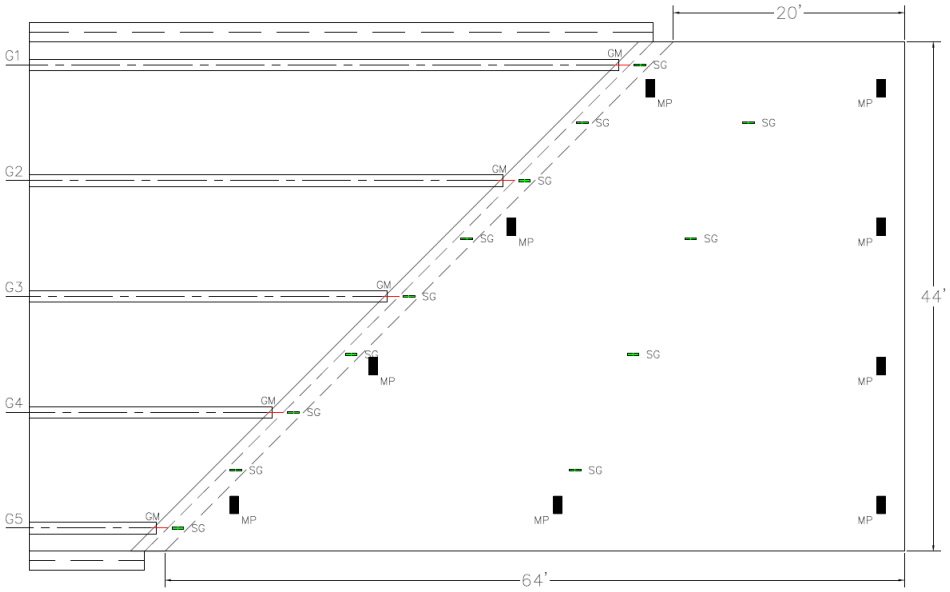

SG: Strain Gage (13 locations)
MP: Monitoring Plate (8 locations)
GM: Gap Meter (5 girders)

Figure 7.4: Instrumentation Plan

7.3 Truck Loading Cases

Various truck loading allocations were considered for the post-construction testing of the deck over backwall concept. For the purpose of this research and continuity, HS-20-44 truck loading conditions were used for this plan. These truck loads were previously shown in Chapter 4, Figure 4.56, Figure 4.57, Figure 4.58, and Figure 4.59, for the FE model of the Marshall County bridge with the approach slab. During the discussion that follows, the middle and rear axle of the trucks would be used for allocation purposes. Therefore, even if a different truck with different dimensions and tire spacing is used in the real-life simulations, these same axles could be used for the truck allocation.

The different truck cases can be seen in Figure 7.5, Figure 7.6, Figure 7.7, and Figure 7.8 as Case 1, Case 2, Case 3, and Case 4 respectively. The first truck loading case that was considered corresponds to the truck loading case used in the test specimen discussed in Chapter 6. Because of this, Case 1 also correlates with the Story County bridge FE model. While this model is a non-skewed bridge, the difference between a skewed bridge and a non-skewed bridge can be appreciated. For this case, the rear axle of the truck would be located at the midspan of the 20 feet section of the new approach slab. Case 2 corresponds to two trucks back-to-back at the midspan of the 64 feet section. This would maximize deflection values and stress levels in the approach slab. Case 3 corresponds to two trucks side-by-side with the rear axle close to the abutment interface. This would maximize the live load abutment reactions while causing deflection in the abutment interface. Case 4 corresponds to two trucks side-by-side at the midspan of the 64 feet section and at the center of the approach slab. This would provide high magnitudes of midspan deflection values and stress levels while adding to the live load abutment reactions of both the exterior and the interior supports. Therefore, adding live load to the bearing loads.

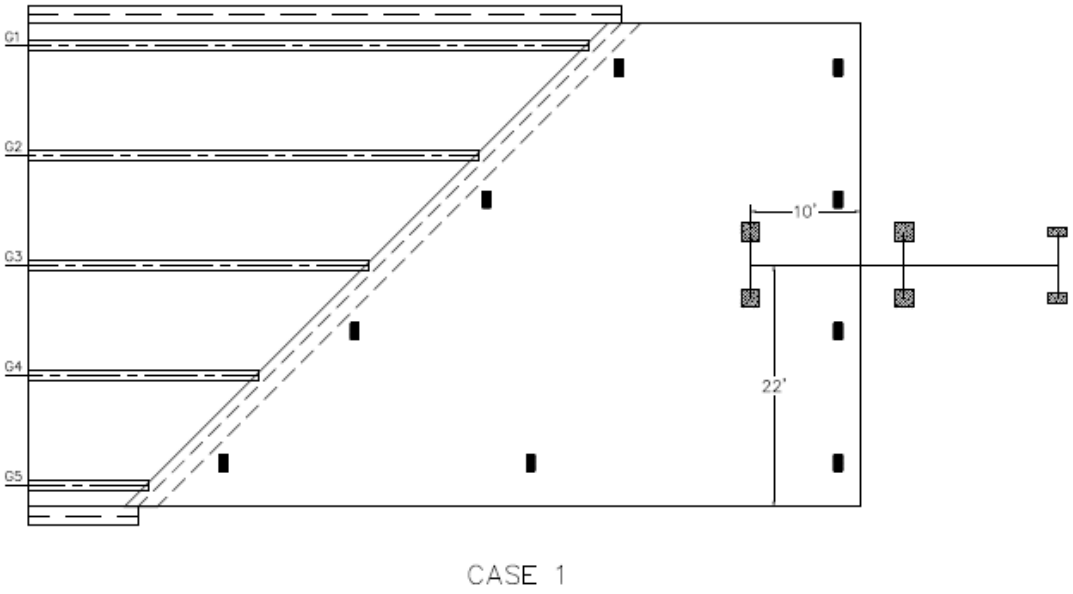

Figure 7.5: Truck Loading Case 1

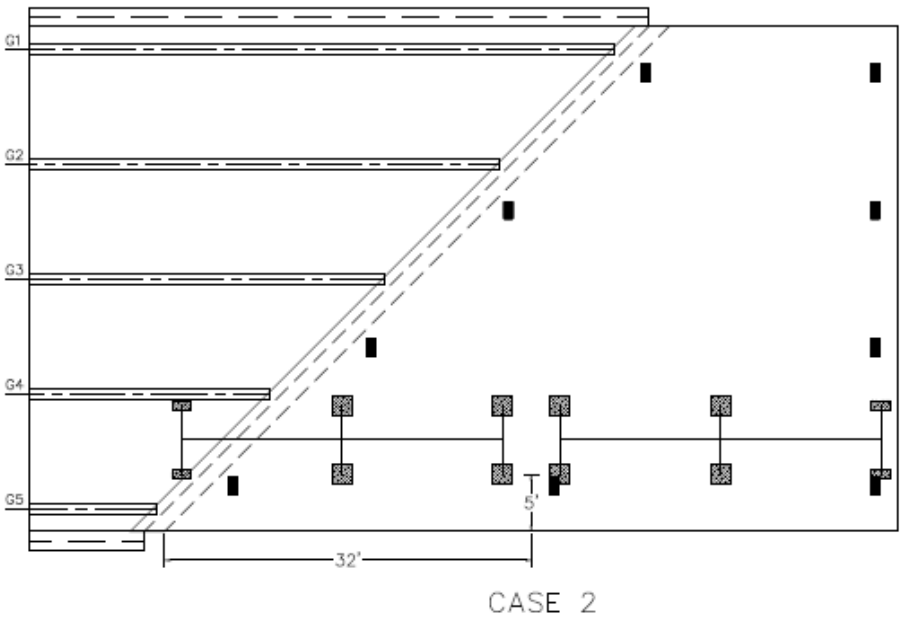

Figure 7.6: Truck Loading Case 2

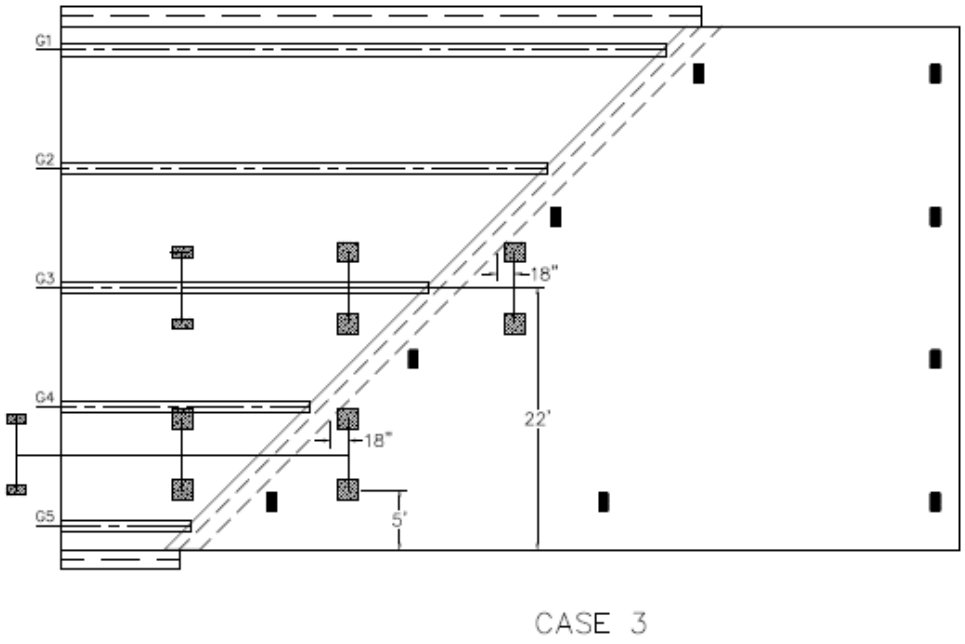

Figure 7.7: Truck Loading Case 3

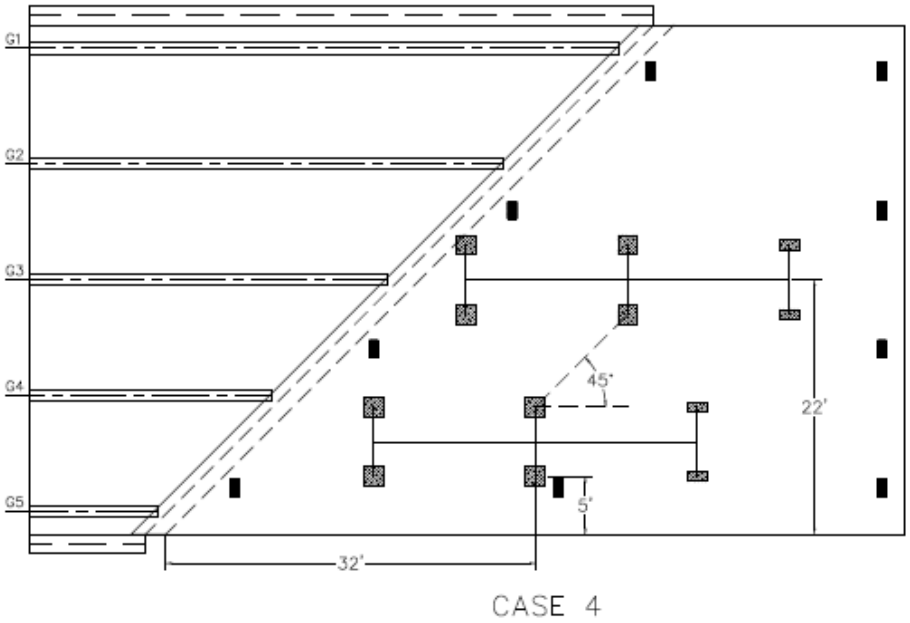

Figure 7.8: Truck Loading Case 4

CHAPTER 8. CONCLUSIONS AND FUTURE WORK

The objectives of the research set out in Chapter 1 were accomplished realizing the different chapters of the research. Conclusions were drawn from each chapter and possible future work alternatives were determined. These are shown and discussed in detail in the following pages.

8.1 Joint Detailing

Further development of the deck over backwall concept was accomplished in Chapter 3. The research team proposed various options with many different alternatives being considered by the research team and the Iowa DOT. Iowa DOT developed a joint taking into account the research team options and various factors.

While the Iowa DOT might move forward with the joint they developed, further detailing can be realized on the deck over backwall concept. There are still various options for several of the joints in the Iowa DOT joint detailing like the opposite end of the abutment interface and the joint 15 feet from the abutment stud wall. Possible options for these joints include a sleeper slab, subdrain, EF joint, CF joint, CD joint, or any combination of the previously mentioned.

8.2 Finite Element Modeling And Analysis

Full-scale FE models of two different bridges were realized and detailed in Chapter 4. These models were analyzed with various loading conditions from dead loads, temperature loading, and live loads which corresponds to various truck loading cases. Both models were validated using the original drawing plans. The same process of modeling was used for both

models in terms of material properties, boundary conditions, constraints, and loading conditions, etc.

The impact of the deck over backwall concept was studied with the Marshall County bridge model showing an increment in bearing loads due to the additional dead load of the approach slab and in live loads with the truck loading conditions. Relevant deflection values and stress levels at various points of interest across the abutment interface and the midspan of the approach slab were also determined. These FE results provide the Iowa DOT with the necessary knowledge to confidently design and further develop the deck over backwall concept.

A parametric study of various bridge skew angles (no skew, 30 degrees, 45 degrees, and 60 degrees) was also realized with the Marshall County bridge. Results for models without soil show that generally the increase in the bridge skew angle leads to the increase in all points of interest under study. These being the dead load abutment reactions and temperature deformation of the bridges with and without the approach slab, live load abutment reactions, deflection values and stress levels at the abutment interface and in the midspan of the approach slab. Results for models with soil show more variance and do not follow a general trend due to several factors.

With these models, future correlations between the models and real-life situations can be accomplished. The Story County bridge model, being a non-skewed bridge, will be compared and correlated with the future experimental investigation results. This is explained in Chapter 6. While the Marshall County bridge will be compared and correlated with the future post-construction testing. This is explained in Chapter 7.

While these models served the purpose of this research to study and develop the deck over backwall, further analysis could always be realized. One way this can be done is by incorporating the steel bar reinforcement and studying their behavior at the abutment interface and at midspan of the approach slab. This could be beneficial and provide more information for future designs of the deck over backwall concept. In addition, a plastic analysis could also be realized under certain truck loading conditions. The FE models were verified with loading conditions used at the time of construction. While those loads are not entirely different from the loads used at the time of writing, the FE models can be calibrated with current design loads.

Further modification of the FE models would also need to be made with the post-construction testing. This is detailed in 8.5.

8.3 Cost Analysis

A comparison between the different types of joints and the deck over backwall concept in terms of cost was realized and detailed in Chapter 5. When combining the repair or replacement costs and the construction cost of the deck over backwall concept, the concept was the best alternative among the nine types of joints considered for a bridge service life of 50 years. For a bridge service life of 25 years, the deck over backwall concept has a higher cost than other comparable types of joints. The concept usually ranks between 3rd and 4th of lowest cost out of the nine types of joints for most of the cases considered. The high initial cost accounts for most of the costs since the repair or replacement cost of Saw and Seal Deck over Backwall was the lowest of all types of joints by a wide margin. A BEP between the 25 years and 50 years was identified. Beyond that point, the deck over backwall concept would produce the lowest costs among all other types of joints across all different combinations of

cost points and service life stage. Results show a BEP of 44 years for a 2% interest rate and lowers as the interest rate is increased.

Many assumptions and simplifications were made in this study. Numerous factors could have been incorporated in the cost of installation, repair, replacement, and construction of not only the deck over back wall concept but the other types of joints that were considered as well. A more in depth cost analysis can be realized taking into account more factors like the costs of maintenance of the abutment interface, approach slab, steel girders, bearings, steel reinforcement bars of the bridge deck and the abutment, cost of formwork, labor, work zone, lane closures, mobilization, etc. Other methods of realizing a cost analysis can also be used and not necessarily the methods chosen by the research team. One such method could be the development of a probabilistic approach with a Monte Carlo simulation that takes into account the fluctuations in costs of the various project items across the life cycle of the particular project.

8.4 Experimental Investigation

An experimental investigation plan was realized in Chapter 6. The laboratory testing will be conducted on the joint developed by the Iowa DOT. Test results will be compared and correlated with the FE model for the Story County bridge, the non-skewed bridge model. With these results, the Iowa DOT can confidently design and further develop the deck over backwall concept.

Additional testing can be realized for deck over backwall concept. Different truck loading cases can be tested across the approach slab. Soil could be incorporated in the testing plan supporting the approach slab. Soil compaction could be controlled to simulate the three compositions (loose, moderately stiff, and stiff) considered in the FE model.

8.5 Construction Observation And Post-Construction Testing

A plan for construction observation and post-construction testing was developed and detailed in Chapter 7. Implementation of the deck over backwall concept and this plan is expected to be conducted in a future Iowa DOT construction season.

Further modification of the FE models would also need to be made with the post-construction testing. The truck loads used in real-life simulations are expected to be different than the HS-20-44 truck loading conditions used for the purpose of this research. Iowa DOT would use certain trucks with different loads and tire spacing in the post-construction testing. These trucks should be weighted while incorporating them in the FE models. Results of these real-life simulations can be compared with the FE model. The correlations between results from future field testing and predictions will serve to calibrate and improve the accuracy of the FE models.

REFERENCES

ACI – 239 Committee in Ultra-High Performance Concrete, "Minutes of Committee Meeting October 2012", *ACI Annual Conference 2012,* Toronto, Ontario, Canada, 2012.

Aktan, H., Attanayake, U., and Ulku, E. (2008). *Combining Link Slab , Deck Sliding over Backwall , and Revising Bearings*. Lansing MI.

Alampalli, S., and Yannotti, A. P. (1998). "In-Service Performance of Integral Bridges and Jointless Decks." *Transportation Research Record*, 1(1624), 1–7.

Ålenius, M. (2003). "Finite Element Modelling of Composite Bridge Stability." Royal Institute of Technology.

American Association of State Highway and Transportation Officials. (2014). *LRFD Bridge Design Specifications*. Washington, DC.

Au, A., Lam, C., Au, J., and Tharmabala, B. (2013). "Eliminating Deck Joints Using Debonded Link Slabs: Research and Field Tests in Ontario." *Journal of Bridge Engineering*, 18(8), 768–778.

Baker Engineering & Energy. (2006). *Evaluation of Various Types of Bridge Deck Joints*. Phoenix, Arizona.

Bengtsson, R., and Widén, M. (2010). "FE-analysis of Vårby Bridge Investigation of fatigue damage in a composite bridge." Chalmers University of Technology.

Bierwagen, D., Moore, B., and Perry, V., "Revolutionary Concrete Solutions", *Concrete Specifier*, USA, 2006.

Biggs, R. M., Barton, F. W., Gomez, J. P., Massarelli, P. J., and McKeel, W. T. (2000). *Finite Element Modeling and Analysis of Reinforced-Concrete Bridge Decks*. *VTRC 01-R4*, Charlottesville, Virginia.

Civjan, S. A., and Quinn, B. (2016). *Better Bridge Joint Technology*. Boston, MA.

Culmo, M. P. (2011). *Accelerated Bridge Construction Manual - Experience in Design, Fabrication and Erection of Prefabricated Bridge Elements and Systems.pdf*. McLean, VA.

Dunker, K. F., and Abu-Hawash, A. (2005). "Expanding the Use of Integral Abutments in Iowa." *2005 Mid-Continent Transportation Research Symposium*, Ames, IA.

Eom, J., and Nowak, A. S. (2001). "Live Load Distribution for Steel Girder Bridges." *Journal of Bridge Engineering*, 36(December), 489–497.

Federal Highway Administration. (2005). "Integral Abutment and Jointless Bridges." *2005 – FHWA Conference*, Baltimore, Maryland, 343.

Fehling, E., Schmidt, M., Walraven, J., Leutbecher, T., and Fröhlich, S. (2015). *Ultra-High Performance Concrete UHPC: Fundamentals, Design, Examples*.

F. Cosgrove, Edward & Lehane, Barry. (2003). Cyclic loading of loose backfill placed adjacent to integral bridge abutments. International Journal of Physical Modelling in Geotechnics. 3. 09-16. 10.1680/ijpmg.2003.030302.

Fu, C. C., and Zhang, N. (2011). "Investigation of Bridge Expansion Joint Failure Using Field Strain Measurement." *Journal of Performance of Constructed Facilities*, 25(4), 309–316.

Gergely, J., Ogunro, V., and Manus, M. (2009). *Material Property and Quality Control Specifications for Elastomeric Concrete Used at Bridge Deck Joints*. Raleigh, North Carolina.

Giesmann, M. T. (2008). "Evaluation of bridges implementing innovative materials and design." Iowa State University.

Graybeal, B., "Fabrication of an Optimized UHPC Bridge", *PCI National Bridge Conference*, Atlanta, Georgia, USA, 2004.

Graybeal, B. A. (2006). *Material Property Characterization of Ultra-High Performance Concrete*. *FHWA*, McLean, VA.

Graybeal, B., "UHPC in the US Highway Transportation System", *HiPerMat, 2nd International Symposium on UHPC*, Kassel, Germany, 2008.

Graybeal, B. A. (2014). "Design and Construction of Field-Cast UHPC Connections." *FHWA*, (October), 1–36.

Gudimetla, B., and Gopalaratnam, V. S. (2012). "Precast Prestressed Bridge Approach Slab-Cost Effective Designs." University of Missouri – Columbia.

Gunes, O., Yesilmen, S., Gunes, B., and Ulm, F.-J. (2012). "Use of UHPC in Bridge Structures:MaterialModeling and Design." *Advances in Materials Science and Engineering*, 2012, 12.

Hartwell, D. R. (2011). "Laboratory testing of Ultra High Performance Concrete deck joints for use in accelerated bridge construction." Iowa State University.

Helwany, S. (2007). *Applied Soil Mechanics: With ABAQUS Applications*. *Applied Soil Mechanics: With ABAQUS Applications*, John Wiley & Sons, Inc., Hoboken, New Jersey.

Hossain, T. (2012). “Global and local performance of prestressed girder bridges with positive moment continuity detail.” Louisiana State University and Agricultural and Mechanical College.

Iowa DOT. (2018). “Standard Specifications with GS-15006 Revisions.” *Section 2102 - April 17, 2018*, <https://www.iowadot.gov/erl/current/GS/Navigation/nav21.htm> (Mar. 17, 2018).

Iowa DOT Office of Bridges and Structures. (2018b). “Final Bridge Design Software.” *Prepare Cost Estimate 4/25/17*, <https://iowadot.gov/bridge/automation-tools/final-design-software#446761470-iowa-dot-miscellaneous-programs> (Mar. 17, 2018).

Iowa DOT Office of Bridges and Structures. (2018a). *LRFD Bridge Design Manual*. Ames, IA.

Iowa DOT Office of Design. (2018). “Standard Road Plans - BR Series.” *Double Reinforced 12" Approach (Slab Bridge)*, <https://iowadot.gov/design/stdplne-br> (Sep. 28, 2016).

Keiwan, A., and Fadi, P. (2015). “Numerical analysis and model updating of a steel-concrete composite bridge.” KTH Royal Institute of Technology.

Klein, L. E. (2006). “Finite Element Analysis of a Composite Bridge Deck.” University of Southern Queensland.

Lewis, J., McGormley, J. C., and Ladson, R. D. (2014). “Joint Elimination Using Accelerated Bridge Construction Practices on the Indiana Toll Road.” *Transportation Research Board 93rd Annual Meeting. January 12-16, Washington, D.C.*, 1–14.

Li, V. C., Lepech, M., and Li, M. (2005). *Field Demonstration of Durable Link Slabs for Jointless Bridge Decks Based on Strain-Hardening Cementitious Composites*. Lansing, MI.

Liu, D., and Schiff, J. (2016). “Design and Construction of Illinois’s First Precast Deck Panel Bridge with UHPC Joints.” *First International Interactive Symposium on UHPC*, Des Moines, IA, 1–8.

Maruri, R. F., and Petro, S. H. (2005). “Integral Abutments and Jointless Bridges (IAJB) 2004 Survey Summary.” *IAJB 2005*, Baltimore, MD, 12–29.

McDonagh, M. D., and Foden, A. J. (2016). “Benefits of Ultra - High Performance Concrete for the Rehabilitation of the Pulaski Skyway.” *First International Interactive Symposium on UHPC*, Des Moines, IA, 1–10.

Miller, A. M., and Jahren, C. T. 2014. *Rapid Replacement of Bridge Deck Expansion Joints Study – Phase 1*. Ames, IA: Institute for Transportation Construction Management and Technology Program at Iowa State University.

Miller, A. M., and Jahren, C. T. 2015. *Rapid Bridge Deck Joint Repair Investigation - Phase II.* Ames, IA: Institute for Transportation Construction Management and Technology Program at Iowa State University.

Miller, A. M., Nelson, J. S., and Jahren, C. T. (2015). "Rapid Bridge Deck Joint Repair and Rehabilitation." Ames, IA, 17.

Ni, Y. Q., Hua, X. G., Wong, K. Y., and Ko, J. M. (2007). "Assessment of Bridge Expansion Joints Using Long-Term Displacement and Temperature Measurement." *Journal of Performance of Constructed Facilities*, 21(2), 143–151.

Okeil, A. (2016). "Field Monitoring of Link Slab Continuity Detail Under Different Bridge Configurations." *Louisiana Transportation Conference*, Baton Rouge, LA.

Palle, S., Hopwood, T., and Meade, B. W. (2012). *Improved Bridge Expansion Joints*. Lexington, KY.

Perry, V. H., and Corvez, D. (2016). "'An Innovative Technology for Accelerated Bridge Construction – The Owner Designer Dilemma.'" *First International Interactive Symposium on UHPC*, Des Moines, IA, 1–8.

Perry, V., Ghoneim, G., and Carson, G., "UHPC in Footbridges", *Proceedings of the 8th International Conference on Short & Medium Span Bridges"*, Niagara Falls, Ontario, Canada, 2010.

Perry, V. H., and Royce, M. (2010). "Innovative Field-cast UHPC Joints for Precast Bridge Decks (Side-by-Side Deck Bulb-Tees), Village of Lyons, New York: Design, Prototyping, Testing and Construction." *3rd fib International Congress*, Washington, DC, 1–13.

Perry, V. H., and Seibert, P. J. (2013). "Fifteen Years of UHPC Construction Experience in Precast Bridges in North America." *RILEM-fib-AFGC Int. Symposium on Ultra-High Performance Fibre-Reinforced Concrete*, Marseille, France, 229–238.

Phares, B., and Cronin, M. (2015). *Synthesis on the Use of Accelerated Bridge Construction Approaches for Bridge Rehabilitation*. Ames, IA.

Phares, B. M., White, D. J., Bigelow, J., Berns, M., and Zhang, J. (2011). *Identification and Evaluation of Pavement-Bridge Interface Ride Quality Improvement and Corrective Strategies*. *FHWA/OH-2011/1*, Ames, IA.

Rajek, G. S. (2010). "Numerical Modeling of the Performance of Highway Approach Slabs." University of Wisconsin - Madison.

Reyes, J., and Robertson, I. N. (2011). *Precast Link Slabs for Jointless Bridge Decks*. Honolulu, HI.

Ronanki, V. S., Valentim, D. B., and Aaleti, S. (2016). "Development length of reinforcing bars in UHPC: An experimental and analytical investigation." *First International Interactive Symposium on UHPC*, Des Moines, IA, 1–9.

Royce, M. (2016). "Utilization of Ultra-High Performance Concrete (UHPC) in New York." *First International Interactive Symposium on UHPC*, Des Moines, IA, 1–9.

Russell, H. G., and Graybeal, B. A. (2013). *Ultra-High Performance Concrete: A State-of-the-Art Report for the Bridge Community*. McLean, VA.

Ryan, T. W., Eric Mann, J., Chill, Z. M., and Ott, B. T. (2012). *Bridge Inspector's Reference Manual*. *FHWA*, Arlington, Virginia.

Sabatini, P. J., Tanyu, B., Armour, T., Groneck, P., and Keeley, J. (2005). *Micropile design and construction (reference manual for NHI course 132078)*. *FHWA NHI-05-039*, Washington, DC.

Schuettpelz, C. C., Fratta, D., and Edil, T. B. (2010). "Mechanistic Corrections for Determining the Resilient Modulus of Base Course Materials Based on Elastic Wave Measurements." *Journal of Geotechnical and Geoenvironmental Engineering*, 136(8), 1086–1094.

Thiagarajan, G., and Gopalaratnam, V. (2010). *Bridge Approach Slabs for Missouri DOT Looking at Alternative and Cost Efficient Approaches*. Jefferson City, MO.

Thiagarajan, G., Myers, J., and Halmen, C. (2013). *Bridge Approach Slabs for Missouri DOT Field Evaluation of Alternative and Cost Efficient Bridge Approach Slabs*. Jefferson City, MO.

Vorster, M. C., Merrigan, J. P., Lewis, R. W., and Weyers, R. E. (1992). *Techniques for Concrete Removal and Bar Cleaning on Bridge Rehabilitation Projects*. *SHRP-S-336*, Washington, DC.

Wenzlick, J. D. (2002). *Hydrodemolition and Repair of Bridge Decks*. Jefferson City, MO.

White, D., Sritharan, S., Suleiman, M., Mekkawy, M., and Chetlur, S. (2005). *Identification of the Best Practices for Design, Construction, and Repair of Bridge Approaches*. *CTRE Project 02-118*, Ames, IA.

Wing, K. M., and Kowalsky, M. J. (2005). "Behavior, Analysis, and Design of an Instrumented Link Slab Bridge." *Journal of Bridge Engineering*, 331–344.

Wipf, T. J., Phares, B. M., Sritharan, S., Degen, B. E., and Giesmann, M. T. (2009). *Design and Evaluation of a Single-Span Bridge Using Ultra-High Performance Concrete*. Ames, IA.

Wright, J. R., Rajabipour, F., Laman, J. A., and Radlińska, A. (2014). "Causes of Early Age Cracking on Concrete Bridge Deck Expansion Joint Repair Sections." *Advances in Civil Engineering*, 2014, 10.

Yannotti, A. P., Alampalli, S., and White, H. L. (2005). "New York State Department of Transportation's Experience with Integral Abutment Bridges." *IAJB 2005*, Baltimore, MD, 12–29.

Zhu Ding, Dongb, B., and Xingc, F. (2012). "Magnesium Phosphate Cement with large Volume of Fly ash." *Applied Mechanics and Materials*, 802–805.

APPENDIX A. STORY COUNTY BRIDGE PLANS

This page intentionally left blank.

STORY COUNTY

CULVERTS & BRIDGES LETTING DATE

PROJECT NO. I-35-5(18)118--01-85

Oct. 25-1966
Nov. 22-1966
Jan. 4-1966

Bridge

STATE	FED ROAD DIST NO	FISCAL YEAR	SHEET NO	TOTAL SHEETS
IOWA	5			

PROJECT NUMBER

I-35-5 (18)118—01-85

STATE OF IOWA
STATE HIGHWAY COMMISSION

PLANS OF PROPOSED IMPROVEMENT ON THE

INTERSTATE ROAD SYSTEM
STORY COUNTY
CULVERTS AND BRIDGES

ON I-35 FROM APPROX. 5.0 MILES NORTH OF U. S. 30 NORTHERLY TO JUST NORTH OF IA. 221.

THE IOWA STATE HIGHWAY COMMISSION STANDARD SPECIFICATIONS FOR CONSTRUCTION WORK, SERIES OF 1964 SHALL APPLY TO WORK ON THIS PROJECT

Plus current Supplement Specifications and Special Provisions

CONVENTIONAL SIGNS

State Line
Co. Line
Twp. Line
Sec. Line
Corp. Line
Urban Bdry.
R.O.W. Lines (Old / New)
Survey Line (Sta / Ref Point)
Profile Grade
Railroad
Field Tile
Underground Lines (Old / New; G Gas / T Tel)
Culverts (Old / New)
Utility Poles (Power / Tel)
Fences (Barb / Mesh)
Trees Or Brush
Stream
Dike (Old / New)
County Road No.
Primary Road No.
U. S. Road No.
Interstate Road No.

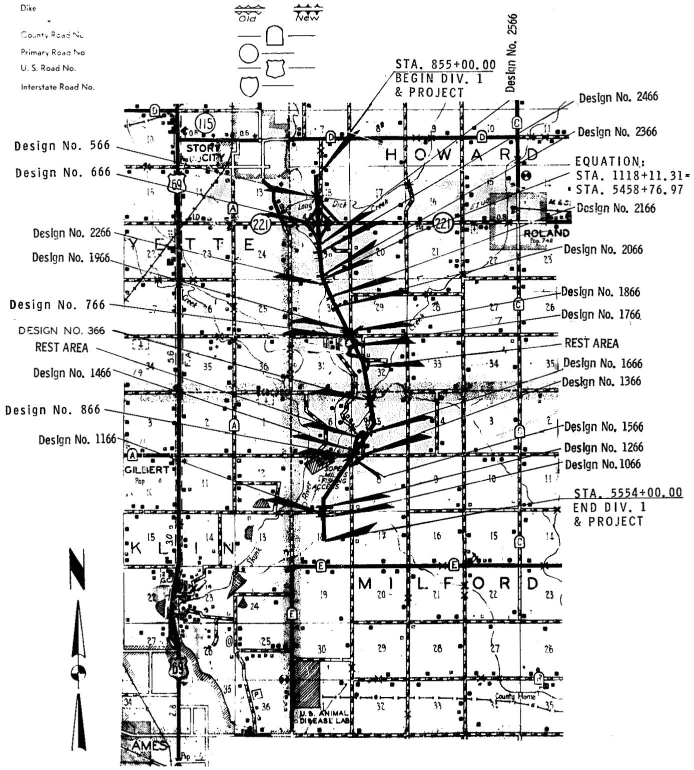

STATE CONTROL SECTION NUMBER

85-1300

LOCATION MAP SCALE

0 1 2 3

miles

DESIGN STRESSES for the following materials are in accordance with A.A.S.H.O. Standard Specifications for Highway Bridges, Series of 1961.

Concrete in accordance with Section 1.4.11 f'c = 3500 psi.
Reinforcing Steel in accordance with Section 1.4.12 "Reinforcement" for Intermediate, Hard, or Rail Steel Grade.

Structural Steel in accordance with INT. 7(62); Section 1.4.2 (B) "Structural Steel", A-36, f_s = 20,000 psi.
Prestressed Concrete in accordance with Section 1.13.7 f'c = 5000 psi.
Prestressing Steel in accordance with Section 1.13.7 f's = 270,000 psi.

NO MILEAGE SUMMARY

MILEAGE SUMMARY

LOCATION	LIN. FT.	MILES
BRIDGE AT STA. 5536+12.00	195.50	.037
BRIDGE AT STA. 996+40.00	343.00	.065

INDEX OF SHEETS 105-3

NO.	DESCRIPTION
1	TITLE SHEET
1A	TABULATION OF REVISIONS
2	ESTIMATE SHEET
3	MISCELLANEOUS DETAIL SHEET
4	MISCELLANEOUS DETAIL SHEET
5	MISCELLANEOUS DETAIL SHEET
6	MISCELLANEOUS DETAIL SHEET CHP2.5-65
7	CULVERT DESIGN NO'S 1066 & 1166
8	CULVERT DESIGN NO. 1266
9-12	CULVERT DESIGN NO. 1366 & 1466
13	CULVERT DESIGN NO. 1566 & 1866
14-15	CULVERT DESIGN NO. 1666
16	CULVERT DESIGN NO. 1766
17	CULVERT DESIGN NO. 1966
18	CULVERT DESIGN NO. 2066
19	CULVERT DESIGN NO. 2166
20	CULVERT DESIGN NO. 2266
21	CULVERT DESIGN NO. 2366
22	CULVERT DESIGN NO. 2466
23	CULVERT DESIGN NO. 2566
23A1 - 23A7	Bridge Design No. 566
23A8 - 23A17	Bridge Design No. 666
23A18 - 23A25	Bridge Design No. 766
23A26 - 23A39	Bridge Design No. 866
23B1-23B13	BRIDGE DESIGN NO. 366
2A	ESTIMATE SHEET

In Letting of Oct. 25-1966 (sheets 3–23)
In Letting of Nov. 22-1966 (sheets 23A1–23A39)
In Letting of Jan. 4-1966 1967 (sheets 23B1–23B13, 2A)

IOWA STATE HIGHWAY COMMISSION STANDARDS REQUIRED
(AVAILABLE AT THE I. S. H. C. STOREROOM)

Standard	Issued	Revised
C1P	1932	1944
CFP	1945	
C4P	1932	1944
C5P	1932	1944
C6P	1932	1944
C6F	1952	1955
C8F	1952	1955
C4J	1959	1964
C5J	1959	1964
C6J	1959	1964
C8J	1959	1964
F4J		1964
F5J		1964
F6J		1964
CBH-00	1960	
CBH-30	1960	1961

DESIGN DESIGNATION
INTERSTATE
HIGHWAY

1966 AADT	7,255	V.P.D.
1986 AADT	12,495	V.P.D.
1986 DHV	1,666	V.P.H.
DIRECTIONAL	60	%
TRUCKS	7	%
DESIGN V	70	M.P.H.

FULL CONTROL OF ACCESS SHALL BE EXERCISED ON THIS PROJECT.

REVISED
SEE FOLLOWING SHEET 1-A

APPROVED D.E. McLean 9-6-66
DIRECTOR OF ENGINEERING DATE
IOWA HIGHWAY COMMISSION

I HEREBY CERTIFY THAT THIS PLAN WAS PREPARED UNDER MY SUPERVISION AND THAT ENGINEERING DECISIONS WITH REGARD TO THE DESIGN WERE MADE BY ME OR BY OTHER DULY REGISTERED PROFESSIONAL ENGINEERS UNDER THE LAWS OF THE STATE OF IOWA.

DATE 8-31 1966, IOWA REG. NO. 2792

DEPARTMENT OF COMMERCE
BUREAU OF PUBLIC ROADS

APPROVED

DIVISION ENGINEER DATE

File No. 22590 STORY COUNTY

PROJECT NUMBER I-35-5(18)118--01-85

STATE	FED ROAD DIST NO	FISCAL YEAR	SHEET NO	TOTAL SHEETS
IOWA	5		1	23

Bench Mark: No. 15A, Sta. 998+35, 178' Rt., RR. spk. in S. side 24" Elm. Elev. = 936.92

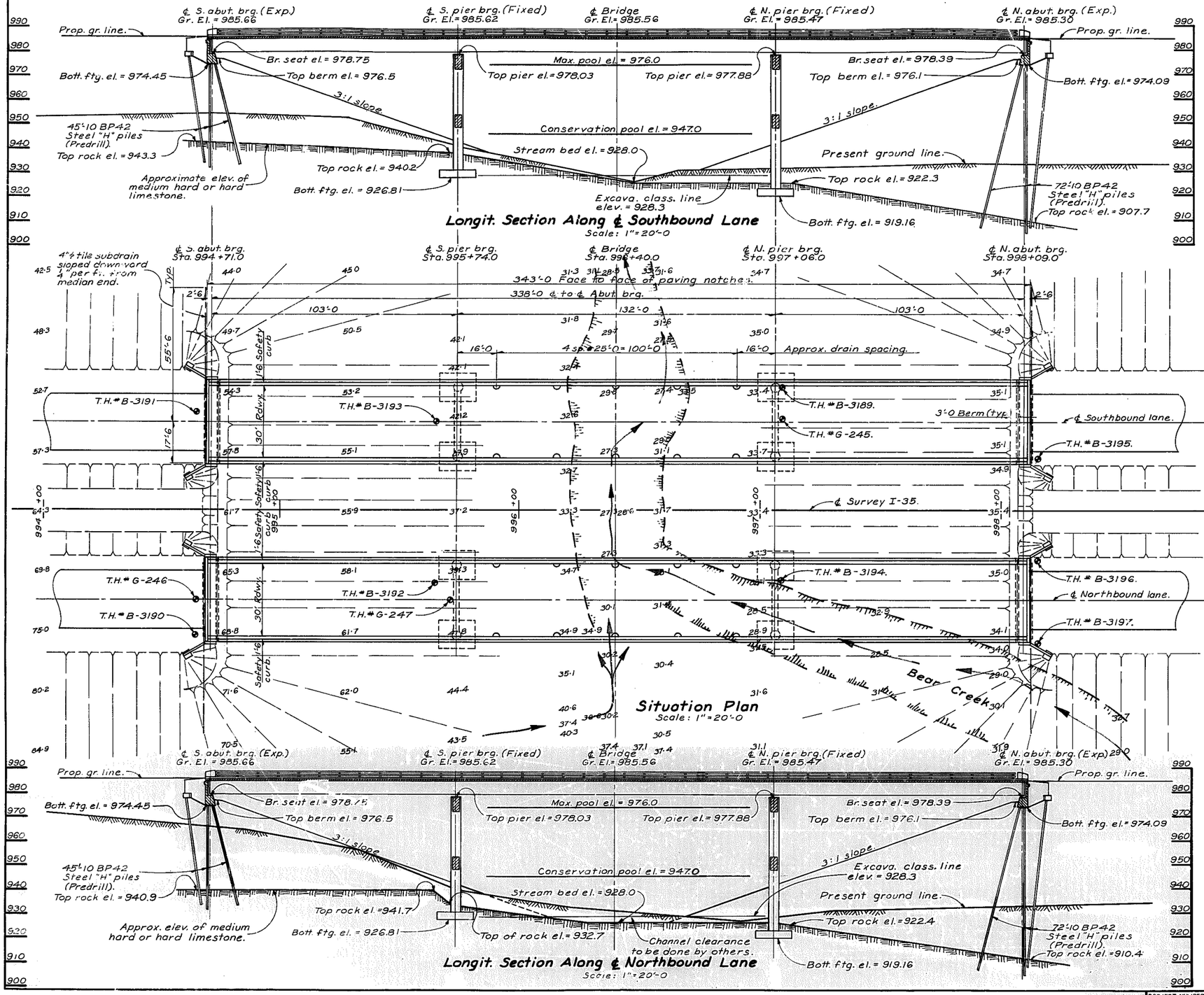

Longit. Section Along ℄ Southbound Lane
Scale: 1" = 20'-0

Situation Plan
Scale: 1" = 20'-0

Longit. Section Along ℄ Northbound Lane
Scale: 1" = 20'-0

+0.24% −0.36%
1,100' V.C.
P.I. Sta. 995+50.00
P.I. El. = 986.46
M.O. = 0.825

Profile Grade Line

Hydraulic Data
D.A. = 28.0 sq. mi. F-GR-R
Des. Discharge = 4,000 cfs

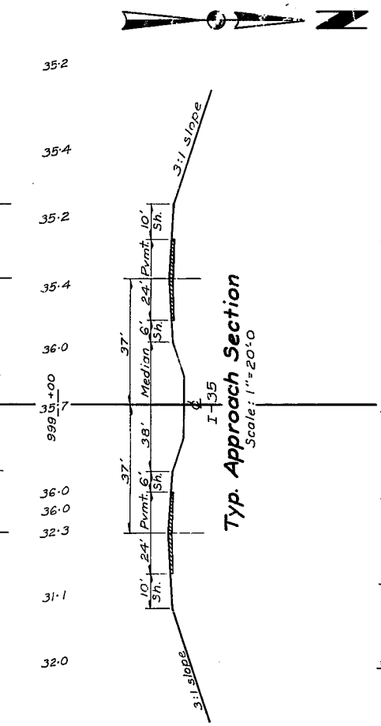

Location:
Section #5
T-84-N, R-23-W
Milford TWP
Story County
I-35 over Bear Cr.

DESIGN NO. 366
FILE NO. 22590
DES. SH. NO. 2 OF 13

Design for
DUAL 338'-0 × 30' CONTINUOUS WELDED PLATE GIRDER BRIDGES
103'-0 End Spans 132'-0 Center Span
SITUATION PLAN
Station 996+40.00 I-35 over Bear Cr. November, 1966
STORY COUNTY
Iowa State Highway Commission

Designed by: MHT Traced by: LB Checked by: LEP

STORY COUNTY

PROJECT NUMBER	STATE	FED. ROAD DIST. NO.	FISCAL YEAR	SHEET NO.	TOTAL SHEETS
I-35-5(18)118--01-85	IOWA	5		23 Bz.	23

DIETZGEN NO. 131 ARKWRIGHT

Bench Mark: No. 45A; Sta. 998+35, 178' Rt, R.R. spk. in S. side 24" elm. Elev. = 936.92

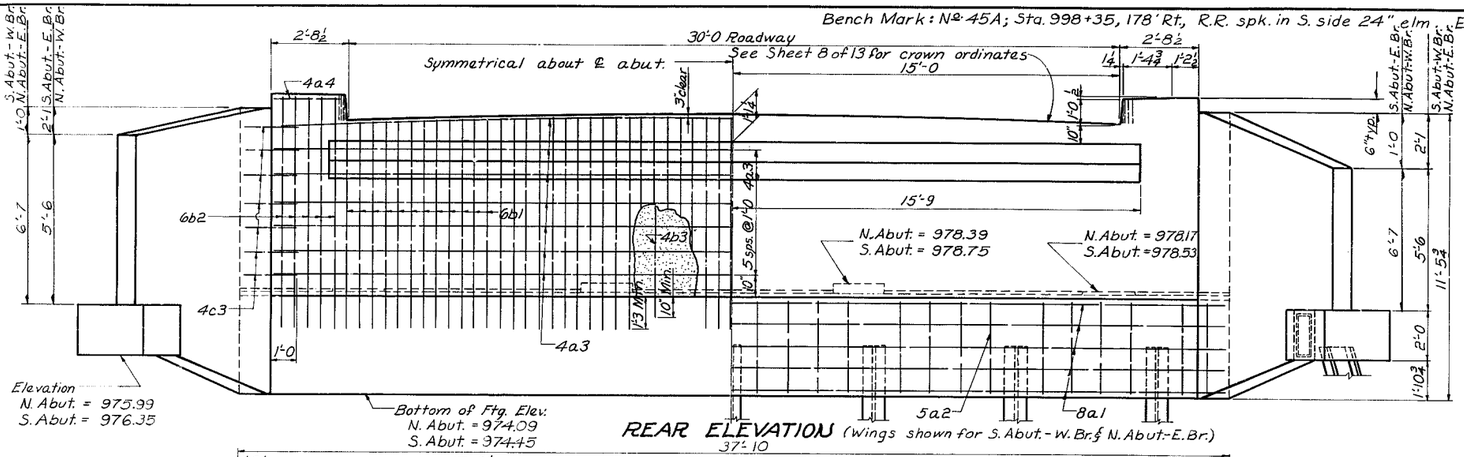

REAR ELEVATION (Wings shown for S. Abut.-W. Br. & N. Abut.-E. Br.)

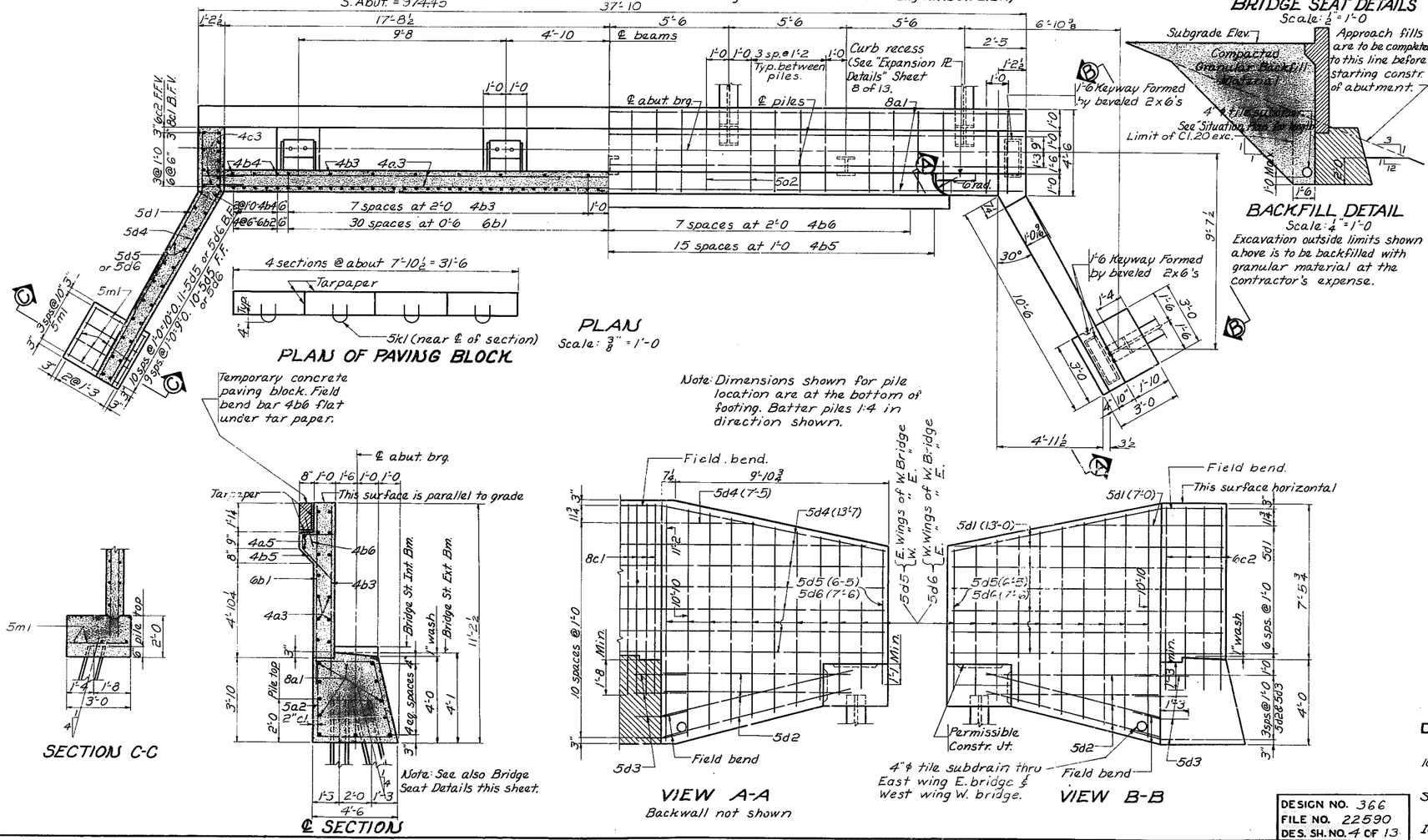

PLAN

Scale: ⅜" = 1'-0

PLAN OF PAVING BLOCK

SECTION C-C

Temporary concrete paving block. Field bend bar 4b6 flat under tar paper.

Note: See also Bridge Seat Details this sheet.

Note: Dimensions shown for pile location are at the bottom of footing. Batter piles 1:4 in direction shown.

VIEW A-A

Backwall not shown

4" ϕ tile subdrain thru East wing E. bridge & West wing W. bridge.

VIEW B-B

BACKFILL DETAIL

Scale: ¼" = 1'-0

Excavation outside limits shown above is to be backfilled with granular material at the contractor's expense.

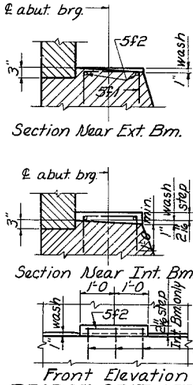

BRIDGE SEAT DETAILS

Scale: ½" = 1'-0

REINFORCING BAR LIST-ONE ABUTMENT

Bar	Location	Shape	No.	Length	Weight
8a1	Footing, Longitudinal		12	37'-6	1,272
5a2	" Hoops		28	15'-5	453
4a3	Backwall, Horiz., B.F. & F.F.		14	35'-2	323
4a4	Curb, Horizontal		4	2'-2	6
4a5	Paving Support, Horiz.		2	31'-2	42
6b1	Backwall, Vertical, B.F.		61	8'-6	779
6b2	" , " , "		10	9'-6	143
4b3	" , " , F.F.		16	8'-1	80
4b4	" , " , "		6	9'-1	36
4b5	Paving Support Tie		31	3'-10	79
4b6	" " Dowels *		15	1'-8	17
8c1	End Wall, Vertical, B.F.		14	9'-2	343
6c2	" " " , F.F.		8	8'-9	105
4c3	" " , Dowels		28	2'-0	37
5d1	Wingwall, Horiz. F.F.		16	Varies	204
5d2	Wing, Horiz., Bottom, F.F. & B.F.		16	9'-0	150
5d3	" , " , " , Dowel		16	2'-6	42
5d4	" , " , B.F.		16	Varies	214
5d5	Wingwall, Vertical, B.F. & F.F.		21	"	132
5d6	" " " " "		21	"	203
5f1	Top of Footing, Under Beams		12	4'-6	56
5f2	" " " " "		8	1'-9	15
5k1	Paving Block Hoops		4	2'-1	9
5m1	Wingwall, Footing		14	2'-8	33
* Structural Grade			Total	lbs.	4,772

BENT BAR DETAILS

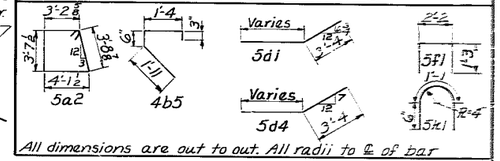

All dimensions are out to out. All radii to ℄ of bar

CONCRETE PLACEMENT QUANTITIES

Item	Quantity
Footing	22.4 c.y.
Backwall	10.6 c.y.
Wingwall & Footing	10.1 c.y.
Paving Block	0.8 c.y.
Total	43.9 c.y.

ESTIMATED QUANTITIES-FOUR ABUTS.

Item			Quantity
Structural Concrete, Class "C"			1756 c.y.
Reinforcing Steel			19,112 lbs.
Class 20 Excavation			228 c.y.
10BP42 Steel Bearing Piling	Furnish	18@45'-⅛", 18@72'	2,106 Lin. Ft.
	Drive	18@45'-⅛", 18@72'	2,106 Lin. Ft.
Granular Backfill			412 c.y.

ABUTMENT NOTES:

All exposed corners 90° or sharper are to be formed with a ¾" dressed and beveled fillet.

Minimum distance from face of concrete to ℄ of near reinforcing bar is to be 2" unless otherwise shown.

The design bearing value is 50 tons per pile. Piles are to be driven to refusal in limestone. Piles shall be driven with a diesel hammer having a ram weighing at least 4000 #. A minimum of 10 blows with a resulting penetration of not over ¼ inch with a hammer as specified above will be considered evidence of refusal.

Bridge Contractor is to backfill abutment between wings to subgrade elevation with granular backfill material complying with Article 4133 of the Specifications.

Abutment backwall is to be poured after superstructure is in place.

Design for
DUAL 338'-0 × 30' CONTINUOUS WELDED PLATE GIRDER BRIDGES
103'-0 End Spans 132'-0 Center Span

ABUTMENT DETAILS

Station: 996+40.00 I-35 over Bear Cr. November, 1966.

STORY COUNTY

Iowa State Highway Commission

DESIGN NO. 366
FILE NO. 22590
DES. SH. NO. 4 OF 13

Designed by: MHT Traced by: LDB Checked by: LEP

STORY COUNTY PROJECT NUMBER I-35-5(18)118--01-85

STATE	FED. ROAD DIST. NO.	FISCAL YEAR	SHEET NO.	TOTAL SHEETS
IOWA	5		33.24	23

DIETZGEN NO. 131 ARKWRIGHT

Bench Mark: No. 45A, Sta. 998+35, 178' Rt., R.R. spk. in S. side of 24" Elm. Elev. = 936.92

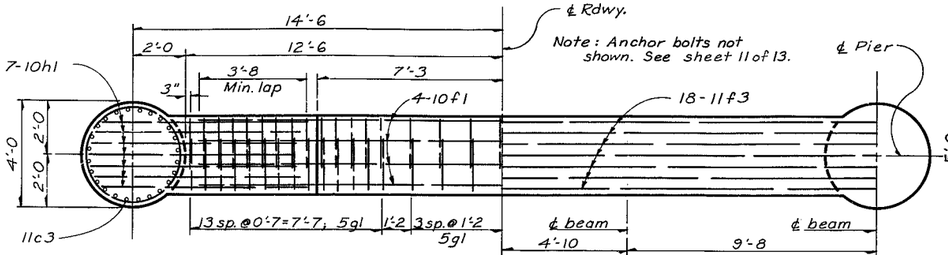

HALF PLAN TOP REINF.

HALF PLAN BOTT. REINF.

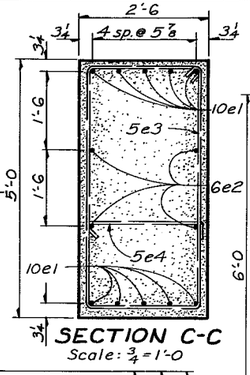

SECTION C-C
Scale: 3/4" = 1'-0

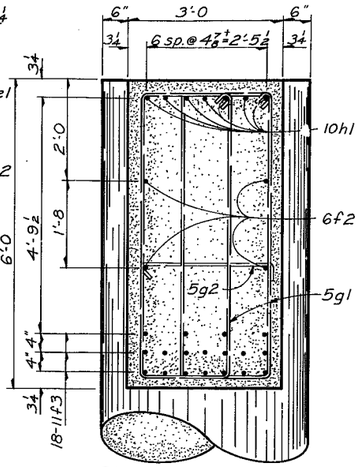

SECTION A-A
Scale: 3/4" = 1'-0

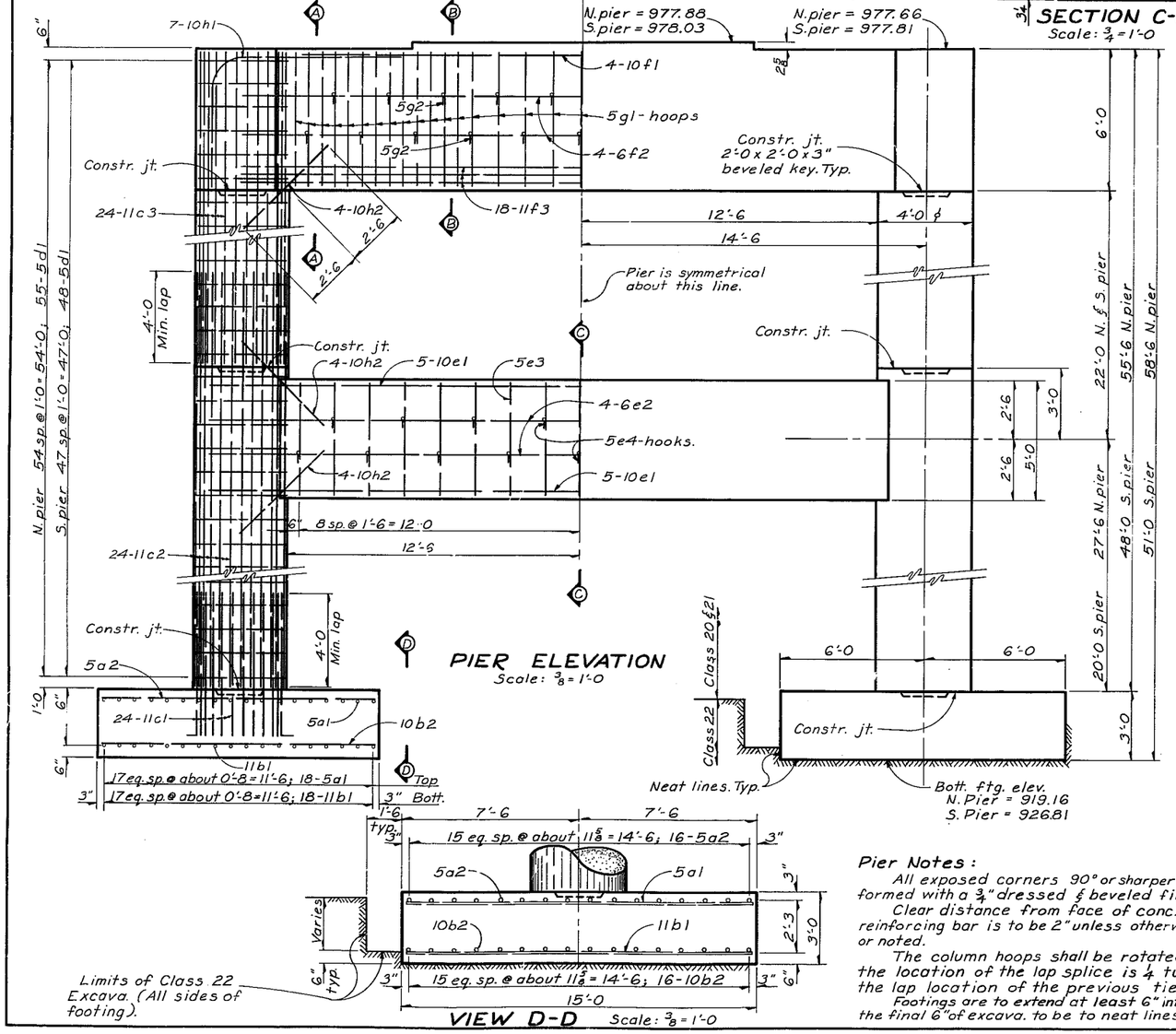

PIER ELEVATION
Scale: 3/8" = 1'-0

VIEW D-D Scale: 3/8" = 1'-0

Limits of Class 22 Excava. (All sides of footing).

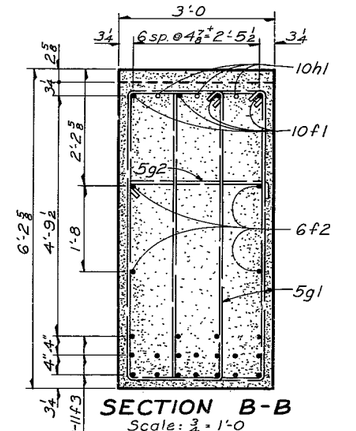

SECTION B-B
Scale: 3/4" = 1'-0

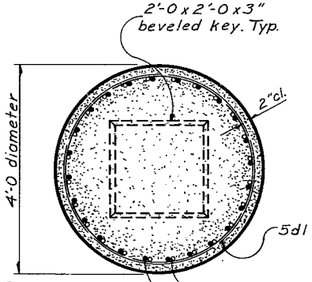

TYP. COLUMN SECTION
Scale: 3/4" = 1'-0

REINF. BAR LIST - ONE PIER

Bar	Location	Shape	No.	Length	Weight N. Pier	Weight S. Pier
5a1	Footing, longit, top	—	36	14'-8	551	551
5a2	" , transv., "	—	32	11'-8	389	389
11b1	" , longit., bott.	—	36	14'-8	2,805	2,805
10b2	" , transv., "	—	32	11'-8	1,606	1,606
11c1	" to column, dowels	⌐	48	6'-9	1,721	1,721
11c2	Column, vert., N. pier	—	48	34'-6	8,798	—
11c2	" " , S. "	—	48	27'-0	—	6,886
11c3	" " , N. & S. pier	—	48	24'-8	6,291	6,291
5d1	" , hoops, N. pier	○	110	13'-0	1,491	—
5d1	" " , S. "	○	96	13'-0	—	1,302
10e1	Strut, longit., top & bott.	—	10	30'-0	1,291	1,291
6e2	" " , sides	—	4	30'-0	180	180
5e3	" , hoops	□	17	14'-5	256	256
5e4	" , hooks	⌐	17	3'-0	53	53
10f1	Pier cap, longit., top	—	4	23'-0	396	396
6f2	" " " , sides	—	4	29'-0	174	174
11f3	" " " , bott.	—	18	29'-0	2,773	2,773
5g1	" " , hoops	□	70	15'-9	1,150	1,150
5g2	" " , hooks	⌐	21	3'-6	77	77
10h1	" " , corners	—	14	13'-6	813	813
10h2	" " "	—	24	5'-0	516	516
				Total (lbs.)	31,331	29,230

BENT BAR DETAILS

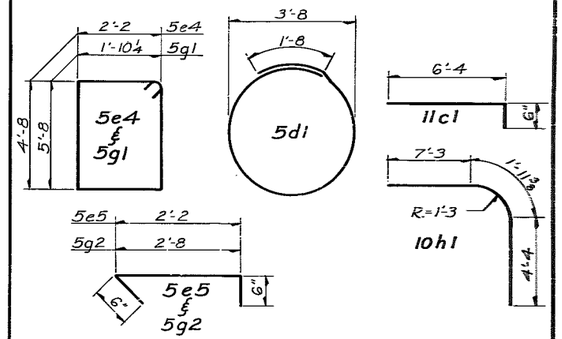

Note: All dimensions are out to out. Radii to ℄ of bar.

CONC. PLACEMENT QUANT.

Location	Units	N. Pier	S. Pier
Footings	Cu.yd.	40.0	40.0
Columns & Strut below Constr. Joint	Cu.yd.	40.1	33.1
Columns between Strut & Pier Cap	Cu.yd.	17.7	17.7
Pier Cap	Cu.yd.	22.9	22.9
Total	Cu.yd.	120.7	113.7

ESTIMATED QUANT.- 4 PIERS

Item	Units	N. Piers	S. Piers	Total
Structural Conc. Class "C"	Cu.yd.	241.4	227.4	468.8
Reinf. Steel	lbs.	62,662	58,460	121,122
Class 20 Excava.	Cu.yd.	600	270	870
Class 21 Excava.	Cu.yd.	162	0	162
Class 22 Excava.	Cu.yd.	200	402	602

Pier Notes:

All exposed corners 90° or sharper are to be formed with a 3/4" dressed & beveled fillet.

Clear distance from face of conc. to near reinforcing bar is to be 2" unless otherwise shown or noted.

The column hoops shall be rotated such that the location of the lap splice is 1/4 turn from the lap location of the previous tie.

Footings are to extend at least 6" into medium hard limestone with the final 6" of excava. to be to neat lines of the footing.

Design for
DUAL 338'-0 x 30' CONTINUOUS WELDED PLATE GIRDER BRIDGES
103'-0 End Spans 132'-0 Center Span

PIER DETAILS

Station: 996 +40.00 I-35 over Bear Cr. November, 1966
STORY COUNTY
Iowa State Highway Commission

DESIGN NO. 366
FILE NO. 22590
DES. SH. NO. 5 OF 13

Designed by: MHT Traced by: LPB Checked by: LEP

STORY COUNTY PROJECT NUMBER I-35-5(18)118--01-85

STATE	FED. ROAD DIST. NO.	FISCAL YEAR	SHEET NO.	TOTAL SHEETS
IOWA	5		23 85	23

DIETZGEN NO. 131 ARKWRIGHT

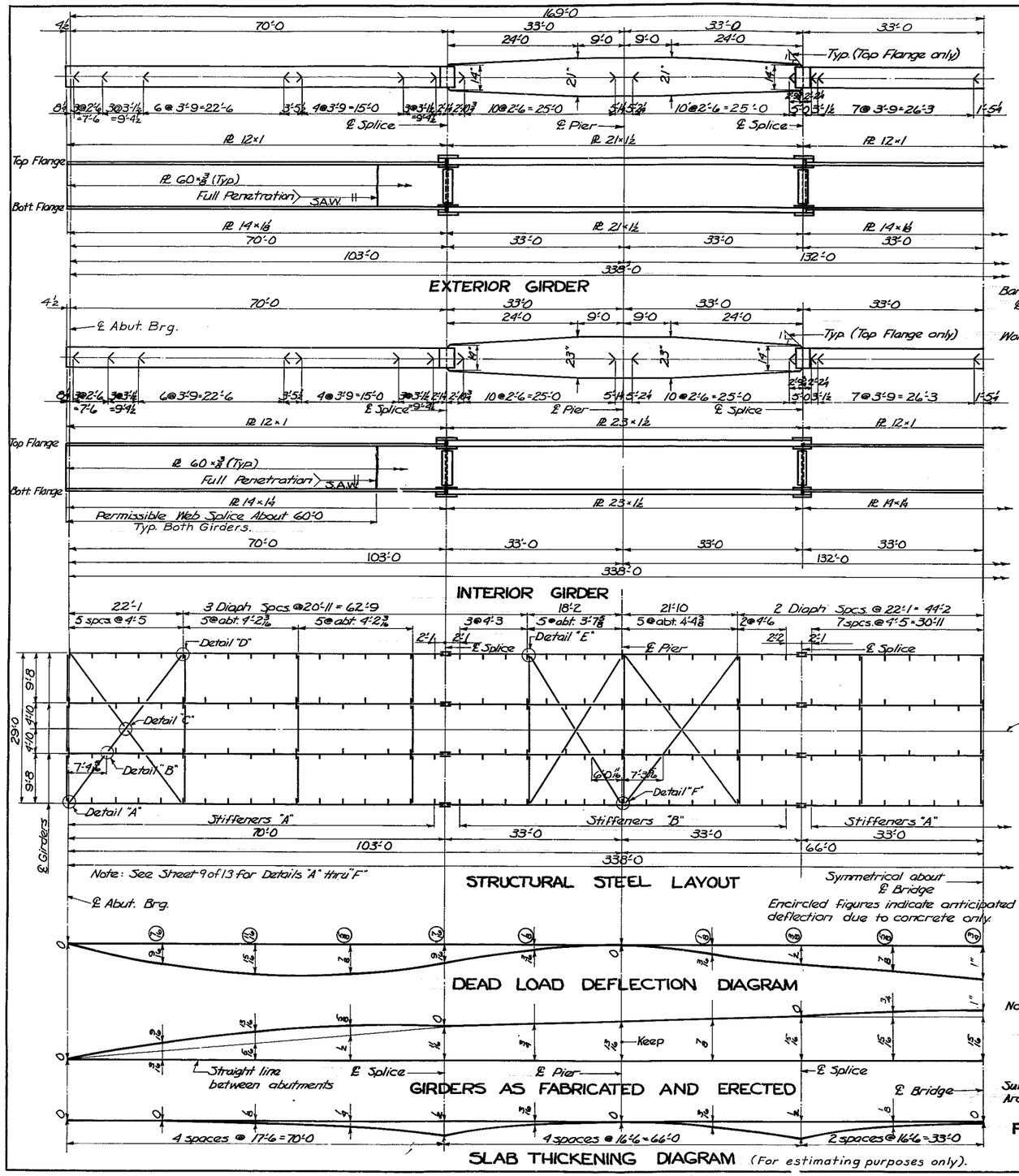

STRUCTURAL STEEL LAYOUT

DEAD LOAD DEFLECTION DIAGRAM

GIRDERS AS FABRICATED AND ERECTED

SLAB THICKENING DIAGRAM (For estimating purposes only).

Note: See Sheet 9 of 13 for Details "A" thru "F"

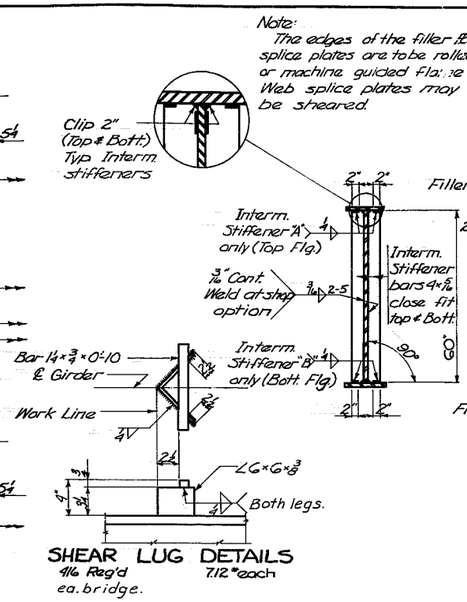

SHEAR LUG DETAILS
416 Req'd ea. bridge.
7/12" each

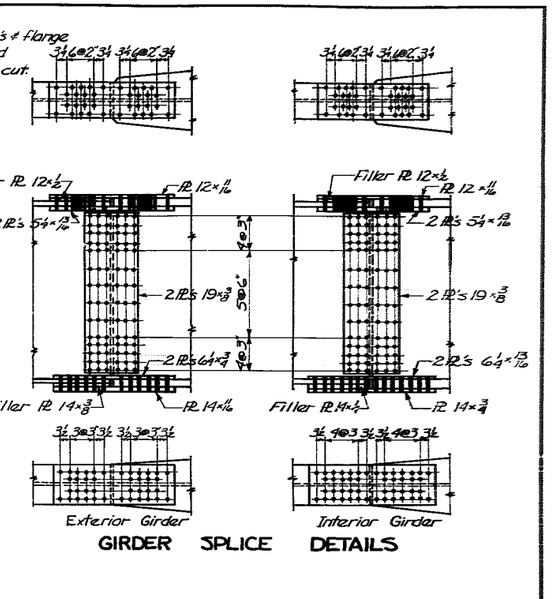

GIRDER SPLICE DETAILS

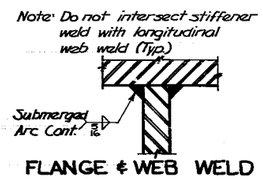

FLANGE & WEB WELD DETAILS

Design for
DUAL 338'-0 x 30' CONTINUOUS WELDED PLATE GIRDER BRIDGES
103'-0 End Spans 132'-0 Center Span
SUPERSTRUCTURE DETAILS
Station: 996+40.00 November, 1966
STORY COUNTY
Iowa State Highway Commission

DESIGN NO. 366					
FILE NO. 22590					
DES. SH. NO. 6 OF 13					
PROJECT NUMBER	STATE	FED. ROAD DIST. NO.	FISCAL YEAR	SHEET NO.	TOTAL SHEETS
I-35-5(18)118--01-85	IOWA	5		2356	23

STORY COUNTY

Designed by: J.D.C. Traced by: Checked by: LEP

DIETZGEN NO. 131 ARKWRIGHT

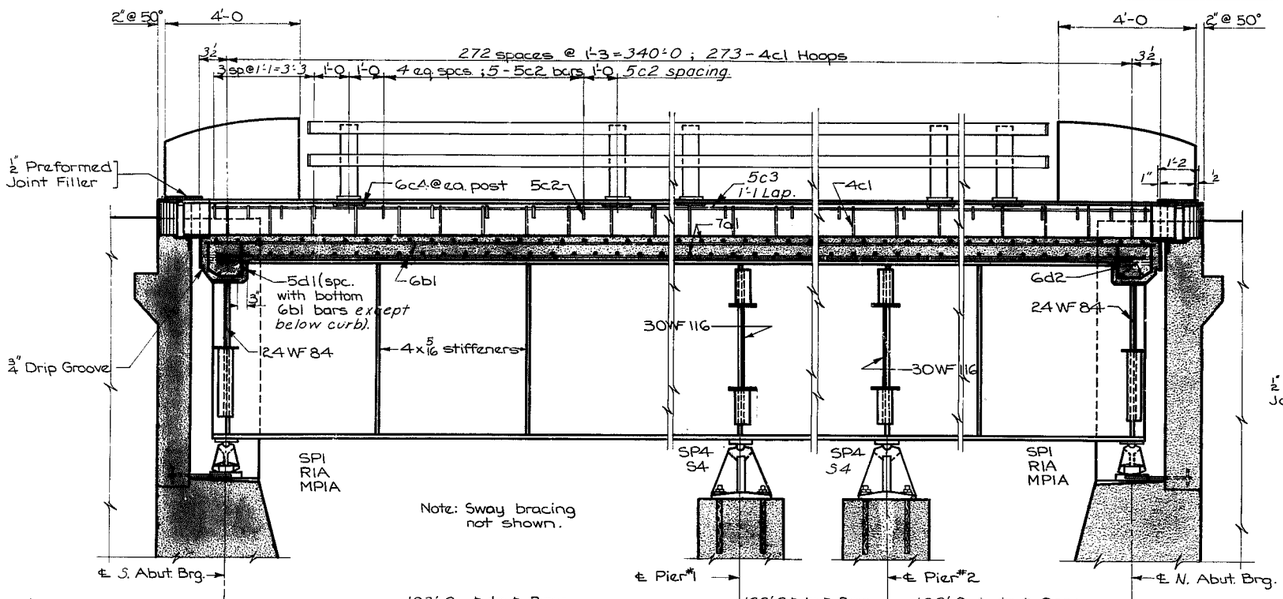

LONGITUDINAL SECTION NEAR CURB

Note: See sheet 12 or 13 of 13 for rail post spacing.

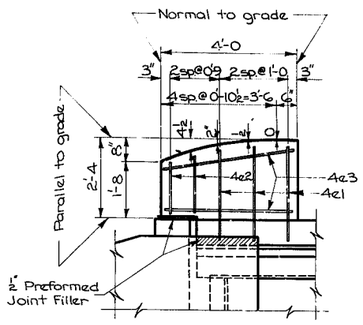

PART SECTION A-A

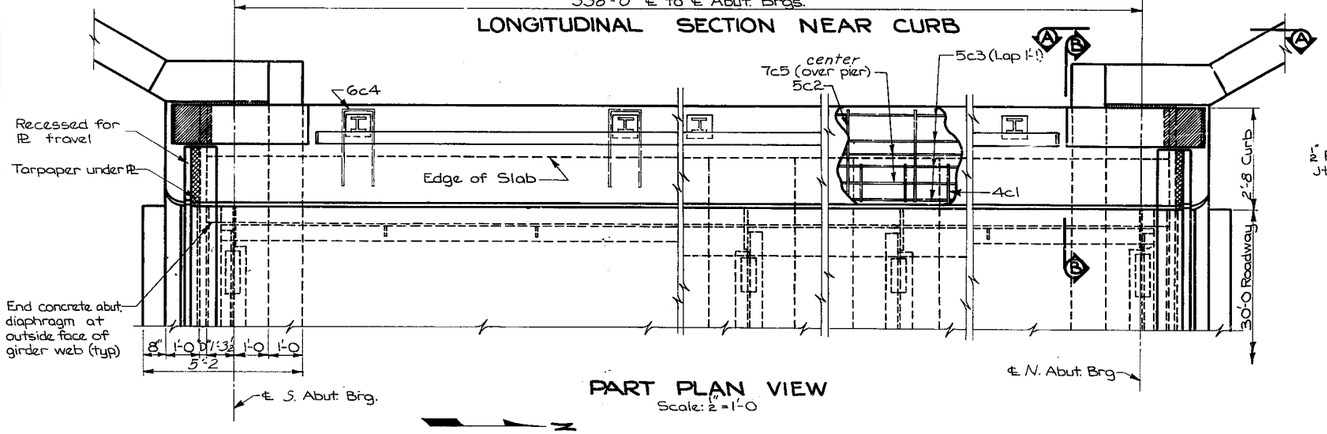

PART PLAN VIEW
Scale: ½" = 1'-0

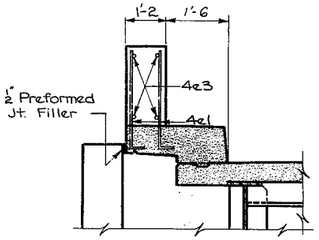

PART SECTION B-B

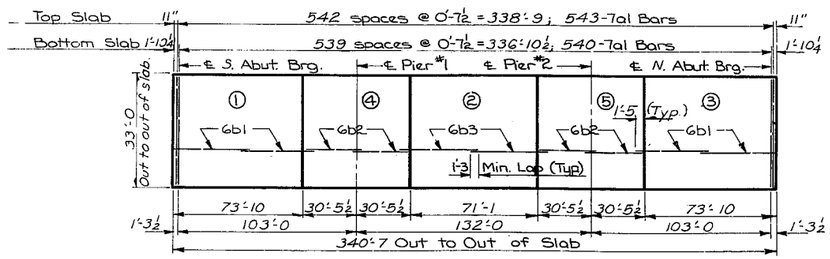

Note: Slab is to be placed in sections and in order indicated by encircled figures. Curbs may be placed continuously. Alternate procedures for placing concrete may be submitted for approval, together with a statement of the proposed method and evidence that the contractor possesses the necessary equipment and facilities to accomplish the required result.

SLAB CONCRETE PLACEMENT DIAGRAM & REINFORCING STEEL LAYOUT

REINFORCING BAR LIST - SUPERSTRUCTURE

Bar	Location	Shape	No.	Length	Weight
7a1	Slab, Trans., Top & Bott.	—	1,083	32'-8	72,313
6b1	Slab, Longit., Top & Bott, Sec ①③	—	204	38'-2	11,695
6b2	" , " , " " " , ④⑤	—	204	30'-11	3,473
6b3	" , " , " " " , ②	—	102	37'-7	5,758
4c1	Curb, Transv., Hoops	⊐	546	4'-7	4,672
5c2	" , "	⌐	406	2'-7	1,094
5c3	" , Longit.	—	80	35'-0	2,920
6c4	Rail Post Anchor	⊃	80	5'-2	621
7c5	Curb, Longit., Over Piers	—	8	40'-0	654
5d1	Abut., Diaphragm, Vert.	⊐	42	3'-4	146
6d2	" , " , Horiz.	—	12	9'-4	168
4e1	End Post, Vert.	⌐	24	3'-0	48
4e2	" " , "	—	16	1'-5	15
4e3	" " , Horiz.	—	16	3'-8	39
			Total lbs.		10,616

BENT BAR DETAILS

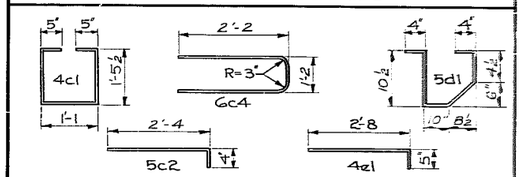

All dimensions are out to out. Radii are to ℄ of bar.

CONCRETE PLACEMENT QUANTITIES - SUPER.

Location		Quantity
Slab	Sections ① & ③ 61.4 cu.yd. each	122.8 cu.yd.
	Section ②	58.3 cu.yd.
	Sections ④ & ⑤ 49.8 cu.yd. each	99.6 cu.yd.
Curbs	2 @ 30.7	61.4 cu.yd.
End Posts		1.5 cu.yd.
	Total	343.6 cu.yd.

TOTAL ESTIMATED QUANT. - TWO SUPER.

Item	Quantity
Structural Conc., Class "D"	687.2 cu.yd.
Reinforcing Steel	213,232 lbs.
Structural Steel	744,560 lbs.

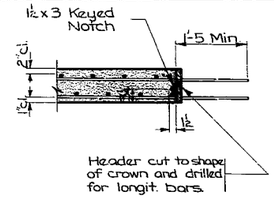

TRANSVERSE CONSTR. JOINT

Moments in Ft. Kips **MOMENTS & REACTIONS** Reactions in Kips

	Loads		Max. Pos. Mom. End Span		Max. Pos. Mom. Center Span		Neg. Moment Pier 146% Increase		Abutment Reactions		Pier Reactions	
	Ext.	Int.	Ext.	Int.	Ext.	Int.	Ext.	Int.	Ext.	Int.	Ext.	Int.
D.L. #1	0.857	1.297	554.0	837.0	480.0	726.0	1,385.0	2,095.0	31.0	47.1	113.4	172.1
D.L. #2	0.568	0.118	405.0	84.2	434.0	90.4	801.0	171.0	21.5	4.5	74.5	15.5
U.L.L.	0.482	0.562	—	—	—	—	764.0	890.0	—	—	67.0	78.0
C.L.L.*	135.5 / 78.578	15.818 / 22.848	—	—	—	—	287.0	335.0	—	—	19.6	22.8
HS 20-16	24.096	28.128	973.0	1,138.0	1,005.0	1,172.0	—	—	48.2	56.3	—	—
Impact	—	—	213.0	249.0	196.0	229.0	217.0	253.0	10.6	12.3	17.9	20.8
Total							3,454.0	3,744.0	111.3	120.2	292.4	309.2

* Upper figure is for moment; lower is for shear.

Note: Positive moments due to D.L. #2, Live Load, & Impact are resisted by composite action of girder and slab. Shear lugs are used to insure composite action. Dead Load #1 includes weight of slab, girders, and diaphragms. Dead Load #2 includes weight of curbs, rail, and future wearing surface.

Design for
DUAL 338'-0 × 30' CONTINUOUS WELDED PLATE GIRDER BRIDGES
103'-0 End Spans 132'-0 Center Span
SUPERSTRUCTURE DETAILS
Station: 996+40.00 November 1966
STORY COUNTY
Iowa State Highway Commission

DESIGN NO. 366
FILE NO. 22590
DES. SH. NO. 7 OF 13

Designed by: J.D.C. Traced by: LPB Checked by: LEP

STORY COUNTY

PROJECT NUMBER	STATE	FED. ROAD DIST. NO.	FISCAL YEAR	SHEET NO.	TOTAL SHEETS
I-35-5(18)118--01-85	IOWA	5		23 57	23

DIETZGEN NO 131 ARKWRIGHT

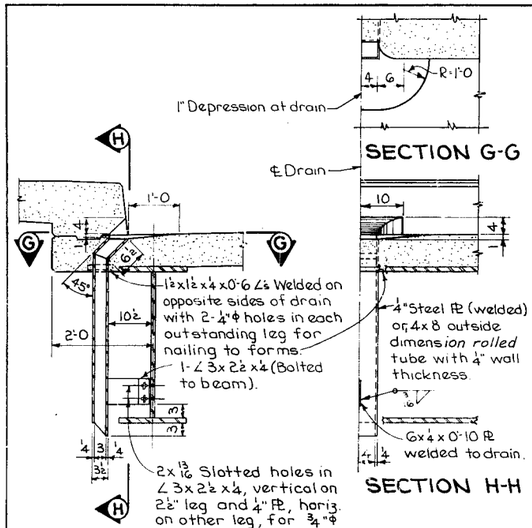

DRAIN DETAILS

Wt. of drain = 126 lb.

10 req'd. ea. bridge.

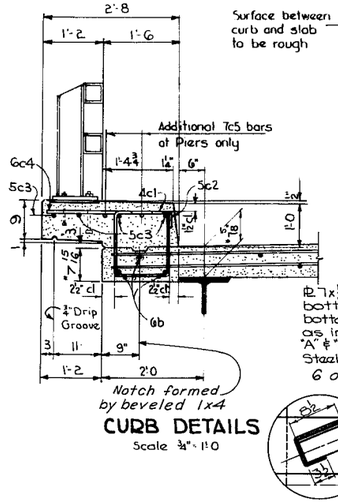

CURB DETAILS

Scale ¾" = 1'-0

HALF INTERMEDIATE SECTION

(Handrail & Reinforcing Steel Not Shown)

Scale: ½" = 1'-0

HALF SECTION NEAR ABUTMENT

△ Dimensions are from top of slab to bottom of top Flange.
* Indicates nominal dimensions.
Note: The bottom of slab is to be a flat surface between girders and 1" above the bottom of top Flange of girders.

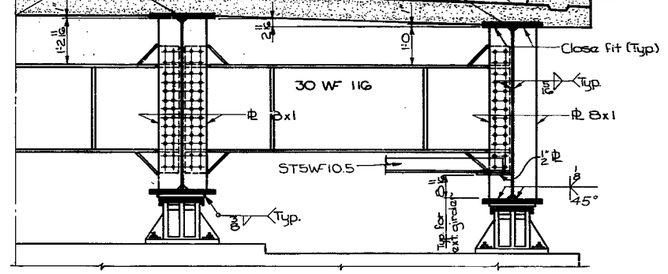

HALF SECTION NEAR PIER

(Handrail & Reinforcing Not Shown)

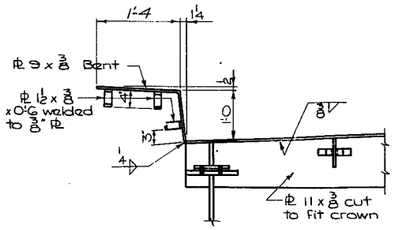

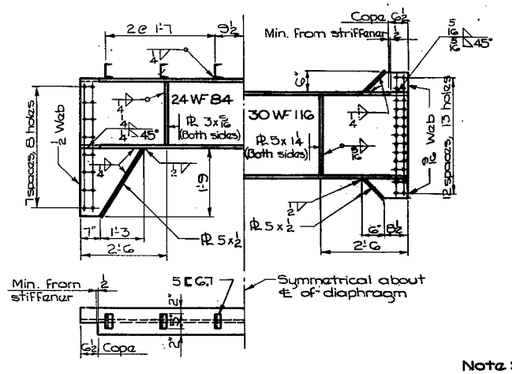

At Abutment At Pier

DIAPHRAGM DETAILS

Note:
Tilt rockers in direction shown for temperature below 50° and in opposite direction for temperature above 50°. Settings for other temperatures are proportional.

ROCKER & EXPANSION PLATE SETTINGS						
	S. Abut.		Pier #1	Pier #2	N. Abut.	
Temp. at time of setting	"D"					"D"
10°	3"	½	0	0	½	3"
50°	2½	0	0	0	0	2½
90°	2"	½	0	0	½	2"

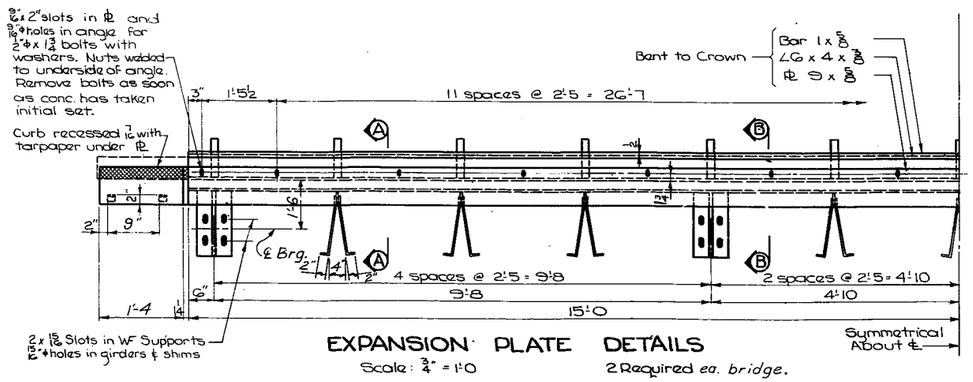

EXPANSION PLATE DETAILS

Scale: ¾" = 1'-0

2 Required ea. bridge.

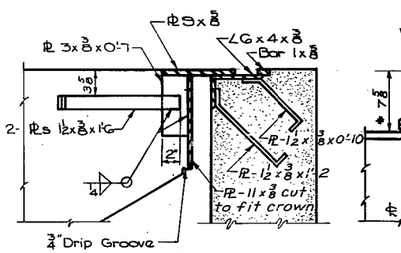

SECTION A-A

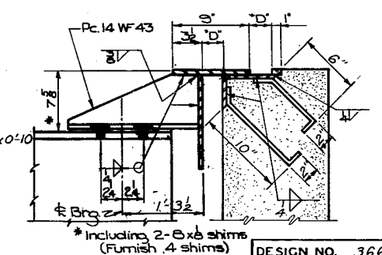

SECTION B-B

Scale: ½" = 1'-0

Design for

DUAL 338'-0 × 30' CONTINUOUS WELDED PLATE GIRDER BRIDGES

103'-0 End Spans 132'-0 Center Span

SUPERSTRUCTURE DETAILS

Station 996+40.00 November, 1966

STORY COUNTY

Iowa State Highway Commission

DESIGN NO.	366
FILE NO.	22590
DES. SH. NO.	6 OF 13

Designed by: J.D.C. Traced by: LEP Checked by: LEP

STORY COUNTY

PROJECT NUMBER I-35-5(18)118--01-85

STATE	FED. ROAD DIST. NO.	FISCAL YEAR	SHEET NO.	TOTAL SHEETS
IOWA	5		23 88	23

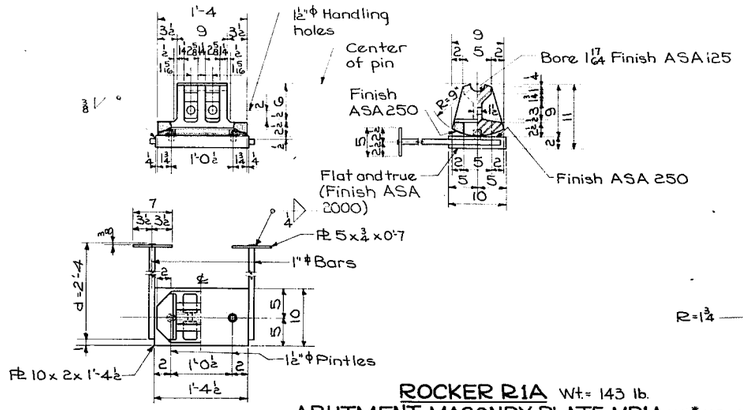

ROCKER R1A Wt.= 143 lb.

ABUTMENT MASONRY PLATE MP1A Wt.*= 110 lb.

* Wt. does not include 1"ϕ bars

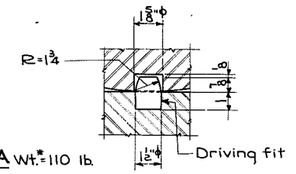

TYPICAL PINTLE DETAIL

SP1 - PL 8x¾x1'-1½
SP2 - PL 8x¾x1'-0½
SP3 - PL 8x¾x1'-2½

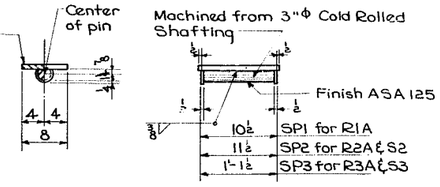

SOLE PLATE SP1, SP2 & SP3

Wt { SP1 = 34 lb. SP2 = 37 lb. SP3 = 43 lb.

BEARING NOTES:

The casting of R1A, R2A, S2, R3A and S3 shall comply with Article 4153.04 of the I.H.C. Standard Specifications. Castings may be Gray Iron or Nodular Iron.

The masonry plates marked MP1A, MP2A, MP2P, MP3A and MP3P shall comply with the requirements of ASTM A-36 steel.

The pins shall comply with Article 4153.02 of the I.H.C. Standard Specifications and with the requirements of ASTM A-108 steel.

All bearings are to be set in paint and canvas.

Anchor bolts shall be set in accordance with Article 2408.47 of the I.H.C. Standard Specifications.

After masonry plates, rockers and shoes are in correct location, pour mortar around anchor bolts to fill the slotted holes.

The weight of bearings shown does not include the weight of paint.

Surfaces finished with an ASA 125 finish shall be shop coated with an application of white lead and tallow as soon as the surfacing process is done. The shop coated surfaces are to be wiped clean and then a field coat of white lead and tallow is to be applied just before the erection of structural steel in the field.

The following materials are to be provided from this sheet.

16-SP1
16-R1A
16-MP1A

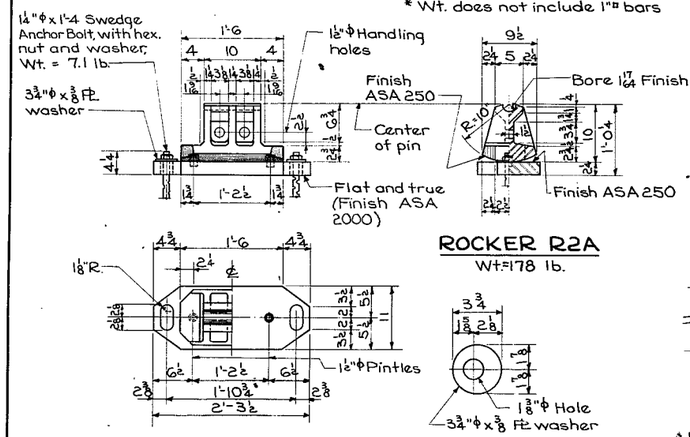

ROCKER R2A

Wt=178 lb.

PIER MASONRY PLATE MP2P

Wt. = 160 lb.

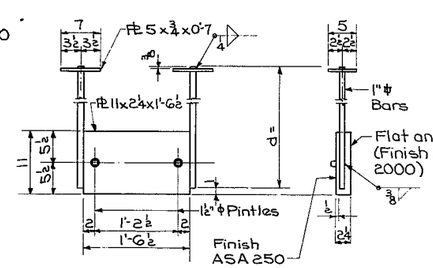

ABUTMENT MASONRY PLATE MP2A

Wt. 146 lb. (Does not include 1"ϕ bars)

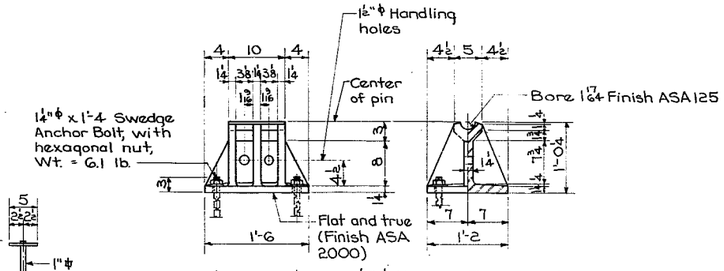

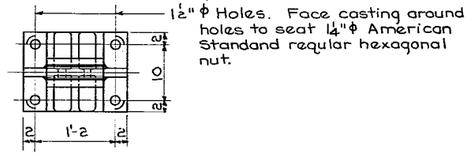

FIXED SHOE S2

Wt.=222 lb.

(Similar to S2 V12-1)

DISTANCE FROM TOP OF SOLE PLATE TO BRIDGE SEAT	
Rockers & Fixed Shoes	D*
R1A	1'-0 11/16
R2A & S2	1'-1 15/16
R3A & S3	1'-4 3/16

* Including 1/16" paint and canvas.

MAXIMUM REACTION (In Kips)		
R1A	R2A S2	R3A S3
132	171	263

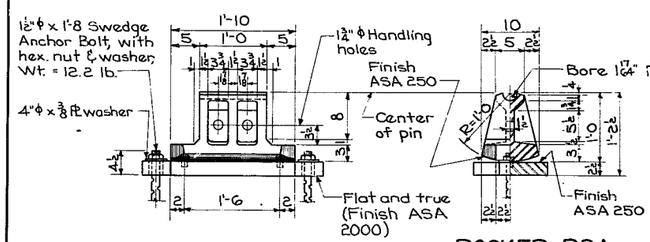

ROCKER R3A

Wt.= 259 lb.

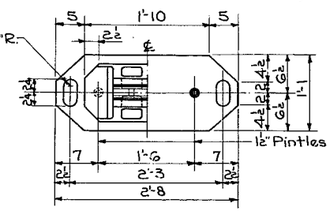

PIER MASONRY PLATE MP3P

Wt. = 249 lb.

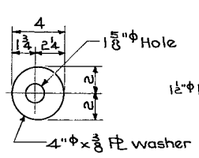

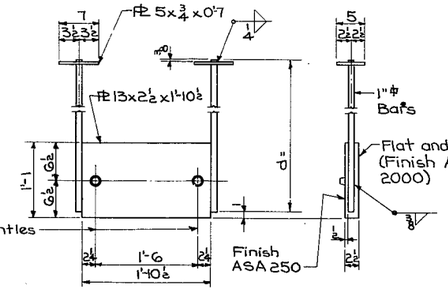

ABUTMENT MASONRY PLATE MP3A

Wt.=224 lb. (Does not include 1"ϕ bars)

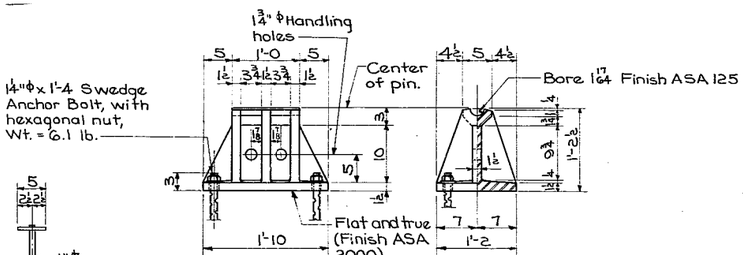

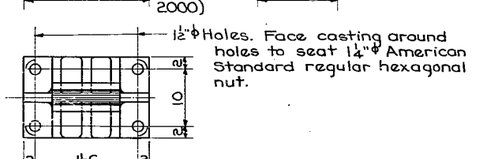

FIXED SHOE S3

Wt.= 349 lb.

(Similar to S1 V10A-7)

Design for

DUAL 338'-0"×30' CONTINUOUS WELDED PLATE GIRDER BRIDGES

103'-0 End Spans 132'-0 Center Span

BEARING DETAILS

Station: 996+40.00 November, 1966

STORY COUNTY Iowa State Highway Commission

Bearing Standard Sheet 1008

DESIGN NO. 366	PROJECT NUMBER	STATE	FED. ROAD DIST. NO.	FISCAL YEAR	SHEET NO.	TOTAL SHEETS
FILE NO. 22590	I-35-5(18)118--01-85	IOWA	5		23B10	25
DES. SH. NO. 10 OF 13						

Designed by: J.D.C. Traced by: Checked by: LEP

1008 STORY COUNTY

Revision (7-6-64) Finish on shoes and masonry plates in contact with concrete added.
Revision (6-1-65) Specifications for Rocker and Shoe material clarified.

DIETZGEN NO. 131 ARKWRIGHT

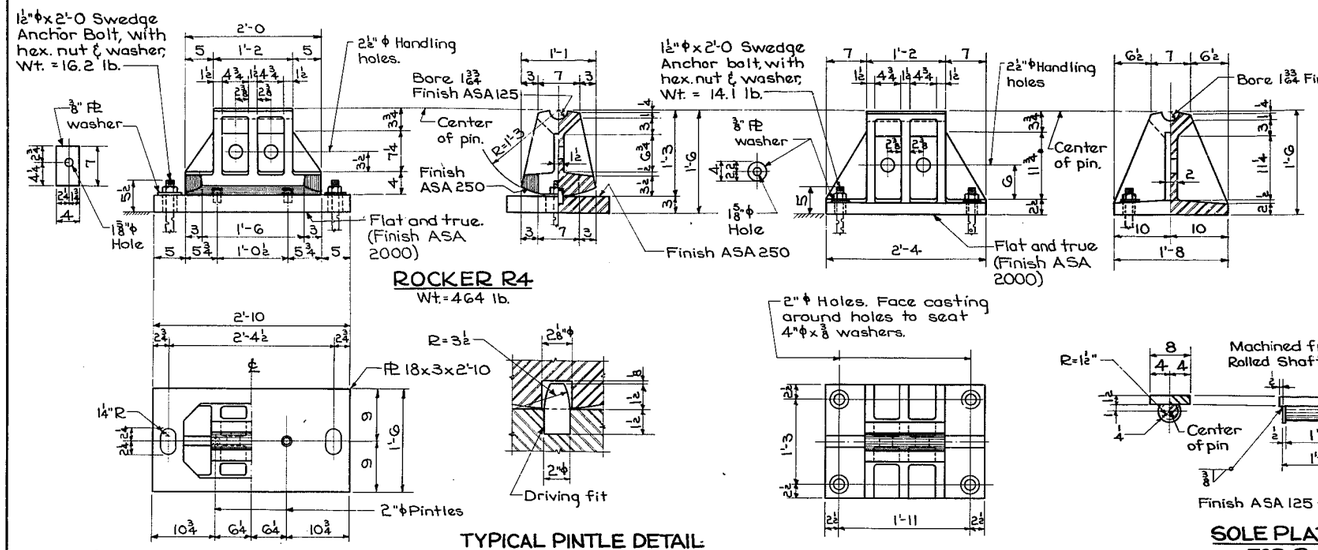

ROCKER R4
Wt.= 464 lb.

TYPICAL PINTLE DETAIL

PIER MASONRY PLATE MP4P
Wt.= 462 lb.

FIXED SHOE S4
Wt.=735 lb.

SOLE PLATES SP4 FOR R4 & S4
Wt.= 85 lb.

BEARING NOTES :

Nodular Iron Castings shall comply with Article 4153.04 of the Standard Specifications except ASTM A-536, Grade 65-45-12 will be required in lieu of ASTM A-339 Grade 60-45-10.

The following shall be Nodular Iron Castings:

R4 MP4P S4
R5 MP5P S5

All plates and bars shall comply with ASTM A-36. Pins shall comply with Article 4153.02 of the Standard Specifications and with ASTM A-108.

All bearings are to be set in paint and canvas.

Anchor bolts shall be set in accordance with Article 2408.47 of the Standard Specifications.

After masonry plates, rockers and shoes are in correct location, pour mortar around anchor bolts to fill slotted holes.

The weight of bearings shown does not include the weight of paint.

Surface finished with an ASA 125 Finish shall be shop coated with an application of white lead and tallow as soon as the surfacing process is done. The shop coated surfaces are to be wiped clean and then a field coat of white lead and tallow is to be applied just before the erection of structural steel in the field.

The following materials are to be provided from this sheet:

16-SP4
16-S4

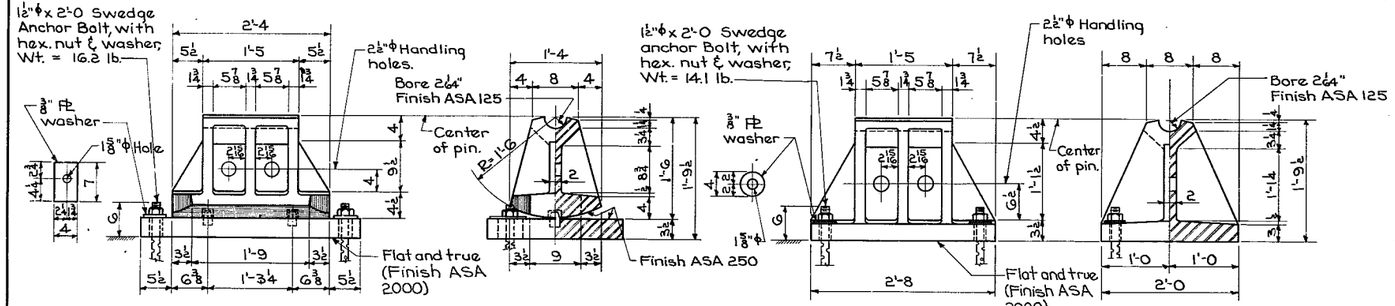

PIER MASONRY PL MP5Pa FOR SPAN LENGTH GREATER THAN 150'
Wt.= 808 lb.

PIER MASONRY PL MP5Pb FOR SPAN LENGTH 101' TO 150'
Wt.= 825 lb.

FIXED SHOE S5
Wt.= 1274 lb.

SOLE PLATES SP5 FOR R5 & S5
Wt. = 159 lb.

DISTANCE FROM TOP OF SOLE PLATE TO BRIDGE SEAT	
Rockers & Fixed Shoes	* D
R4 & S4	1'-8 9/16
R5 & S5	2'-0 13/16

* Including 1/16" paint and canvas.

MAXIMUM REACTION (In Kips)	
R4 S4	R5 S5
475	650

Revision (12-12-62) Pintle size changed
Revision (7-6-64) Finish on shoes and masonry plates in contact with concrete added.
Revision (5-27-65) Weights for MP4P, MP5Pa and MP5Pb changed.
Revision (6-20-66) Nodular Iron Casting ASTM number and grade changed.

Design for
DUAL 338'-0 x 30' CONTINUOUS WELDED PLATE GIRDER BRIDGES
103'-0 End Spans *132'-0 Center Span*
BEARING DETAILS
Station: 996+40.00 *November, 1966*
STORY COUNTY
Iowa *State* *Highway* *Commission*
Bearing Standard Sheet 1009

DESIGN NO. 366	
FILE NO. 22590	
DES. SH. NO. 11 OF 13	

PROJECT NUMBER	STATE	FED. ROAD DIST. NO.	FISCAL YEAR	SHEET NO.	TOTAL SHEETS
I-35-5(18)118--01-85	IOWA	5		23 5 11	13

Designed by: J.D.C. Traced by: Checked by: LEP 1009 STORY COUNTY

DIETZGEN NO. 131 ARKWRIGHT

APPENDIX B. MARSHALL COUNTY BRIDGE PLANS

This page intentionally left blank.

STATE	FED. ROAD DIST. NO.	FISCAL YEAR	SHEET NO.	TOTAL SHEETS
IOWA	5		1	17

PROJECT NUMBER
~~FN-64-7(2)--21-64~~
FN-330-2(2)--21-64

MARSHALL COUNTY — BRIDGE AND CULVERT — LETTING DATE March 5, 1969

PROJECT NO. ~~FN-64-7(2)--21-64~~ FN-330-2(2)--21-64

CONVENTIONAL SIGNS

State Line
Co. Line
Twp. Line
Sec. Line
Corp. Line
Urban Bdry.
R.O.W. Lines
Survey Line — Old / New; Sta. / Ref. Point
Profile Grade
Railroad
Field Tile
Underground Lines — Old / New; Gas / Tel.
Culverts — Old / New
Utility Poles — Power / Tel.
Fences — Barb. / Mesh
Trees Or Brush
Stream
Dike — Old / New
County Road No.
Primary Road No.
U. S. Road No.
Interstate Road No.

DETAIL PLANS REDUCED IN SIZE (DO NOT SCALE)

STATE OF IOWA
STATE HIGHWAY COMMISSION

PLANS OF PROPOSED IMPROVEMENT
ON THE

PRIMARY ROAD SYSTEM
MARSHALL COUNTY
BRIDGE AND CULVERT

REPLACE BRIDGE 2 1/2 MI. S. W. OF MELBOURNE

THE IOWA STATE HIGHWAY COMMISSION STANDARD SPECIFICATIONS FOR CONSTRUCTION WORK, SERIES OF 1964 SHALL APPLY TO WORK ON THIS PROJECT

PLUS CURRENT SUPPLEMENT SPECIFICATIONS AND SPECIAL PROVISIONS

All welding shall meet the requirements of the 1966 Seventh Edition of Specifications for Welded Highway and Railway Bridges of the American Welding Society except as modified by the Standard Specifications.

DESIGN STRESSES:

Design stresses for the following materials are in accordance with AASHO Standard Specifications for Highway Bridges, Series of 1965:
Concrete in accordance with Section 1.5.1 f'c = 3500 psi.
Reinforcing Steel in accordance with Section 1.5.1.
"Reinforcement" for Intermediate, Hard or Rail Steel Grade.
Structural Steel in accordance with Section 1.7.1
ASTM A-36, fs = 20,000 psi.

INDEX OF SHEETS

NO.	DESCRIPTION
1	TITLE SHEET
1A	REVISION SHEET
2	ESTIMATE SHEET
3	MISCELLANEOUS DETAIL SHEET
4-5	~~CULVERT DESIGN NO. 368~~
6-17	BRIDGE DESIGN NO. 168
~~17A~~	~~CULVERT DESIGN NO. 368~~

GENERAL CONTRACTOR = WELDEN BROS. INC.
1969 IOWA FALLS IOWA

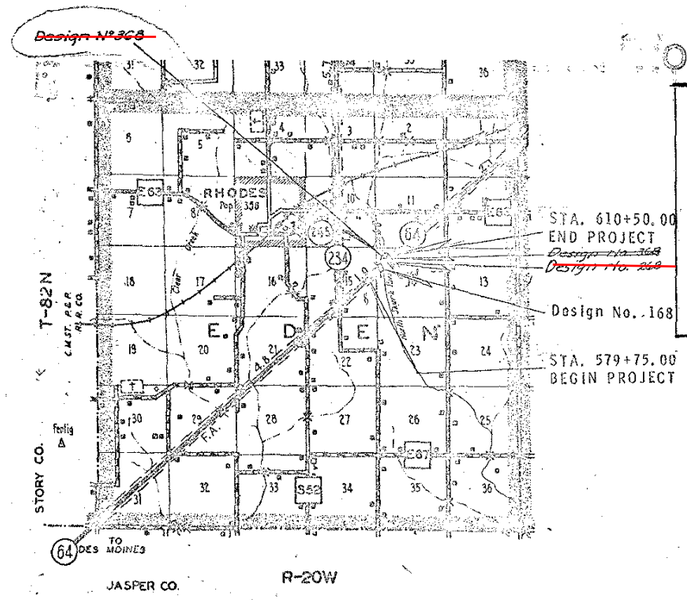

LOCATION MAP

LOCATION MAP SCALE
0 1 2 3
miles

N

STATE CONTROL SECTION NUMBER
64-0900

MILEAGE SUMMARY

CONSTRUCTION PLANS SHOWING PROJECT AS BUILT

PREPARED BY John E. Peters Jr
CONSTRUCTION RESIDENT ENGINEER

DATE December 7, 1971

IOWA STATE HIGHWAY COMMISSION STANDARDS
(Available at the I.S.H.C. Storeroom)

STANDARD	ISSUED	REVISED
C5P	4-1932	6-1944
C1P	1932	8-25-67
C4P	4-1932	
C4J	7-1959	
F4J		6-19-64
CBH-00	1-1960	
P10A	1959	
CHP2.5-65	1965	8-25-65

101-4

DESIGN DATA RURAL

1969 AADT 2900 V.P.D.
1989 AADT 4400 V.P.D.
1969 DHV 500 V.P.H.
DIRECTIONAL 55 %
TRUCKS 17 %
DESIGN V 70 M.P.H.
PARTIAL ACCESS CONTROL

REVISED:
SEE FOLLOWING SHEET 1A

APPROVED
E. A. Owen 2/3/69
DEPUTY CHIEF ENGINEER — DATE
IOWA HIGHWAY COMMISSION

I HEREBY CERTIFY THAT THIS PLAN WAS PREPARED UNDER MY SUPERVISION AND THAT ENGINEERING DECISIONS WITH REGARD TO THE DESIGN WERE MADE BY ME OR BY OTHER DULY REGISTERED PROFESSIONAL ENGINEERS UNDER THE LAWS OF THE STATE OF IOWA.
DATE Feb. 3 1969 IOWA REG. NO. 2792

U.S. DEPT. TRANSPORTATION
BUREAU OF PUBLIC ROADS
APPROVED
DIVISION ENGINEER — DATE

BGM RAK Jan. 31, 1969 1-31-69

Rev (30)

MARSHALL CO. PROJECT NO. ~~FN-64-7(2)--21-64~~ FN-330-2(2)--21-64 FILE NO. 23033

STATE	FED. ROAD DIST. NO.	FISCAL YEAR	SHEET NO.	TOTAL SHEETS
IOWA	5		1	17

Marshall JA 330 #9

221

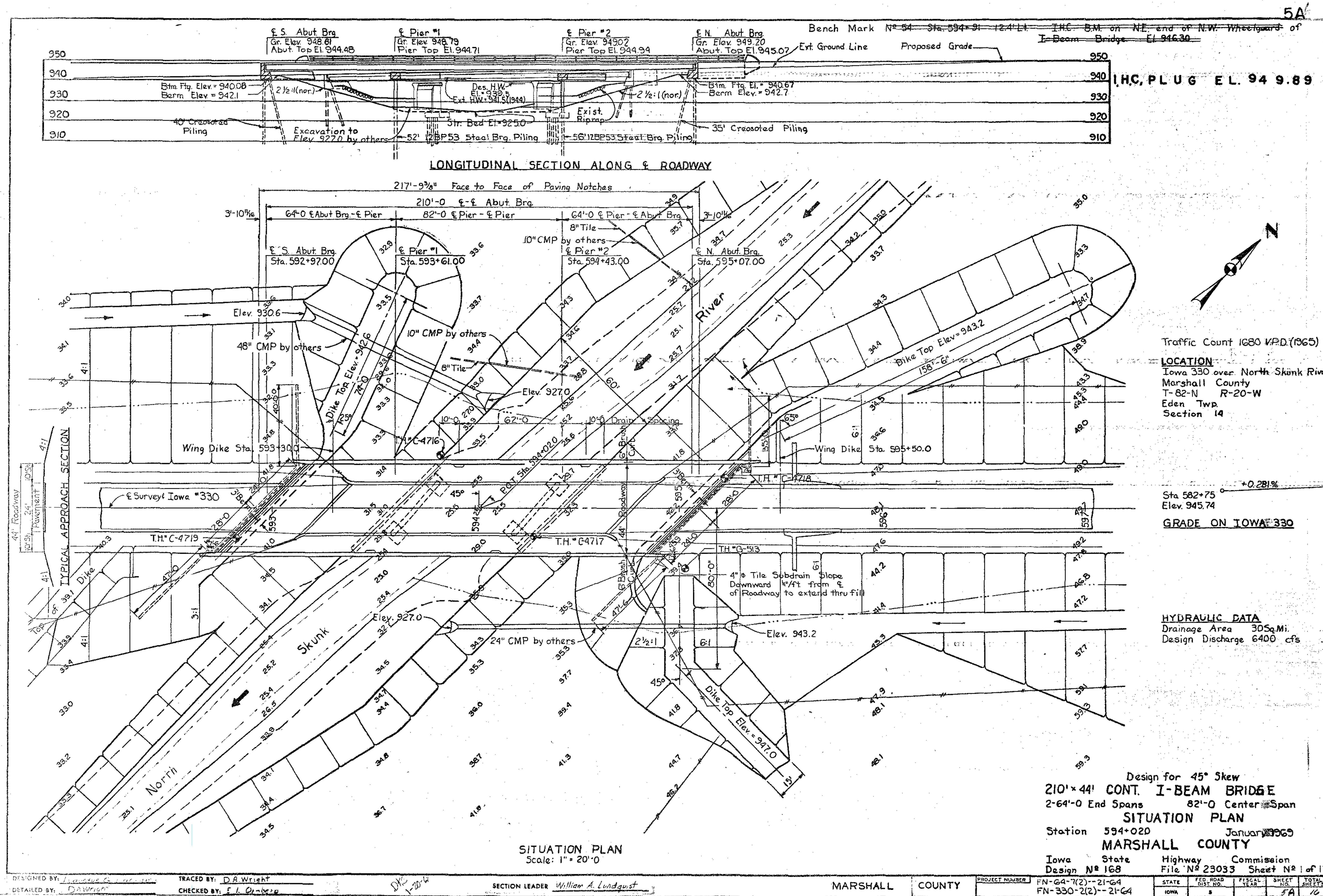
5A
Bench Mark No 54 Sta. 594+91 12.4' Lt. I.H.C. B.M. on N.E. end of N.W. Wheelguard of I-Beam Bridge El. 946.30
I.H.C. PLUG EL. 949.89
℄ S. Abut. Brg. Gr. Elev. 948.61 Abut. Top El. 944.48
℄ Pier #1 Gr. Elev. 948.79 Pier Top El. 944.71
℄ Pier #2 Gr. Elev. 949.02 Pier Top El. 944.94
℄ N. Abut. Brg. Gr. Elev. 949.20 Abut. Top El. 945.07
Ext. Ground Line
Proposed Grade
Btm. Ftg. Elev. = 940.08
Berm Elev. = 942.1
Btm. Ftg. El. = 940.67
Berm Elev. = 942.7
Des. H.W. El. = 939.5
Ext. HW-941.5 (1944)
Str. Bed El. = 925.0
Exist. Riprap
40' Creosoted Piling
35' Creosoted Piling
Excavation to Elev. 927.0 by others
52' 12BP53 Steel Brg. Piling
56' 12BP53 Steel Brg. Piling
LONGITUDINAL SECTION ALONG ℄ ROADWAY
217'-9⅜" Face to Face of Paving Notches
210'-0 ℄-℄ Abut. Brg.
64'-0 ℄ Abut. Brg.-℄ Pier
82'-0 ℄ Pier-℄ Pier
64'-0 ℄ Pier-℄ Abut. Brg.
℄ S. Abut. Brg. Sta. 592+97.00
℄ Pier #1 Sta. 593+61.00
℄ Pier #2 Sta. 594+43.00
℄ N. Abut. Brg. Sta. 595+07.00
10" CMP by others
48" CMP by others
24" CMP by others
8" Tile
Elev. 930.6
Elev. 927.0
Elev. 943.2
Dike Top Elev. = 942.6
Dike Top Elev. = 943.2
Dike Top Elev. = 947.0
Wing Dike Sta. 593+30.0
Wing Dike Sta. 595+50.0
P.O.T. Sta. 594+02.0
℄ Survey Iowa #330
T.H. # C-4719
T.H. # C-4717
T.H. # C-4716
T.H. # C-4718
T.H. # G-513
4" Tile Subdrain Slope Downward ¼"/ft. from ℄ of Roadway to extend thru fill
North Skunk River
TYPICAL APPROACH SECTION
44' Roadway
24' Pavement
Traffic Count 1680 V.P.D. (1965)
LOCATION
Iowa 330 over North Skunk River
Marshall County
T-82-N R-20-W
Eden Twp.
Section 14
Sta 582+75
Elev. 945.74
+0.281%
GRADE ON IOWA 330
HYDRAULIC DATA
Drainage Area 305 Sq. Mi.
Design Discharge 6400 cfs
SITUATION PLAN
Scale: 1" = 20'-0
Design for 45° Skew
210' × 44' CONT. I-BEAM BRIDGE
2-64'-0 End Spans 82'-0 Center Span
SITUATION PLAN
Station 594+020
January 1969
MARSHALL COUNTY
Iowa State Highway Commission
Design No 168
File No 23033
Sheet No 1 of 12
DESIGNED BY:
DETAILED BY: D.A. Wright
TRACED BY: D.A. Wright
CHECKED BY:
SECTION LEADER William A. Lundquist
MARSHALL COUNTY
FN-64-7(2)--21-64
FN-330-2(2)--21-64
IOWA
5A
16
222

Bench Mark: No. 54 ~~Sta 594+91 12.4' Lt. I.H.C. B.M. on N.E. end of N.W. Wheelguard of I-Beam Bridge El. 946.30~~

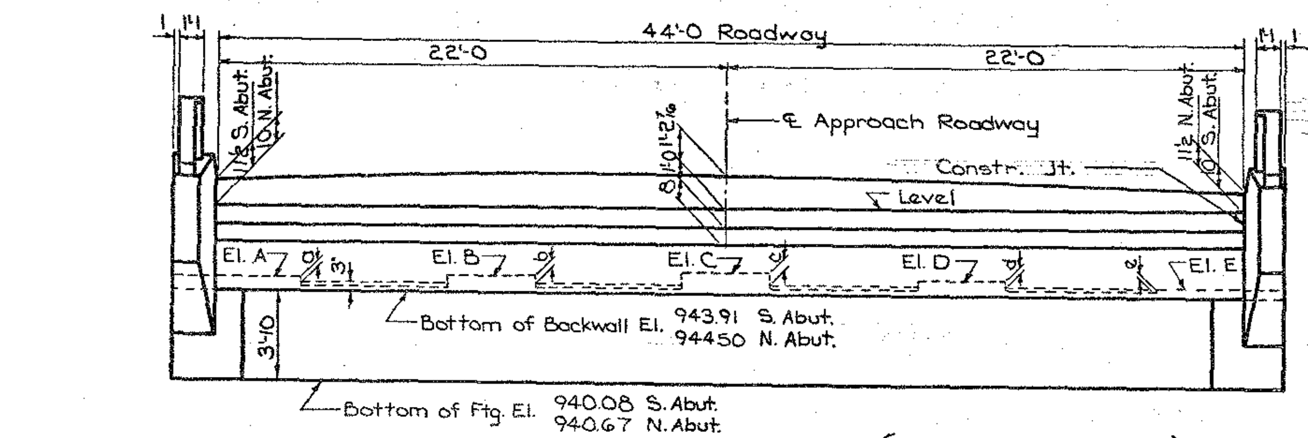

REAR ELEVATION (Looking North - S. Abut. / Looking South - N. Abut.)

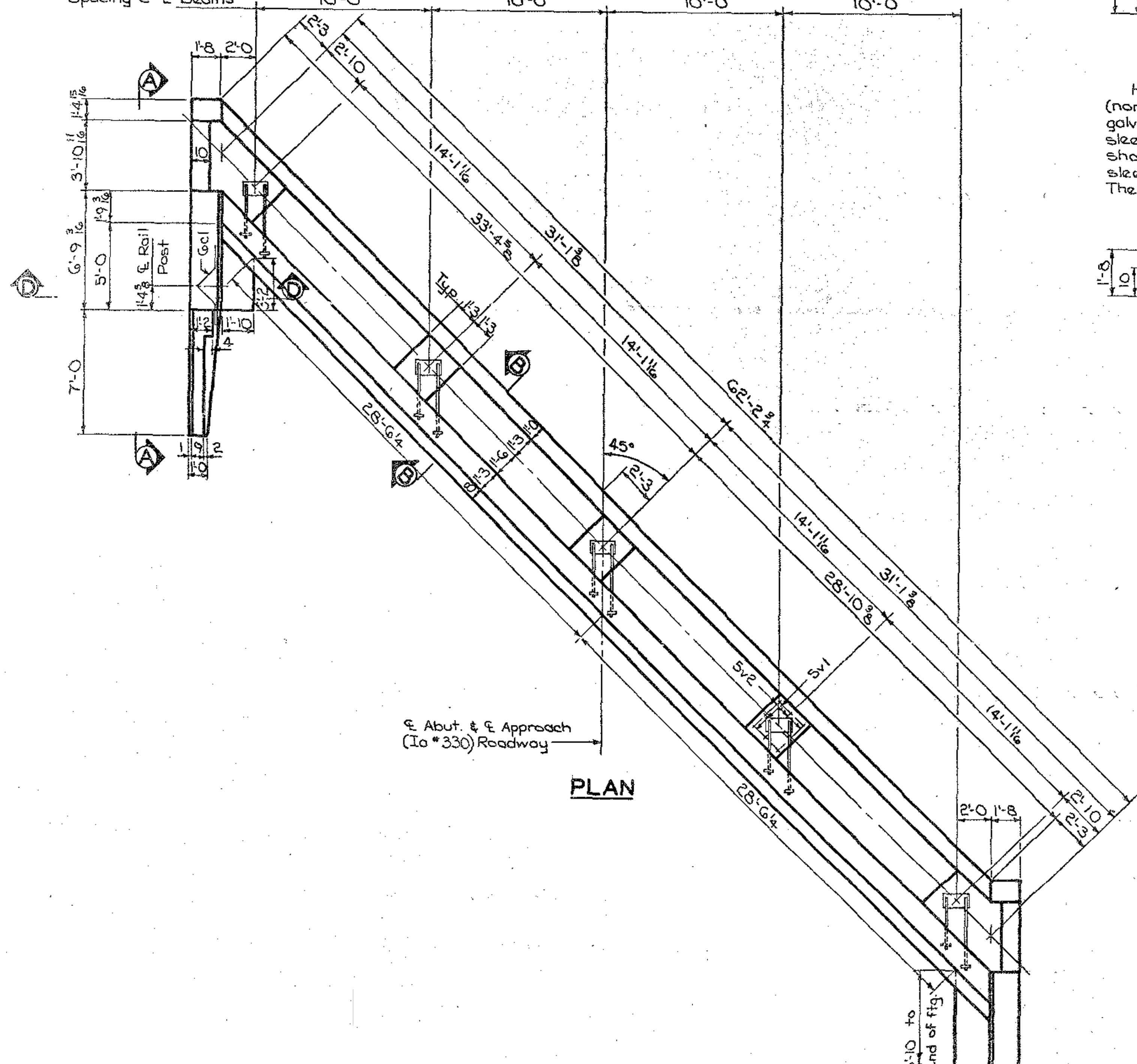

PLAN

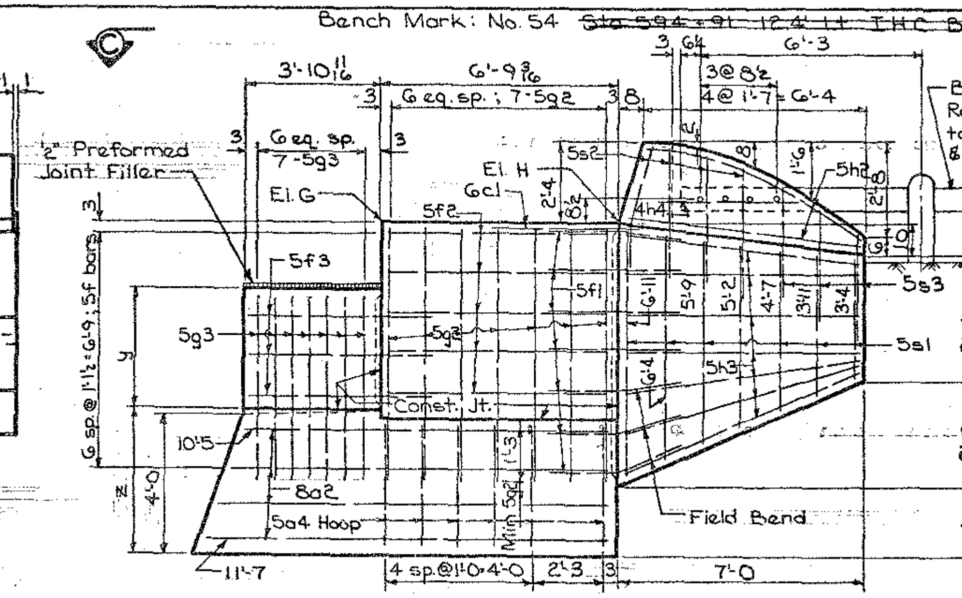

VIEW A-A

Holes for ⅞"ϕ bolts are to be formed with 1"ϕ (nominal dia.) St'd. steel pipe sleeves which are to be galvanized after cutting to proper length. The pipe sleeves shall be securely fixed in exact location as shown before concrete is poured. The cost of pipe sleeves is to be included in the price bid for concrete. The ⅞"ϕ bolts are to be furnished and placed by others.

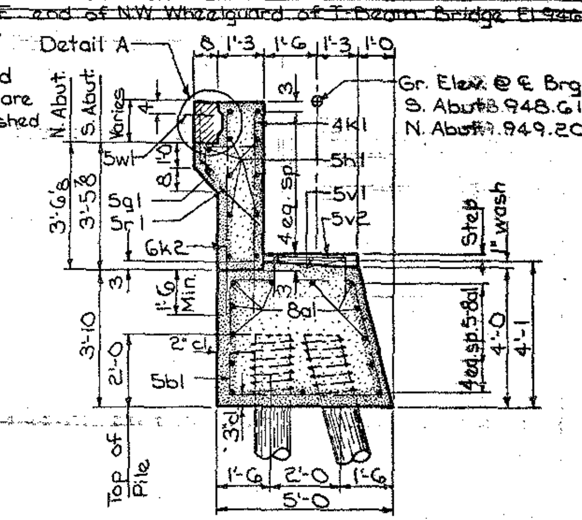

SECTION B-B

NOTE: Before the concrete paving block is poured bend down dowels (structural grade) and line the notch with tar paper to prevent bond. Block is to be removed and bars straightened before pavement is placed.

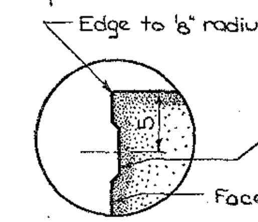

DETAIL A

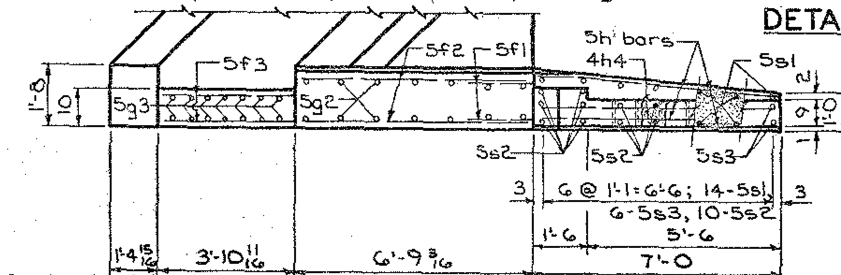

VIEW C-C

ELEVATIONS & DIMENSIONS						
		El. H	El. G	j	y	z
S. Abut.	W. End	949.36	949.40	1'-11 11/16	3'-4 7/8	4'-2 3/8
	E. End	949.26	949.28	1'-10 3/16	3'-4 3/4	4'-1
N. Abut.	W. End	950.02	950.00	2'-0 5/16	3'-4 7/8	4'-2 3/8
	E. End	949.90	949.88	1'-10 13/16	3'-4 3/4	4'-1

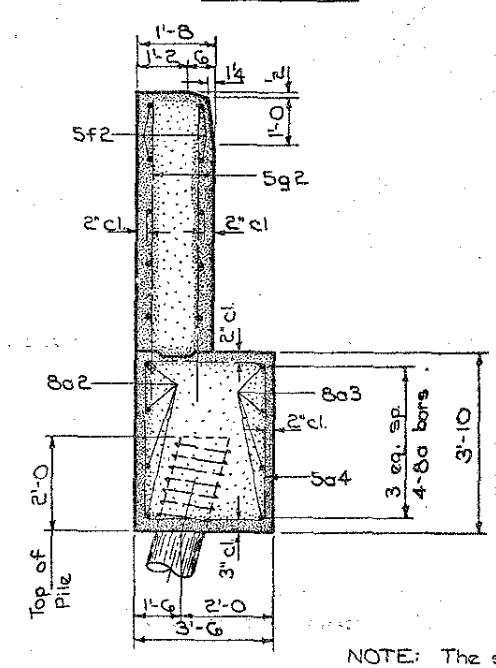

SECTION D-D

STEP ELEV. & DIMENSIONS		
	S. Abut.	N. Abut.
Elevation A	944.27	944.75
" B	944.38	944.92
" C	*944.48	*945.07
" D	944.33	944.97
" E	944.16	944.86
Step a	1 3/8	0
" b	2 1/16	2
" c	3 7/8	3 7/8
" d	2	2 1/16
" e	0	1 3/8

* Abut. Top

NOTE: The spirals at the top of each pile are made up of 7 turns of ¼" ϕ rod, 21" diameter, 3" pitch, with 2-⅜ CO69 spacers punched to hold spiral.

Design For 45° Skew

210'-0 × 44'-0 CONTINUOUS I-BEAM BRIDGE

64'-0 End Spans 82'-0 Interior Span

ABUTMENT DETAILS

Station: 594+02.0 January 1969

MARSHALL COUNTY

IOWA STATE HIGHWAY COMMISSION

Des. Sh. No. 3 of 12 File No. 23033 Des. No. 168

DESIGNED BY: Augustus G. Larkus TRACED BY: Darwin Backous
DETAILED BY: Darwin Backous CHECKED BY: E.L. Ornberg

MARSHALL COUNTY

PROJECT NUMBER		STATE	FED. ROAD DIST. NO.	FISCAL YEAR	SHEET NO.	TOTAL SHEETS
	FN-64-7(2)--21-64 FN-330-2(2)--21-64	IOWA	5		7	16

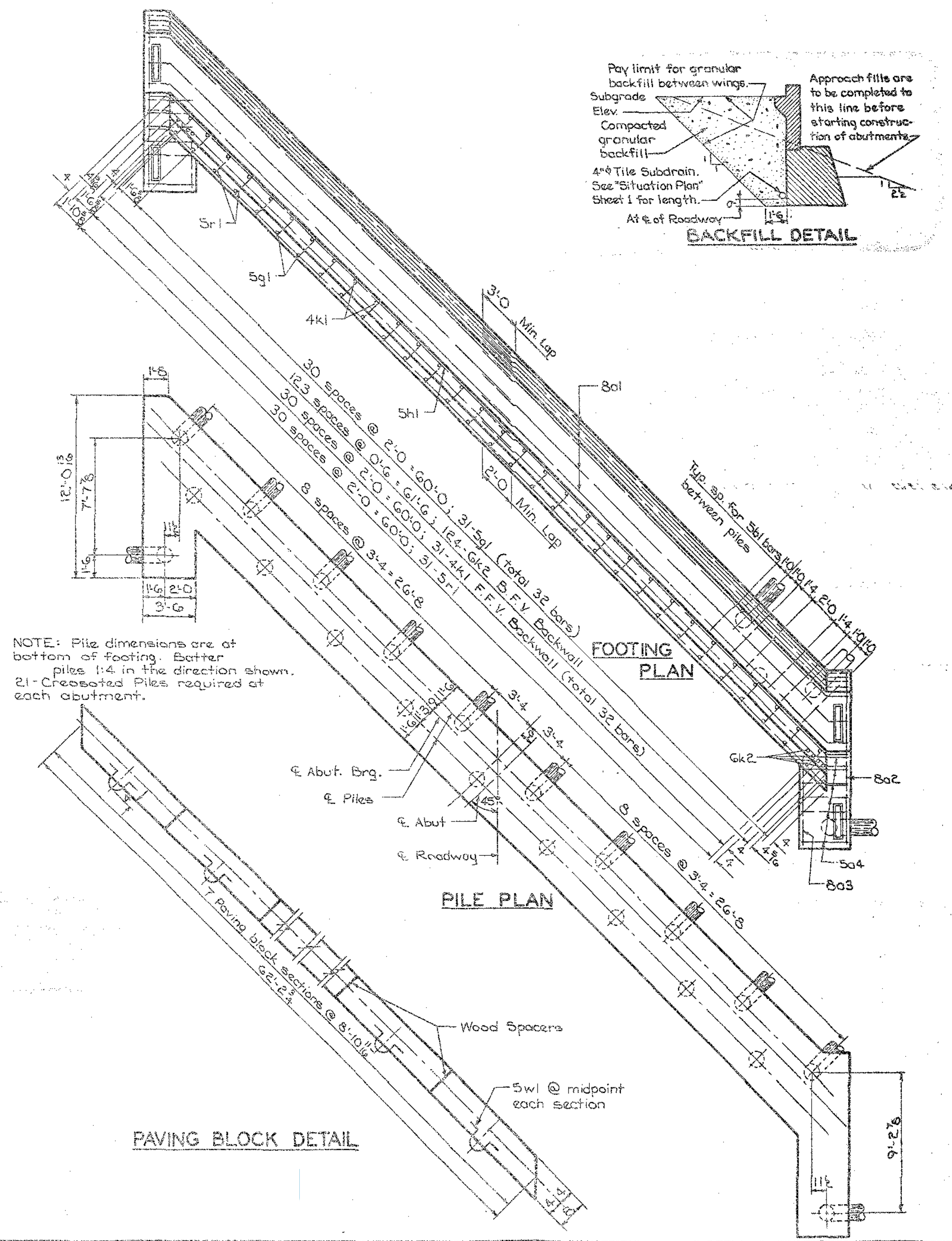

BACKFILL DETAIL

FOOTING PLAN

PILE PLAN

PAVING BLOCK DETAIL

CONC. PLACEMENT QUANT.-ONE ABUT.		
Item	Unit	Quantity
Footing & Steps	Cu. Yd.	48.4
Backwall	Cu. Yd.	15.2
Wings	Cu. Yd.	3.8
Wingwalls	Cu. Yd.	4.5
Maskwalls	Cu. Yd.	0.8
End Posts	Cu. Yd.	0.8
*Paving Block	Cu. Yd.	1.6
Total Cu. Yd.		75.1

* Paving Block may be Class "C" or Class "D" concrete.

ESTIMATED QUANT.-TWO ABUTS.		
Item	Unit	Quantity
Structural Concrete Class C	Cu. Yd.	150.2
Reinforcing Steel	Lbs.	14,824
Class 20 Excavation	Cu. Yd.	200
Granular Backfill	Cu. Yd.	178
Creosoted Piling 21@40', 21@35'	L.F.	1,575

ABUTMENT NOTES:

All exposed corners 90° or sharper are to be filleted with a 3/4" dressed and beveled strip.

Reinforcing steel is to be securely wired in place before concrete is poured.

Minimum clear distance from face of concrete to near reinforcing bar is to be 2" unless otherwise noted or shown.

All backfill behind the abutment between wings is to be granular backfill. The remainder of the abutment excavation is to be backfilled with soil.

Cost of all preformed joint and compressible materials is to be included in price bid for concrete.

The portion of the backwall containing the abutment anchorage of the expansion plate is to be poured after the bridge floor is placed.

The Mask Wall ~~is to be~~ was poured before the superstructure slab is poured.

Construction joint keyways are to be formed with beveled 2 x 6's.

Beams and masonry plates ~~are to be set~~ were before backwall is placed. Masonry plates are included in the superstructure estimate.

Piles ~~are to~~ were be driven to full penetration if practicable, but to not less than 20 tons nor more than 40 tons bearing value per pile.

REINFORCING BAR LIST-ONE ABUTMENT					
Bar	Location	Shape	No.	Length	Weight
8a1	Footing Longitudinal		26	34'-2	2372
8a2	Wing Footing Longitudinal		8	Varies	235
8a3	" " "		8	8'-10	189
5a4	" " Hoops		12	13'-11	174
5b1	Footing Hoops		38	16'-2	641
6c1	Rail Post Anchors		2	5'-0	15
5f1	Wing Dowels		28	3'-10	112
5f2	" Horizontal		20	6'-6	136
5f3	Maskwall Horizontal		12	5'-2	65
*5g1	Paving Dowels		32	2'-0	67
5g2	Wing Vertical		28	6'-9	197
5g3	Maskwall Vertical		28	4'-9	139
5h1	Backwall Horizontal		24	33'-7	841
5h2	End Post "		8	6'-8	56
5h3	Wing Horizontal		28	6'-8	195
4h4	End Post "		4	3'-0	8
4k1	Backwall F.F.V.		32	6'-1	130
6k2	" B.F.V.		124	6'-1	1133
5r1	Paving Notch Transverse		31	4'-2	135
5s1	Wing Vertical		28	Varies	150
5s2	End Post Wing		20	3'-9	78
5s3	" " "		12	3'-0	38
5v1	Beam Step Longitudinal		15	2'-2	34
5v2	" " Transverse		15	4'-4	68
5w1	Paving Block Lifting Hoop		7	2'-3	16
	Pile Spiral ¼" ϕ rod		21	38'-6	135
	Spiral Spacers ⅞ E O.69		42	1'-10	53
* Structural Grade			Total lbs.		7,412

BENT BAR DETAILS

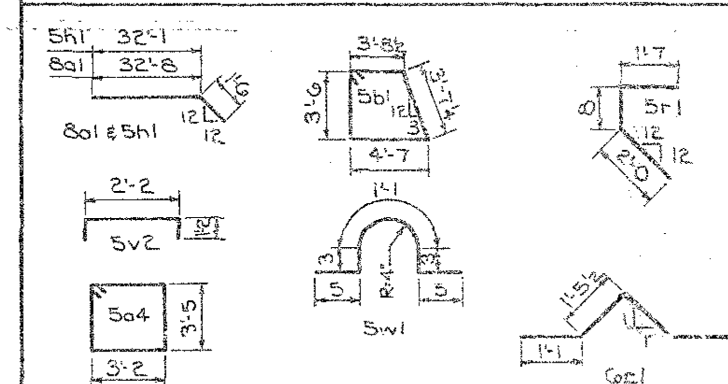

NOTE: All dimensions are out to out. Radii are to ℄ bar.

Design For 45° Skew
210'-0 x 44'-0 CONTINUOUS I-BEAM BRIDGE
64'-0 End Spans 82'-0 Interior Span
ABUTMENT DETAILS
Station: 594+02.0 January 1969
MARSHALL COUNTY
IOWA STATE HIGHWAY COMMISSION
Des. Sh. No. 4 of 12, File No. 23033 Des. No. 168

DESIGNED BY: Augustus G. Lerkus TRACED BY: Darwin Backous
DETAILED BY: Darwin Backous CHECKED BY: E.L. Ornberg

MARSHALL COUNTY

PROJECT NUMBER	STATE	FED. ROAD DIST. NO.	FISCAL YEAR	SHEET NO.	TOTAL SHEETS
FN-64-7(2)--21-64 FN-330-2(2)--21-64	IOWA	5		8	16

224

Bench Mark: No. ~~54 Sta. 594+91 12.4' Lt. T.H.C. B.M. on N.E. end of N.W. Wingwall of I Beam Bridge Elev. 950.00~~

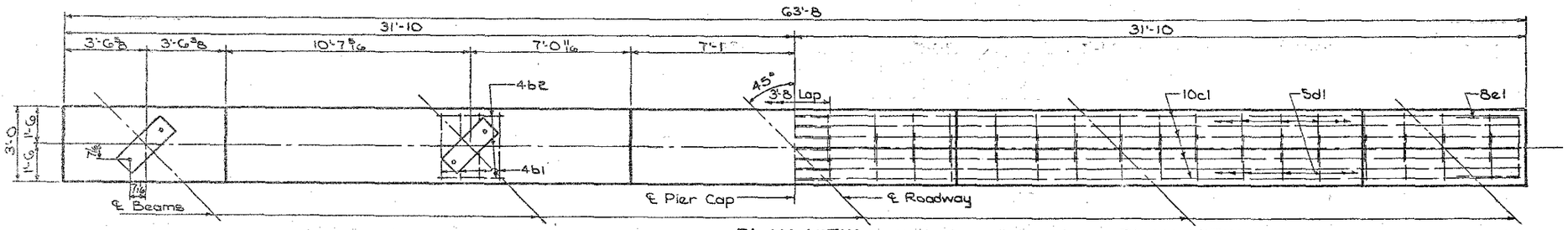

PLAN VIEW

PIER ELEVATIONS		
Elev.	Pier #1	Pier #2
A	944.50	944.73
B	944.62	944.85
* C	944.71	944.94
D	944.56	944.79
E	944.39	944.62

* Pier Top Elev.

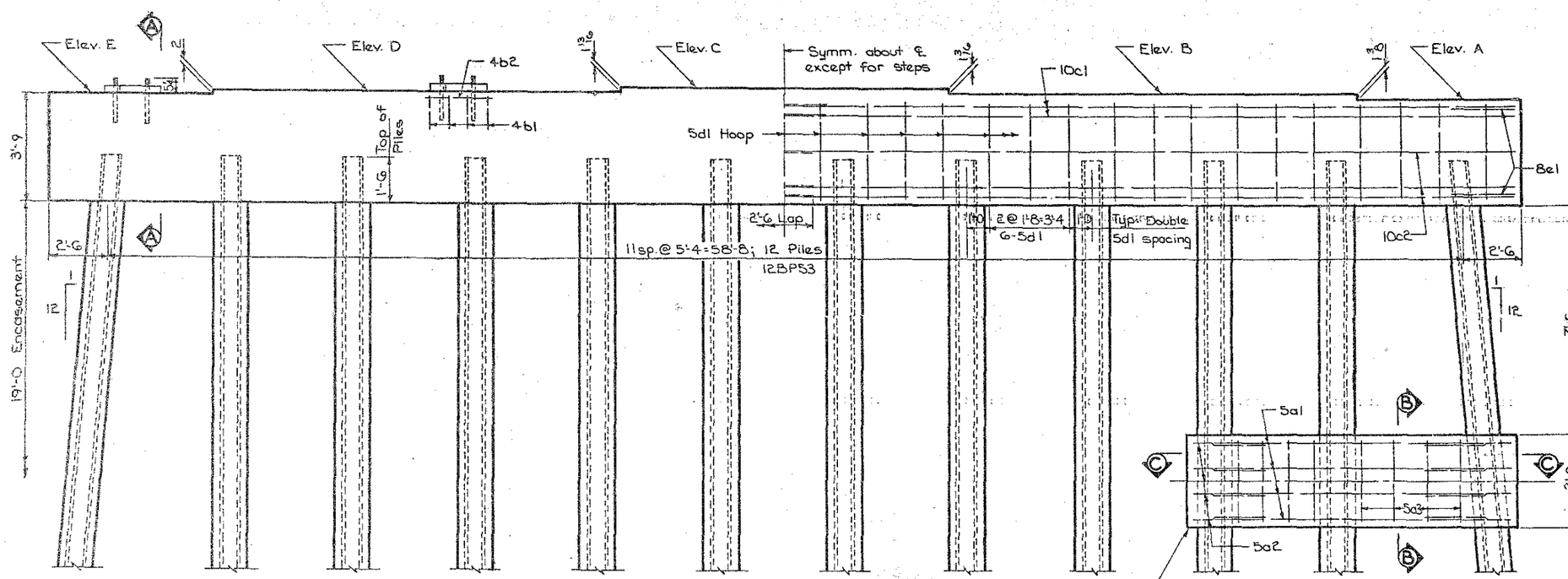

ELEVATION
Looking West

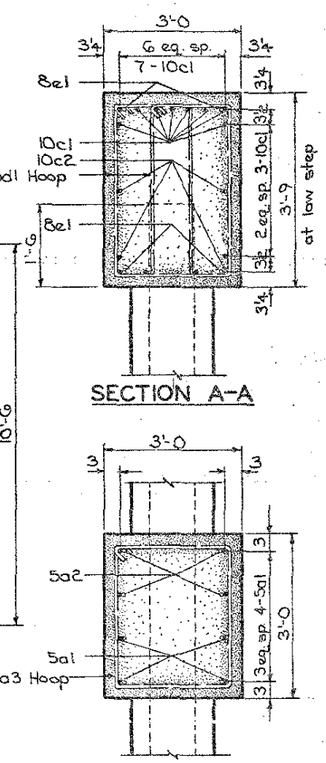

SECTION A-A

SECTION B-B

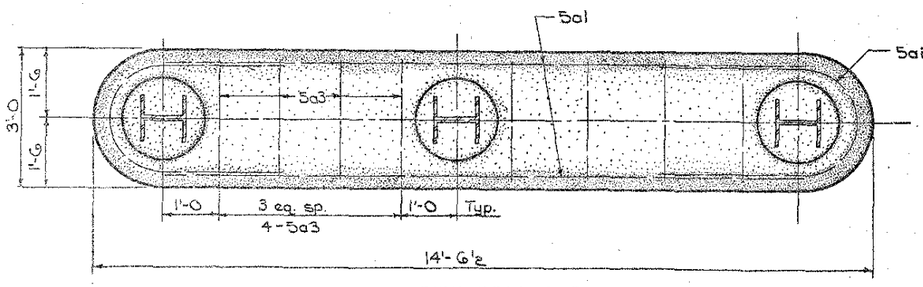

SECTION C-C

NOTE: For pier notes & quantities see sht. 6

Design For 45° Skew
210'-0 × 44'-0 CONTINUOUS I-BEAM BRIDGE
64'-0 End Spans 82'-0 Interior Span
PIER PILE BENT DETAILS
Station: 594 +02.0 January 1969
MARSHALL COUNTY
IOWA STATE HIGHWAY COMMISSION
Des. Sh. No. 5 of 12 File No. 23033 Des. No. 1685

DESIGNED BY: Engineering Personnel TRACED BY:
DETAILED BY: Darwin Backous CHECKED BY: E. L. Ornberg

MARSHALL COUNTY

PROJECT NUMBER	STATE	FED. ROAD DIST. NO.	FISCAL YEAR	SHEET NO.	TOTAL SHEETS
FN-64-7(2)--21-64 FN-330-2(2)--21-64	IOWA	8		9	16

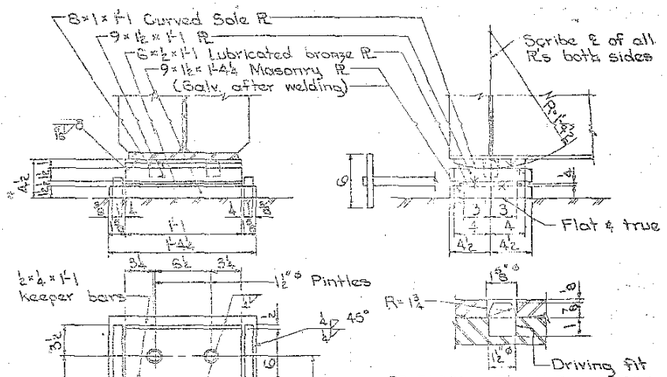

TYPICAL PINTLE DETAIL

Surfaces marked "V" shall be finished ASA 250, surfaces marked "V" shall be finished ASA 125. Bronze PL shall be lubricated in accordance with I.S.H.C. Spec. Art. 4190.06 (Sliding surface only). Top edges of bronze PL shall be beveled ⅛". All bearings to be set in paint & canvas. Pintle plates and masonry plates are a part of the Superstructure Structural Steel Quantity.

ABUTMENT BEARING DETAILS

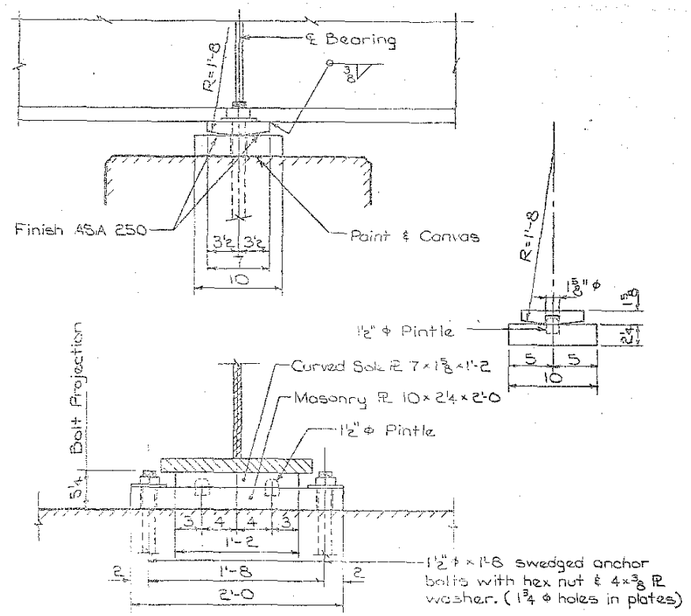

BEARING DETAILS AT PILE BENTS

PIER NOTES:

Reinforcing steel is to be securely wired in place before concrete is poured.

Minimum clear distance from face of concrete to near reinforcing bar is to be 2" unless otherwise noted or shown.

Anchor bolts are to be preset in piers in accordance with the Standard Specifications. The weight of anchor bolts is included in the structural steel quantity.

Reinforcing bars may be shifted slightly to clear anchor bolts.

All piling ~~shall be~~ driven to full penetration if practicable but to at least 46 ton bearing value per pile.

For encasement details see I.H.C. std. P-10A Type V dated June 1959.

REINFORCING STEEL - ONE PIER

Bar	Location	Shape	No.	Length	Weight
5a1	Collar Longitudinal		8	11'-4	95
5a2	Collar Ends		8	9'-7	76
5a3	Collar Hoop		8	11'-5	95
4b1	Pier Cap Transverse		20	4'-7	61
4b2	Pier Cap Longit		15	2'-10	28
10c1	Pier Cap Longit. Top		18	33'-6	2595
10c2	Pier Cap Longit. Bottom		16	32'-11	2266
5d1	Pier Cap Hoops		70	11'-3	821
8e1	Pier Cap Ends		4	7'-7	81
				Total lbs	6118

BENT BAR DETAILS

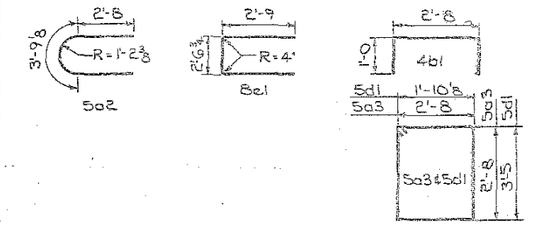

Note: All dimensions are out to out. Radii to ℄ bar.

ESTIMATED QUANTITIES - TWO PIERS

Item			Unit	Quantity
* Structural Concrete Class C			Cu. Yds.	63.6
Reinforcing Steel			Lbs.	12,236
12BP53 Steel Bearing Piles	Furnish	12 @ 56' 12 @ 52'	L.F.	1296
	Drive	12 @ 56' 12 @ 52'	L.F.	1296
	Encase.	12 @ 19' 12 @ 19'	L.F.	456

*Includes 55.8 Cu.Yd. for Caps & 7.8 Cu.Yd. for Collars.

Design For 45° Skew

210'-0 × 44'-0 CONTINUOUS I-BEAM BRIDGE

64'-0 End Spans 82'-0 Interior Span

BEARING DETAILS

Station: 594 +02.0 January 1969

MARSHALL COUNTY

Iowa State Highway Commission

Des Sh. No. 6 of 12 File No. 23033 Des No. 168

DESIGNED BY: Louisiana C.E. Students TRACED BY:

DETAILED BY: Darwin Beckous CHECKED BY: E.L. Ongberg

MARSHALL COUNTY

PROJECT NUMBER		STATE	FED. ROAD DIST. NO.	FISCAL YEAR	SHEET NO.	TOTAL SHEETS
FN-64-7(2)--21-64		IOWA	5		12	12
FN-330-8(2)--21-64						

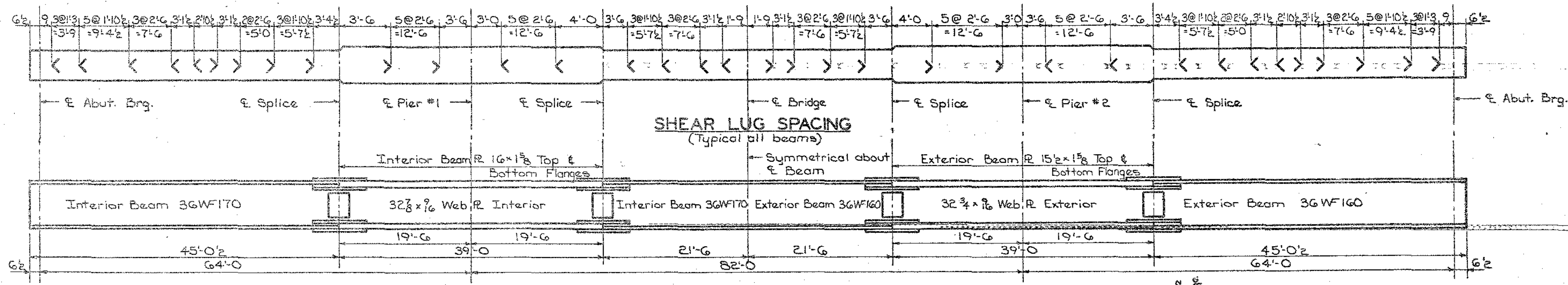

SHEAR LUG SPACING
(Typical all beams)

INTERIOR AND EXTERIOR BEAMS

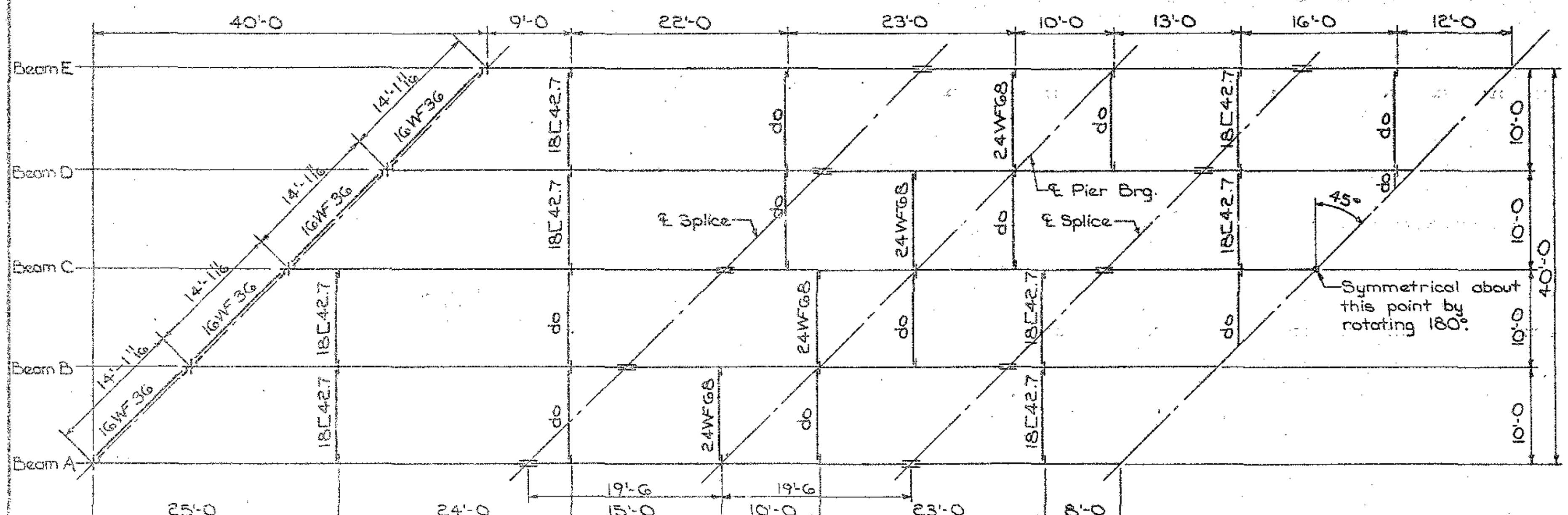

STRUCTURAL STEEL LAYOUT

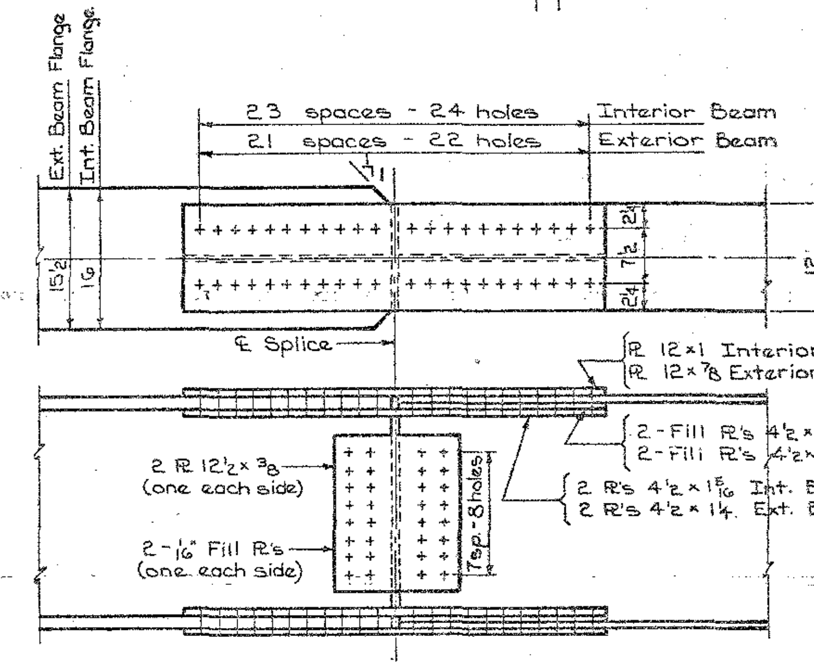

EXTERIOR & INTERIOR BEAM SPLICE DETAIL

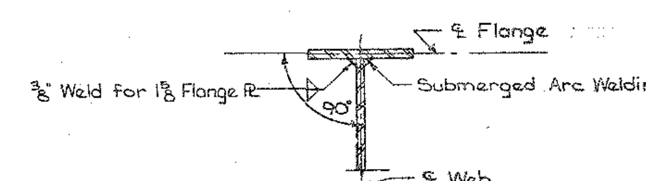

FLANGE TO WEB DETAILS

Encircled figures indicate deflection due to concrete alone.

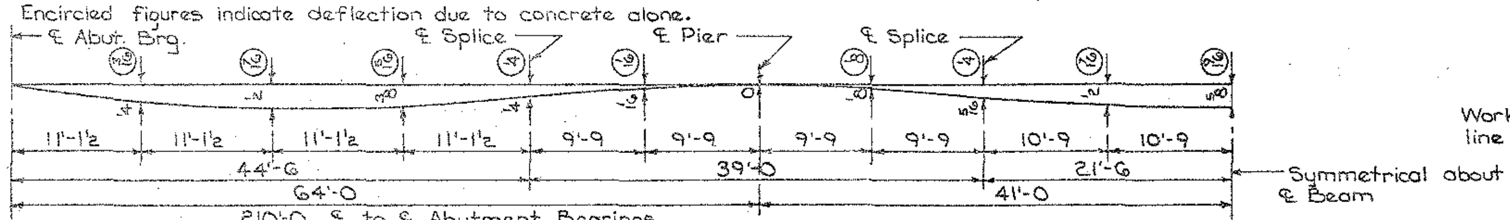

ANTICIPATED DEAD LOAD DEFLECTION

BEAMS AS FABRICATED & ERECTED

HAUNCH THICKENING DIAGRAM
(For estimating purposes only)

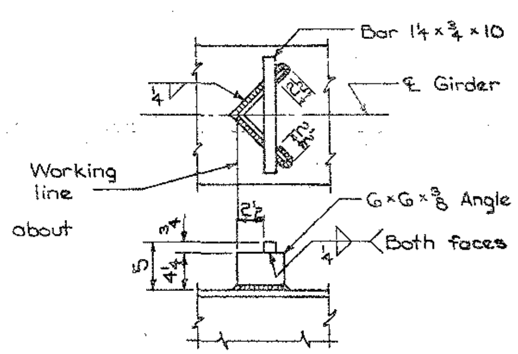

SHEAR LUG DETAIL

400 Required Wt. = 8.36# each

NOTE: Shear lugs are spaced in multiples of transverse reinforcing bars & are located to clear the bottom transverse bars.

Design For 45° Skew

210'-0 × 44'-0 CONTINUOUS I-BEAM BRIDGE

64'-0 End Spans 82'-0 Interior Span

SUPERSTRUCTURE DETAILS

Station: 594+02.0 January 1969

MARSHALL COUNTY

Iowa State Highway Commission

Des. Sh. No. 7 of 12 File No. 23033 Des No. 168

227

DESIGNED BY: [illegible] TRACED BY: Darwin Backous

DETAILED BY: Darwin Backous CHECKED BY: E.L. Ornberg

MARSHALL COUNTY

PROJECT NUMBER FN-64-7(2)--21-64 FN-330-2(2)--21-64

STATE IOWA SHEET NO. 11 TOTAL SHEETS 14

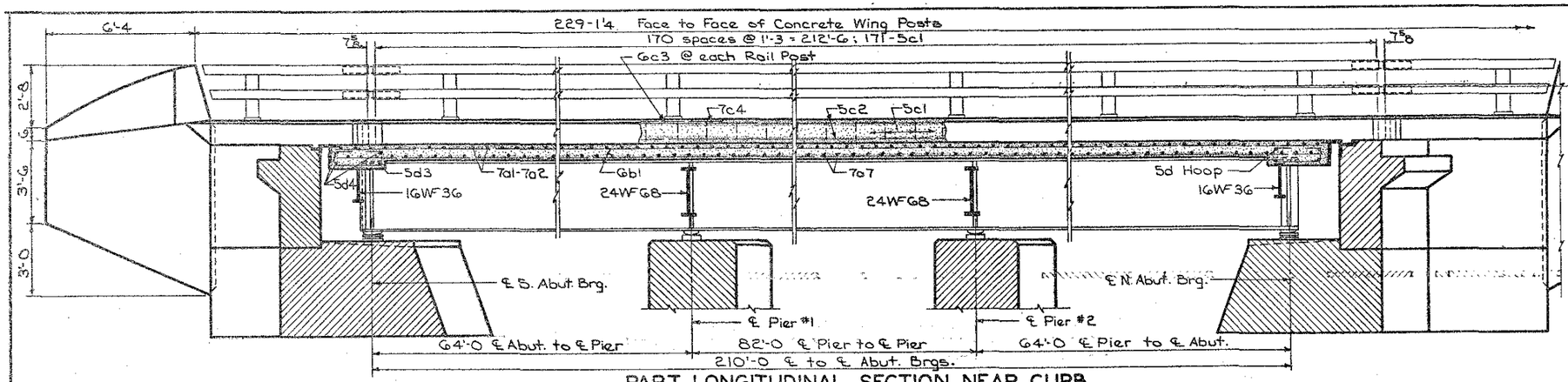

PART LONGITUDINAL SECTION NEAR CURB

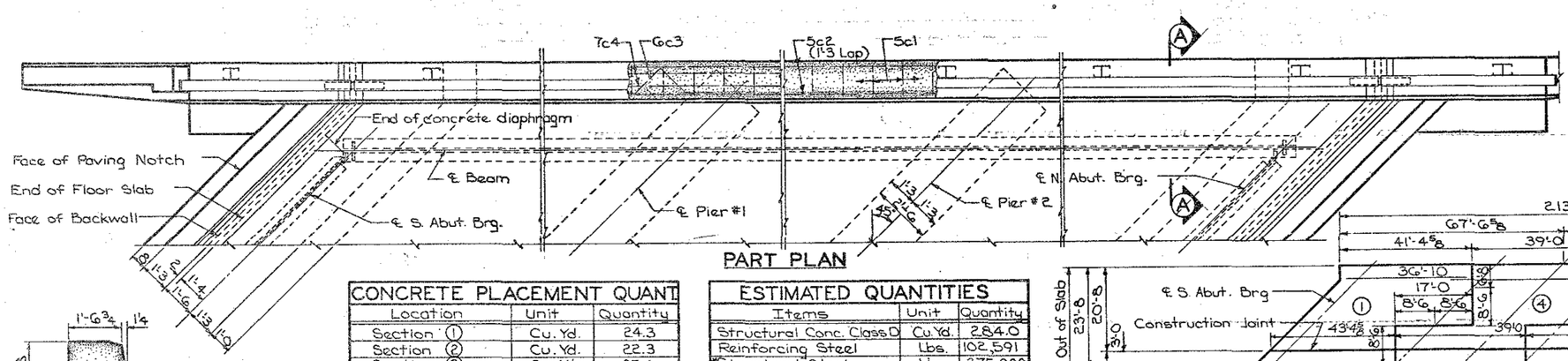

PART PLAN

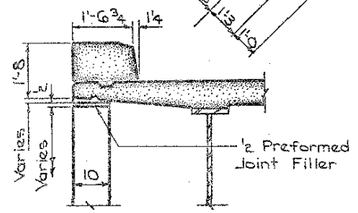

SECTION A-A

CONCRETE PLACEMENT QUANT		
Location	Unit	Quantity
Section (1)	Cu. Yd.	24.3
Section (2)	Cu. Yd.	22.3
Section (3)	Cu. Yd.	25.1
Section (4)	Cu. Yd.	20.2
Section (5)	Cu. Yd.	20.2
Section (1A)	Cu. Yd.	32.4
Section (2A)	Cu. Yd.	28.9
Section (3A)	Cu. Yd.	31.6
Section (4A)	Cu. Yd.	26.1
Section (5A)	Cu. Yd.	26.1
Curbs 2 @ 13.4	Cu. Yd.	26.8
Total	Cu. Yd.	284.0

ESTIMATED QUANTITIES		
Items	Unit	Quantity
Structural Conc. Class D	Cu. Yd.	284.0
Reinforcing Steel	Lbs.	102,591
*Structural Steel	Lbs.	275,000

* Includes 120 lbs. of bronze

REINFORCING BAR LIST					
Bar	Location	Shape	No.	Length	Weight
7a1	Slab Transverse Top		297	29'-5	17858
7a2	" " "		313	19'-5	12422
7a3	" " "		45	Varies	1426
7a4	" " "		41	Varies	1243
7a5	" " "		29	Varies	622
7a6	" " "		25	Varies	498
7a7	" " Bottom		610	24'-5	30444
7a8	" " "		66	Varies	1698
7a9	" " "		72	Varies	1919
6b1	Slab Longit.- Top & Bott.		468	36'-10	25891
5c1	Curb Hoops		342	5'-10	2081
5c2	Curb Longitudinal		24	36'-8	918
6c3	Rail Post Anchors		52	5'-0	391
7c4	Slab & Curb Longit. @ Piers		72	30'-0	4415
5d1	Slab Hoops @ Abut.		36	3'-8	138
5d2	" " " "		36	4'-0	150
5d3	Slab Trans. @ Abut.		8	13'-9	115
5d4	" " " "		12	28'-11	362
				Total (lbs)	102591

BENT BAR DETAILS

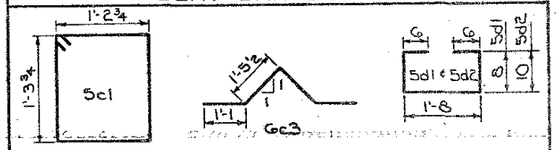

NOTE: All dimensions are out to out.

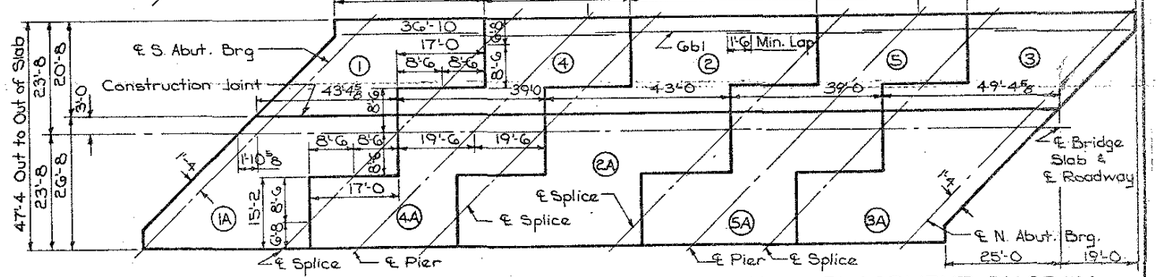

SLAB LONGITUDINAL REINFORCING LAYOUT AND CONCRETE PLACEMENT DIAGRAM

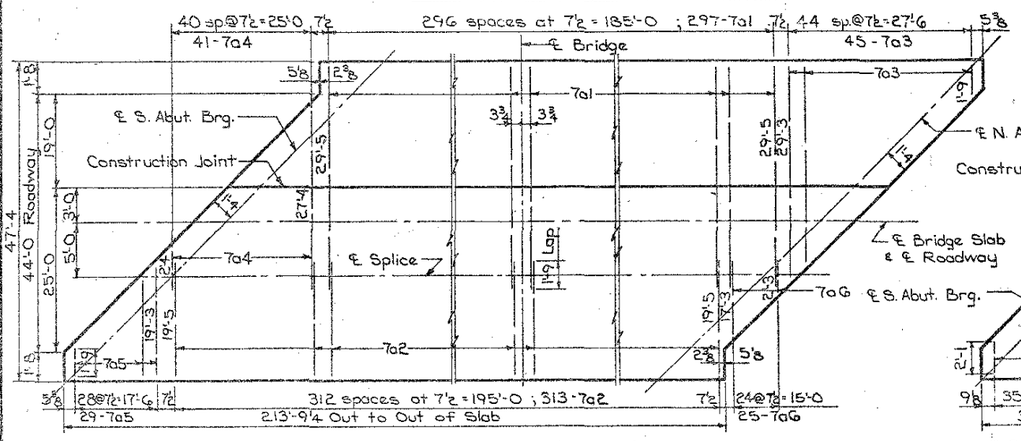

TOP SLAB TRANSVERSE REINFORCING LAYOUT

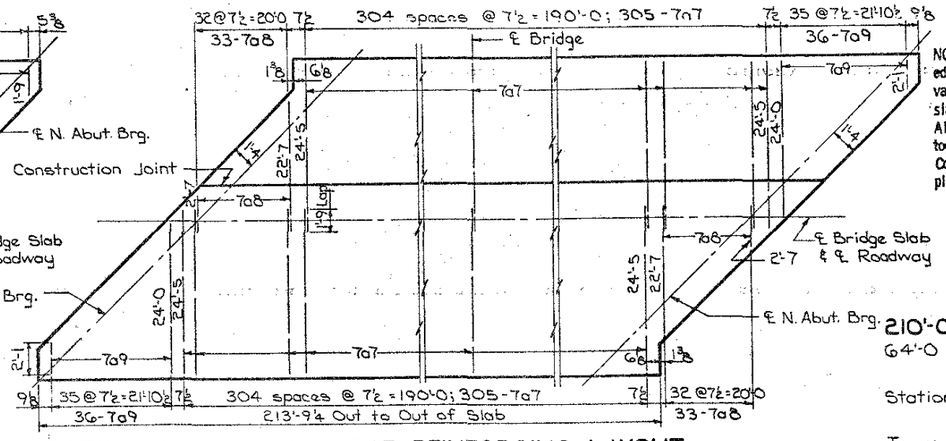

BOTTOM SLAB TRANSVERSE REINFORCING LAYOUT

NOTE: Roadway slab shall be placed in sections and in sequence indicated by encircled numbers on placement diagram and preferably at intervals not exceeding 24 hours. Curbs may be placed continuously. All slab reinforcing steel is to be in place before any section is poured. Alternate procedures for placing concrete may be submitted for approval, together with a statement of the proposed method, and evidence that the Contractor possesses the necessary equipment and facilities to accomplish the required result.

Design For 45° Skew

210'-0 × 44'-0 CONTINUOUS I-BEAM BRIDGE

64'-0 End Spans 82'-0 Interior Span

SUPERSTRUCTURE DETAILS

Station: 594+02.0 January 1969

MARSHALL COUNTY

IOWA STATE HIGHWAY COMMISSION

Des. Sh No. 8 of 12 File No. 23033 Des. No. 1688

DESIGNED BY: Authentic Solutions TRACED BY: Darwin Backous

DETAILED BY: CHECKED BY: E.L. Ornberg

MARSHALL COUNTY

PROJECT NUMBER	STATE	FED. ROAD DIST. NO.	FISCAL YEAR	SHEET NO.	TOTAL SHEETS
FN-G4-7(2)--21-G4 FN-330-2(2)--21-G4	IOWA	3		12	16

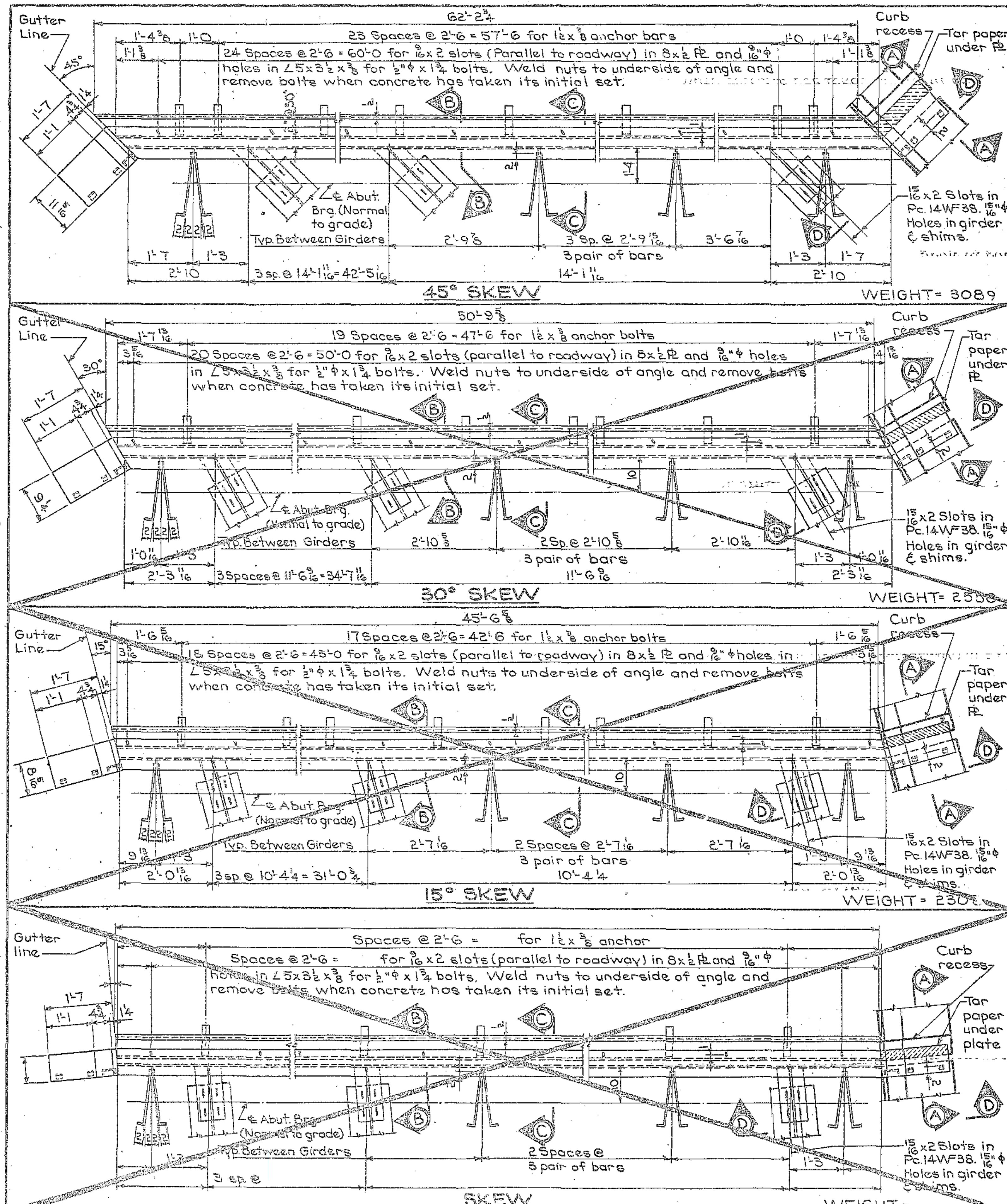

EXPANSION PLATE SETTINGS

Temp. at time of setting	South Abut.		Pier 1	Pier 2	North Abut.	
	D					D
10°	2¼	−5/16	—	—	−5/16	2¼
50°	2	0	—	—	0	2
90°	1¾	+5/16	—	—	+5/16	1¾

NOTE: Settings for other temperatures are proportional.

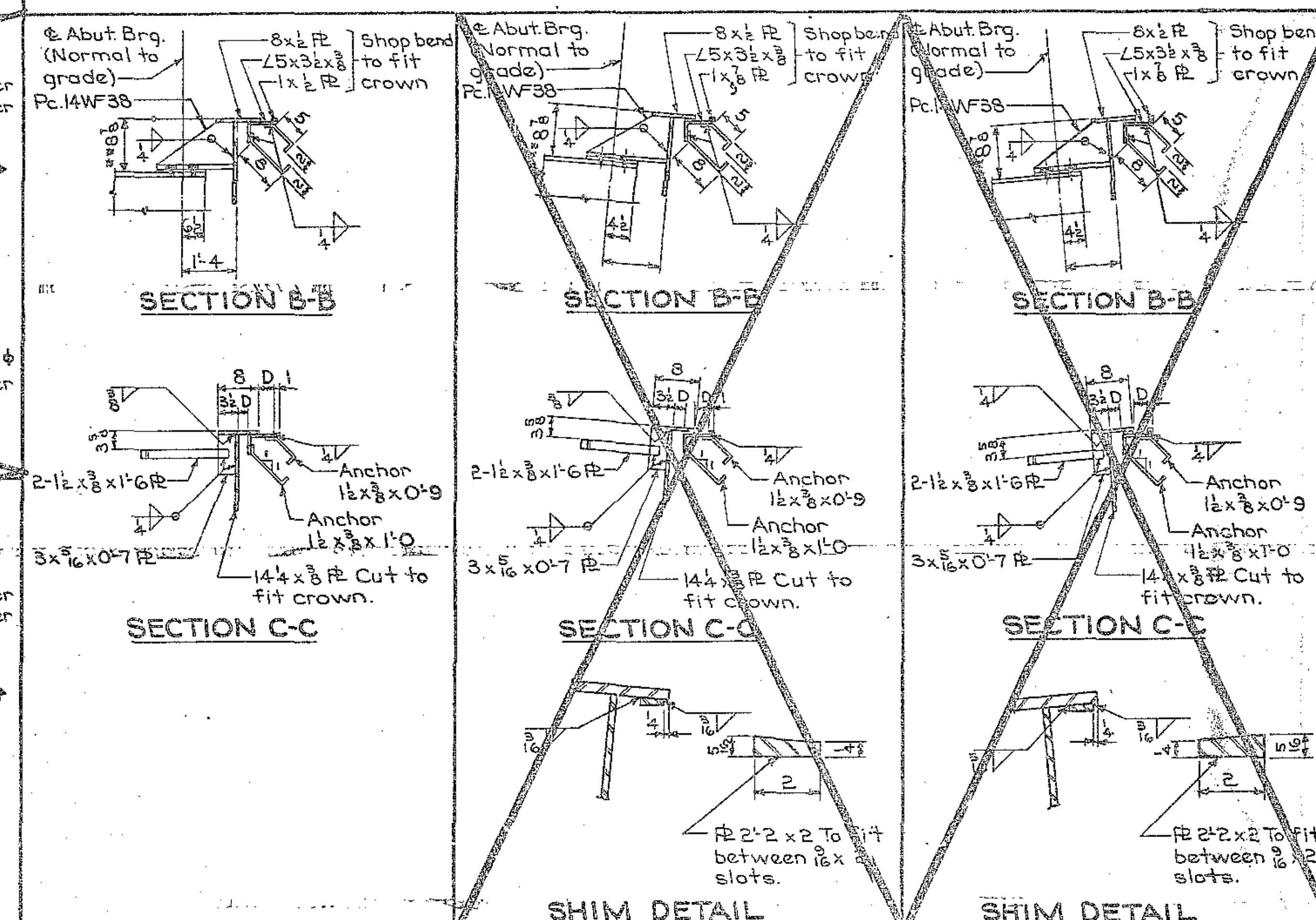

NOTE: Dimension "D" is 2" for a temperature off 50°F. See "Expansion Plate Setting" diagram on this sheet for Settings for 10°F and 90°F. Expansion Plate weights are for a level plate, and do not include the girder connection bolts. One permissible shop splice may be made in any expansion plate providing the pieces are joined with a prequalified single groove weld and all surfaces not in contact with concrete are ground flush.

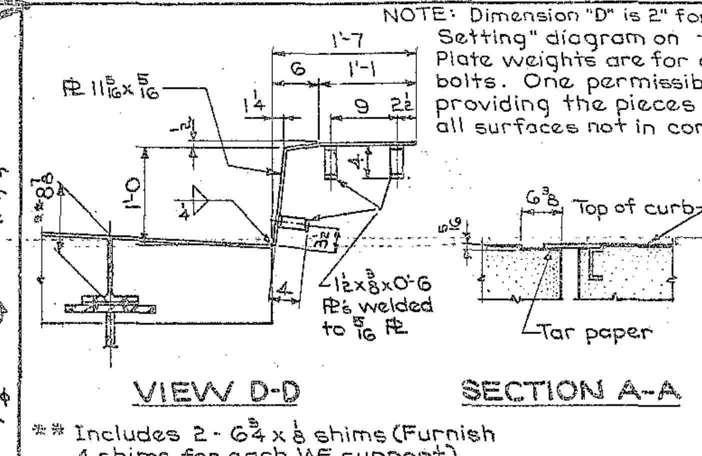

** Includes 2 - 6¾ x ⅛ shims (Furnish 4 shims for each WF support).

Design For 45° Skew
210'-0 x 44'-0 CONTINUOUS I-BEAM BRIDGE
64'-0 End Spans 82'-0 Interior Span
EXPANSION PLATE DETAILS
Station: 594 + 02.0 January 1969
MARSHALL COUNTY

IOWA STATE HIGHWAY COMMISSION
Design Sheet № 9 Of 12 File № 23033 Design № 168
EXPANSION PLATE DETAILS - 44'-0 RDWY. - SKD. LT. AHEAD | STD. SHT.

DESIGNED BY: Augustus C. Lortius TRACED BY:
DETAILED BY: Darwin Backous CHECKED BY: E. L. Ornburs

MARSHALL COUNTY

PROJECT NUMBER	STATE	FED. ROAD DIST. NO.	FISCAL YEAR	SHEET NO.	TOTAL SHEETS
FN-64-7(2)--21-64 FN-330-2(2)--21-64	IOWA	5		245	14

229

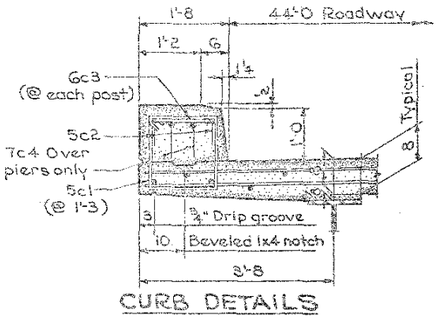

CURB DETAILS

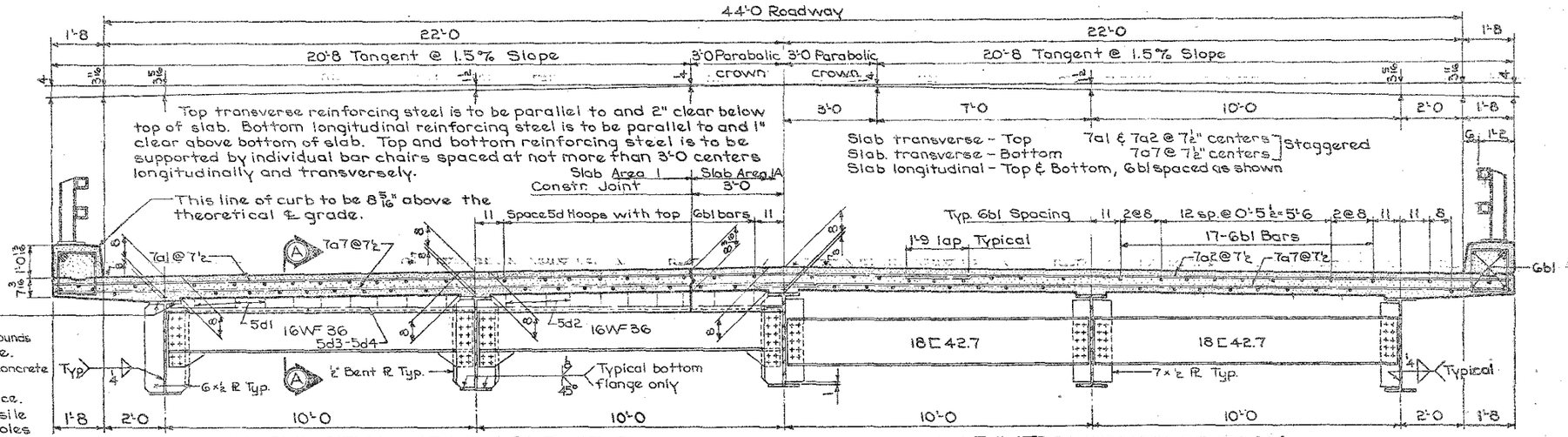

HALF SECTION NEAR ABUTMENT

HALF INTERMEDIATE SECTION

NOTE: Bottom of slab is a straight line between tops of haunches.

SUPERSTRUCTURE NOTES:

Close fit at top

This bridge is designed for HS20-44 loading, plus 20 pounds per square foot of roadway for future wearing surface.

Minimum clear distance from edge of bar to face of concrete is to be 2" unless otherwise noted or shown.

The floor slab as shown includes ½" of wearing surface.

All field connections are to be bolted using "High Tensile Strength Bolts." Unless otherwise noted, all open holes are to be 15/16" ϕ and all bolts are to be ⅞" ϕ.

Bottom flanges are to be perpendicular to webs at the reaction points.

All paint is to be omitted on tops of top flanges and on other steel surfaces in contact with concrete. The parts inaccessible after erection are to be given three coats of paint in the shop.

Forms for the slab and curb are to be supported by the beams.

Fill thicknesses shown on plans are based on the nominal beam dimensions. These thicknesses are to be verified or adjusted during fabrication to secure a close fit. Each fill plate shall fit to the nearest 1/16" in thickness and single plates are required at any fill location. Beams are to be truly square at splice points with flanges perpendicular to webs.

The design drawings indicate AWS pre-qualified welded joints, and unless otherwise noted the design joint details are for manual shielded metal-arc welding. Alternate joint details may be submitted for approval.

Magnetic particle inspection of welds, in accordance with Article 2408.15 of the Standard Specifications, will be required for the bearing stiffener welds of the beams & girders and the web to flange welds of the girders.

Approved stud shear connector may be used as an alternate for the angle shear connectors shown. If studs are used, each angle lug is to be replaced by a group of 10 x ⅞" ϕ x 5" studs. The centroid of the stud group is to be in the approximate location of the angle lug replaced. Maximum spacing between stud rows is to be 24" and where the angle lug spacing exceeds 24" the equivalent studs are to be located in two or more rows so that the maximum spacing is not exceeded. Studs are to be welded in the shop at locations shown on shop drawings approved by the Iowa State Highway Commission.

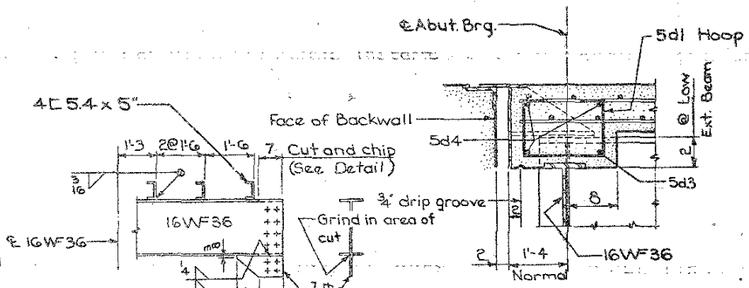

ABUTMENT DIAPHRAGM CONNECTION

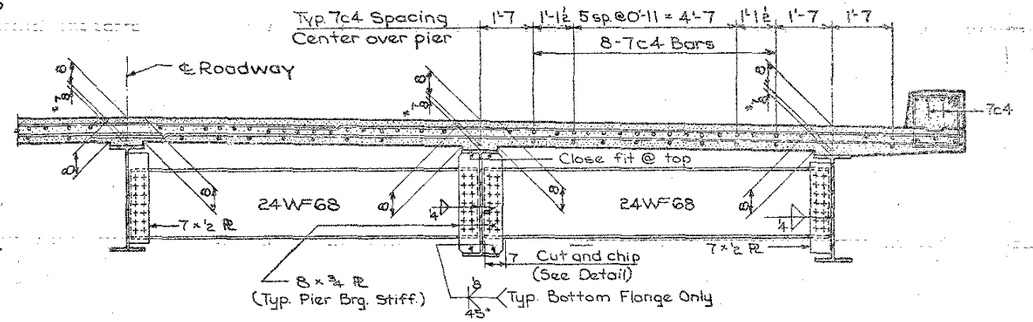

PART SECTION NEAR PIER

SECTION A-A

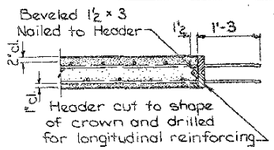

TRANSVERSE FLOOR CONSTRUCTION JOINT

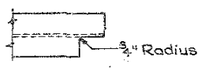

TYPICAL CUT AND CHIP DETAIL

* The haunch dimensions shown are nominal haunch dimensions at bearings. For the slab thickness over the beam at any location the nominal haunch dimension is to be increased by the amount indicated on the "Haunch Thickening Diagram" shown on Sheet 7 and may be further increased or decreased a maximum of ¼" due to beam camber inaccuracies.

NOTE: Faying surfaces of diaphragm connections are to be given the shop coat of paint.

Area of Slab			
	Area IA	=	18.0555 sq. ft.
	Area I	=	13.9370 sq. ft.
Area of One Curb		=	1.693 sq. ft.

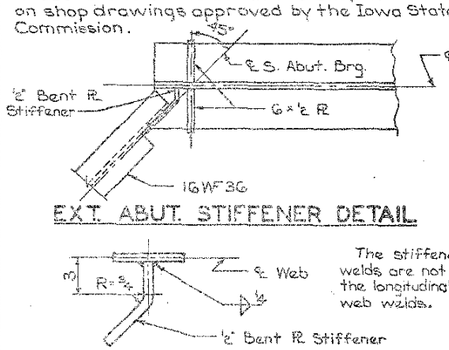

EXT. ABUT. STIFFENER DETAIL

The stiffener to flange welds are not to intersect the longitudinal flange to web welds.

ABUT. BENT PL STIFF. DETAIL

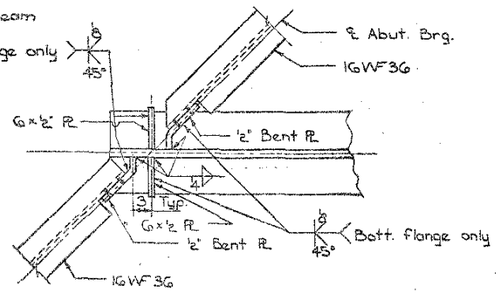

INT. ABUT. STIFF. DETAIL

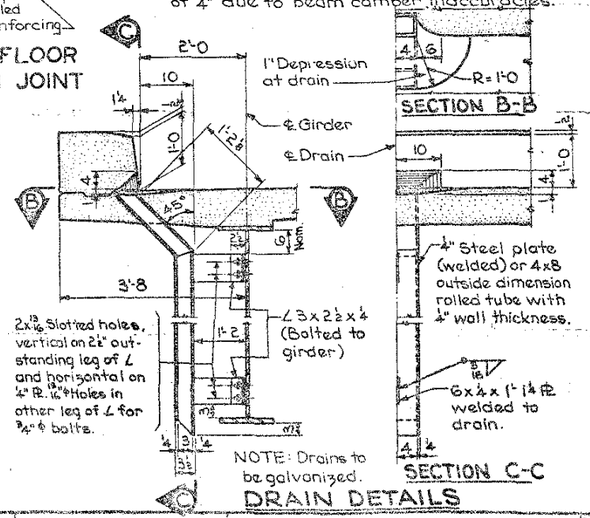

NOTE: Drains to be galvanized.

DRAIN DETAILS

Design For 45° Skew

210'-0 x 44'-0 CONTINUOUS I-BEAM BRIDGE

64'-0 End Spans 82'-0 Interior Span

SUPERSTRUCTURE DETAIL

Station: 594 +02.0 January 1969

MARSHALL COUNTY

IOWA STATE HIGHWAY COMMISSION

Design Sheet No 10 Of 12 File No 23033 Design No 168

DESIGNED BY: Richard G. Martens
DETAILED BY: Darwin Backous
TRACED BY:
CHECKED BY: E.L. Ornberg

STEEL CROSS SECTION - 44' ROADWAY | STANDARD SHEET | MARSHALL COUNTY

PROJECT NUMBER	STATE	FED. ROAD DIST. NO.	FISCAL YEAR	SHEET NO.	TOTAL SHEETS
FN-64-7(2)--21-64	IOWA	5		12	12
FN-330-2(2)--21-64					